

DISPLACEMENT OF OIL BY CARBON DIOXIDE

Final Report

Work Performed for the Department of Energy  
Under Contract DE-AC21-78ET12082

Date Published—May 1981

New Mexico Institute of Mining & Technology  
Socorro, New Mexico



**National Petroleum Technology Office**  
**U. S. DEPARTMENT OF ENERGY**  
**Tulsa, Oklahoma**

## DISCLAIMER

"This book was prepared as an account of work sponsored by an agency of the United States Government. Neither the United States Government nor any agency thereof, nor any of their employees, makes any warranty, express or implied, or assumes any legal liability or responsibility for the accuracy, completeness, or usefulness of any information, apparatus, product, or process disclosed, or represents that its use would not infringe privately owned rights. Reference herein to any specific commercial product, process, or service by trade name, trademark, manufacturer, or otherwise, does not necessarily constitute or imply its endorsement, recommendation, or favoring by the United States Government or any agency thereof. The views and opinions of authors expressed herein do not necessarily state or reflect those of the United States Government or any agency thereof."

Available from the National Technical Information Service, U.S. Department of Commerce, Springfield, Virginia 22161.

### NTIS price codes

Paper copy:	\$11.00
Microfiche copy:	\$ 3.50

DISPLACEMENT OF OIL BY CARBON DIOXIDE

Final Report

*Contributors:*

C. L. Lien  
H. K. Wainwright  
M. K. Silva  
M. T. Pelletier

F. M. Orr, Jr. and J. J. Taber  
*Principal Investigators*  
New Mexico Institute of Mining and Technology  
Socorro, New Mexico 87801

Leo Noll, *Technical Project Officer*  
Bartlesville Energy Technology Center  
Bartlesville, Oklahoma 74003

Prepared for the Department of Energy  
Under Contract No. DE-AC21-78ET12082

Date Submitted—December 1980  
Date Published—May 1981

U.S. DEPARTMENT OF ENERGY

TABLE OF CONTENTS

	<u>PAGE NO.</u>
LIST OF TABLES . . . . .	iv
LIST OF FIGURES . . . . .	v
ABSTRACT . . . . .	ix
1. Introduction . . . . .	1
2. Task 1. Design of High Pressure Equipment . . . . .	3
2.1 PVT Apparatus . . . . .	3
Volumetric Calibrations . . . . .	3
Densitometer Calibrations . . . . .	5
Capillary Tube Viscometer Calibrations . . . . .	5
Experimental Procedures . . . . .	5
High Pressure Sampling Technique . . . . .	8
2.2 Displacement Apparatus . . . . .	9
Slim Tube, Core and Mixing Cell Configurations . . . . .	9
Fluid Production and Sample Collection System . . . . .	12
Continuous Multiple Contact Apparatus . . . . .	15
2.3 Chemical Analysis of CO <sub>2</sub> -Hydrocarbon Mixtures . . . . .	17
Equipment . . . . .	19
Analysis of Hydrocarbon Liquid Samples . . . . .	22
Analysis of High Pressure CO <sub>2</sub> -Crude Oil Mixtures . . . . .	25
Analysis of Produced Gas Samples . . . . .	29
2.4 Task 1: Summary and Conclusions . . . . .	30
3. Task 2. Displacement Experiments . . . . .	31
3.1 Slim Tube Displacement Results . . . . .	31
3.2 Comparison of Slim Tube, Core and Mixing Cell Displacements . . . . .	39
3.3 Phase Behavior and Fluid Properties of CO <sub>2</sub> -Crude Oil Mixtures . . . . .	46
Results of Single Contact Experiments . . . . .	47

Results of a Batch Multiple Contact Experiment . . . . .	54
Results of Mixing Cell Displacements . . . . .	62
Measurement of Phase Compositions by Continuous Multiple Contacts . . . . .	64
Discussion . . . . .	73
3.4 Summary and Conclusions for Task 2 . . . . .	74
4. Task 3. Mathematical Modeling of CO <sub>2</sub> Displacements . . . . .	76
4.1 Validation of the Simulator . . . . .	77
4.2 Simulation of Slim Tube Displacements . . . . .	80
4.3 Summary and Conclusions for Task 3 . . . . .	94
5. Task 4. Application of Laboratory Results to Field Problems . . . . .	96
5.1 Process Description . . . . .	98
5.2 Slim Tube Displacements . . . . .	100
5.3 Core Floods . . . . .	103
5.4 PVT Experiments . . . . .	105
5.5 Continuous Multiple Contact Experiment . . . . .	107
5.6 Task 4: Conclusions . . . . .	107
6. Summary . . . . .	109
Acknowledgement . . . . .	111
References . . . . .	112
Appendix A . . . . .	118
Appendix B . . . . .	135

LIST OF TABLES

	<u>PAGE</u> <u>NO.</u>
Table 2.1 Gas Chromatograph Operating Conditions . . . . .	21
Table 3.1 Properties of Maljamar Separator Oil at Atmospheric Pressure . . . . .	33
Table 3.2 Solubility of CO <sub>2</sub> in Maljamar Separator Oil at 32.2°C . . . . .	36
Table 3.3 Effective CO <sub>2</sub> Injection at Breakthrough . . . . .	37
Table 3.4 Density and Viscosity of Mixtures of CO <sub>2</sub> with Maljamar Separator Oil and Recombined Reservoir Fluid (RRF) . . . . .	51
Table 3.5 Composition and Properties of Maljamar Recombined Reservoir Fluid (RRF) . . . . .	52
Table 3.6 Compositions of Gas Samples Recovered During Blowdown of Reverse Contact Upper Phases (Mol Percent) . . . . .	60
Table 3.7 Compositions (Weight Percent) of Fluids Produced in a Continuous Multiple Contact Displacement of Maljamar Separator Oil . . . . .	67
Table 4.1 Component Properties for Slim Tube Simulations . . . . .	81
Table 5.1 Characteristics of Slim Tube Displacement Experiments . . . . .	101
Table 5.2 Characteristics of CO <sub>2</sub> Displacements in Cores . . . . .	104

LIST OF FIGURES

	<u>PAGE</u> <u>NO.</u>
Figure 2.1 Apparatus for measurements of phase volumes, compositions, densities and viscosities . . . . .	4
Figure 2.2 Comparison of high pressure measurements of the density of CO <sub>2</sub> at 32.2°C with data from Michels et al. (1957) . . . . .	6
Figure 2.3 Comparison of viscosity measurements with literature values for decane and CO <sub>2</sub> . . . . .	7
Figure 2.4 High pressure sampling system . . . . .	10
Figure 2.5 Apparatus for CO <sub>2</sub> displacements in a slim tube, core or mixing cell . . . . .	11
Figure 2.6 Servo-controlled back pressure regulator . . . . .	13
Figure 2.7 Servo amplifier for the back pressure regulator . . . . .	14
Figure 2.8 Apparatus for continuous measurement of equilibrium phase compositions for CO <sub>2</sub> -crude oil mixtures . . . . .	16
Figure 2.9 Comparison of phase compositions determined at 24°C by static equilibrium experiments (dashed tie lines) and by continuous multiple contact experiments (solid tie lines) . . . . .	18
Figure 2.10 Gas chromatography equipment . . . . .	20
Figure 2.11 Chromatograms for a crude oil sample . . . . .	23
Figure 2.12 Effect of sample size on hydrocarbon response factors . . . . .	26
Figure 2.13 Effect of molecular size on hydrocarbon response factors . . . . .	27
Figure 2.14 Comparison of analyses of Maljamar separator oil by gas chromatography and by true boiling point distillation . . . . .	28
Figure 3.1 Recovery of Maljamar separator oil from slim tubes by continuous displacement with CO <sub>2</sub> at 32.2°C (90°F) . . . . .	32

	<u>PAGE</u> <u>NO.</u>
Figure 3.2 Pressure drops (normalized by the initial pressure drop) during slim tube displacements . . . . .	34
Figure 3.3 Summary of oil recovery in slim tube displacements of Maljamar separator oil at 32.2°C (90°F) . . . . .	38
Figure 3.4 Composition of liquids produced during a slim tube displacement of Maljamar separator oil at 5.52 MPa (800 psi) and 32.2°C (90°F) . . . . .	40
Figure 3.5 Composition of liquids produced during a slim tube displacement of Maljamar separator oil at 6.89 MPa (1000 psi) and 32.2°C (90°F) . . . . .	41
Figure 3.6 Composition of liquids produced during a slim tube displacement of Maljamar separator oil at 8.27 MPa (1200 psi) and 32.2°C (90°F) . . . . .	42
Figure 3.7 Composition of liquids produced during a slim tube displacement of Maljamar separator oil at 9.65 MPa (1400 psi) and 32.2°C (90°F) . . . . .	43
Figure 3.8 Oil recovered from displacements of Maljamar oil by CO <sub>2</sub> at 8274 kPa (1200 psi) and 32.2°C (90°F) . . . . .	44
Figure 3.9 Phase behavior of binary mixtures of CO <sub>2</sub> with Maljamar separator oil at 32.2°C (90°F) . . . . .	48
Figure 3.10 Volumetric behavior of two CO <sub>2</sub> -crude oil mixtures at 32.2°C (90°F) . . . . .	49
Figure 3.11 Pressure ranges for liquid-liquid-vapor behavior in CO <sub>2</sub> -crude oil systems . . . . .	55
Figure 3.12 Summary of volumes transferred in a batch multiple contact experiment with recombined Maljamar oil at 32.2°C (90°F) . . . . .	56
Figure 3.13 Volumetric behavior of mixture F <sub>2</sub> . . . . .	58
Figure 3.14 Volumetric behavior of mixture R <sub>1</sub> . . . . .	59

	PAGE <u>NO.</u>
Figure 3.15	Compositions of blowdown liquids from mixtures R <sub>1</sub> -R <sub>4</sub> . . . . . 61
Figure 3.16	Weight fraction of hydrocarbons extracted by CO <sub>2</sub> from Maljamar separator oil at 32.2°C (90°F) . . . . . 63
Figure 3.17	Compositions of hydrocarbons produced during displacement of Maljamar separator oil from a mixing cell at 8274 kPa (1200 psi) and 32.2°C (90°F) . . . . . 65
Figure 3.18	Weight ratio of gas to oil production in a continuous multiple contact displacement of Maljamar separator oil at 8274 kPa (1200 psi) and 32.2°C (90°F) . . . . . 68
Figure 3.19	Calculated molecular weights of hydrocarbons produced in upper and lower phase samples . . . . . 69
Figure 3.20	Compositions of liquids collected from upper and lower phase samples . . . . . 70
Figure 3.21	Pseudo-ternary phase diagram (in mole fractions) for CO <sub>2</sub> and Maljamar separator oil at 8274 kPa (1200 psi) and 32.2°C (90°F) . . . . . 71
Figure 4.1	Comparison of calculated (solid line) and experimental (data points) component recovery for isooctane (IC <sub>8</sub> ) displacing 50 vol % isopropanol (IPA) - 50 vol % brine (2 wt. % CaCl <sub>2</sub> ) . . . . . 78
Figure 4.2	Comparison of calculated (solid line) and experimental (data points) component recovery for isooctane (IC <sub>8</sub> ) displacing 85 vol % IPA - 15 vol % brine . . . . . 79
Figure 4.3	Pseudo-ternary phase diagram used in one-dimensional simulation of slim tube displacement at 5516 kPa (800 psi) . . . . . 82
Figure 4.4	Pseudo-ternary phase diagram used in one-dimensional simulation of slim tube displacement at 6895 kPa (1000 psi) . . . . . 83

	PAGE <u>NO.</u>
Figure 4.5	Pseudo-ternary phase diagram used in one-dimensional simulation of slim tube displacement at 8274 kPa (1200 psi) . . . . . 84
Figure 4.6	Calculated oil recovery in slim tube displacements . . . . . 85
Figure 4.7	Comparison of computed and experimental oil recovery at one pore volume injection in slim tube displacements . . . . . 86
Figure 4.8	Effect of CO <sub>2</sub> density on computed recovery for a slim tube displacement at 5516 kPa (800 psi) . . . . . 88
Figure 4.9	Comparison of calculated to experimental oil recovery in slim tube displacements . . . . . 89
Figure 4.10	Computed saturation and composition distributions for slim tube displacement at 5516 kPa (800 psi) . . . . . 90
Figure 4.11	Computed saturation and composition distributions for slim tube displacement at 6895 kPa (1000 psi) . . . . . 90
Figure 4.12	Computed saturation and composition distribution for slim tube displacement at 8274 kPa (1200 psi) . . . . . 90
Figure 4.13	Overall composition path of fluids present at the outlet grid block at 5516 kPa (800 psi) . . . . . 91
Figure 4.14	Overall composition path of fluids present at the outlet grid block at 6895 kPa (1000 psi) . . . . . 92
Figure 4.15	Overall composition path of fluids present at the outlet grid block at 8274 kPa (1200 psi) . . . . . 93
Figure 5.1	Ideal one-dimensional displacement of oil by CO <sub>2</sub> . . . . . 99

## Abstract

Results of a comprehensive research program on factors influencing CO<sub>2</sub> flooding are reported. Equipment constructed for static equilibrium measurements of phase volumes, compositions, densities and viscosities is described. Design of an apparatus used for a variety of displacement tests is also reported. Apparatus and experimental procedures are described for a new experiment in which equilibrium phase compositions can be measured rapidly and continuously.

Results of displacements of crude oil from slim tubes, cores and mixing cells are presented and interpreted in terms of detailed measurements of the phase behavior and fluid properties of the CO<sub>2</sub>-crude oil mixtures. The complex (liquid-liquid and liquid-liquid-vapor) phase behavior of low temperature CO<sub>2</sub>-crude oil mixtures is described and compared with similar behavior for CO<sub>2</sub>-alkane mixtures. A simple correlation is offered for the ranges of reservoir temperature and pressure at which liquid-liquid and liquid-liquid-vapor phase behavior should be expected to occur. Direct evidence is presented of the efficiency with which a CO<sub>2</sub>-rich liquid phase can extract hydrocarbons from a crude oil.

A simple one-dimensional process simulator for CO<sub>2</sub> flooding applications is described. Simulation results are compared with experimental data from slim tube displacements. Good agreement is reported between calculated and experimental results as long as the volume change of CO<sub>2</sub> on mixing with the oil is not too great. Sensitivity of calculated results to phase behavior and fluid properties is discussed. Comparison of displacement results, phase behavior measurements, and model calculations provides strong evidence that the high displacement efficiency which can be obtained when pressure is high enough and viscous fingering is controlled is the result of efficient extraction of a broad range of hydrocarbons by a dense CO<sub>2</sub>-rich phase which is a liquid if the temperature is below about 50°C (130°F).

Factors such as phase behavior, viscous fingering, gravity segregation and core heterogeneity influencing laboratory experiments are reviewed. Uses and limitations of laboratory experimental data to support field scale performance predictions are discussed.

Reprints of two papers which provide additional analysis of CO<sub>2</sub>-crude oil phase behavior are given in Appendices A and B.



## 1. INTRODUCTION

Injection of CO<sub>2</sub> into an oil reservoir causes a complicated series of interactions between CO<sub>2</sub>, oil and water. Initially, injected CO<sub>2</sub> dissolves in both the oil and water present near the injection well. As injection continues, the concentration of CO<sub>2</sub> in the fluids around the injector rises. When the solubility limit of CO<sub>2</sub> in the oil is reached, the CO<sub>2</sub>-oil system divides into two phases: an oil rich phase, and a CO<sub>2</sub>-rich phase. The oil-rich phase contains a high concentration of dissolved CO<sub>2</sub>, while the CO<sub>2</sub>-rich phase contains hydrocarbons extracted from the oil. The relative movement of the CO<sub>2</sub>-rich, oil-rich and water phases, in conjunction with transfer of CO<sub>2</sub> and hydrocarbon components between phases determines the local displacement efficiency of a particular CO<sub>2</sub> flood. That relative movement, however, is not independent of the effects of mass transfer between phases. Phase densities and viscosities (which are functions of reservoir pressure and temperature and the phase compositions) along with phase relative permeabilities control the rates at which the phases move under the imposed pressure gradient. Those rates, in turn, influence compositions of a second generation of phases which result when rapidly moving primary phases encounter and mix with those moving more slowly. On a larger scale that mixing process can be strongly influenced by viscous fingering, gravity segregation, reservoir heterogeneity and dispersion. Thus, a CO<sub>2</sub> flood is a complex collection of competing effects, the sum of which determines displacement efficiency.

In this report we summarize work performed during the past two years to characterize various features of the process. Our goal was to measure the ranges of phase compositions and properties likely to exist during a CO<sub>2</sub> flood, to understand how such composition variations influence displacement efficiency, and to understand how phase behavior interacts with factors such as viscous fingering and dispersion to alter process efficiency.

Three experimental systems were developed during the project. These are reviewed in §2. Equipment constructed to perform static equilibrium measurements of phase compositions and properties is described, and related techniques developed for sampling and analysis of high pressure mixtures of CO<sub>2</sub> and oil are outlined. Design of a second system used in high pressure slim tube and core displacement tests is also reported. We also describe a new apparatus developed to perform measurements of phase compositions during a displacement test. The new experiment, a continuous multiple contact experiment (Orr et al. 1980b), can be used to determine phase compositions much more rapidly than can be done in standard static equilibrium experiments.

In §3, results of a series of displacement tests in slim tubes, cores and in the continuous multiple contact apparatus are reported. Results of supporting measurements of phase behavior and fluid properties are also

given. The results give some insight into the roles and interactions of viscous fingering and phase behavior and illustrate the difficulties encountered in interpreting displacement experiments in which more than one displacement mechanism is operating.

One-dimensional simulations of the displacement process are reported in §4. Variations of composition and fluid properties in the transition zone which develops in a CO<sub>2</sub> flood are discussed, and the sensitivity of recovery efficiency to variations in phase behavior and fluid properties is examined.

In §5, a review of the types of experiments used to evaluate a CO<sub>2</sub> flood is undertaken. Relationships between various kinds of equilibrium and displacement experiments are discussed, the types of information obtained are outlined, and the uses and limitations of the data are reviewed. In the final section, conclusions from this study are summarized.

## 2. TASK 1. DESIGN OF HIGH PRESSURE EQUIPMENT

### 2.1 PVT Apparatus

Figure 2.1 shows a schematic of the (PVT) equipment used for static equilibrium measurements of phase behavior and fluid properties. The PVT system developed in this project is much more versatile than standard systems because it allows simultaneous measurement of phase volumes, densities, viscosities and compositions. The heart of the system consists of two 190 cm<sup>3</sup> high pressure windowed cells mounted on a single rotating plate in a temperature controlled air bath. Cell contents are mixed by repeated rotation of the cells to an inverted position. The cells have windows on both sides so that the cell contents can be viewed in transmitted light, an essential feature since phase separations at high pressures can be very difficult to see in reflected light alone. The cells are connected so that fluids can be transferred from one cell to the other. A two barrel Ruska pump is used to transfer fluids at nearly constant pressure by displacing mercury into one cell and withdrawing mercury from the second cell at the same rate. System pressure is measured by a Setra 204 0-10,000 psig transducer. Phase viscosities are measured by transferring the appropriate phase from one cell to the other. The transfer loop between the cells includes a capillary tube (across which pressure drop can be measured to determine phase viscosity), a high pressure densitometer (Mettler/Paar DMA 512), and a Valco high pressure sampling valve through which samples are extracted from the pressurized system for analysis by gas chromatography.

### Volumetric Calibrations

Precise measurement of phase volumes and accurate metering of fluids into the high pressure cells require careful volumetric calibration of the pumps, tubing and windowed cells that make up the PVT apparatus. First, the volumetric delivery of each pump barrel was calibrated by comparing the actual volume of mercury removed from the pump at various pressures to pump scale readings. Next, the expansion of the tubing manifold leading from the pumps to the cells was measured as a function of system pressure by compressing mercury into the manifold. Manifold compressibility measurements were made at 100°F and 250°F. Finally, PVT cell volumes were also measured at 100°F and 250°F at various pressure levels. A known volume of mercury was metered into each cell against a constant back pressure. The position of the mercury interface was then measured with a cathetometer. Volumetric calibration data were incorporated into a computer program which calculated volume of a phase from the position of the interfaces bounding it (Yu 1980).

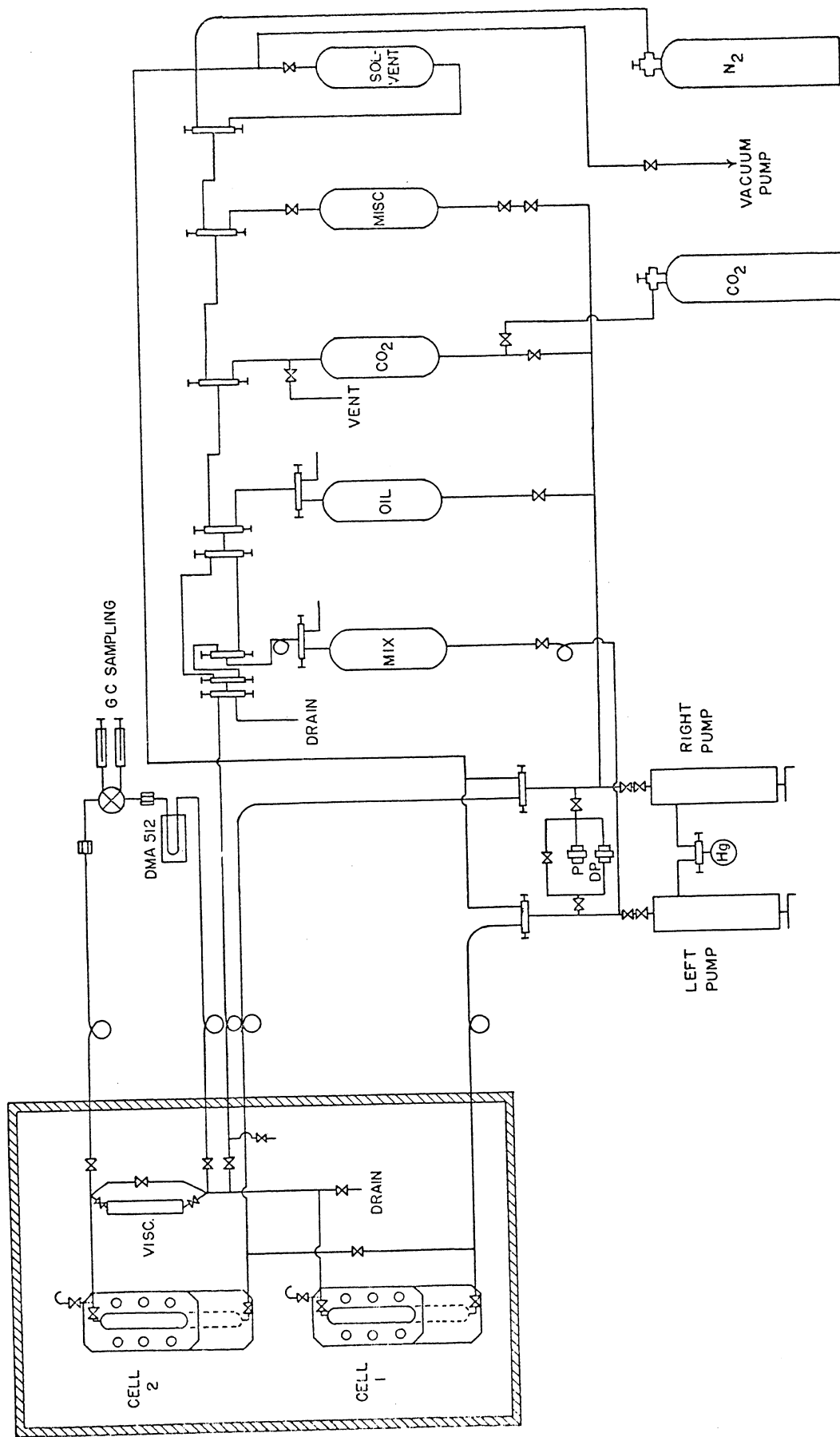


Figure 2.1 Apparatus for measurements of phase volumes, compositions, densities and viscosities.

### Densitometer Calibrations

Calibration of the high pressure densitometer (Mettler/Par 512) was also carried out at elevated temperature and pressure. Temperature of the DMA 512 cell was controlled to within  $\pm 0.1^\circ\text{C}$  by a Neslab Exacal 100. A Ruska manual positive displacement pump was used to generate test pressures to 4000 psi. Pressure was measured by a Setra 204 transducer (absolute accuracy:  $\pm 0.5$  psi). Air,  $\text{CO}_2$  and degassed distilled water were used as calibration fluids. Results show that densities of order  $1 \text{ g/cm}^3$  can be measured at elevated temperature and pressure with an accuracy of  $\pm 0.1\%$  (Spaulding 1980). A test measurement of the density of pure  $\text{CO}_2$  at  $90^\circ\text{F}$  showed excellent agreement with published values (Michels et al. 1957) even after almost a year of operation without recalibration. Results of that test are shown in Figure 2.2.

### Capillary Tube Viscometer Calibrations

Phase viscosities were measured by transferring the phase in question from one windowed cell to the other at a known rate through a 0.0152 cm ID stainless steel capillary tube of length 30.5 cm. Pressure drop across the capillary tube was determined by measuring differential pressure between the two high pressure cells using two Setra 204 transducers. Calibration experiments were performed with decane and  $\text{CO}_2$  for pressures between 1000 and 4000 psi (6895 to 27579 kPa). An effective capillary tube diameter of 0.0165 cm was calculated from calibration runs with decane at a variety of rates. That diameter is about 9% larger than the nominal value for the tubing. A comparison of measured viscosities for decane and  $\text{CO}_2$  with values given by Lee (1965) and Michels et al. (1957) is given in Figure 2.3. The agreement for decane is good since those data were used to determine the capillary tube diameter. Agreement for the  $\text{CO}_2$  data is less satisfactory. Values measured in our apparatus exceed those reported by Michels et al. (1957) by about 0.05 cp. The principal sources of error were probably the pressure transducers. We conclude that the viscosity measurements reported below are probably accurate to within 10% for viscosities of order 1. Percentage errors are, of course, much larger for low viscosity fluids.

### Experimental Procedures

The apparatus shown in Figure 2.1 was used to perform both single and multiple contact phase behavior studies. In single contact studies, metered volumes of hydrocarbons or  $\text{CO}_2$  were charged into one of the visual cells. The fluid to be charged was displaced from a supply vessel by mercury from pump 1 while an equal volume of mercury was withdrawn from the visual cell into the barrel of pump 2 (the two mercury pumps are actually a single Ruska pump with two  $250 \text{ cm}^3$  barrels). Thus, fluids could be transferred from the supply vessels to the high pressure cells at nearly constant pressure. The volume of the resulting mixture of known

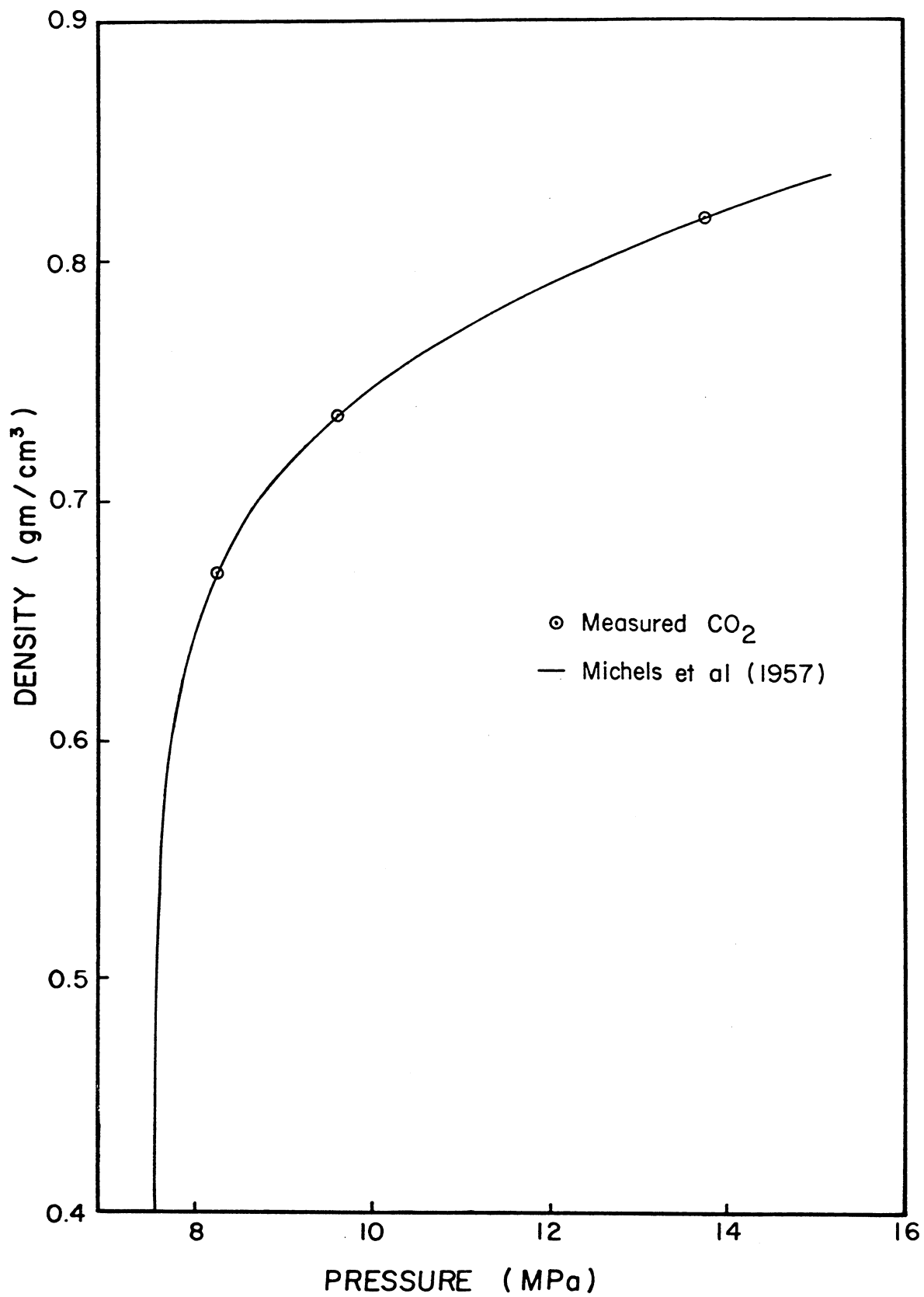


Figure 2.2 Comparison of high pressure measurements of the density of CO<sub>2</sub> at 32.2°C with data from Michels et al. (1957).

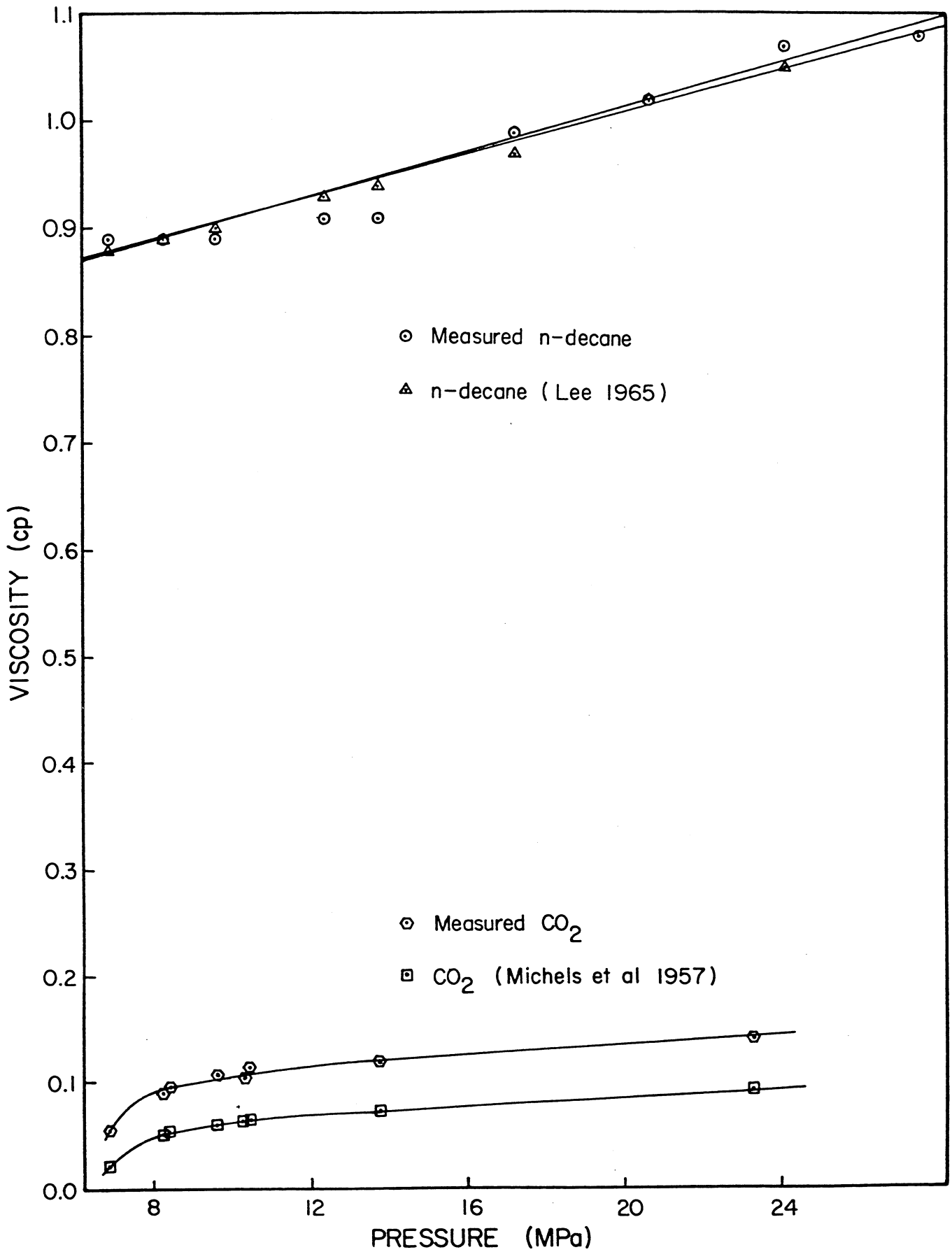


Figure 2.3 Comparison of viscosity measurements with literature values for decane and CO<sub>2</sub>.

overall composition was then varied by injecting or removing mercury from the cell. Appearance or disappearance of phases was determined visually and from measurements of the overall compressibility of the cell contents. Bubble point pressures were easily detected since there is a large change in system compressibility when a gas phase appears or disappears. Liquid-liquid saturation pressures and dew point pressures were determined visually since the appearance or disappearance of a liquid phase in the presence of a gas or another liquid phase has only a small effect on the overall compressibility of the system. Phase volumes were determined from cathetometer measurements of the positions of interfaces between phases.

The two-cell arrangement shown in Figure 2.1 is particularly useful for multiple contact phase behavior studies (Gardner et al. 1979). Results of one such experiment are reported in §3.2. In that experiment, a two phase mixture of CO<sub>2</sub> and crude oil was made in one of the cells, just as in a single contact study. Then the upper, CO<sub>2</sub>-rich phase was transferred to the second cell and mixed with fresh crude oil. Volumetric behavior of the resulting mixture was then determined at a variety of pressures. The mixture of the CO<sub>2</sub>-rich phase with fresh crude oil is referred to below as a forward contact mixture because it simulates the mixing which takes place when a low viscosity, and hence highly mobile, CO<sub>2</sub>-rich phase mixes with uncontacted crude oil near the leading edge of a transition zone in a CO<sub>2</sub> displacement. The behavior of oil left behind as the CO<sub>2</sub> front passes was simulated by mixing fresh CO<sub>2</sub> with the lower phase remaining after the removal of the CO<sub>2</sub>-rich phase. Such mixtures will be referred to as reverse contact mixtures.

#### High Pressure Sampling Technique

Representative samples of high pressure mixtures, particularly CO<sub>2</sub>-hydrocarbon mixtures, are difficult to obtain. The aim of any sampling procedure is to transfer a representative sample taken at high pressure and the system temperature to the injection port of a gas chromatograph, which is at low pressure and high temperature, without losing part of the sample. CO<sub>2</sub>-crude oil samples are particularly difficult to handle because CO<sub>2</sub> extracts even heavy hydrocarbons very effectively from crude oil. Those hydrocarbons remain in solution in the CO<sub>2</sub>-rich phase only as long as the pressure remains high. If the pressure is reduced, as would occur if a high pressure sampling valve were used to obtain the sample and inject it into the gas chromatograph, the heavy hydrocarbons would be left behind in the valve unless the valve was at very high temperature. To be representative, however, the sample would have to be taken at the experimental temperature and pressure and then heated, while still under pressure, to a temperature high enough to vaporize the heavy hydrocarbons into a helium stream. Unfortunately, sampling valves which can withstand high pressure and temperature simultaneously are not available.

Sampling with a syringe capable of sealing to hold a sample at high pressure is an attractive alternative. Research is underway at Louisiana

State University (Whitehead and Kimbler 1979) on the use of that technique using experimental prototype syringes provided by Precision Sampling Company. The syringe being used by the Louisiana State group has not yet been made available for purchase by other research groups, however.

Accordingly, a sampling technique was developed which uses a combination of sampling valve and syringes able to withstand low positive pressures. High pressure samples from the PVT cell were obtained by the procedure outlined schematically in Figure 2.4. Before sampling, the sample groove (volume  $1.5\mu\ell$ ) in the sampling valve (Valco CV-6-UHPA-HC) was cleaned and filled with carbon disulfide ( $CS_2$ ). The valve was then rotated to the vent position and a very small amount of sample vented to remove the  $CS_2$  from the system. Then, with the valve in the load position a large volume of the phase to be sampled was displaced from one windowed cell to the other through the sample groove. Finally, the sample was allowed to relieve pressure into a  $50\mu\ell$  syringe which could stand pressures up to 1700 kPa (250 psi). Any hydrocarbons which condensed in the valve during blowdown were displaced into the sample syringe with  $CS_2$ . The nose valve on the syringe was then closed and the sample injected immediately into the gas chromatograph. Details of the chromatographic techniques used for  $CO_2$ -hydrocarbon mixtures are given in §2.3.

## 2.2 Displacement Apparatus

### Slim Tube, Core and Mixing Cell Configurations

Figure 2.5 is a schematic of the equipment used for high pressure displacements of oil from a tube, core, or mixing cell.

Slim tube studies were performed using a 12.2 m (40 ft.), 0.635 cm ( $\frac{1}{4}$  in.) ID stainless steel tube packed with 170-200 mesh glass beads. The slim tube had a pore volume of  $147.3\text{ cm}^3$  and a permeability of 5800 md. The packed tube was rolled into a 25.4 cm (10 in.) diameter coil, and installed in a temperature controlled water bath. In all slim tube displacements, the bead pack was first completely saturated with oil, then  $CO_2$  was injected into the top, and fluids were produced from the bottom of the coiled tube. Just prior to the start of  $CO_2$  injection, oil was displaced through the pack at the run displacement rate to establish a pressure gradient. Then,  $CO_2$  injection was started at the same rate. Pressure drop across the pack was recorded continuously. A capillary sight glass was installed at the outlet of the slim tube so that produced fluids could be observed. The amount of oil recovered was determined by weight rather than by less accurate volumetric measurements.

Core flood studies used a Berea sandstone core 5.1 cm (2 in.) in diameter and 75 cm (29.5 in.) long with a pore volume of  $283\text{ cm}^3$  and a permeability of 180 md. The core was coated with epoxy and mounted in a core holder. Overburden pressure of 16200 kPa (2350 psia) was maintained

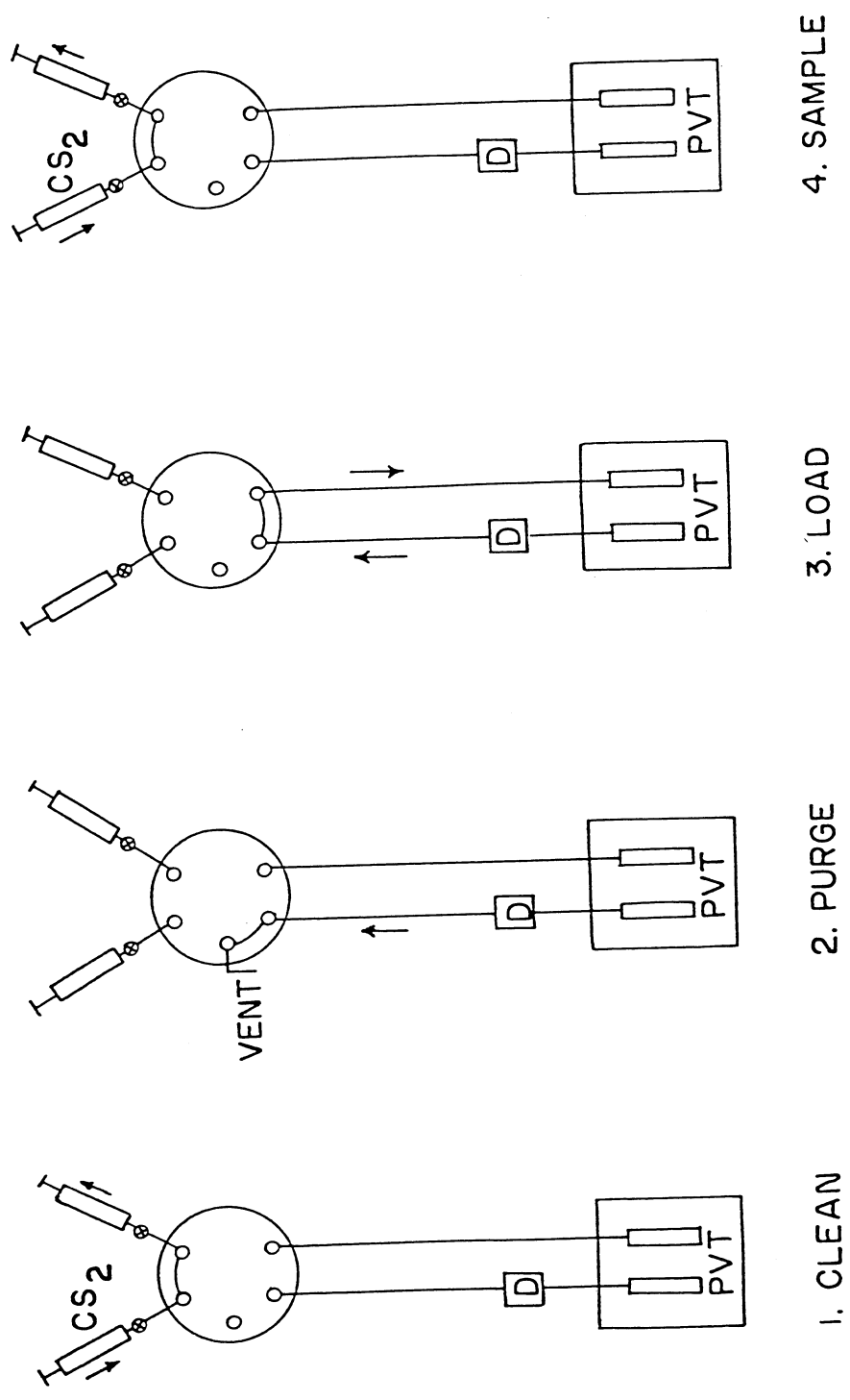


Figure 2.4 High pressure sampling system.

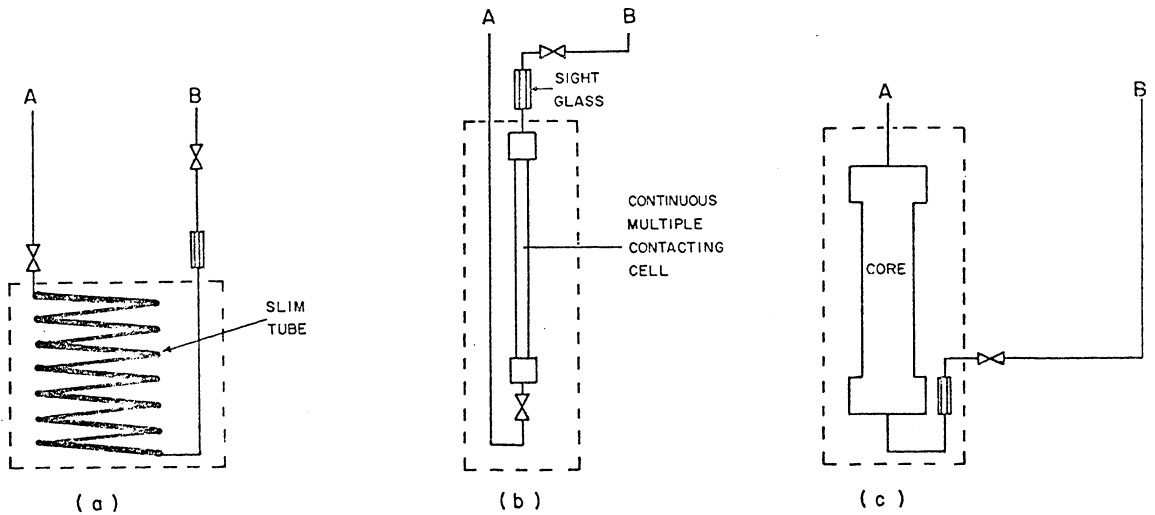
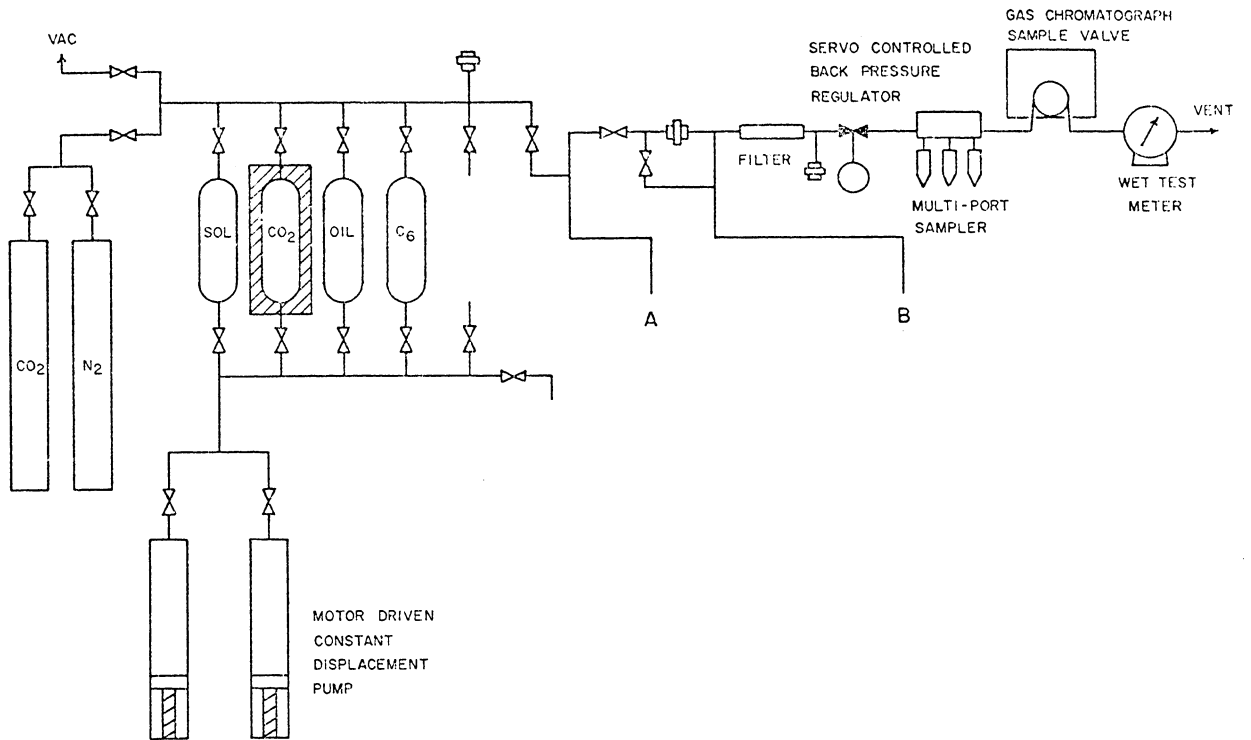


Figure 2.5 Apparatus for CO<sub>2</sub> displacements in a slim tube, core or mixing cell.

by ethylene glycol in the annulus between the core and the core holder. The core holder was wrapped with heating tape and covered with insulation. A platinum RTD temperature sensor was placed between the heating tape and the surface of the core holder. The temperature controller used held the temperature fluctuations at the surface of the core holder to within  $\pm 1^\circ\text{F}$ . Because the thermal mass of the core holder was large, the temperature variation within the core was substantially less than  $1^\circ\text{F}$ . In all core floods, the core was oriented vertically,  $\text{CO}_2$  was injected from the top, and fluids were produced from the bottom.

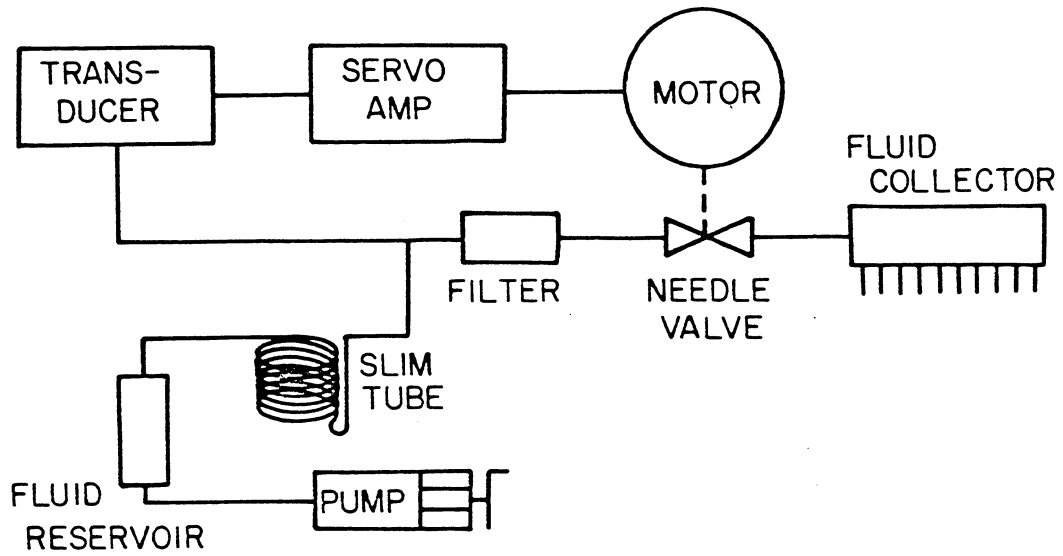
Two apparatus configurations were tested in mixing cell displacements. The first configuration used a  $55\text{ cm}^3$  Daniel sight gauge (not shown in Figure 2.4) installed in a temperature controlled ( $\pm 0.2^\circ\text{F}$ ) water bath. The cell was initially filled with oil,  $\text{CO}_2$  was injected slowly, and  $\text{CO}_2$ -hydrocarbon mixtures were produced from the top of the cell. The fluids in the cell were agitated only by the  $\text{CO}_2$  bubbling upward through the cell.

The second configuration used a 1.27 cm ID,  $66.8\text{ cm}^3$  stainless steel tube (shown in Figure 2.5). This same cell was used again in the continuous multiple contact system described below. The cell was wrapped with heating tape and insulation, and a temperature controller maintained the surface of the cell to within  $\pm 1^\circ\text{F}$  of the desired temperature. For the cell displacement tests reported in §3.1, the cell was filled initially with oil,  $\text{CO}_2$  was injected into the bottom of the cell, and  $\text{CO}_2$ -hydrocarbon mixtures were produced through a back pressure regulator with the separator system (see below). Again, cell contents were agitated only by bubbles of  $\text{CO}_2$  rising through the oil in the cell.

#### Fluid Production and Sample Collection System

Fluids from the displacement element of the apparatus (slim tube, core or mixing cell) were produced through a back pressure regulator into a multiport gas-liquid separator (see Figure 2.5). The back pressure regulator was designed to provide more precise pressure control at low flow rates ( $\sim 5\text{ cm}^3/\text{hr}$ ) than we were able to achieve with commercially available regulators. Figure 2.6a is a diagram of the servo back pressure regulator system. The servo back pressure regulator consists of a pressure transducer, servo amplifier, servo motor, and a fine metering valve in a servo loop with the transducer sensing system pressure at the slim tube output. The mechanical linkage between the motor and the metering valve is shown in Figure 2.6b. The servo amplifier (Figure 2.7) compares the transducer signal with an adjustable set point and produces a  $\pm 15\text{ VDC}$  signal that reverses polarity as required to drive the motor so that the valve continuously adjusts output flow. When the transducer signal is greater than the set point, the valve is driven in the open direction until the increase in flow reduces pressure at the transducer, and vice versa. As constructed, the servo back pressure regulator maintains back pressure at set point pressure  $\pm 1\text{ psi}$  for liquid flow down to  $1\text{ ml/hr}$  to a maximum back pressure of  $2000\text{ psi}$ . The back pressure limitation of  $2000\text{ psi}$  is dictated by the needle valve pressure limit. Currently a Nupro type SS-2SG is in use

a. Components



b. Mechanical linkage between valve and drive motor

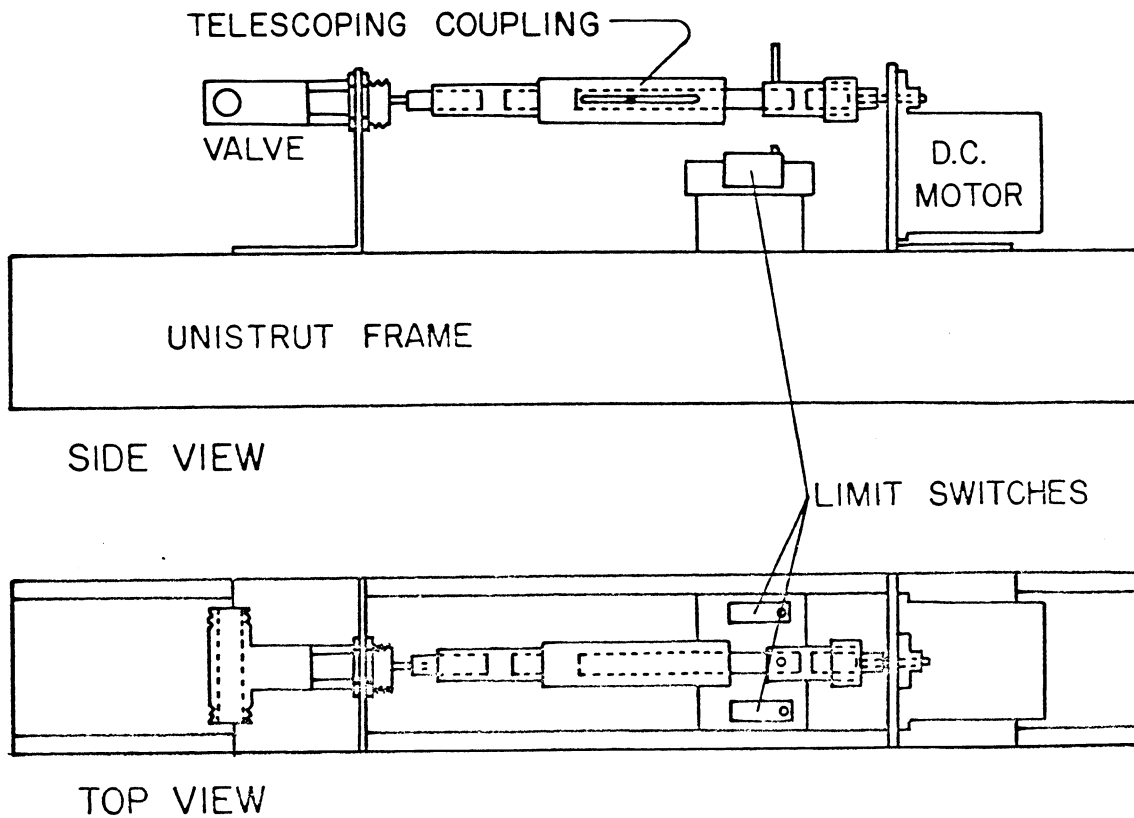


Figure 2.6 Servo-controlled back pressure regulator.

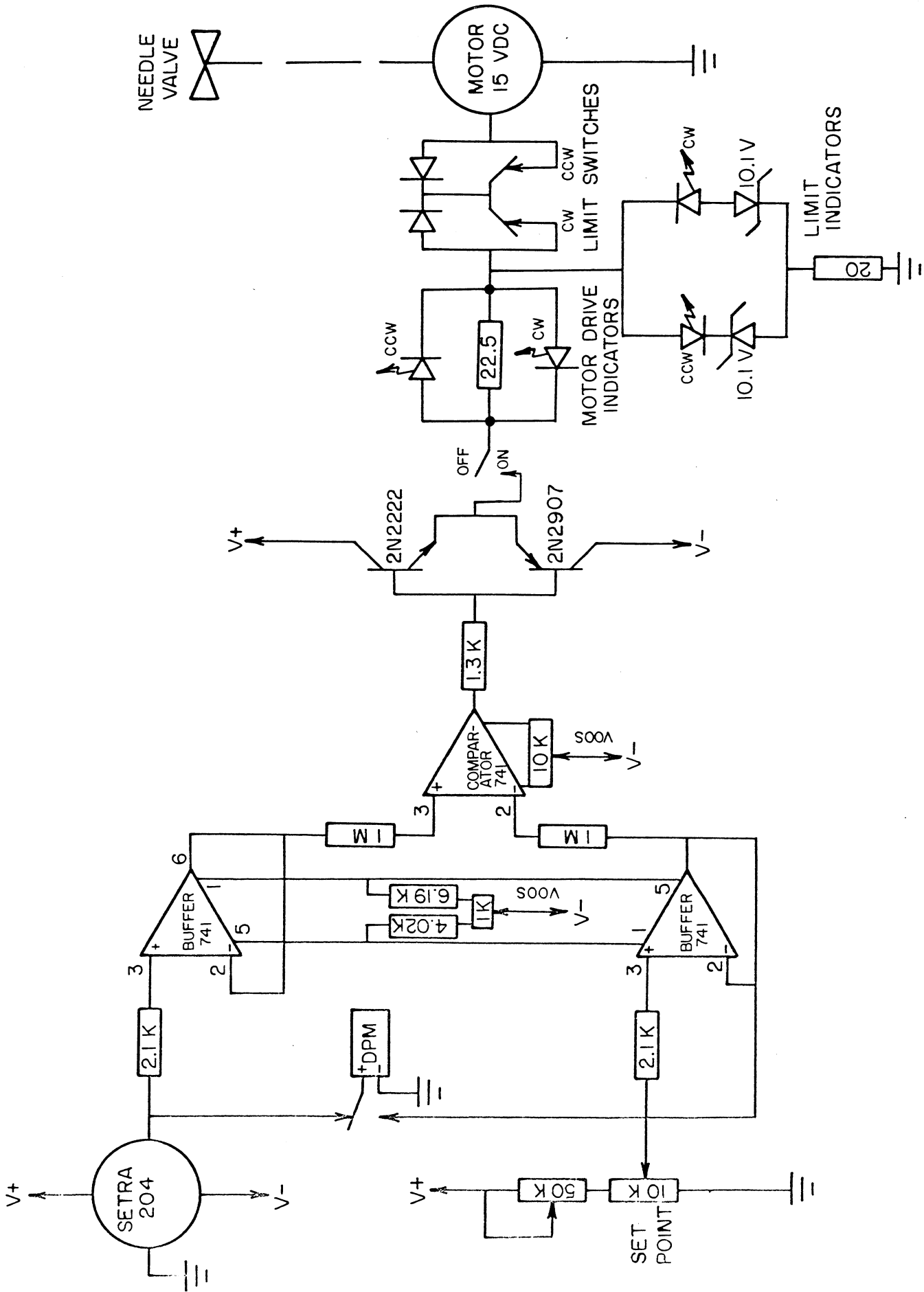


Figure 2.7 Servo amplifier for the back pressure regulator.

because it offers a 0.1 ml dead volume; Ideal-Aerosmith type P54-1-11 needle valve offers a pressure limit of 5000 psi at a sacrifice of approximately 1 ml dead volume.

Gas-liquid mixtures leaving the back pressure regulator were routed to an automatically switched 20 port sampling valve which then directed the produced fluids into one of a succession of centrifuge tubes. The liquid portion of the sample was retained in the centrifuge tube. Gases were vented from the sampling array through an automatic gas sampling valve in a Hewlett-Packard 5840A gas chromatograph and then through a recording wet test meter where produced gas volumes were measured. Produced gas compositions were determined on-line, but hydrocarbon liquid sample analyses, which take approximately one hour per sample, were performed after completion of the displacement test (see §2.3).

### Continuous Multiple Contact Apparatus

Experimental results from the static equilibrium PVT apparatus described in §2.1 are essential for understanding the relative importance of phase behavior, compositional effects on phase densities and viscosities, viscous fingering and other factors on local displacement efficiency. Unfortunately, such experiments are time consuming as well as expensive and hence, are not routinely performed. Figure 2.8 shows a schematic of an apparatus developed as part of this project to reduce the experimental effort required to measure equilibrium phase compositions. The experimental technique is similar to that described above for mixing cell displacements except that fluids are circulated in the cell to improve mixing and samples are taken simultaneously from both the top and bottom of the cell. It is substantially faster than static phase equilibrium experiments because it operates continuously rather than in discrete steps.

Results of continuous multiple contact (CMC) experiments are reported in §3.3. In those experiments, oil was loaded into a 1.27 cm ID, 66.8 cm<sup>3</sup> stainless steel mixing cell (identical to that described above). The contents of the cell were continuously mixed by circulating fluid from the top of the cell through a 0.076 cm (0.030 in.) ID external line into the bottom of the cell. A circulation rate of 160 cm<sup>3</sup>/hr was maintained by a Milton-Roy metering pump. CO<sub>2</sub> was injected into the circulating stream at a rate of 8 cm<sup>3</sup>/hr. The connections of the circulation line were designed to allow the ends of the line to protrude 1/2 in. into each end of the mixing cell. This configuration provides two small quiescent zones in which samples of upper and lower phases can accumulate and be continuously extracted. The production rate of lower phase samples was regulated by a Nupro SS-2SG fine metering valve which was set to allow lower phase production at about one quarter of the rate of injection of CO<sub>2</sub>. Upper phase samples were produced at the rate established by the back pressure regulator (described above).

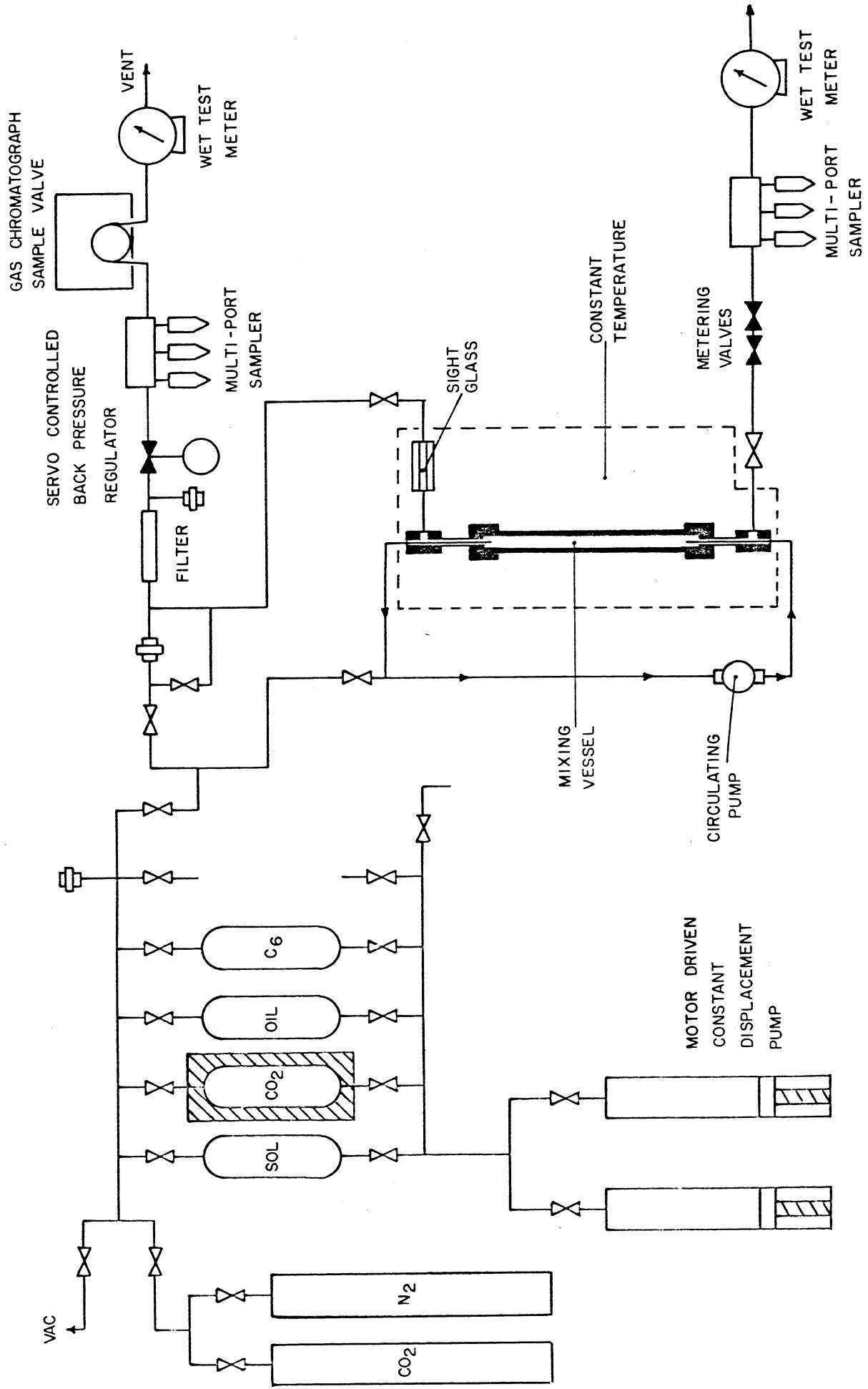


Figure 2.8 Apparatus for continuous measurement of equilibrium phase compositions for CO<sub>2</sub>-crude oil mixtures.

Gas and liquid samples were routed through parallel sample collection systems similar to that described above. Produced gases were analyzed on-line, and produced liquids were held for later analysis. Produced gas volumes were measured by separate wet test meters.

Experiments were performed with a ternary system of known phase behavior to demonstrate that the apparatus (shown in Figure 2.8) could be used to measure equilibrium phase compositions accurately. Figure 2.9 shows a comparison of the results of two CMC experiments with those of static equilibrium phase composition measurements. In the first experiment, a mixture of 79 vol % isopropanol (IPA) with 21 vol % brine (2 wt. %  $\text{CaCl}_2$ ) was displaced by isooctane (IC<sub>8</sub>). In the second, a 50-50 vol % mixture of brine and IC<sub>8</sub> was displaced by IPA. Figure 2.9 shows excellent agreement between results of static equilibrium and continuous multiple contact measurements for both tie line slopes and location of the binodal curve. The small differences in lower phase compositions were probably the result of evaporation of IC<sub>8</sub> from small lower phase samples.

The displacement of the 79-21 vol % IPA-brine mixture was a stringent test of the apparatus and experimental technique, because the first two phase mixtures which occurred as IC<sub>8</sub> was injected had interfacial tensions less than 0.1 dynes/cm. At the circulation rates used, the entire central portion of the mixing cell was filled with a very finely divided suspension of the two phases in each other. Nevertheless, there was no evidence of contamination of either upper or lower phase samples with the other phase. Thus, the design of the circulation and sampling system shown in Figure 2.8 successfully provided good mixing between phases and representative phase samples.

### 2.3 Chemical Analysis of CO<sub>2</sub>-Hydrocarbon Mixtures

Most phase composition analyses reported for CO<sub>2</sub>-crude oil mixtures do not resolve components heavier than heptanes (C<sub>7</sub>), because standard low temperature fractional distillation techniques analyze only out to "heptanes-plus" (C<sub>7+</sub>) with extensions to "undecanes-plus" (C<sub>11+</sub>) possible without too much difficulty. Nevertheless, where more detailed analyses have been reported (Gardner et al. 1979, Simon et al. 1977, Orr et al. 1980a) experimental results clearly indicate that, under appropriate conditions of temperature, pressure and composition, CO<sub>2</sub> can extract hydrocarbons at least as heavy as eicosane (C<sub>20</sub>). In fact, results from recent studies (Orr et al. 1980b, 1981) show that CO<sub>2</sub> can extract substantial quantities of hydrocarbons as heavy as C<sub>35</sub> from crude oil. It appears, therefore, that the traditional definition of intermediates as C<sub>2</sub>-C<sub>6</sub> hydrocarbons is not consistent with the extractive power of high pressure CO<sub>2</sub>. It is clear that analytical techniques which provide better resolution of hydrocarbons heavier than C<sub>11</sub> would help to improve understanding of the role of component partitioning in the generation of miscibility, would aid in the choice of pseudo-components for process simulation, and may be

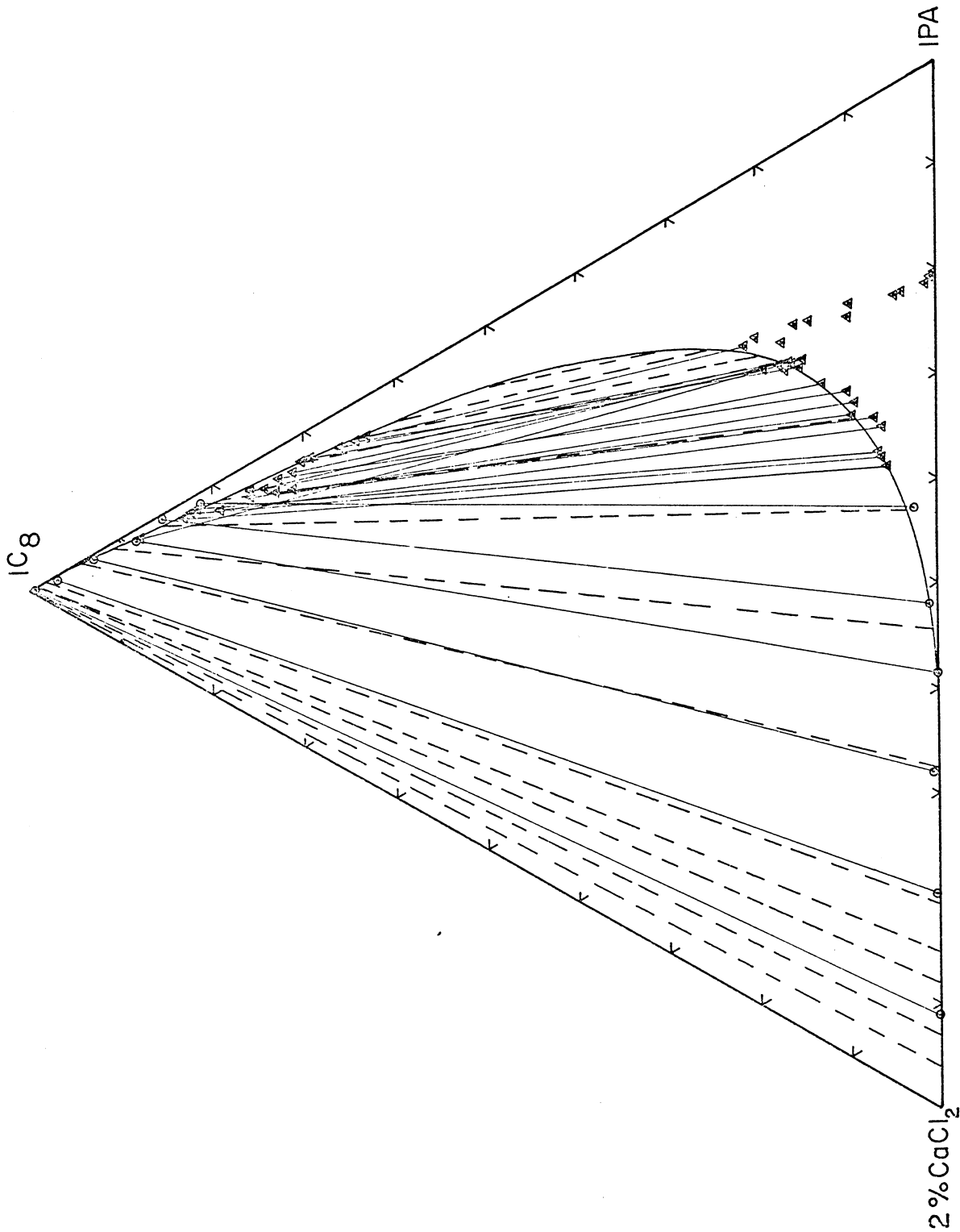


Figure 2.9 Comparison of phase compositions determined at 24°C by static equilibrium (dashed tie lines) and by continuous multiple contact experiments (solid tie lines). Circular points indicate data from displacements of 79 vol % isopropanol (IPA) - 21 vol % brine (2 wt. % CaCl<sub>2</sub>) by isooctane (IC8). Triangular points are data from displacement of 50 vol % brine - 50 vol % IC8 by IPA.

necessary for adequate representation of phase behavior with an equation of state (Fussell 1977). Fortunately, chromatographic techniques have developed to the point that good resolution can be obtained for hydrocarbons lighter than about C<sub>40</sub>. Chromatography requires only small samples, offers better precision and repeatability than low temperature fractional distillation, and is much less time consuming. Described below are the chromatographic techniques used for three types of samples analyzed in this project:

- (1) Liquid hydrocarbon samples
- (2) High pressure CO<sub>2</sub>-crude oil mixtures
- (3) Produced gas samples

Samples of hydrocarbon liquids at atmospheric pressure were analyzed according to a proposed ASTM method (1976) which estimates the boiling range of the sample as well as the percentage of hydrocarbons heavier than the limit of the analysis. High pressure samples of CO<sub>2</sub>-crude oil mixtures were analyzed by a method similar to the ASTM method except that light ends (CO<sub>2</sub>, methane through butane) were included in the analysis while the amount of hydrocarbons heavier than C<sub>36</sub> was not determined. Produced gas samples were analyzed by straightforward methods.

#### Equipment

Figure 2.10 shows a schematic of the gas chromatograph and associated equipment. The instrument used was a Hewlett-Packard 5840A gas chromatograph equipped with dual thermal conductivity (TCD) and flame ionization (FID) detectors, and with an automatic gas sampling valve. The TCD and FID were connected in series so that the TCD could be used to detect CO<sub>2</sub> and light hydrocarbons (C<sub>1</sub>-C<sub>4</sub>) and the more sensitive FID used to detect hydrocarbons C<sub>5</sub> and heavier present in CO<sub>2</sub>-crude oil mixtures.

Columns and operating conditions used for the three types of analyses are listed in Table 2.1. Low pressure gas mixtures of CO<sub>2</sub> and light hydrocarbons were analyzed on a 6 ft. x 1/8 in. Porapak Q column. A 10 ft. x 1/8 in. OV-101 column was used for analyses of both high pressure CO<sub>2</sub>-crude oil mixtures and atmospheric pressure hydrocarbon liquid samples. Separations of CO<sub>2</sub> and the C<sub>1</sub>-C<sub>4</sub> hydrocarbons present in high pressure samples were made by starting the analysis at an oven temperature of -65°C. Thus, the analysis was performed on a single column without the use of column switching or backflush valves. It is important to avoid the use of valves in the oven, if possible, because the high temperature limit for valves currently available is much lower than the oven temperature required to elute the heavy hydrocarbons present in a crude oil. The technique used has the advantage of being less expensive as well. The price paid for the simplicity of the analysis is that the separation of the light ends

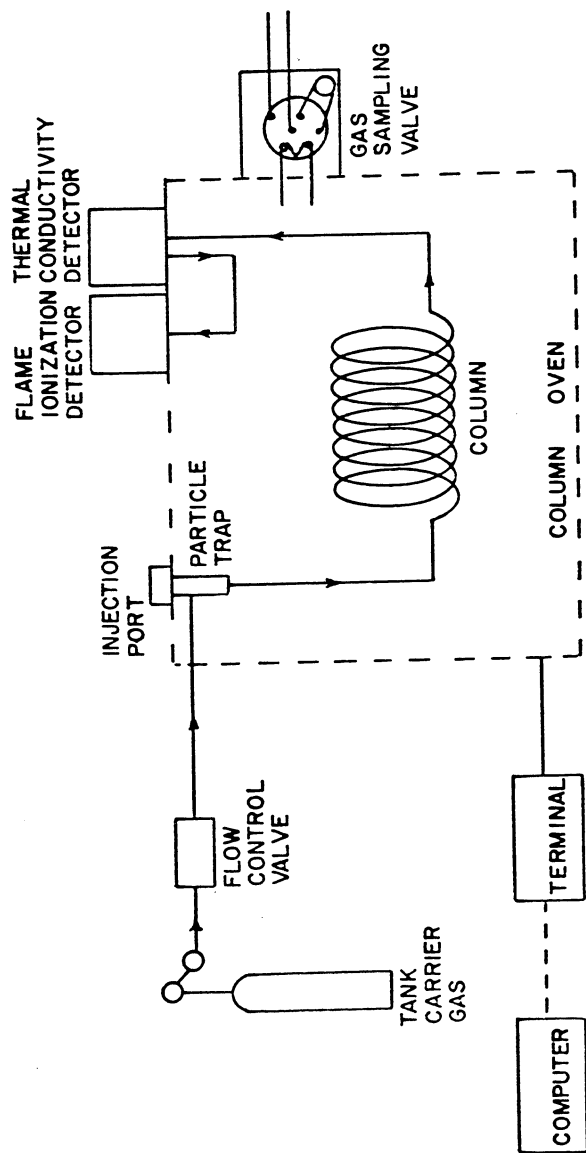


Figure 2.10 Gas chromatography equipment.

Table 2.1 Gas Chromatograph Operating Conditions

<u>Mixture</u>	<u>Column</u>	<u>Temperature</u>		<u>Column</u>	<u>Sample Size</u>
		<u>Injection Port</u>	<u>Detector</u>		
CO <sub>2</sub> -light hydrocarbon (C <sub>1</sub> ~ C <sub>7</sub> )	1/8" x 6' Porapak Q 80/100 mesh	250°C	250°C (TCD)	60°C 2 min. hold to 250°C at 30°C/min. rate 5 min. final hold	0.5 ml
High Pressure CO <sub>2</sub> + Crude Oil	1/8" x 10' 10% OV-101 on 80/100 m chromosorb W-HP	370°C	370°C (TCD) 380°C (FID)	-65°C 1 min. hold 30°C/min. rate for 4 min., then at 15°C/min. rate Final temp. 370°C 5 min. final hold	1 µl
Crude Oil	1/8" x 10' 10% OV-101 on 80/100 m chromosorb W-HP	370°C	370°C (TCD) 380°C (FID)	0°C 1 min. hold to 370°C at 15°C/min. rate 5 min. final hold	1 µl

is not as efficient as could be achieved with other columns at higher temperatures. Because the silicone rubber liquid phase in the OV-101 column solidifies at some temperature above  $-65^{\circ}\text{C}$ , some tailing of the light end peaks occurs. Nevertheless, the advantages of a single column analysis far outweigh the disadvantages.

Analysis of low pressure liquid hydrocarbon samples (simulated distillation) required some processing of the raw area percent data for each run (see below). To avoid manual data entry of the several hundred lines of data from each run, the gas chromatograph was interfaced with a Hewlett-Packard 2645A computer terminal with which run data were recorded on tape cartridges. The terminal was then used to transfer the run data to a Digital Equipment DEC-20/50 for processing.

### Analysis of Hydrocarbon Liquid Samples

The principal difficulty encountered in the analysis of crude oil samples is estimation of the amount of hydrocarbons present which are heavier than those eluted from the column at its maximum operating temperature. One technique for making such estimates is given by a proposed ASTM test method for analysis of crude oils (1976). The method requires that two runs be performed for each sample, one in which a mixture of sample plus an internal standard is injected (Run A), and another in which only the sample is injected (Run B). Typical results of two such runs are shown in Figure 2.11. The estimate of the amount not eluted is calculated by comparing the areas of the chromatograms for the two runs. Let  $A_{IS}$  be the area of the segment which contains the internal standard in the chromatogram for Run A (see Figure 2.11). If  $A$  is the total area for that run, then the ratio of the areas of the internal standard segment to the remaining area is

$$R_{IS} = \frac{A_{IS}}{A - A_{IS}} \quad (2.1)$$

Because the total areas of the two runs may not be the same (due to small differences in injected sample sizes), an estimate of the area of the internal standard which would have resulted had the amount injected in Run A been identical to that in Run B is

$$C_{IS} = R_{IS} (B - B_{IS}) \quad (2.2)$$

where  $B$  is the total area of Run B and  $B_{IS}$  is the area of the internal standard segment of Run B. Thus, the area of the internal standard is

$$D_{IS} = C_{IS} - B_{IS} \quad (2.3)$$

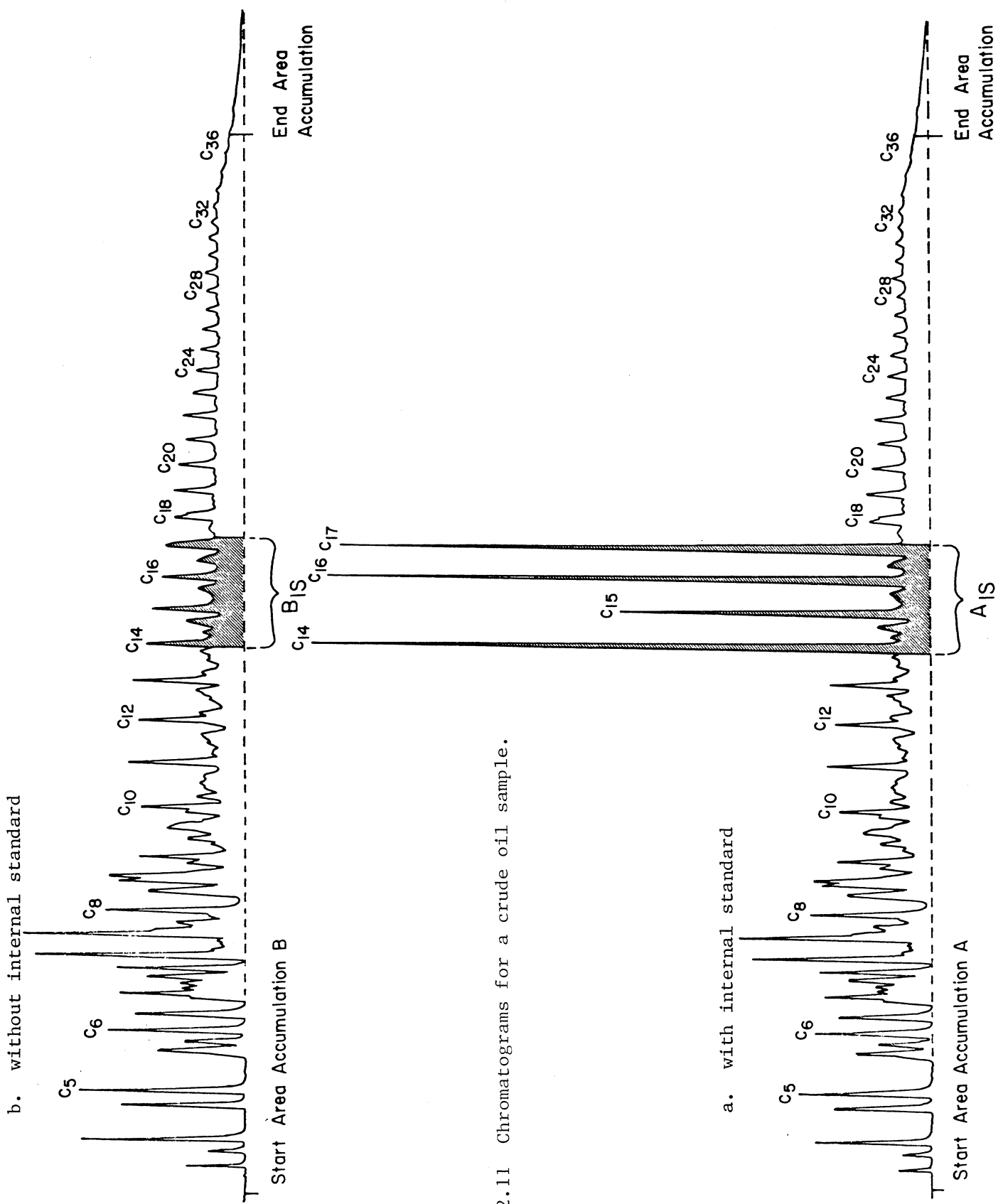


Figure 2.11 Chromatograms for a crude oil sample.

Now, if area is proportional to the weight of sample injected (for a flame ionization detector) then the ratio of the area of the internal standard to the area of the hydrocarbon sample is

$$\frac{D_{IS}}{T} = \frac{W}{1 - W} \quad (2.4)$$

where  $W$  is the weight fraction of the internal standard in sample A, and  $T$  is the total theoretical area of the hydrocarbon sample. Thus, the estimate of the total area of the crude chromatogram had all components been eluted is

$$T = \frac{D_{IS}(1-W)}{W} = \left\{ \frac{A_{IS}}{(A-A_{IS})} (B-B_{IS}) - B_{IS} \right\} \frac{(1-W)}{W} \quad (2.5)$$

and the weight fraction of heavy components not eluted is

$$W_H = 1 - \frac{B}{T} \quad (2.6)$$

The column used for crude oil analyses separates hydrocarbons, approximately at least, in boiling point order. Carbon number cuts were determined on the assumption that the normal alkane of a given carbon number eluted last. Thus, hydrocarbons with retention times between those of  $C_n$  and  $C_{n+1}$  were assumed to be  $C_{n+1}$ . The molecular weight of the normal alkane was used as an estimate of the molecular weight for each carbon number cut.

Inherent in the proposed ASTM method is the assumption that response factors are independent of sample size and the carbon number of the hydrocarbon. That assumption implies that in a given chromatogram, the area of a particular peak reflects the weight percent (for a flame ionization detector) or volume percent (for a thermal conductivity detector) of that component in the sample. To test this assumption, a check of response factors was carried out for various hydrocarbons.

In the first series of tests, different sample sizes of  $nC_6$  were injected and a response factor was calculated using  $R_i = W_i/A_i$  where  $R_i$  is the response factor for component  $i$ ,  $W_i$  the weight of sample injected, and  $A_i$  the area of the peak. The sample size was carefully measured by pulling the plunger back to draw the sample out of the needle and into the syringe barrel. After the sample was injected, the amount of sample left in the needle was measured by the same technique. The weight of the sample injected was calculated from the actual volume of the sample injected.

Results of isothermal runs using a 10 ft. x 1/8 in. OV-101 column with the oven at 69°C, and the flame ionization detector (FID) at three temperatures are shown in Figure 2.12. The measured response factors showed essentially no dependence on sample size, and detector temperature. The results shown in Figure 2.12 indicate that detector response is very nearly linear for the amounts of hydrocarbons to be injected during analysis of crude oil samples or of CO<sub>2</sub>-crude oil mixtures. The scatter in the data is evidence of the difficulty of measuring accurately the very small volumes injected.

The second series of tests investigated the variation of response factors with molecular size. Response factors were measured by the technique described above for normal alkanes ranging from C<sub>5</sub> to C<sub>40</sub>. The analyses were performed with the FID at 380°C. The oven temperature was set to the temperature at which the hydrocarbon would elute when using the proposed ASTM method. Figure 2.13 presents results of the response factor determinations for normal alkanes from C<sub>5</sub> to C<sub>40</sub>. Response factors do increase slightly with increasing carbon number, but the difference is only slightly greater than the scatter inherent in the measurement. Furthermore, crude oils are not mixtures of normal alkanes, so a slight correction for molecular size does not appear warranted unless a much more detailed investigation of response factors for crude oil constituents is undertaken. Thus, the assumption of equal response factors for all hydrocarbon components appears reasonable, though not exact.

Results of an analysis of crude oil from the Maljamar field (Lea County, New Mexico) are compared with results of an ASTM D1160 true boiling point distillation in Figure 2.14. As expected the distillation results show more scatter than the chromatography results but overall, the agreement is good. Similar chromatographic analyses were obtained for liquid samples collected during slim tube, core and continuous multiple contact displacements.

The analysis scheme described here provides much better definition of hydrocarbons in the range C<sub>11</sub>-C<sub>36</sub> than distillation methods, but it does not attempt to separate every component present in a crude oil. Even more detailed separations could be obtained on a capillary column, for instance, but the amount of data collected for each sample would be very large. The technique used here is a reasonable compromise in that it provides good resolution of hydrocarbons out to about C<sub>36</sub> but does not produce unmanageable amounts of data.

#### Analysis of High Pressure CO<sub>2</sub>-Crude Oil Mixtures

The analysis scheme for liquid samples was not used for high pressure samples because it is difficult to add internal standards to very small high pressure samples, especially with the accuracy needed to quantitatively determine the amount of heavy ends, and because the assumption that

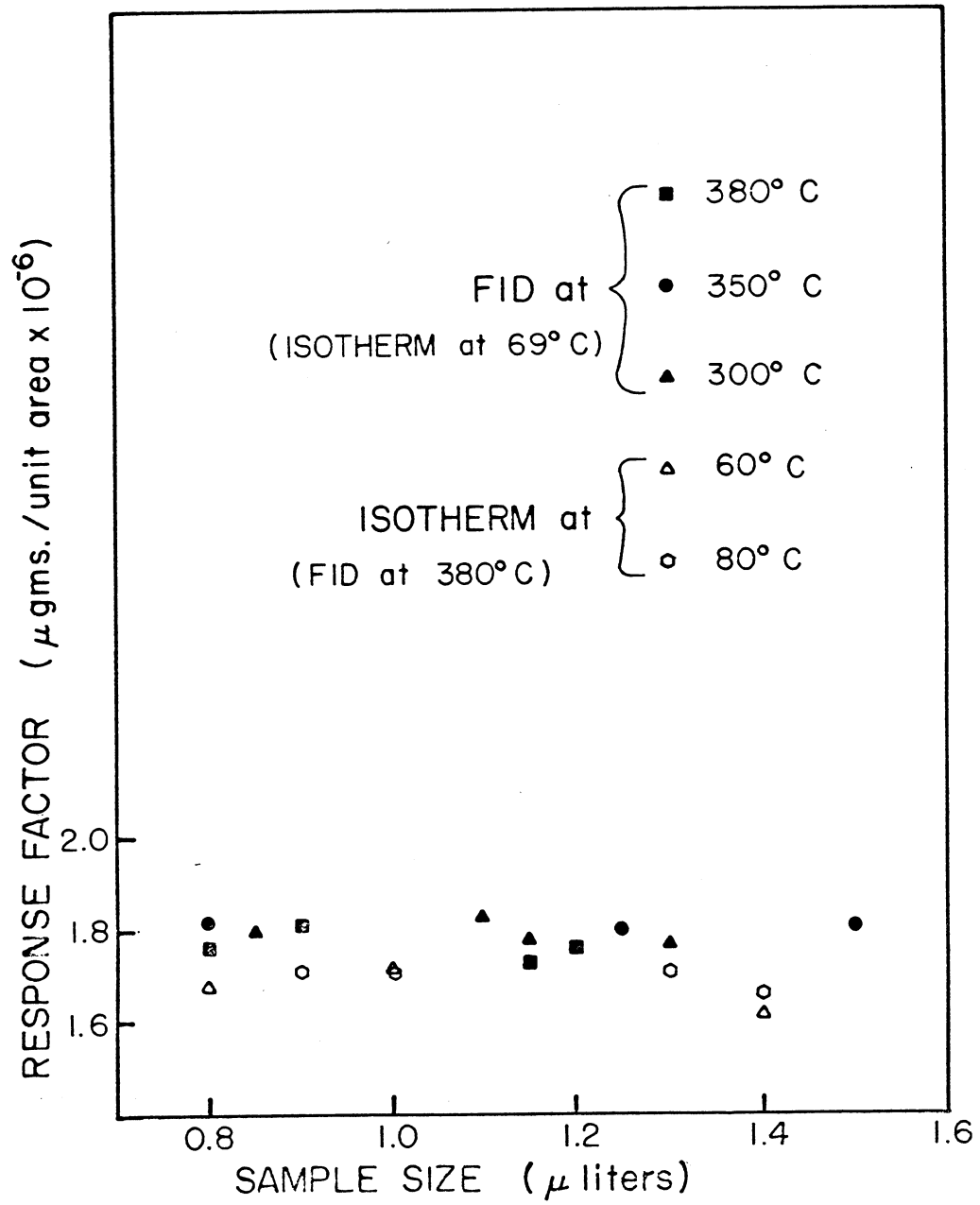


Figure 2.12 Effect of sample size on hydrocarbon response factors.

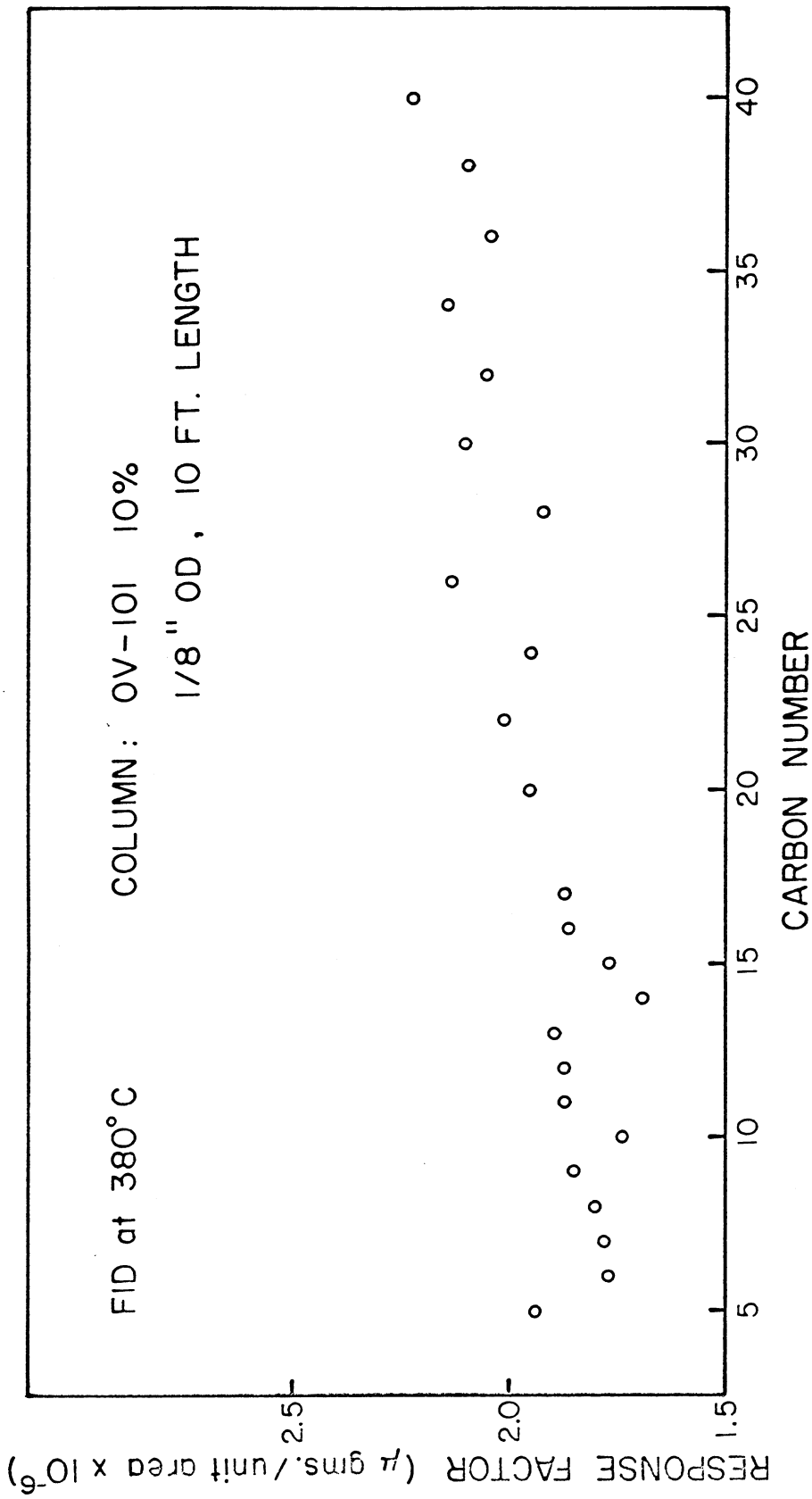


Figure 2.13 Effect of molecular size on hydrocarbon response factors.

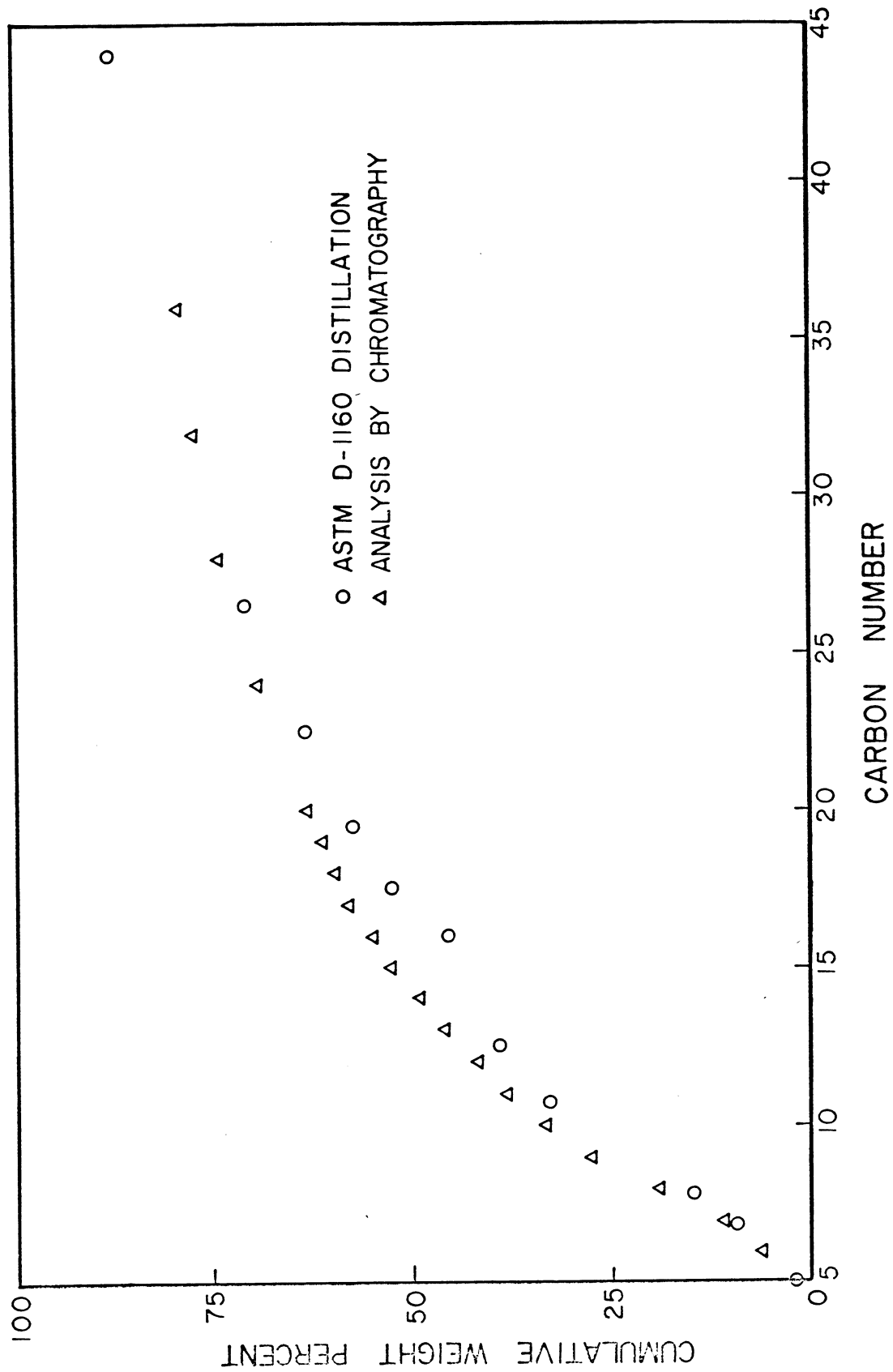


Figure 2.14 Comparison of analyses of Maljamar separator oil by gas chromatography and by true boiling point distillation.

response factors are equal for all components is not satisfied, even approximately, when CO<sub>2</sub> and C<sub>1</sub>-C<sub>4</sub> hydrocarbons are present. Therefore, high pressure sample analyses included only components which actually eluted from the column. No attempt was made to estimate amounts of hydrocarbons not eluted.

As indicated in Table 2.1, high pressure samples were analyzed on the same OV-101 column used for low pressure liquid samples. The lightest components CO<sub>2</sub>, C<sub>1</sub>, and C<sub>2</sub> were separated by starting the analysis at a very low temperature (-65°C), thereby immobilizing heavier hydrocarbons while the light gases eluted. A thermal conductivity detector was used to detect CO<sub>2</sub> and hydrocarbons C<sub>1</sub>-C<sub>4</sub> because CO<sub>2</sub> is not detected by a flame ionization detector. Hydrocarbons heavier than C<sub>4</sub> were detected with the FID plumbed in series with the TCD.

Calibration mixtures containing CO<sub>2</sub> and hydrocarbons C<sub>1</sub>-C<sub>35</sub> are not available. Therefore, the following sequence of calibration analyses was performed. Mixtures of known composition of CO<sub>2</sub>, C<sub>1</sub> and a synthetic oil composed of C<sub>5</sub>, C<sub>10</sub>, C<sub>16</sub> and C<sub>30</sub> were made in the PVT apparatus. High pressure samples were then used to obtain response factors for CO<sub>2</sub> and C<sub>1</sub> which were consistent with previously determined response factors for the heavier hydrocarbons. Then, response factors for C<sub>2</sub>-C<sub>4</sub> were obtained by analyzing gas mixtures containing CO<sub>2</sub>, C<sub>1</sub> and C<sub>2</sub>-C<sub>4</sub> hydrocarbons.

The sampling and analysis scheme for high pressure CO<sub>2</sub>-hydrocarbon mixtures was tested with a variety of mixtures of CO<sub>2</sub> with well-characterized hydrocarbon mixtures. Details of the results of those experiments are given in Appendix B. The procedure used worked well for the well-characterized mixtures, producing consistent composition data for liquid-liquid-vapor mixtures of known overall composition. It was less successful for CO<sub>2</sub>-crude oil mixtures. Substantial scatter was observed in compositions determined from high pressure samples. Reasons for the additional scatter are still under investigation.

#### Analysis of Produced Gas Samples

Because repeatable and reliable high pressure samples are difficult to obtain and because the technique described above does not provide an estimate of amounts of heavy ends not eluted, we believe that the technique used to analyze displacement test fluid samples offers a more accurate method for analyzing high pressure mixtures provided large sample sizes can be tolerated. In that method, produced gas was separated from produced liquid at atmospheric pressure. Gas samples were routed through a sampling valve controlled by the gas chromatograph which injected a 0.5 cm<sup>3</sup> gas sample at timed intervals. The analysis was performed on a Porapak Q column with the operating conditions given in Table 2.1. Volumes of produced gas were measured with a wet test meter. Liquid samples were weighed and then

analyzed by the proposed ASTM method described above. Finally, the overall composition of the produced fluid was calculated from the amounts and compositions of gas and liquid. The method has the disadvantage that two analyses are required, so that there are two sources of error, but it has the advantage that sampling is straightforward and calibrations for the analyses are simpler.

#### 2.4 Task 1: Summary and Conclusions

High pressure equipment for a variety of measurements to evaluate CO<sub>2</sub> flood behavior has been designed, constructed and tested. New equipment and techniques have been developed to:

- (1) sample high pressure mixtures
- (2) analyze high pressure CO<sub>2</sub>-crude oil mixtures by gas chromatography
- (3) control back pressure at low flow rates
- (4) measure equilibrium phase compositions in a continuous experiment.

The development of the continuous multiple contact experiment is particularly important because it is a much more efficient technique for measurement of phase behavior data needed to support compositional reservoir simulations and because it offers the potential, with further development, of simultaneous measurements of phase compositions, densities and viscosities. Better measurements of phase behavior and fluid properties are an important step toward improved correlations for reservoir simulation, better understanding of CO<sub>2</sub>-crude oil displacement mechanisms and better understanding of the roles and interactions of phase behavior, gravity segregation and viscous fingering.

### 3. TASK 2. DISPLACEMENT EXPERIMENTS

Interpretation of CO<sub>2</sub> displacement tests is complicated by the variety of factors which operate even in the simplest of flow geometries. Because different displacement mechanisms may produce results which are qualitatively similar, core flood and slim tube displacement results must be interpreted carefully if the details of the displacement mechanisms are to be correctly identified. For instance, unfavorable phase behavior, high levels of dispersion and viscous fingering can all act to broaden a transition zone between oil and CO<sub>2</sub>. Because the three effects scale differently, it is important to understand which of the effects dominates in a particular laboratory displacement. In this section, results of seven CO<sub>2</sub> displacements are compared. The results shed some light on the roles of phase behavior and mixing in CO<sub>2</sub> displacements.

#### 3.1 Slim Tube Displacement Results

Results of four displacements of separator oil from the Maljamar field (Lea County, New Mexico) from a slim tube are shown in Figure 3.1. Properties of the oil are given in Table 3.1. The displacements were performed at 32.2°C (90°F) at four pressures: 5520, 6890, 8270 and 9650 kPa (800, 1000, 1200 and 1400 psi). In each displacement, the slim tube was filled with oil at the displacement pressure. Just prior to the start of CO<sub>2</sub> injection, oil was displaced through the pack at the run displacement rate (5 cm<sup>3</sup>/hr) to establish a pressure gradient. Then, CO<sub>2</sub> was injected continuously until the test was terminated.

The scales used to plot Figure 3.1 deserve some comment. The time scale is presented as pore volumes of CO<sub>2</sub> are injected. Because the run temperature was very near the critical temperature of CO<sub>2</sub>, the density of CO<sub>2</sub> was sensitive to the change in pressure gradient which occurred as low viscosity CO<sub>2</sub> replaced high viscosity oil. The volume of CO<sub>2</sub> injected at a point during the run was calculated as the volume of mercury injected into the thermostated CO<sub>2</sub> supply vessel plus the expansion of the total volume of CO<sub>2</sub> in the system to the inlet pressure at that point. Overall pressure drops for each of the four displacements are given in Figure 3.2. The fraction of oil recovered was determined by weight, which could be measured more accurately than volumes of produced liquids.

It is clear from Figure 3.1 that the volume of CO<sub>2</sub> calculated as described above is not an accurate measure of the actual volume of oil displaced in the displacements at 5520 and 6890 kPa (800 and 1000 psi). In those displacements, the amount of oil recovered early in the runs was significantly less than the apparent volume injected, and in both runs CO<sub>2</sub> breakthrough occurred at an apparent injection of more than one pore volume. The explanation for the observed behavior lies in the interplay of the solubility of CO<sub>2</sub> in the oil, volume change on mixing, and the effect of

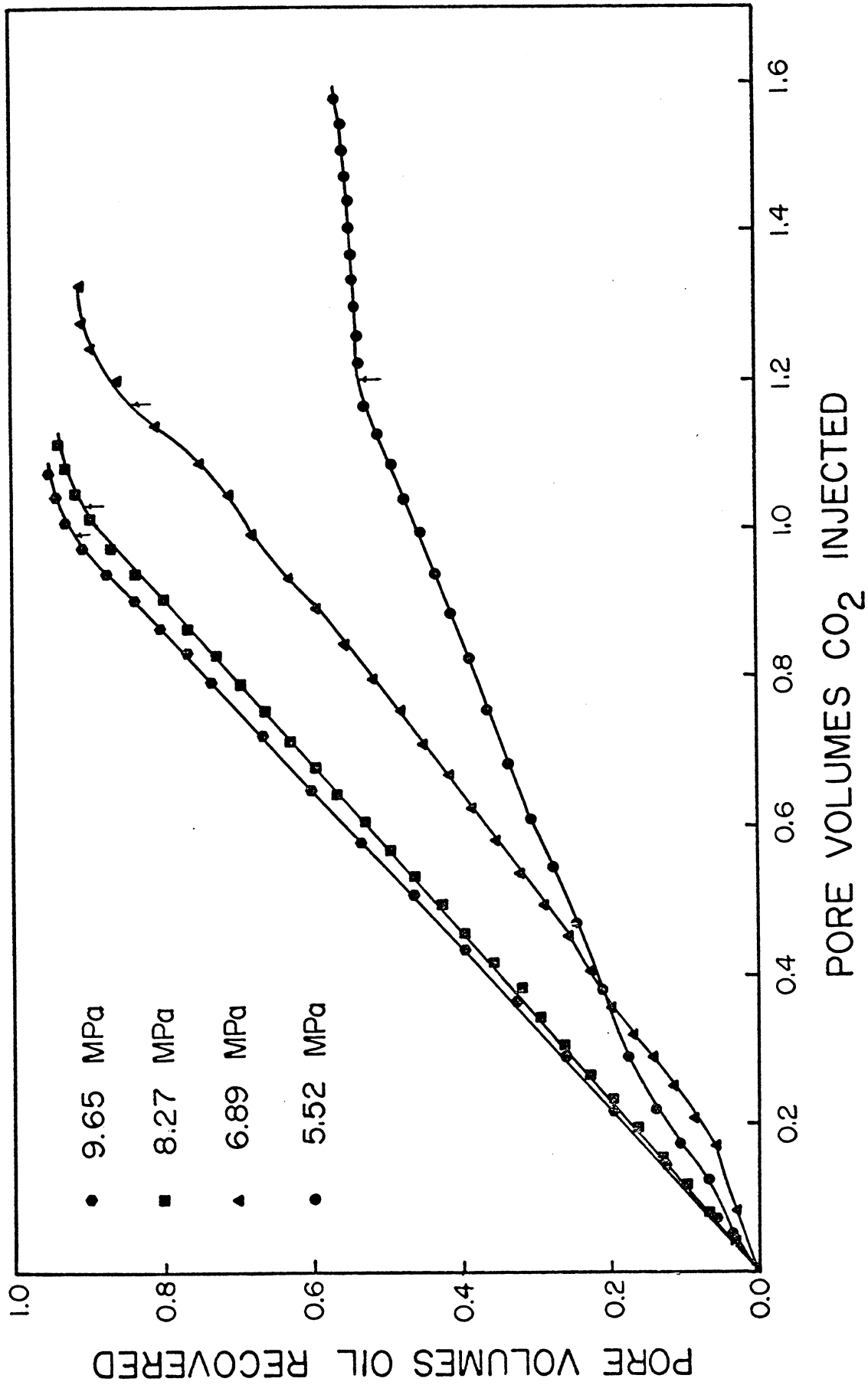


Figure 3.1 Recovery of Maljamar separator oil from slim tubes by continuous displacement with CO<sub>2</sub> at 32.2°C (90°F). Arrows indicate CO<sub>2</sub> breakthrough.

Table 3.1 Properties of Maljamar Separator Oil  
at Atmospheric Pressure

Density (15.6°C)	0.8294 g/cm <sup>3</sup>
Viscosity (34.4°C)	2.8 mPa·s
Molecular Weight	183.7
Molecular Weight of C <sub>7+</sub> *	199.3
Density of C <sub>7+</sub> (15.6°C)*	0.8441 g/cm <sup>3</sup>

\* Calculated from measured values of molecular weight and density and oil composition.

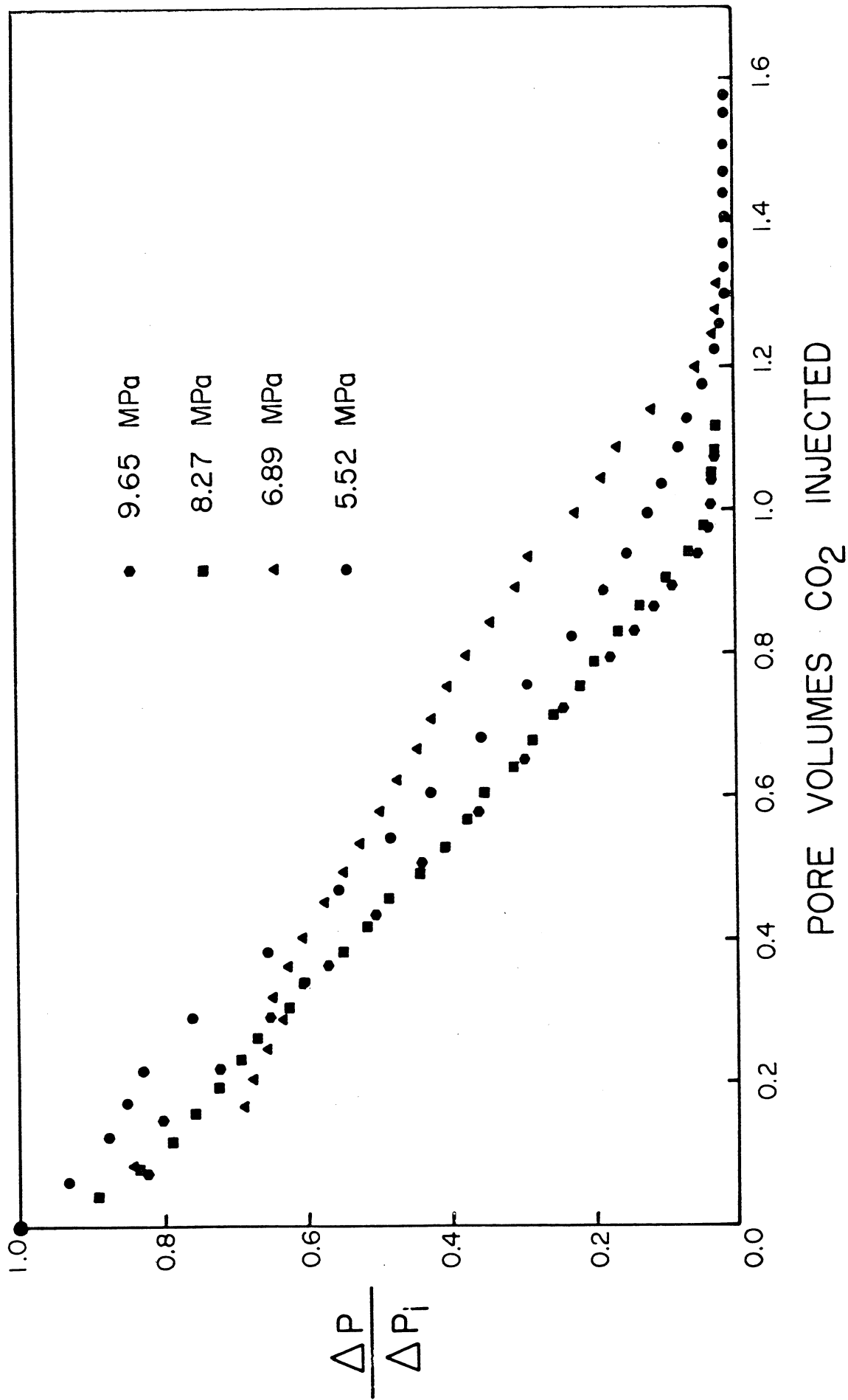


Figure 3.2 Pressure drops (normalized by the initial pressure drop) during slim tube displacements.

component partitioning on displacement efficiency. In the displacement at the lowest pressures, little extraction of hydrocarbons by CO<sub>2</sub> occurred. Consequently, the displacement was immiscible, the local displacement efficiency was low and a large residual saturation was left behind. For instance, at 5520 kPa (800 psi), almost 50 percent of the oil was left in the bead pack at CO<sub>2</sub> breakthrough. That oil was saturated with CO<sub>2</sub>, however, and since the quantity of oil left behind was large, the amount of CO<sub>2</sub> required to saturate it was also large. The apparent density of CO<sub>2</sub> dissolved in the oil (defined as the mass of CO<sub>2</sub> dissolved divided by the volume increase of the swollen oil over original oil) is, however, much higher than the density of pure CO<sub>2</sub> at the same pressure. Thus, the effect of the volume change of CO<sub>2</sub> upon dissolution in the oil is to reduce the effective volume of CO<sub>2</sub> injected. Table 3.2 summarizes results of PVT measurements of the solubility of CO<sub>2</sub> in Maljamar separator oil and compares the apparent density of the CO<sub>2</sub> in the oil with the density of pure CO<sub>2</sub>. Table 3.3 shows results of calculations of the effective volume of CO<sub>2</sub> injected at breakthrough when effects of volume change on mixing are included. In Table 3.3, the pore volumes of CO<sub>2</sub> injected were calculated (as in Figure 3.1) from the injection rate and the density of pure CO<sub>2</sub> at the injection pressure. The volume occupied by CO<sub>2</sub> in solution in the oil was calculated from the PVT data for the mole fraction of CO<sub>2</sub> in the saturated oil and the corresponding swelling factor given in Table 3.2. The total volume change on mixing was calculated as the difference between the volume which would have been occupied by the CO<sub>2</sub> dissolved in the oil had that CO<sub>2</sub> been segregated from the oil minus the volume actually occupied by the dissolved CO<sub>2</sub>. The effective volume of CO<sub>2</sub> injected, then, was estimated as the total volume injected minus the volume change on mixing. The effective CO<sub>2</sub> volume injected should match the volume of oil produced at breakthrough. While the agreement is not exact, the results shown in Table 3.3 indicate clearly that the combination of poor local displacement efficiency with the volume decrease of dissolved CO<sub>2</sub> accounts for the fact that CO<sub>2</sub> breakthrough occurred at apparent injection volumes exceeding one pore volume in the low pressure displacements.

The displacements at 8270 and 9650 kPa (1200 and 1400 psi) were affected much less by volume change on mixing for two reasons. First, the density of pure CO<sub>2</sub> was much nearer the apparent density of CO<sub>2</sub> in solution so that there was much less volume change on mixing. Second, the local displacement efficiency was much higher, and hence there was much less oil remaining to be saturated with CO<sub>2</sub>. Hence, the corrections for volume change on mixing were much smaller at the higher pressures.

Figure 3.3 summarizes oil recovery data for the four displacements. As Figure 3.3b indicates, the "minimum miscibility pressure" was approximately 8000 kPa (1160 psi) which agrees nicely with a prediction made previously (Orr, Yu and Lien 1980) with the one-dimensional simulator developed as part of this project (see §4) and with a range of 7580-7930 kPa (1100-1150 psi) observed by Yellig and Metcalfe (1980) for a West Texas oil of similar composition at 35°C.

Table 3.2 Solubility of CO<sub>2</sub> in Maljamar Separator  
Oil at 32.2°C

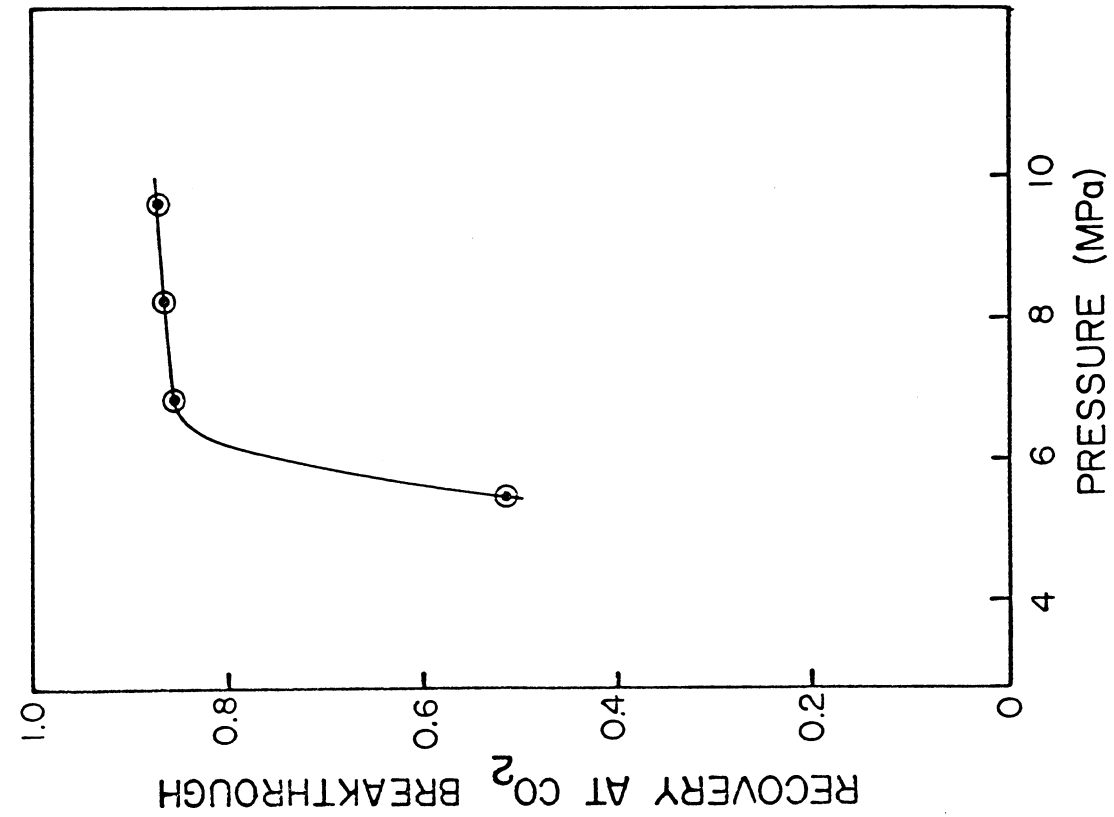
<u>Pressure (kPa)</u>	<u>Mole Fraction Dissolved CO<sub>2</sub></u>	<u>Swelling Factor*</u>	<u>Pure CO<sub>2</sub> Density (g/cm<sup>3</sup>)</u>	<u>Apparent Density of Dissolved CO<sub>2</sub> (g/cm<sup>3</sup>)</u>
5529	0.5950	1.348	0.144	.795
6915	0.7370	1.481	0.234	1.099
8287	0.7399	1.464	0.660	1.117
9673	0.7427	1.450	0.731	1.190

\* Volume of Oil + CO<sub>2</sub> at Saturation Pressure  
Volume of Oil at Atmospheric Pressure

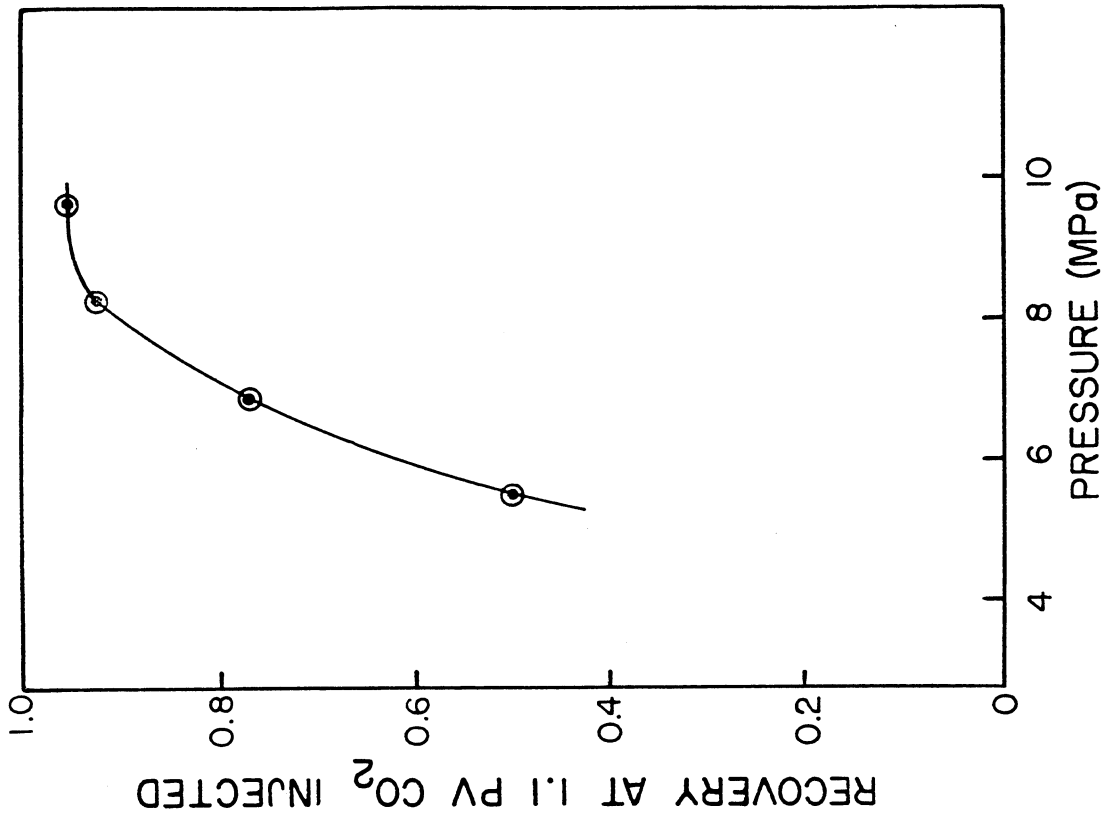
Table 3.3 Effective CO<sub>2</sub> Injection at Breakthrough

Pressure (kPa)	Oil Recovery at Breakthrough (PV)	Volume of CO <sub>2</sub> Injected (PV)*	Volume of CO <sub>2</sub> in Solution (PV)	Volume of Dissolved CO <sub>2</sub> at Injection Conditions (PV)	Volume Change on Mixing (PV)	Effective CO <sub>2</sub> Injection
5529	.515	1.143	.179	.987	.808	0.335
6915	.856	1.190	.075	.353	.278	0.912
8287	.862	.971	.068	.116	.048	0.919
9673	.869	.931	.064	.104	.040	0.890

\* Based on density of pure CO<sub>2</sub> at 32.2°C (90°F) and the injection pressure



a. Oil recovered at CO<sub>2</sub> breakthrough



b. Oil recovered at 1.1 PV injected

Figure 3.3 Summary of oil recovery in slim tube displacements of Maljamar separator oil at 32.2°C (90°F).

Separate samples of produced liquids were collected during each run (see §2.2) so that variations in the composition of produced hydrocarbon liquids could be detected. Figures 3.4-3.7 give results of simulated distillation analyses of those samples (see §2.3). Comparison of the compositions of the produced hydrocarbon liquids gives some additional evidence concerning the effect of component partitioning on the displacement process. Figure 3.4 compares carbon number distributions for produced liquid samples taken before and after CO<sub>2</sub> breakthrough in the displacement at 5516 kPa (800 psi). The compositions of the two liquids differed only slightly. The primary difference is that some light hydrocarbons in the C<sub>5</sub>-C<sub>9</sub> range were stripped out by the large volume of produced gas which accompanied the sample taken after breakthrough. Two phase production of oil and gas was observed in the sight glass after breakthrough. Thus, the oil produced after breakthrough in that run was very nearly the same as the original oil. Such behavior would be typical of an immiscible gas-oil displacement.

Figure 3.5 gives similar comparisons for the displacement at 6895 kPa (1000 psi), this time plotted as cumulative weight percent curves which also indicate amounts of hydrocarbons heavier than C<sub>35</sub>. The composition of the sample taken at 0.708 PV oil produced was within experimental error of the original oil composition. Breakthrough occurred at 0.856 PV oil produced. The liquids produced after breakthrough showed some evidence of enrichment with hydrocarbons in the C<sub>5</sub>-C<sub>20</sub> range. Again, two phase production was observed after CO<sub>2</sub> breakthrough. The liquid hydrocarbon compositions shown in Figure 3.5 are consistent with a displacement in which most hydrocarbons are produced after breakthrough in a phase consisting of original oil with CO<sub>2</sub> dissolved in it. Extraction of limited amounts of hydrocarbons into the CO<sub>2</sub>-rich phase would explain the slight enrichment of the produced liquids with C<sub>5</sub>-C<sub>20</sub> hydrocarbons.

Substantially larger composition variations were observed for samples taken in the displacements at 8287 and 9673 kPa (1200 and 1400 psi). In those runs, the hydrocarbons produced well after breakthrough, which occurred at 0.862 and 0.869 PV oil produced, were substantially lighter than the original oil. The composition data in Figures 3.6 and 3.7 suggest that the hydrocarbons produced late in those runs had been extracted into the CO<sub>2</sub>-rich phase. Results of mixing cell displacements (§3.2), batch multiple contact experiments (§3.3), and continuous multiple contact experiments (§3.3) substantiate that conclusion.

### 3.2 Comparison of Slim Tube, Core and Mixing Cell Displacements

Results of three displacements of Maljamar crude from a slim tube, a Berea sandstone core, and a mixing cell are shown in Figure 3.8. All three displacements were conducted at 1200 psig (8.27 MPa) and 90°F (32.2°C) in the apparatus shown in Figure 2.5. In the slim tube and mixing cell displacements, CO<sub>2</sub> was injected at 5 cm<sup>3</sup>/hr. The core floods were conducted with an injection rate of 4 cm<sup>3</sup>/hr.

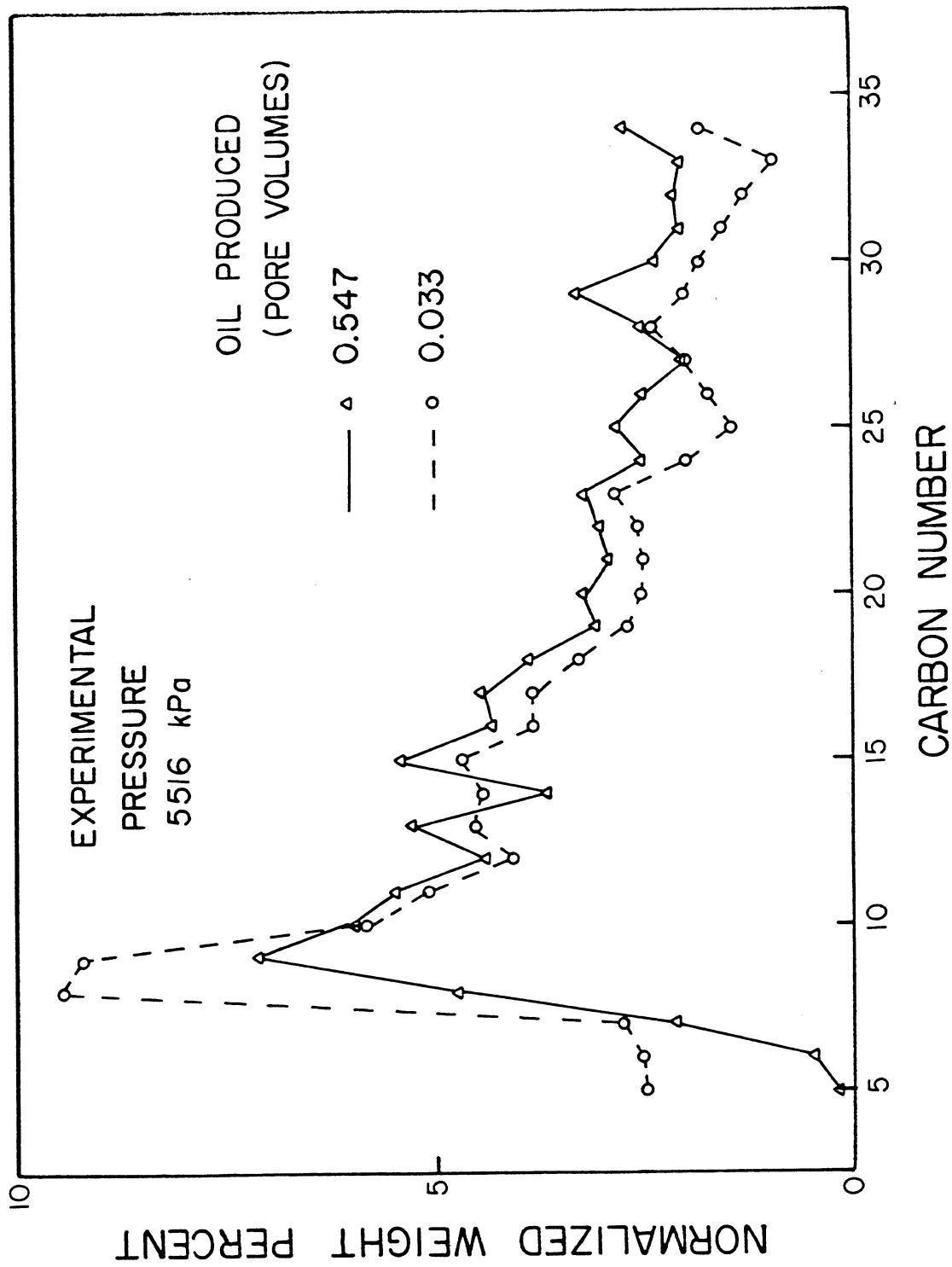


Figure 3.4 Composition of liquids produced during a slim tube displacement of Maljamar separator oil at 5.52 MPa (800 psi) and 32.2°C (90°F).

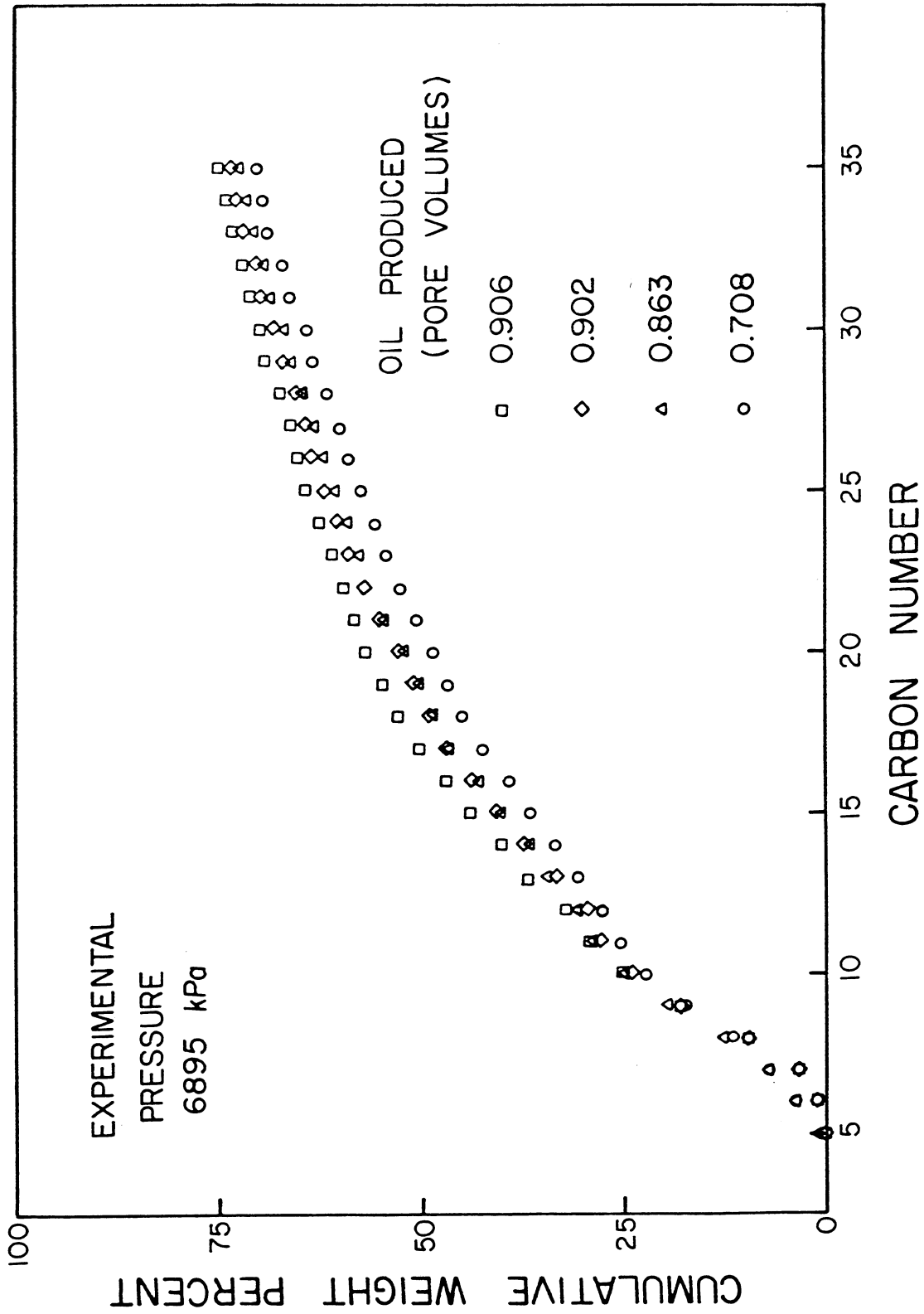


Figure 3.5 Composition of liquids produced during a slim tube displacement of Maljamar separator oil at 6.89 MPa (1000 psi) and 32.2°C (90°F).

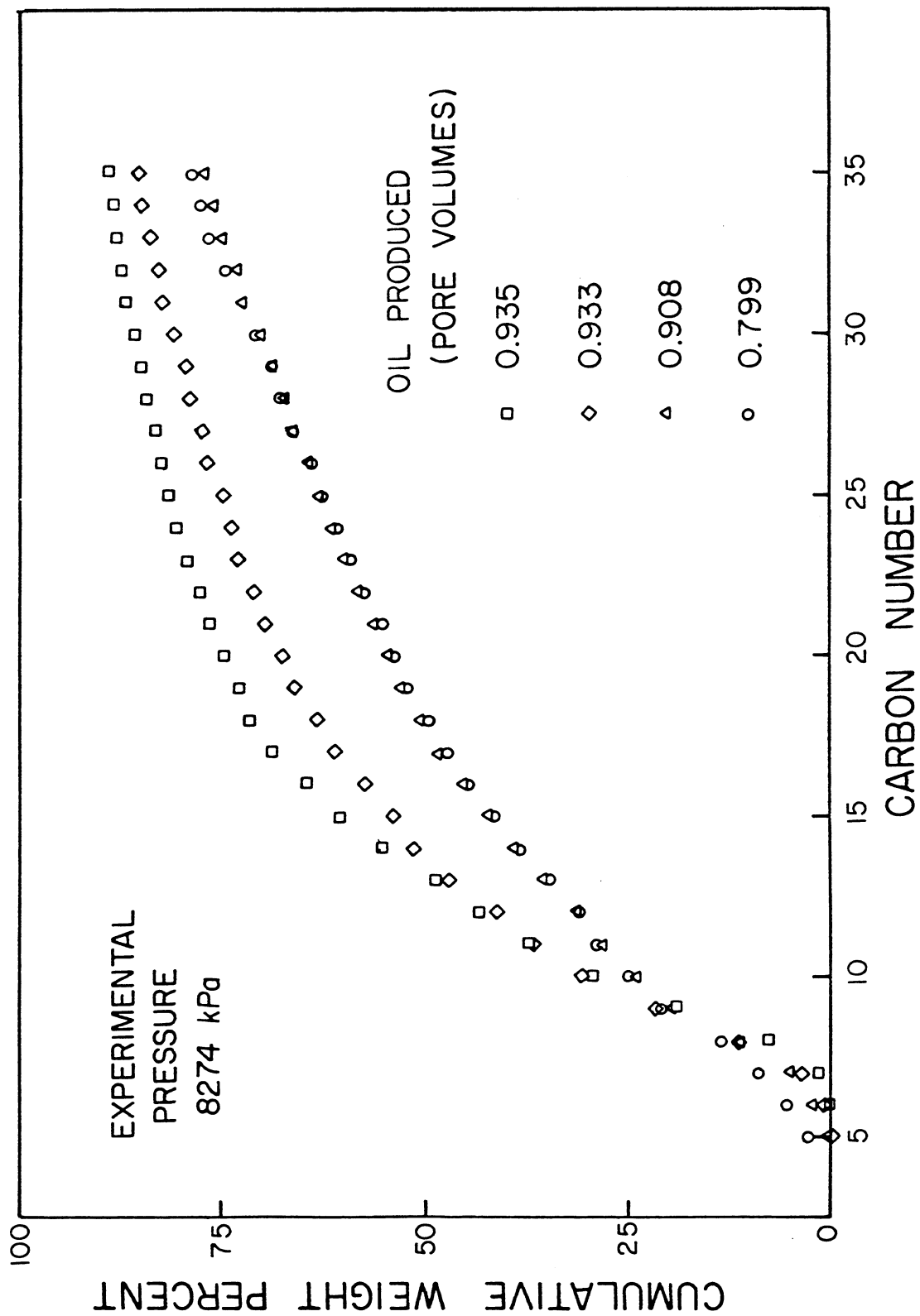


Figure 3.6 Composition of liquids produced during a slim tube displacement of Maljamar separator oil at 8.27 MPa (1200 psi) and 32.2°C (90°F).

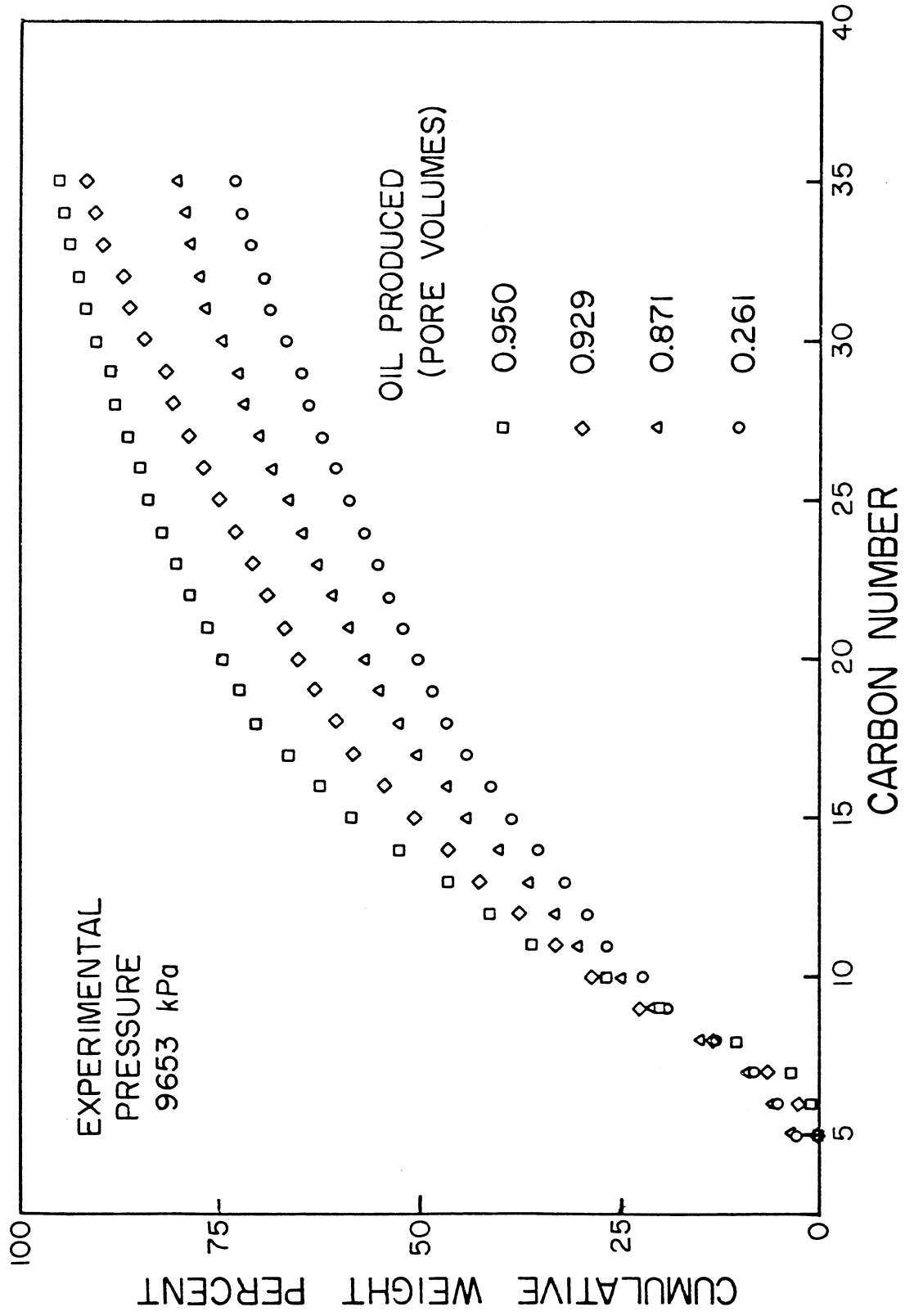


Figure 3.7 Composition of liquids produced during a slim tube displacement of Maljamar separator oil at 9.65 MPa (1400 psi) and 32.2°C (90°F).

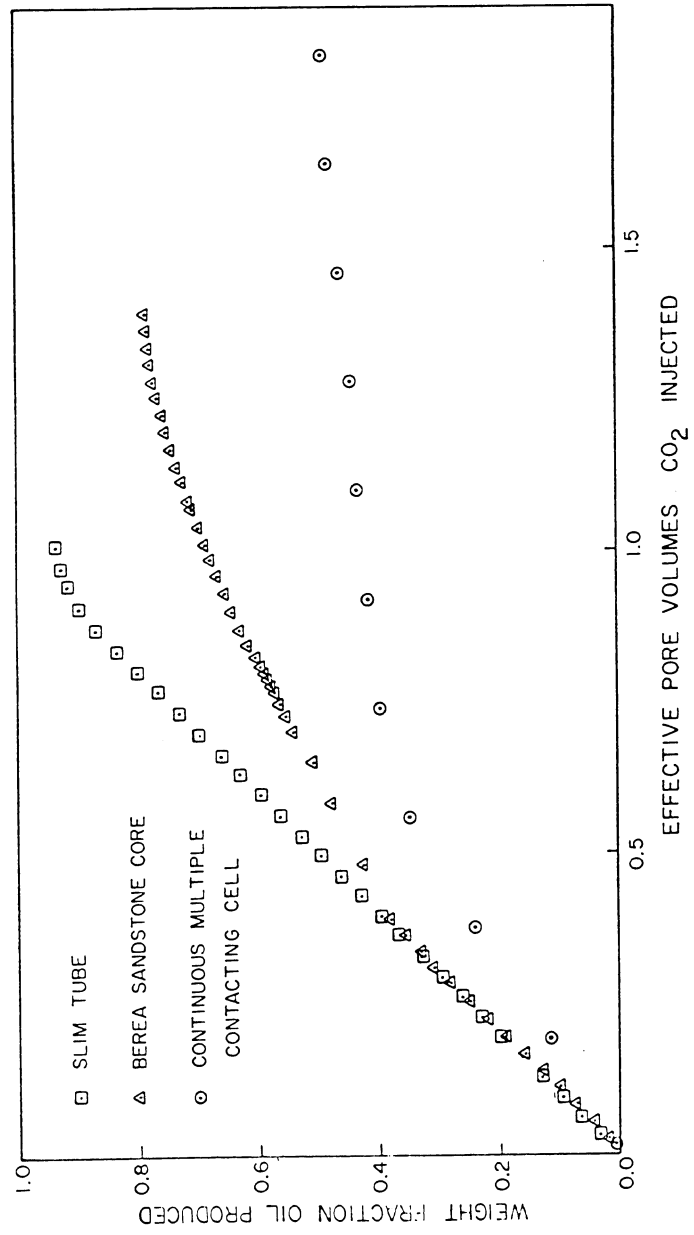


Figure 3.8 Oil recovered from displacements of Maljamar oil by CO<sub>2</sub> at 8274 kPa (1200 psi) and 32.2°C (90°F).

The results shown in Figure 3.8 indicate some of the difficulties which are encountered during experiments to determine the efficiency of CO<sub>2</sub>-oil displacements. The slim tube displacement, which is a standard experiment for evaluation of an oil for CO<sub>2</sub> flooding, yielded very high oil recovery. The core displacement, however was much less efficient than the slim tube displacement and the mixing cell displacement recovered still less oil. The reasons for the differences lie in the interaction of phase behavior with the length scales over which mixing occurred. At the rates at which the slim tube and core flood experiments were conducted, the displacements were unstable. In principle the difference in density between CO<sub>2</sub> and oil can be used to damp viscous fingers in downward displacements if the flow velocity is low enough but in practice, very low flow rates may be required. Estimates of the maximum velocity for gravity stabilized miscible displacements  $v_c$  have been given by Hill (1949) and Dumore (1964) as

$$v_c = k \frac{\Delta\rho}{\Delta\mu} g \sin\theta \quad (3.1)$$

where  $k$  is the permeability,  $\theta$  the dip angle measured from the horizontal axis, and  $\Delta\rho$  and  $\Delta\mu$  the density and viscosity differences between the displaced and displacing phases. The critical flow velocities for the slim tube and core are calculated from equation (1) to be .0295 and .0366 cm/hr., respectively (.0035 and .1381 cm<sup>3</sup>/hr.). Actual flow velocities exceed the critical velocity by factors of 1400 and 29, respectively. Despite the fact that the ratio of the flow velocity to the critical velocity in the slim tube is much higher than it is in the core, the recovery of oil by CO<sub>2</sub> displacement is higher. This occurs because finger growth is limited in the slim tube by the small flow diameter and because the initial instability generates a transition zone which in turn helps to stabilize the flood. Watkins (1978) used Perrine's (1961a, b) analysis of stability requirements for miscible displacements to construct estimates of the minimum length of a transition zone (in pore volumes) required to stabilize an otherwise unstable displacement

$$\Delta L_{\min} = \frac{(1 - \frac{v_c}{v}) \ln \frac{\mu_{oil}}{\mu_{CO_2}}}{\frac{\pi^2 k_t + L}{vd^2}} \quad (3.2)$$

where  $k_t$  is the transverse dispersion coefficient (Perkins and Johnson 1963),  $L$  the length of the core or slim tube,  $v$  is the flow velocity and  $d$  the flow diameter. According to equation (2), the minimum transition zone length is 0.07 PV for the slim tube, but is 2.2 PV for the core. Thus, a transition zone which stabilizes the flood develops quickly in the slim tube, and most of the displacement is efficient. In the core flood, however, the CO<sub>2</sub> breakthrough occurs long before a transition zone long enough to stabilize the flood can develop.

The foregoing discussion ignores the effects of phase behavior on the displacement process, though component partitioning clearly affects both phase volumes and phase properties in the transition zone. Indeed, transition zone length is not the only requirement which must be satisfied. The compositions in the transition zone must be such that if a second phase occurs, it appears only in small quantities. The results of the mixing cell displacement give an indication of the magnitude of the effect. In that experiment, CO<sub>2</sub> was injected into the cell, and a mixture of oil and CO<sub>2</sub> was produced until enough CO<sub>2</sub> had been injected to exceed the solubility of CO<sub>2</sub> in the oil. Then, the CO<sub>2</sub>-rich liquid phase at the top of the cell was produced. After the second liquid phase appeared, oil was recovered only by stripping, a much slower process than displacement, and a large percentage of the original oil in place was left behind in the immobile lower phase. If, however, the injected fluid had been enriched with light and intermediate hydrocarbons stripped from the crude rather than pure CO<sub>2</sub>, then the volume of the lower phase and hence the amount of oil left behind would have been smaller. It is the steady enrichment of the CO<sub>2</sub> at the leading edge of the displacement which accounts for the high displacement efficiency of CO<sub>2</sub> in stable displacements in a porous medium. If the displacement is unstable, however, then the volume over which mixing occurs increases. Purer CO<sub>2</sub> dilutes the enriched CO<sub>2</sub> near the leading edge of the displacement, overall compositions fall deeper into the two phase region, and displacement efficiency decreases by more than the decrease in sweep efficiency which would be observed in an unstable miscible displacement. That is, viscous fingering causes lower oil recovery not only because sweep efficiency is lower, but also because the residual oil saturation is higher in the swept zone.

Thus, the role of viscous fingering in core and field displacements is to increase the length scale over which fluids are mixed in a way which negates, at least partly, the beneficial effects of CO<sub>2</sub>-crude oil phase behavior. Displacement in a slim tube is efficient because viscous fingering is inhibited and only local mixing occurs. Flow in a core at the same conditions may be efficient or not depending on whether it is stable. If it is unstable then the increased mixing volume leads to lower recovery due to the interaction with phase behavior. A similar interaction is observed if the level of dispersion is increased in displacements in which phase behavior is important (Gardner, Orr and Patel 1979; Orr, Yu and Lien 1980). The mixing cell displacement is the limiting case of increased mixing in which minimum benefit is derived from extraction of hydrocarbons by the CO<sub>2</sub>.

### 3.3 Phase Behavior and Fluid Properties of CO<sub>2</sub>-Crude Oil Mixtures

Though CO<sub>2</sub> flooding processes are often referred to as "miscible" floods, it is clear that CO<sub>2</sub> is not strictly miscible with crude oil. That is, CO<sub>2</sub>-crude oil mixtures do not satisfy the requirement that such mixtures form only one phase no matter what the proportions in which they are mixed. It is more accurate to describe CO<sub>2</sub> as "partially miscible" with crude oil. CO<sub>2</sub> is quite soluble in crude oils, and at high enough pressures some hydrocarbons are quite soluble in CO<sub>2</sub>. The effect of the distribution of CO<sub>2</sub>

and hydrocarbon components between phases on local displacement efficiency has been well documented in the work of Hutchinson and Braun (1961), Rathmell et al. (1971), Holm and Josendal (1974, 1980), Metcalfe and Yarborough (1979), Gardner et al. (1979), and Orr et al. (1980a), and it has been analyzed elegantly by Helfferich (1979). It is apparent that a detailed interpretation of results of displacement tests must rest upon an adequate description of the partitioning of CO<sub>2</sub> and hydrocarbon components which takes place in the mixtures which occur during a displacement.

### Results of Single Contact Experiments

In this section, results of experiments to determine the behavior of mixtures of CO<sub>2</sub> and crude oil are reported. Those results form the basis for one-dimensional simulations of the displacement process which are discussed in §4. The phase behavior of CO<sub>2</sub> with Maljamar crude oil at 32.2°C (90°F) was investigated in four experiments which included:

- (1) measurements in the PVT system (Fig. 2.1) described in §2.1 of phase volumes, fluid properties and saturation pressures for single contact mixtures of CO<sub>2</sub> and oil;
- (2) measurements, again in the PVT system (Fig. 2.1), of phase volumes and saturation pressures for multiple contact mixtures;
- (3) displacements of oil from an unstirred mixing cell (Fig. 2.5b); and
- (4) continuous multiple contact experiments to measure phase compositions (Fig. 2.8).

The results presented here illustrate clearly the complexity of the phase behavior of CO<sub>2</sub>-crude oil mixtures at conditions typical of the large Permian Basin fields for which CO<sub>2</sub> flooding is the most likely enhanced recovery technique.

Results of a single contact phase behavior study for binary mixtures of CO<sub>2</sub> and Maljamar separator oil are summarized in Figure 3.9 (see §2.1 for a description of the experimental procedures used). Binary mixtures of CO<sub>2</sub> and Maljamar separator oil containing less than about 75 mol % CO<sub>2</sub> formed vapor-liquid mixtures at low pressures and single phase mixtures at pressures above the bubble point pressure. That is, all the CO<sub>2</sub> present dissolved in the oil at pressures above that given by the curve labeled 100% L<sub>1</sub> in Figure 3.9. Mixtures containing more than about 75 mol % formed two liquid phases at high pressures, while at low pressures, liquid and vapor phases were observed. There was a small range of pressures over which three phases, two liquids and a vapor, coexisted. Figure 3.10a shows the sequence of phase volumes observed for a mixture containing 79.7 mol % CO<sub>2</sub> in Maljamar separator oil. At 6550 kPa (950 psi), that mixture formed a liquid

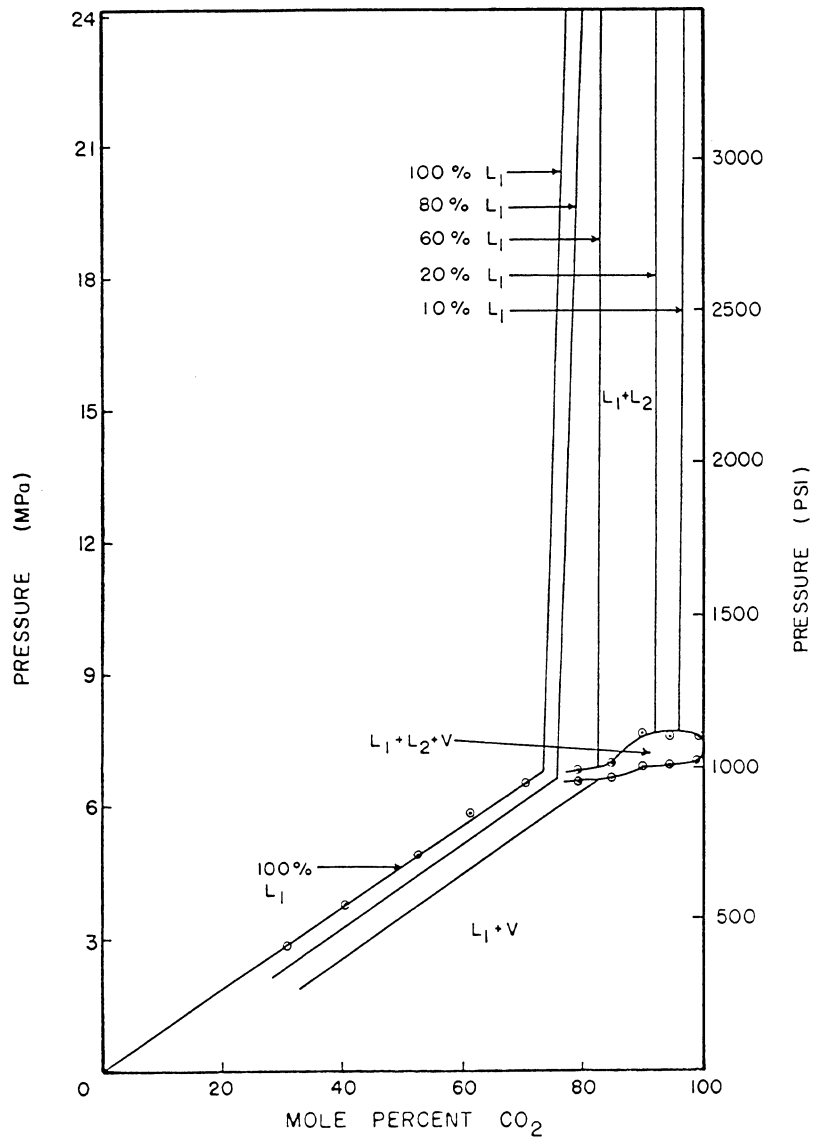


Figure 3.9 Phase behavior of binary mixtures of CO<sub>2</sub> with Maljamar separator oil at 32.2°C (90°F).

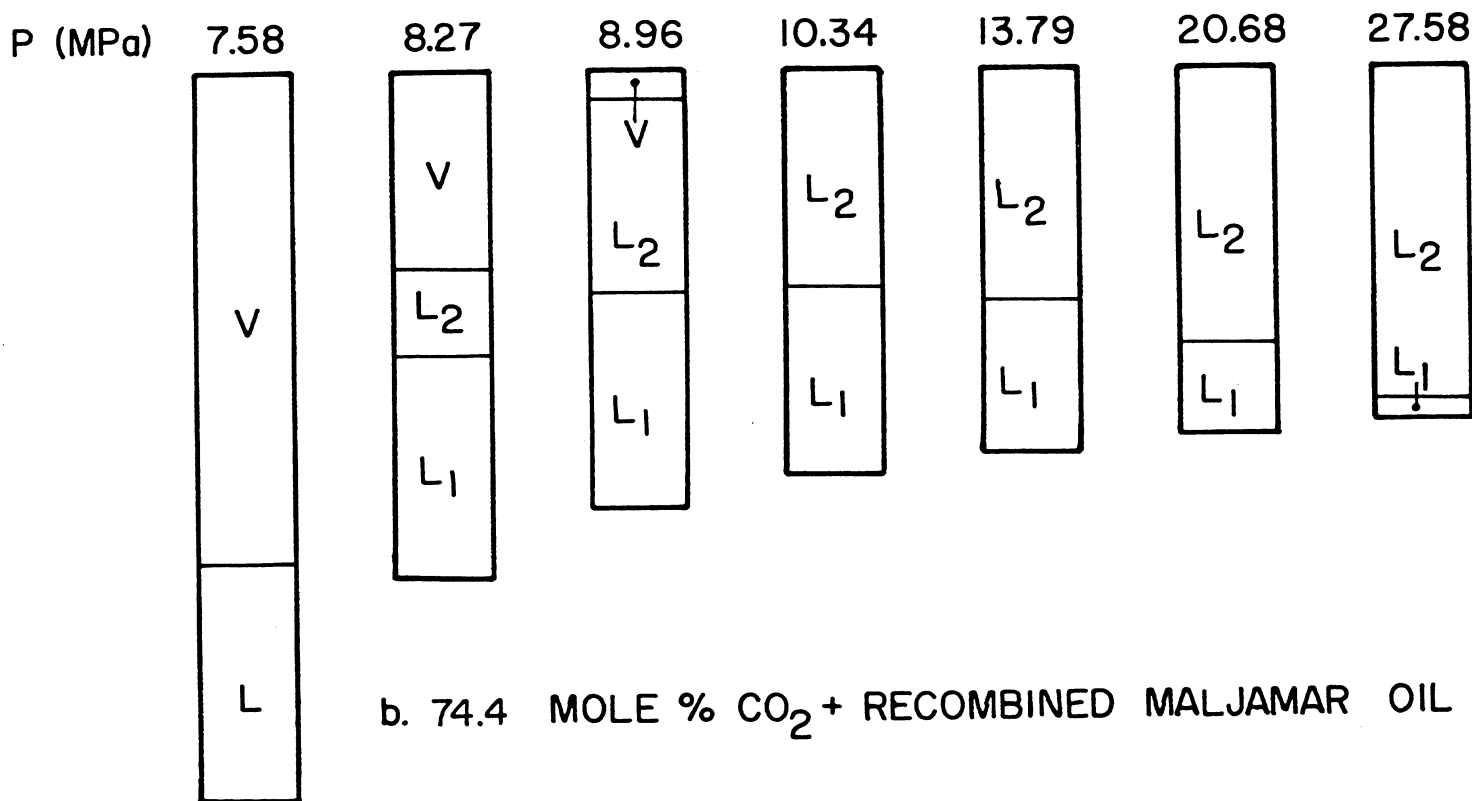
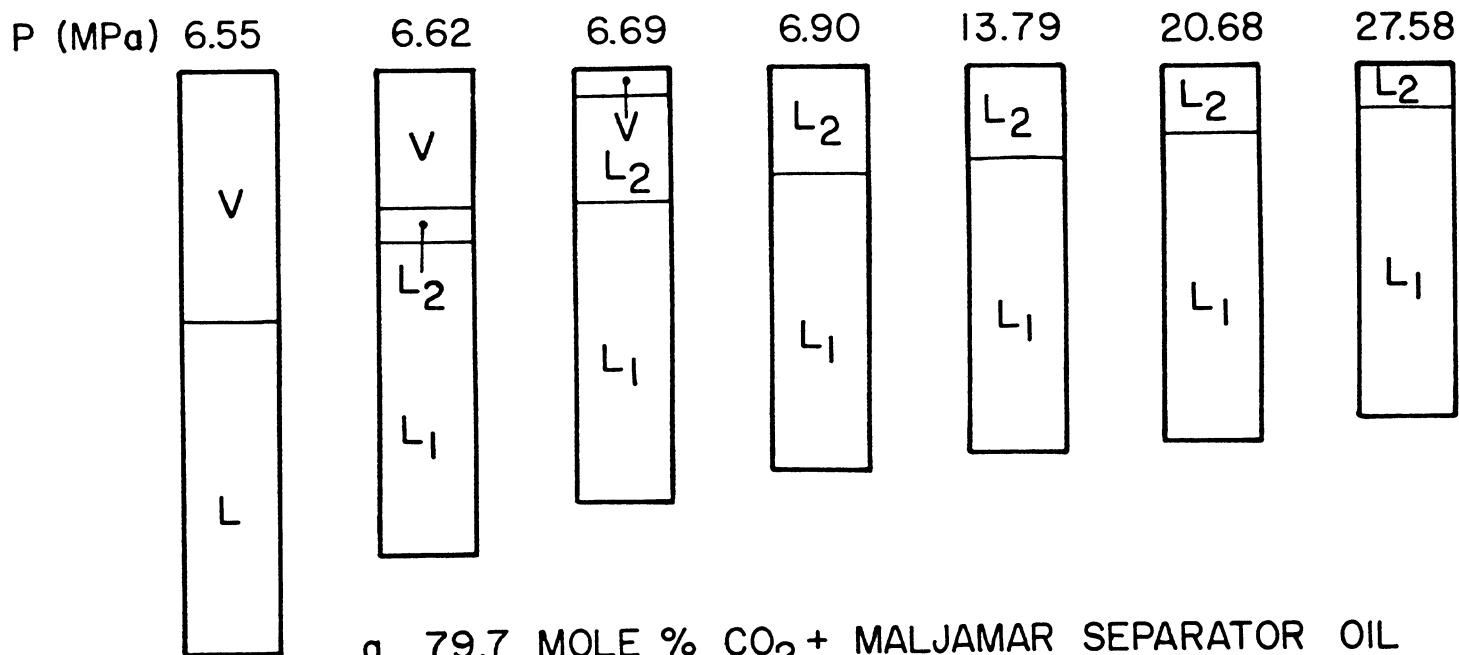


Figure 3.10 Volumetric behavior of two CO<sub>2</sub>-crude oil mixtures at 32.2°C (90°F).

and a vapor, but with a small increase in pressure to 6620 kPa (960 psi), a second liquid phase appeared between the lower liquid and vapor phases. The lower liquid ( $L_1$ ) phase was black, as was the original oil, while the upper liquid ( $L_2$ ) phase was a clear yellow color. The vapor phase was colorless. With additional small increases in pressure, but large decreases in volume, the vapor phase disappeared, leaving two liquid phases in the cell. Very little change was observed in the volume or appearance of the  $L_1$  phase over the range of pressures in which the upper liquid appeared and the vapor disappeared. It was as if the vapor phase was being liquefied with little accompanying change in the  $L_1$  phase. Large pressure increases were required to change the volumes of the two liquid phases, as indicated in Figure 3.10a. As the pressure was increased, the upper liquid phase changed gradually to a dark burgundy at 24130 kPa (3450 psi) and then became black at 27580 kPa (4000 psi). The presence of the upper phase could be detected only in ultraviolet light.

The volumetric behavior shown in Figure 3.10a was typical of mixtures containing 79.7%  $\text{CO}_2$  or more except that as concentration of  $\text{CO}_2$  was increased, the volume fraction of the  $\text{CO}_2$ -rich phases ( $L_2$  and V) also increased. Even at 99.49%  $\text{CO}_2$ , a region of  $L_1$ - $L_2$ -V coexistence was observed. Apparently, the addition of even a very small amount of crude oil to  $\text{CO}_2$  raised the critical temperature of the resulting mixture enough that a liquid  $\text{CO}_2$ -rich phase could be formed at 90°F.

Small amounts of heavy resinous material were observed adhering to the cell windows for mixtures containing more than about 70 mol %  $\text{CO}_2$ . Thus, at some  $\text{CO}_2$  concentrations and pressures, as many as four phases were present in the cell simultaneously. Fluid property measurements were made for both upper and lower liquid phases at various pressures for mixtures of  $\text{CO}_2$  and separator oil containing 79.3, 80.0 and 90.0 mol %  $\text{CO}_2$ . Results of density and viscosity measurements are reported in Table 3.4. Those results show that the viscosity of the  $\text{CO}_2$ -rich liquid phase was about three times higher than the viscosity of pure  $\text{CO}_2$  at the same conditions. The lower phase viscosity was about one fourth of the original separator oil. Thus, it is apparent that the contrast between the viscosities of the phases which result from mixing of  $\text{CO}_2$  and crude oil is not as adverse as would be expected from the viscosities of pure  $\text{CO}_2$  and the original oil. In this case the actual viscosity ratio (oil-rich phase to  $\text{CO}_2$ -rich phase) is about four while the ratio of original oil to  $\text{CO}_2$  was about fifty. Clearly, phase viscosities are strongly affected by component partitioning. Phase densities and viscosities were only mildly affected by pressure, however, as might be expected for liquid-liquid systems.

One additional experiment was performed to assess the effect of solution gas on the phase behavior of mixtures of  $\text{CO}_2$  and Maljamar crude. Gas of the composition given in Table 3.5 was added to separator oil to give a recombined reservoir fluid (RRF) with a bubble point of 10.52 MPa (~650 SCF/BBL). A mixture of 74.4 mol %  $\text{CO}_2$  and RRF was then examined in the high pressure cell for pressures between 7.58 and 31.03 mPa. A comparison of the volumetric behavior of this mixture with that observed for the mixture

Table 3.4 Density and Viscosity of Mixtures of CO<sub>2</sub> with Maljamar Separator Oil and Recombined Reservoir Fluid (RRF)

Overall Composition (Mol % CO <sub>2</sub> )	Oil	Phase	Pressure (kPa)	Density (g/cm <sup>3</sup> )	Viscosity (mPa.s)
0	Separator	-	5516	0.829	2.51
0	Separator	-	8274	0.830	2.71
0	Separator	-	9653	0.831	2.85
0	Separator	-	13790	0.834	2.88
0	Separator	-	17240	0.836	2.95
0	RRF	-	12410	0.7393	0.84
0	RRF	-	14820	0.7419	0.85
0	RRF	-	17230	0.7444	0.87
0	RRF	-	20680	0.7474	0.90
79.3	Separator	Upper	14920	-	0.19
79.3	Separator	Lower	14920	0.8495	0.76
79.3	Separator	Lower	15130	0.8802	0.77
80.0	Separator	Upper	8274	0.8038	0.18
80.0	Separator	Lower	8274	0.8596	0.67
80.0	Separator	Upper	9653	0.8166	-
80.0	Separator	Lower	9653	0.8601	-
90.0	Separator	Upper	8274	0.7803	0.18
90.0	Separator	Lower	8274	0.8358	1.07
90.0	Separator	Upper	9653	0.8079	0.28
90.0	Separator	Lower	9653	0.8471	-
90.0	Separator	Upper	12410	0.8396	-
90.0	Separator	Lower	12410	0.8830	-
90.0	Separator	Upper	17240	0.8637	0.21
90.0	Separator	Lower	17240	0.8965	0.65

Table 3.5 Composition and Properties of Maljamar  
Recombined Reservoir Fluid (RRF)

	Gas (Mol %)	Oil (Mol %)	RRF <sup>1</sup> (Mol %)
C <sub>1</sub>	56.55	-	29.39
C <sub>2</sub>	19.61	-	10.19
C <sub>3</sub>	16.06	-	8.35
C <sub>4</sub>	6.37	-	3.31
C <sub>5</sub>	1.41	3.90	2.61
C <sub>6</sub>	-	9.37	4.50
C <sub>7</sub>	-	10.27	4.93
C <sub>8</sub>	-	13.54	6.50
C <sub>9</sub>	-	11.91	5.72
C <sub>10</sub>	-	7.50	3.60
C <sub>11+</sub>	-	43.51	20.90
	<hr/> 100.00	<hr/> 100.00	<hr/> 100.00
Molecular Wt.	26.77	183.7	102.14
Density	-	0.834 <sup>2</sup>	0.7393 <sup>3</sup>
Bubble Point Pressure (MPa)		-	10.51

<sup>1</sup> Calculated for the approximate recombination GOR of 650 SCF/STB

<sup>2</sup> At 13.79 MPa and 32.2°C

<sup>3</sup> At 12.41 MPa and 32.2°C

containing 79.7% CO<sub>2</sub> and separator oil is shown in Figure 3.10. At low pressures both mixtures formed a dark liquid and a clear vapor, and as pressure was increased, a second liquid phase appeared. With additional increases in pressure, the vapor phase disappeared, leaving two liquids. Substantial differences occurred at higher pressures, however. The separator oil mixture showed small reductions in the volume of the upper phase with increasing pressure, while in the RRF mixture the upper phase grew at the expense of the lower phase. While the actual disappearance of the lower phase was not observed, an extrapolation of the volume of the L<sub>1</sub> phase vs. pressure gives a saturation pressure of above 30.06 mPa. Thus, it appeared that for the separator oil mixture, the single-phase region would be approached with the disappearance of the upper phase--a bubble point except that these are liquid-liquid equilibria rather than vapor-liquid equilibria--while in the RRF mixture it would occur with the disappearance of the lower phase--a dew point in vapor-liquid parlance. These data suggest that the full phase diagram for CO<sub>2</sub>-RRF mixtures would be similar to those reported by Gardner et al. (1979) and Stalkup (1978), with retrograde behavior in the liquid-liquid region of the pressures and compositions. Apparently, addition of the solution gas to the separator oil causes a substantial change in the location of the liquid-liquid critical point. Thus, at high CO<sub>2</sub> concentrations and high pressure, the RRF mixture is more easily extracted into the CO<sub>2</sub> rich phase.

Results which show L<sub>1</sub>-L<sub>2</sub> and L<sub>1</sub>-L<sub>2</sub>-V behavior similar to that presented in Figures 3.9 and 3.10 have been reported for five other crude oil systems by Rathmell et al. (1971), Huang and Tracht (1974), Shelton and Yarborough (1977), Stalkup (1978), and Gardner et al. (1979). Other phase behavior studies have reported only liquid-vapor phase separations (Simon et al. 1978; Graue and Zana 1978; Peterson 1978; Rathmell et al. 1971; and Perry et al. 1978). A review of published phase behavior data for mixtures of CO<sub>2</sub> with well-characterized hydrocarbons was conducted to provide a conceptual framework with which the complexity of CO<sub>2</sub>-crude oil phase behavior could be understood. Details of that review have been reported in a paper by Orr et al. (1980a), a copy of which is reproduced in Appendix A. The review indicated that liquid-liquid and liquid-liquid-vapor phase behavior could be expected to occur as long as the reservoir temperature was below about 50°C. Based on the review, and results of phase behavior experiments with crude oil recombined with solution gas, a prediction was also made in that paper that some qualitative differences would be observed for CO<sub>2</sub>-hydrocarbon mixtures which contained a supercritical hydrocarbon component as well as supercritical CO<sub>2</sub> when the behavior of such mixtures was compared with that of CO<sub>2</sub>-hydrocarbon mixtures containing only subcritical hydrocarbons. Experiments were then conducted for a CO<sub>2</sub>-C<sub>1</sub>-C<sub>16</sub> system and for a CO<sub>2</sub>-synthetic oil system which confirmed the existence of what Orr et al. (1980a) called "type II" phase behavior. Details of those experiments are reported in a second paper reproduced in Appendix B.

Analysis of the results of those experiments also indicated that a simple correlation exists for the pressure required to avoid L<sub>1</sub>-L<sub>2</sub>-V separations in a CO<sub>2</sub>-crude oil system. The correlation is based on the

idea that such separations must occur at pressures near the vapor pressure of CO<sub>2</sub>, extrapolated for temperatures above the critical temperature of CO<sub>2</sub>. Figure 3.11 compares the vapor pressure of CO<sub>2</sub>, calculated from the equation given by Newitt et al. (1956), to pressure ranges reported for L<sub>1</sub>-L<sub>2</sub>-V behavior in CO<sub>2</sub>-hydrocarbon systems (Orr et al. 1980a; Shelton and Yarborough 1977; Meldrum and Nielsen 1955; Gardner et al. 1979; Huang and Tracht 1974; and Henry and Metcalfe 1980). Despite wide variations in the composition of the crude oils, particularly in the amount of methane present, pressure ranges for L<sub>1</sub>-L<sub>2</sub>-V behavior lie within a band given by vapor pressure plus 1750 kPa (250 psi) and minus 1000 kPa (150 psi). Thus, a reasonable estimate of a pressure high enough to avoid three phase separations is given by

$$P = 101.325 \exp \left\{ \frac{-2015.9}{T} + 10.9122 \right\} + 1750 \quad (3.3)$$

where P is the pressure in kPa, and T the temperature in °K.

#### Results of a Batch Multiple Contact Experiment

The binary mixtures of CO<sub>2</sub> and oil which are studied in a single contact phase behavior do not completely represent phases which will occur during a CO<sub>2</sub> displacement. Consider, for instance, the start of CO<sub>2</sub> injection into an oil saturated core. When the concentration of CO<sub>2</sub> has reached a level high enough that two phases are present, the mixtures which occur downstream are no longer simple binary mixtures of CO<sub>2</sub> and oil. They are the result of a mixing process which depends on the rates at which two phases of different composition move ahead to contact fresh oil. Presumably, the less viscous CO<sub>2</sub>-rich phase moves relatively faster than the more viscous oil-rich phase. Thus, additional CO<sub>2</sub> injection causes mixing of fresh CO<sub>2</sub> with oil-rich phase left behind by the more rapidly moving CO<sub>2</sub>-rich phase. It is clear, therefore, that multiple contact experiments can, qualitatively at least, investigate mixture compositions which are more representative of compositions occurring during a CO<sub>2</sub> flood than those considered in single contact studies.

Figure 3.12 summarizes the volumes of crude oil and CO<sub>2</sub> transferred during a multiple contact phase behavior experiment performed in the PVT apparatus (§2.1). Properties and composition of the recombined reservoir fluid (RRF) are given in Table 3.5. Two series of mixtures were studied. In the forward contact experiments, the CO<sub>2</sub>-rich upper phase was mixed with fresh RRF while in the reverse contact experiments, fresh CO<sub>2</sub> was mixed with the lower phase remaining from the previous contact. The forward contacts simulate mixtures which occur at the leading edge of the transition zone, while the reverse contacts model the behavior of fluids near an injection well.

The initial mixture (F<sub>1</sub>) was made by charging nearly equal volumes of RRF and CO<sub>2</sub> into the cell at 13.79 MPa (2000 psi). For comparison purposes, the charge volumes shown in Figure 3.12 have been corrected to 17240 kPa

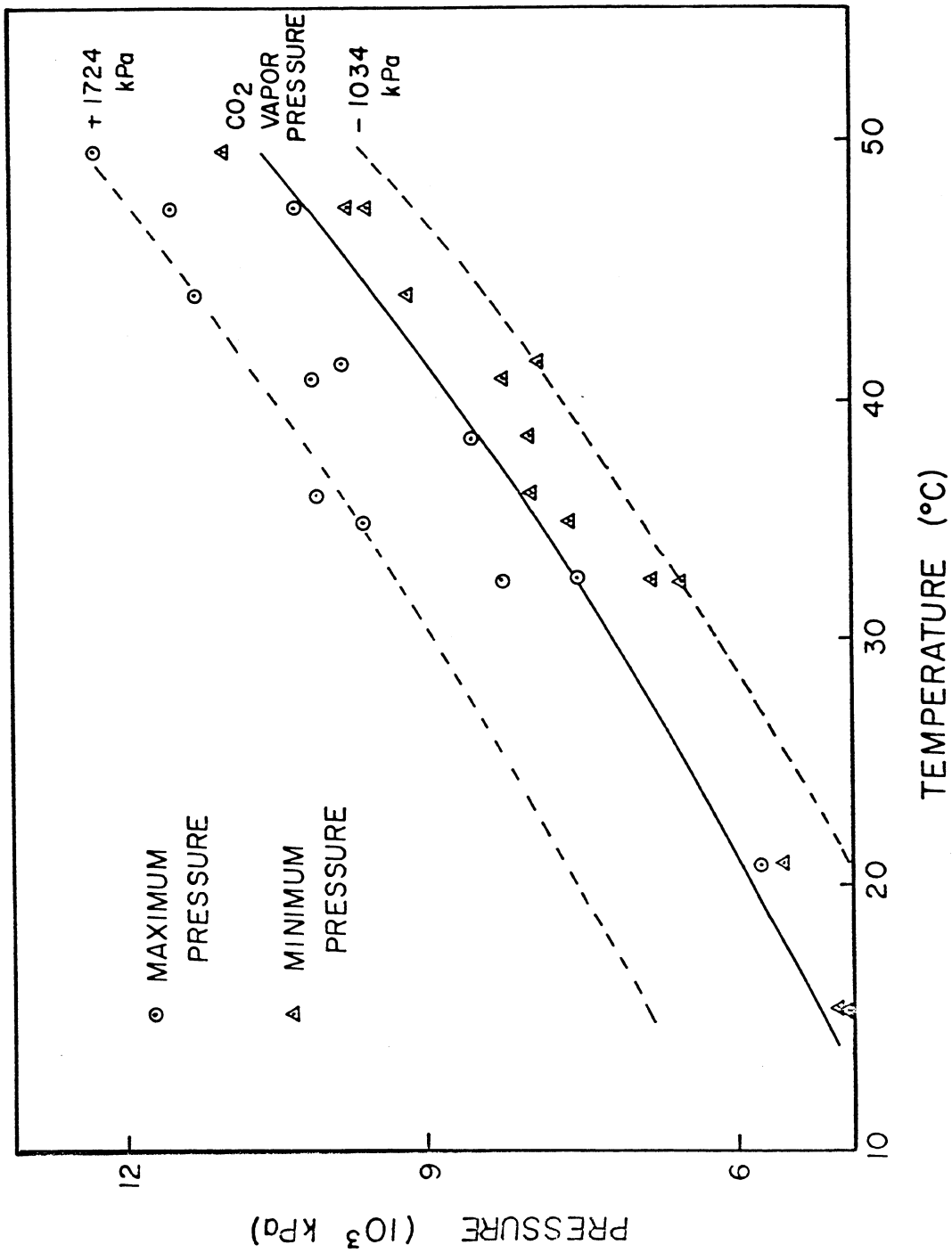


Figure 3.11 Pressure ranges for liquid-liquid-vapor behavior in CO<sub>2</sub>-crude oil systems.

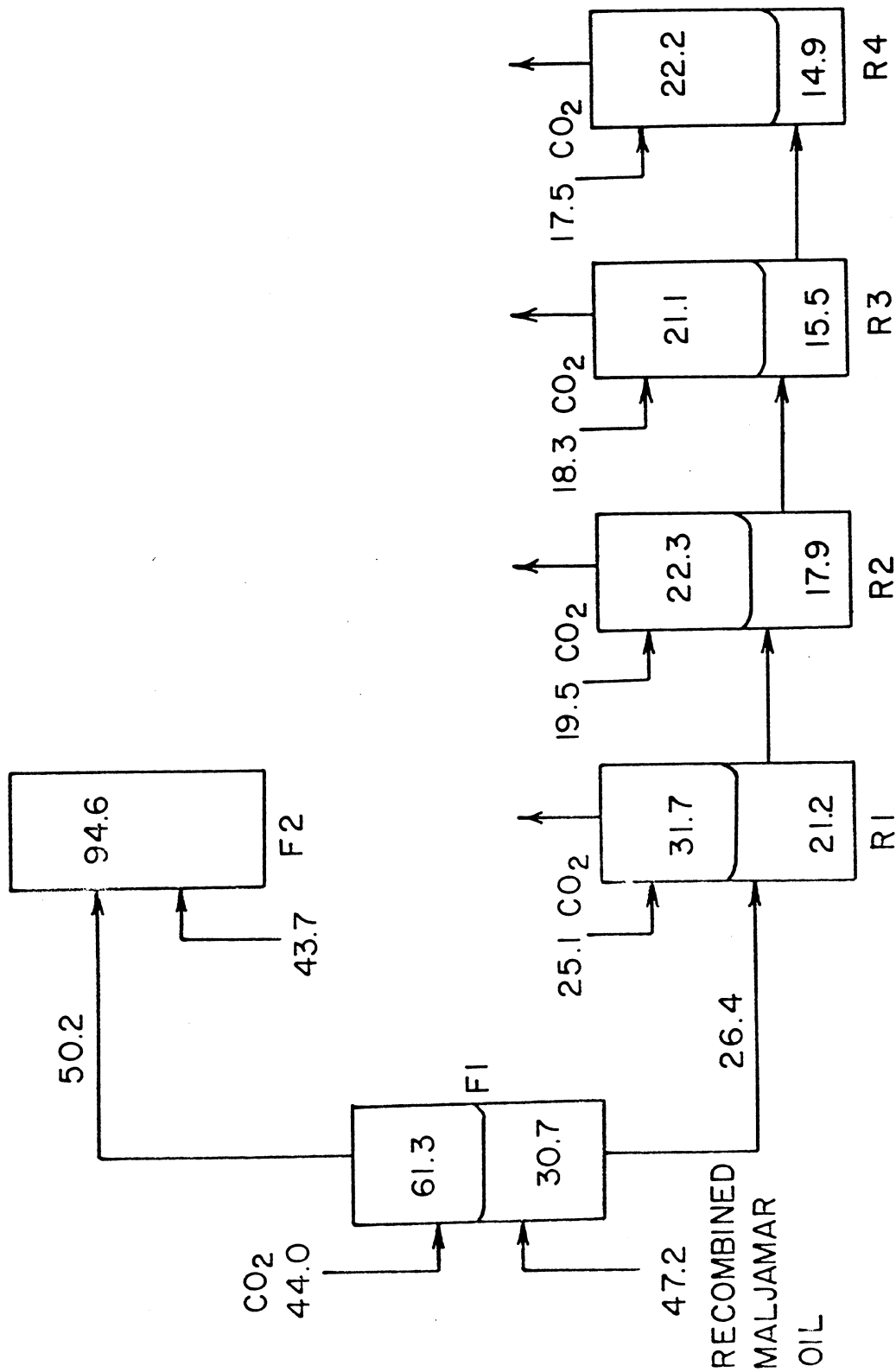


Figure 3.12 Summary of volumes transferred in a batch multiple contact experiment with recombined Maljamar oil at 32.2°C (90°F). Phase volumes and volumes of CO<sub>2</sub> charged are in cm<sup>3</sup> at 17.24 MPa (2500 psi) and 32.2°C (90°F).

(2500 psi). The resulting mixture  $F_1$  contained 74.4 mol %  $CO_2$ . After equilibration at 17240 kPa (2500 psi), two phases were observed, an upper,  $CO_2$ -rich liquid phase ( $L_2$ ) and a lower, oil-rich liquid ( $L_1$ ) phase. The volumetric behavior of this mixture at various pressures is shown in Figure 3.10b. As pressure was reduced from high levels 30000 kPa (4300 psi), the lower liquid phase volume increased. At 9240 kPa (1340 psi) a vapor phase appeared and with further reductions in pressure, the upper liquid phase decreased in volume, disappearing at 7140 kPa (1036 psi). Below that pressure, only liquid and vapor were observed.

The contents of the cell were then compressed to 17240 kPa (2500 psi) and 50.2 cm<sup>3</sup> of the upper phase were transferred to the second cell which contained 43.7 cm<sup>3</sup> of original RRF. This mixture ( $F_2$ ) was a single phase at 17240 kPa (2500 psi) and did not show  $L_1$ - $L_2$ -V phase behavior as Figure 3.13 indicates. The bubble point of the mixture  $F_2$  was 11930 kPa (1730 psi). Evidently, the  $CO_2$  concentration in  $F_2$  was low enough that the three phase region was not encountered.

Four reverse contact experiments were performed. In each contact, a volume of  $CO_2$  roughly equal to the remaining oil phase volume was added to the cell. Figure 3.12 shows the trend of phase volumes with succeeding contacts and Figure 3.14 reports volume fractions as a function of pressure for mixture  $R_1$ . The volumetric behavior of the reverse contact mixtures was similar to that observed for  $CO_2$  and Maljamar separator oil (see Figure 3.10a). That is,  $L_1$ - $L_2$ -V behavior occurred but the retrograde extraction of hydrocarbons with increasing pressure, observed for the  $CO_2$ -RRF mixture  $F_1$ , did not occur.

In each contact for mixtures  $R_1$  through  $R_4$ , the volume of the  $CO_2$ -rich liquid phase was greater than that of the  $CO_2$  charged. Furthermore, the volume of the remaining oil-rich liquid phase was reduced with each additional contact as hydrocarbons were extracted into the  $CO_2$ -rich phase. Table 3.6 reports results of the analyses of gas produced during blowdown after each reverse contact. Those results show that most of the light ends of the RRF were removed during the initial contact ( $F_1$ ). Thus, hydrocarbons  $C_5$  and heavier being extracted into the  $CO_2$ -rich phase account for the volume increase of the upper phase in contacts  $R_1$  through  $R_4$ . Additional evidence of the depth of extraction is shown in Figure 3.15. Liquid produced during blowdown of the upper phase from each reverse contact was collected and analyzed by gas chromatography (see §2.3). Carbon number distributions for each sample are shown in Figure 3.15 along with that of the oil remaining after blowdown of the lower phase remaining after the last reverse contact. The results show that the early contacts ( $R_1$  and  $R_2$ ) extract oils richer in the  $C_5$  to  $C_{18}$  range. The oil recovered from blowdown of the upper phase from the last contact ( $R_4$ ) was substantially lighter in color than the original oil, and the carbon number distribution for that sample reflects the smaller amount of heavy ends ( $C_{36+}$ ) in the sample. Apparently, the amount of  $C_{36+}$  extracted decreased as the amount  $C_5$ - $C_{18}$  hydrocarbons present in the upper phase decreased. The amount of  $C_5$ - $C_{18}$  hydrocarbons in

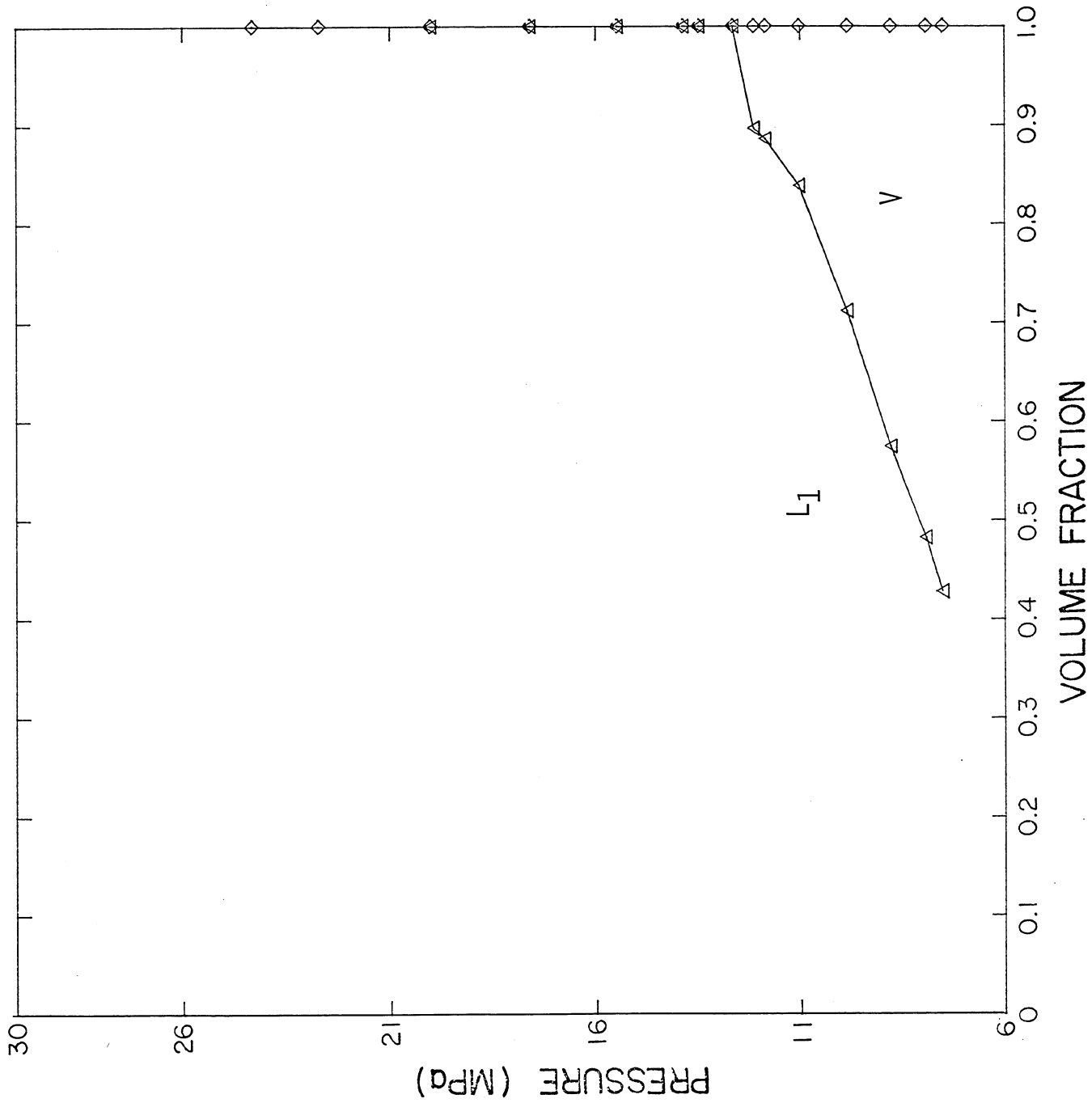


Figure 3.13 Volumetric behavior of mixture F<sub>2</sub>.

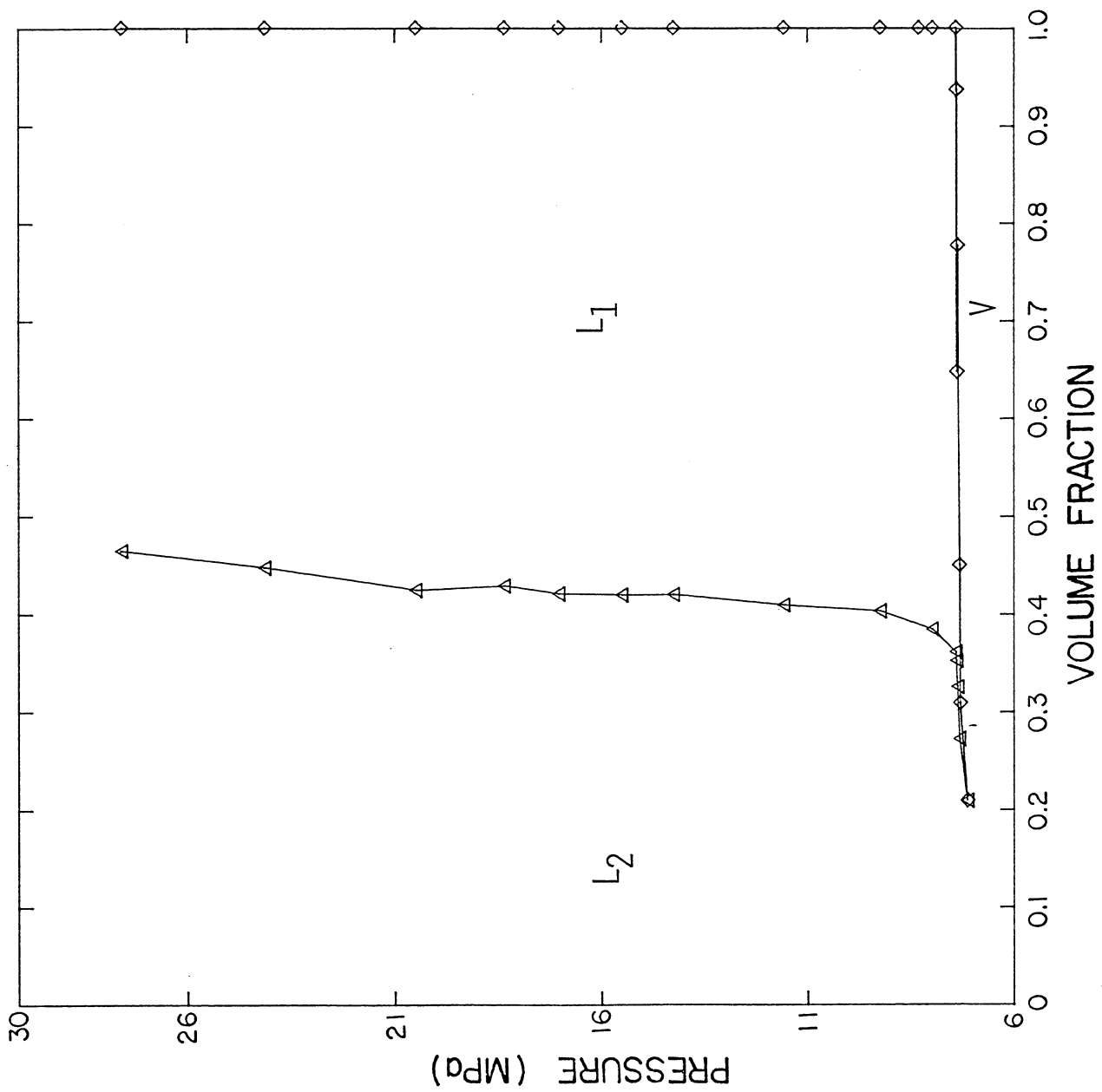


Figure 3.14 Volumetric behavior of mixture R<sub>1</sub>.

Table 3.6 Compositions of Gas Samples Recovered During  
Blowdown of Reverse Contact Upper Phases  
(Mol Percent)

<u>Component</u>	<u>R<sub>1</sub></u>	<u>R<sub>2</sub></u>	<u>R<sub>3</sub></u>	<u>R<sub>4</sub></u>
CO <sub>2</sub>	94.663	98.252	99.332	99.726
C <sub>1</sub>	2.834	0.809	0.272	0.104
C <sub>2</sub>	1.121	0.389	0.150	0.062
C <sub>3</sub>	0.967	0.365	0.157	0.062
C <sub>4</sub>	0.415	0.183	0.089	0.045
	<u>100.00</u>	<u>100.00</u>	<u>100.00</u>	<u>100.00</u>

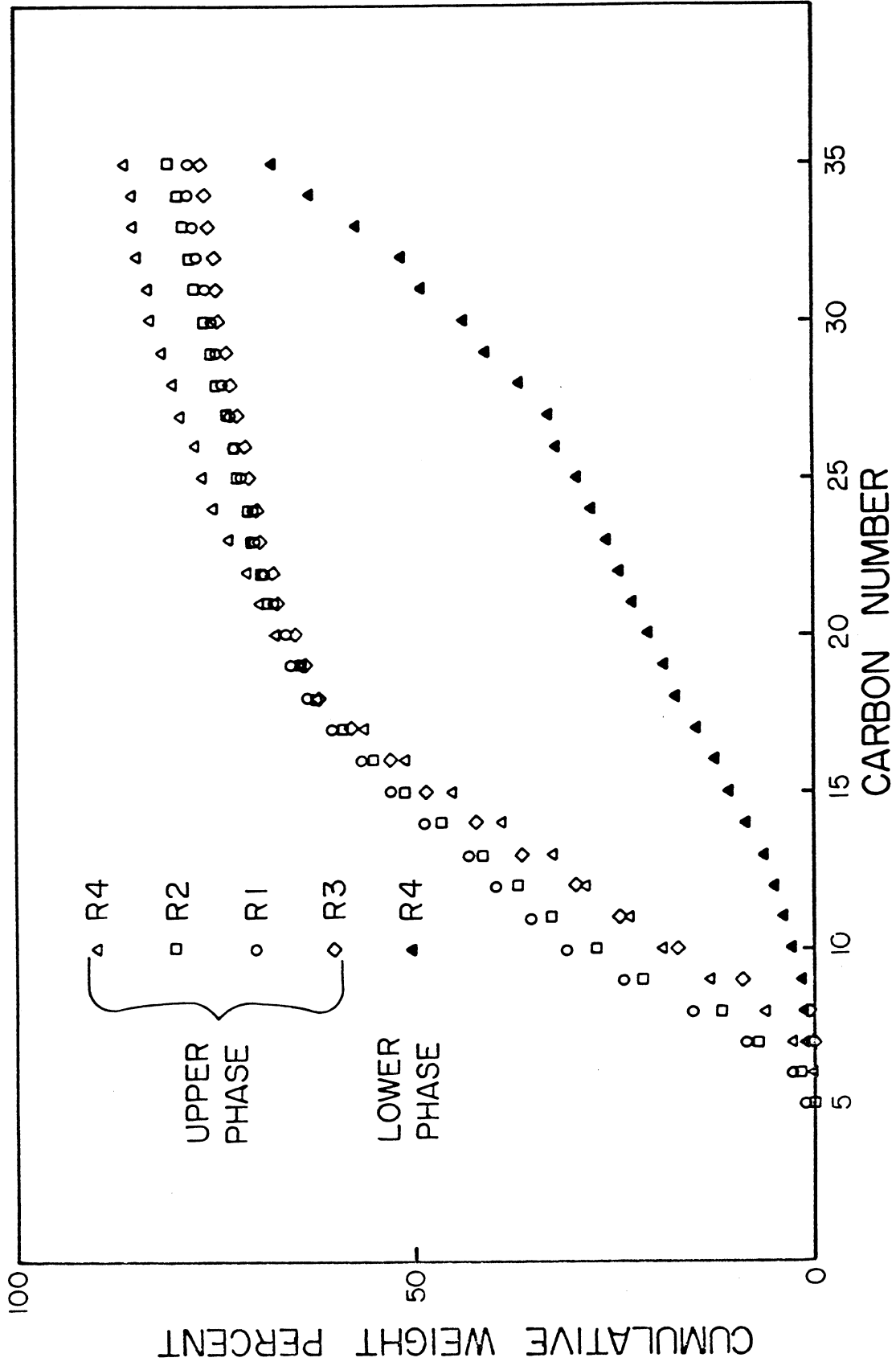


Figure 3.15 Compositions of blowdown liquids from mixtures R<sub>1</sub>-R<sub>4</sub>.

the upper phase decreased because previous contacts had removed most of the hydrocarbons in that range.

The composition of the liquid remaining after blowdown of the R<sub>4</sub> lower phase (Figure 3.15) clearly shows the effects of repeated preferential extraction of the lighter hydrocarbons. That oil was much heavier and much more viscous than the original oil because substantial quantities of the hydrocarbons over the entire molecular weight range were extracted, though, of course, lighter hydrocarbons were extracted more effectively.

### Results of Mixing Cell Displacements

In a CO<sub>2</sub> flood, the compositions of the phases that are present at a point in the flow system are the result of a continuous contacting process rather than a batch multiple contact process such as that described above. As the transition zone passes that point, the overall composition of the mixture present there will change continuously from mostly oil to mostly CO<sub>2</sub>. As Figure 3.15 indicates, the composition of the hydrocarbons extracted also varies as the transition zone passes. When the CO<sub>2</sub>-rich phase first appears, it is rich in the light and intermediate hydrocarbons extracted from the oil in contacts which occurred upstream of the point in question. Continued extraction of hydrocarbons leaves an oil which becomes steadily heavier. In addition, the total amount of hydrocarbons extracted changes with transition zone passage. Amounts of hydrocarbons extracted were measured in two experiments in which Maljamar separator oil was displaced by CO<sub>2</sub> from a visual cell (see §2.2) at 32.2°C (90°F). CO<sub>2</sub> was injected at 5 cm<sup>3</sup>/hr into the bottom of the cell, and samples were produced from the top of the cell. Contents of the cell were agitated only by the bubbles of injected CO<sub>2</sub> rising through the cell.

Figure 3.16 reports the weight fraction of oil in samples produced from the top of the cell for displacements conducted at 7308 and 8274 kPa (1060 and 1200 psi). Produced gas compositions were not measured in those experiments.

The weight fractions plotted in Figure 3.16 were calculated as the ratio of the weight of liquid sample produced to the sum of the weights of gas and liquid produced. Later experiments indicated that the gas contained 2-4 mol % hydrocarbons. In addition, because the cell contents were not agitated, the phases present may not have been in "chemical" equilibrium. Thus, the results shown in Figure 3.16 should be viewed as approximate rather than firm quantitative determinations of the extraction of hydrocarbons from crude oil.

In both displacements, the CO<sub>2</sub> injected initially dissolved completely in the oil. Hence, the weight fraction of oil in the produced fluid declined from one as the concentration of dissolved CO<sub>2</sub> rose. When the solubility of CO<sub>2</sub> in the oil was reached, a second phase appeared at the top of the cell. In the displacement at 8274 kPa (1200 psi), a second phase, light yellow in color, appeared in the cell at about 0.6 cell

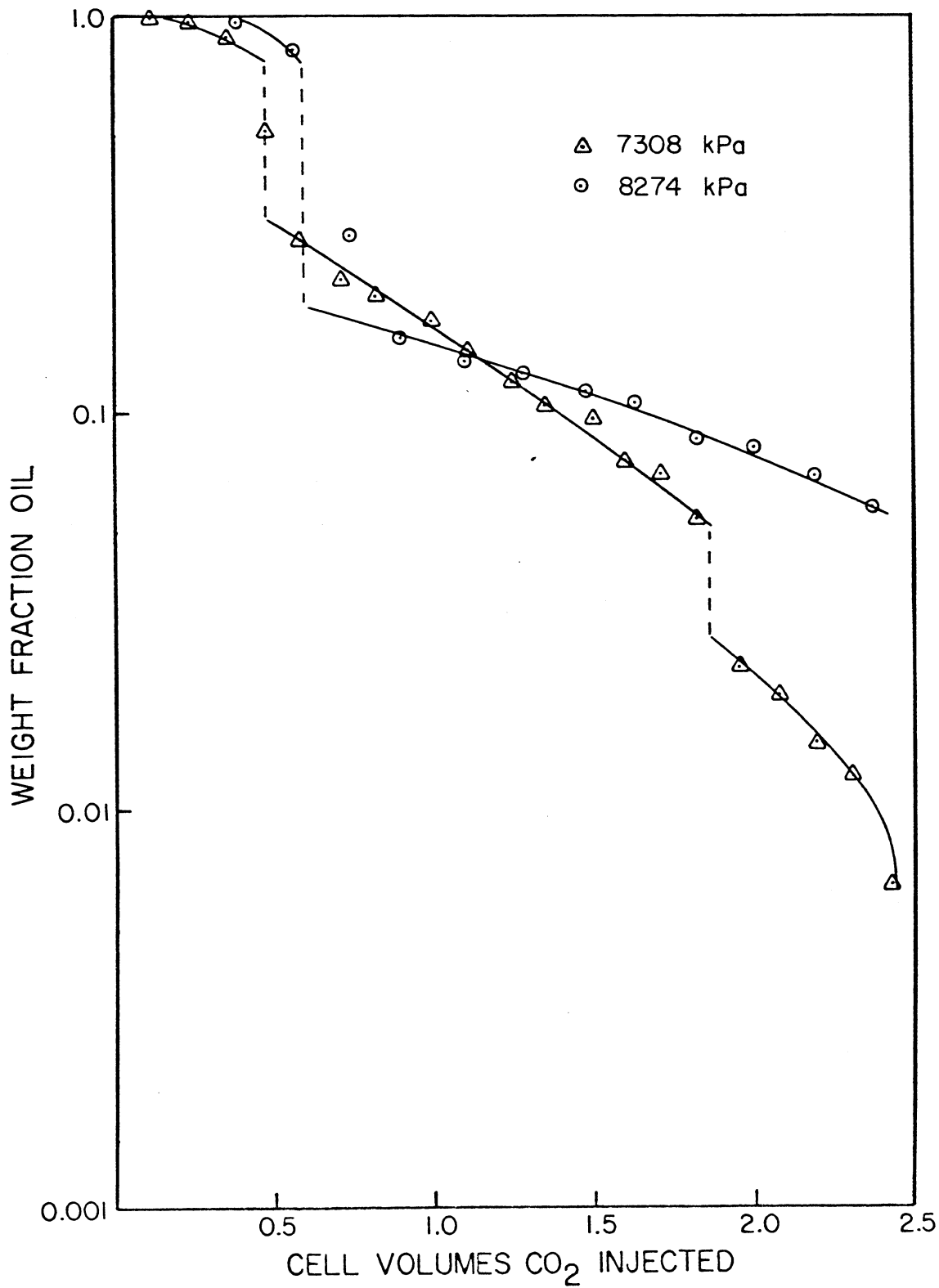


Figure 3.16 Weight fraction of hydrocarbons extracted by CO<sub>2</sub> from Maljamar separator oil at 32.2°C (90°F).

volumes injected. As Figure 3.9 indicates, the second phase was a CO<sub>2</sub>-rich liquid phase. At that point, the weight fraction of oil in the produced fluid dropped sharply because the new phase was richer in CO<sub>2</sub> than the single phase mixture present just prior to the phase split. Then, as CO<sub>2</sub> injection continued, the weight fraction of oil extracted into the CO<sub>2</sub>-rich phase declined slowly as the light and intermediate hydrocarbons were removed from the mixture in the cell.

Similar behavior was observed in the displacement at 7308 kPa (1060 psi). A second liquid phase appeared at about 0.48 cell volumes injected. The amount of hydrocarbons extracted dropped sharply at that point and then declined slowly until about 1.85 cell volumes injected when the amount extracted dropped sharply again. The second step change in the weight fraction of oil in the produced fluid coincided with the appearance of a vapor phase at the top of the cell. Thus, the coexistence of two liquids and a vapor, observed in the single contact phase behavior study (see Figure 3.9), was also observed in the continuous displacement of oil from the mixing cell.

The results for the 7308 kPa (1060 psi) displacement indicate clearly that the less dense vapor phase extracted hydrocarbons less efficiently than the CO<sub>2</sub>-rich liquid phase. The data in Figure 3.16 confirm directly, therefore, the argument given by Orr et al. (1980a) that the vapor phase must be richest in CO<sub>2</sub> for a CO<sub>2</sub>-separator oil system (see Appendix A for a detailed discussion of the reasons for that behavior). Similar results were obtained in static equilibrium measurements of phase compositions for mixtures of CO<sub>2</sub> with well-characterized hydrocarbon mixtures. Details are given in Appendix B.

Compositions of hydrocarbon liquids produced during the 8274 kPa (1200 psi) run were analyzed by simulated distillation (§2.3). The composition of the sample taken at 0.38 cell volumes should have been and was close to that of the original oil (minus a small amount of light ends stripped off in the separator by the flashed CO<sub>2</sub>). Produced samples taken later in the run were upper phase samples. The compositions of the other samples again give direct evidence of the depth of extraction by CO<sub>2</sub>, since the hydrocarbons collected were those in the upper liquid phase only. Substantial quantities of components heavier than C<sub>36</sub> were found even in samples taken late in the run, though, of course, the light and intermediate hydrocarbons were extracted more efficiently as the composition of the oil remaining in the cell after completion of the experiment shows. The trend of hydrocarbon compositions shown in Figure 3.17 agrees well with that observed for slim tube displacements (Figures 3.6 and 3.7) and for the batch multiple contact experiment (Figure 3.15).

#### Measurement of Phase Compositions by Continuous Multiple Contacts

The mixing cell displacements discussed above provided clear qualitative evidence of the extractive properties of CO<sub>2</sub>, but the results of phase composition calculations suggested that the fluids in the cell were

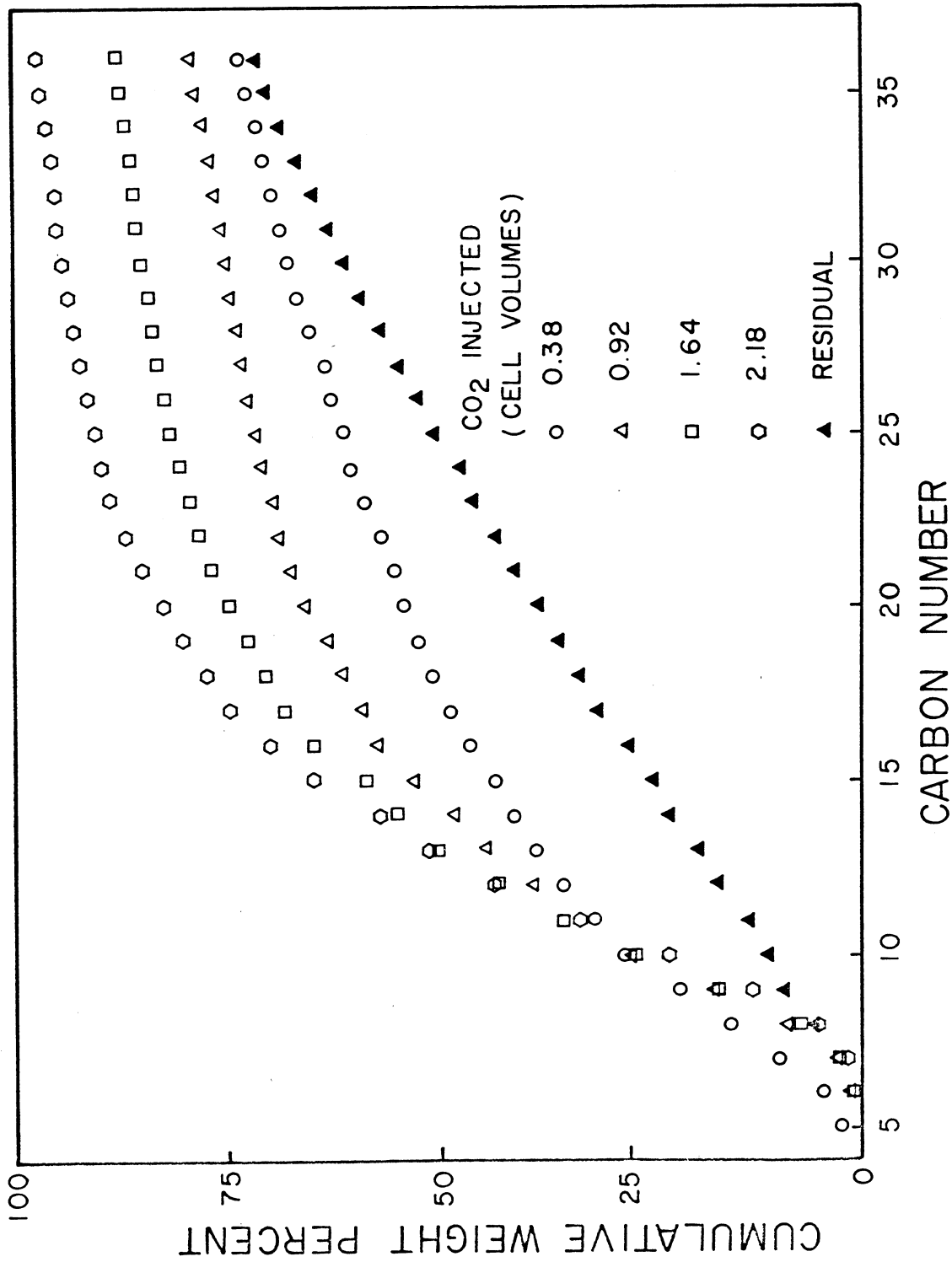


Figure 3.17 Compositions of hydrocarbons produced during displacement of Maljamar separator oil from a mixing cell at 8274 kPa (1200 psi) and 32.2°C (90°F).

not well enough mixed to be in chemical equilibrium. Accordingly, a new apparatus was designed (see Figure 2.8) which provided much better mixing by circulating the fluids in the cell. In addition, samples were taken from both the top and the bottom of the cell, so that equilibrium phase compositions could be determined. Design of the apparatus, operating procedures, and experiments performed to test the apparatus are discussed in detail in §2.2.

Maljamar separator oil was displaced in a continuous multiple contact experiment at 8274 kPa (1200 psi) and 32.2°C (90°F). Results of that experiment are summarized in Table 3.7 and Figures 3.18-3.21. Figure 3.18 reports gas-oil ratio (GOR) data for upper and lower samples. The GOR is expressed as weight of gas to weight of liquid because weights of liquid samples could be measured much more accurately than volumes. As in the mixing cell displacement described above, the first CO<sub>2</sub> injected dissolved completely in the oil. At the displacement conditions, CO<sub>2</sub> was quite soluble in the oil. Figure 3.9 indicates that mixtures can contain up to about 74 mol % CO<sub>2</sub> at 8274 kPa (1200 psi). Thus, early in the run, the samples produced from the top and bottom of the cell were the same single phase mixture. The appearance of the second liquid phase in the mixing cell was detected two ways. First, an LED and a photo-transistor mounted in the sight glass at the top of the cell showed a sharp change in the intensity of light transmitted through the upper sample flowing through the sight glass. Second, a step change was observed in the gas-oil ratio of the upper sample, as shown in Figure 3.18. The appearance of the second phase, which was much richer in CO<sub>2</sub>, caused an immediate increase in the amount of gas produced with the upper phase sample, and a corresponding decrease in the amount of oil produced. A material balance calculation indicated that the second phase appeared when the CO<sub>2</sub> mole fraction in the vessel was 0.736 which agrees well with previous single contact equilibrium measurements.

As the run progressed, the GOR of the lower phase samples decreased. As CO<sub>2</sub> stripped more and more of the intermediate hydrocarbons from the oil remaining in the lower phase, the solubility of the CO<sub>2</sub> in the remaining hydrocarbons also declined. There was a corresponding increase in the upper phase GOR as the amount of intermediate hydrocarbons available to be extracted declined. Liquid hydrocarbon samples collected from the upper phase became steadily lighter in color during the course of the run. Samples collected shortly after the phase change were a clear yellow color while those collected near the end of the run were nearly colorless. The lower phase liquid samples, on the other hand, became steadily heavier and more viscous, as the fraction of intermediate hydrocarbons in the lower phase decreased. The composition trends are summarized in Figure 3.19 which shows average molecular weights of the upper and lower phases calculated from compositional analyses of gas and liquid samples produced for each phase. Calculated molecular weights of upper phase samples declined rapidly and then stayed roughly constant while those of lower phase samples climbed throughout the displacement.

Table 3.7 Compositions (Weight Percent) of Fluids Produced in a Continuous Multiple Contact Displacement of Maljamar Separator Oil

Component	Original Oil	SAMPLES AT 1.57 CELL VOLUMES INJECTED					
		Lower Phase			Upper Phase		
		Liquid	Gas	Overall	Liquid	Gas	Overall
CO <sub>2</sub>			93.30	20.11		93.30	82.44
C <sub>2</sub>	] 2.18		0.06	0.01		0.06	0.05
C <sub>3</sub>							
C <sub>4</sub>			0.29	0.06		0.29	0.26
C <sub>5</sub>		0.13	1.14	0.35	0.06	1.14	1.01
C <sub>6</sub>	2.52	0.62	2.62	1.05	1.02	2.62	2.44
C <sub>7</sub>	4.49	1.72	2.59	1.90	3.97	2.59	2.75
C <sub>8</sub>	7.33	3.22		2.53	9.09		1.06
C <sub>9</sub>	5.83	3.34		2.62	10.53		1.22
C <sub>10</sub>	4.75	2.99		2.35	9.20		1.07
C <sub>11</sub>	3.62	2.46		1.93	6.65		0.77
C <sub>12</sub>	3.95	2.92		2.29	6.86		0.80
C <sub>13</sub>	3.42	2.78		2.18	5.66		0.66
C <sub>14</sub>	2.93	2.42		1.90	4.27		0.50
C <sub>15</sub>	3.03	2.69		2.11	4.15		0.48
C <sub>16</sub>	3.46	3.30		2.59	4.38		0.51
C <sub>17</sub>	2.21	2.13		1.67	2.54		0.30
C <sub>18</sub>	2.24	2.23		1.75	2.36		0.27
C <sub>19</sub>	1.98	2.07		1.63	1.90		0.22
C <sub>20</sub>	2.45	2.66		2.09	2.11		0.25
C <sub>21</sub>	1.90	2.14		1.68	1.48		0.17
C <sub>22</sub>	1.35	1.58		1.24	0.98		0.11
C <sub>23</sub>	1.83	2.18		1.71	1.25		0.15
C <sub>24</sub>	1.74	2.12		1.66	1.10		0.13
C <sub>25</sub>	1.70	2.15		1.68	1.07		0.12
C <sub>26</sub>	1.13	1.48		1.16	0.70		0.08
C <sub>27</sub>	1.65	2.21		1.73	0.99		0.12
C <sub>28</sub>	1.11	1.50		1.18	0.65		0.08
C <sub>29</sub>	1.13	1.57		1.23	0.66		0.08
C <sub>30</sub>	1.11	1.57		1.23	0.66		0.08
C <sub>31</sub>	1.08	1.57		1.23	0.70		0.08
C <sub>32</sub>	1.06	1.59		1.25	0.75		0.09
C <sub>33</sub>	1.03	1.58		1.24	0.80		0.09
C <sub>34</sub>	1.03	1.61		1.26	0.87		0.10
C <sub>35</sub>	.97	1.53		1.20	0.87		0.10
C <sub>36</sub>	.88	1.40		1.10	0.85		0.10
C <sub>37+</sub>	22.91	34.54		27.10	10.87		1.26
Ave. Mole Wt.		279.96	45.48	132.64	183.83	45.48	49.83
Wt. Percent		78.46	21.54	100.00	11.62	88.38	100.00

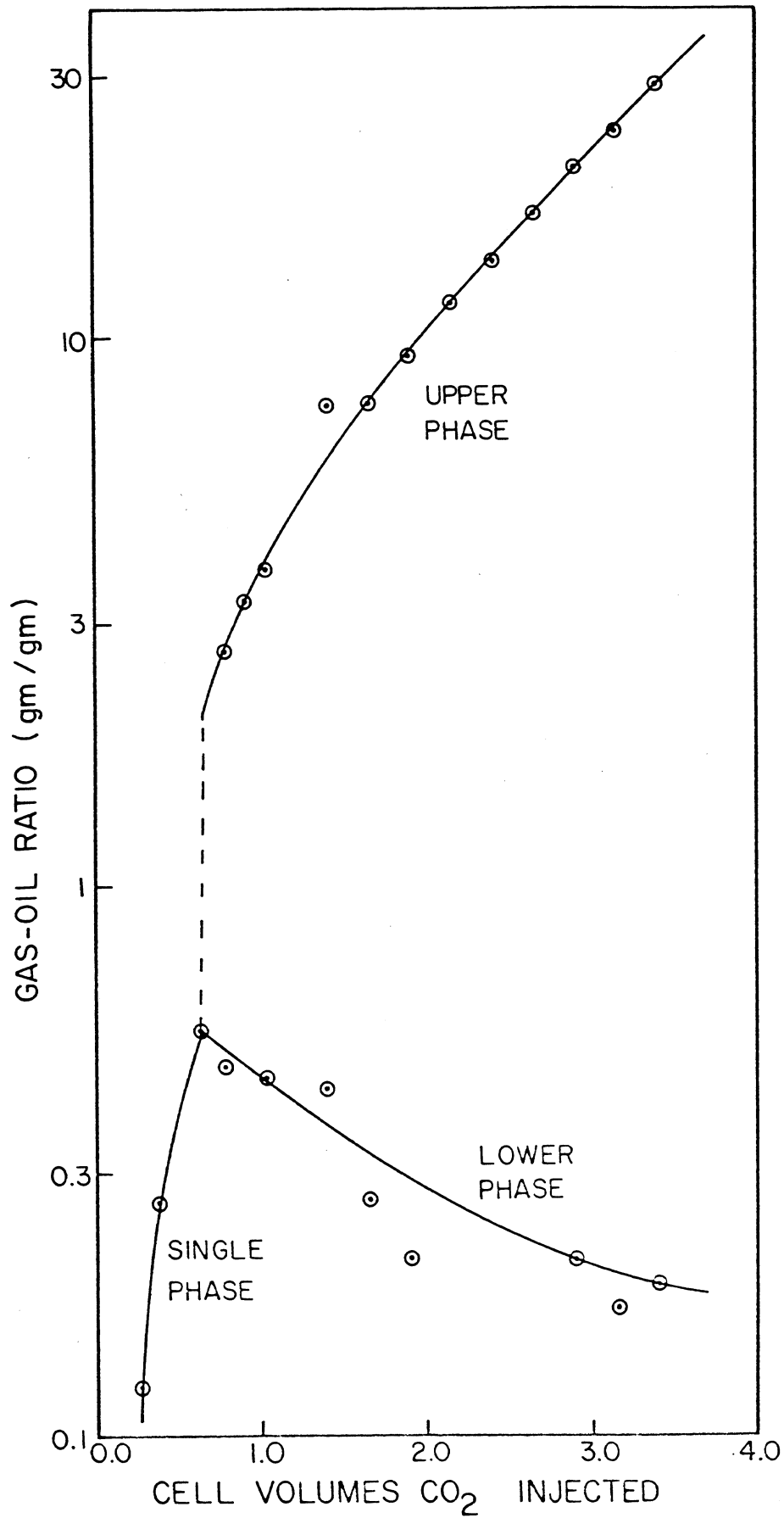


Figure 3.18 Weight ratio of gas to oil production in a continuous multiple contact displacement of Maljamar separator oil at 8274 kPa (1200 psi) and 32.2°C (90°F).

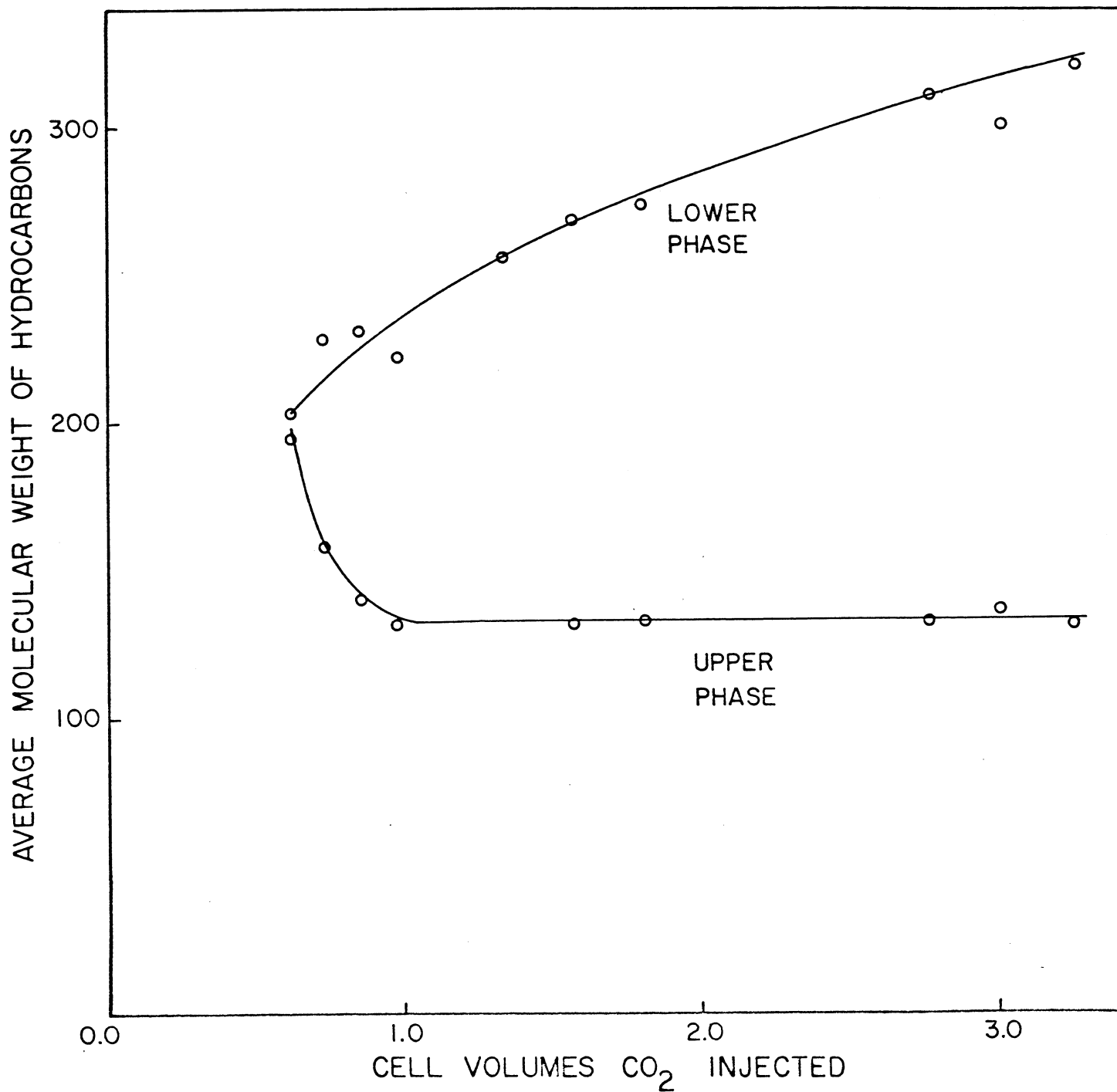


Figure 3.19 Calculated molecular weights of hydrocarbons produced in upper and lower phase samples.

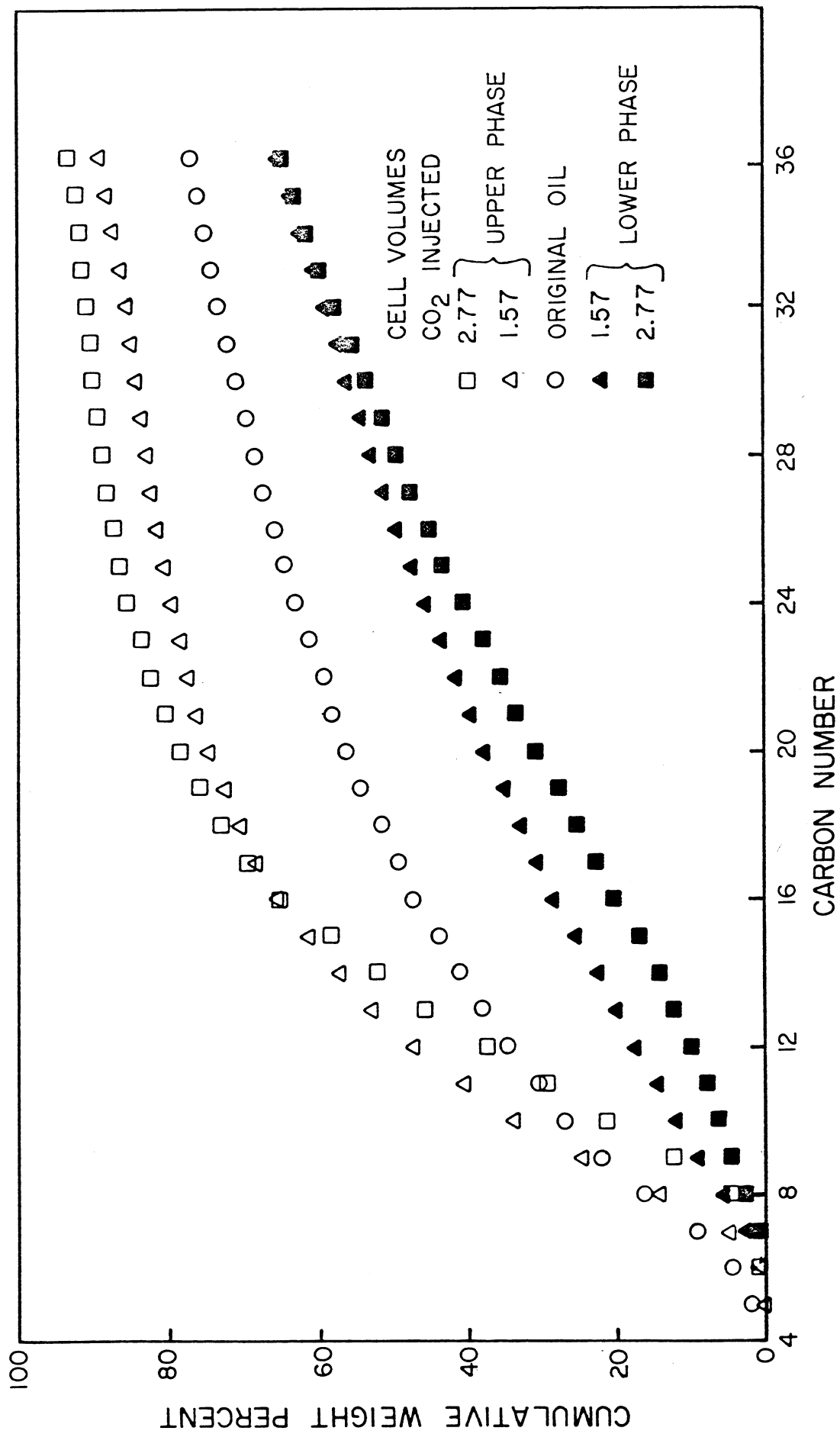


Figure 3.20 Compositions of liquids collected from upper and lower phase samples.

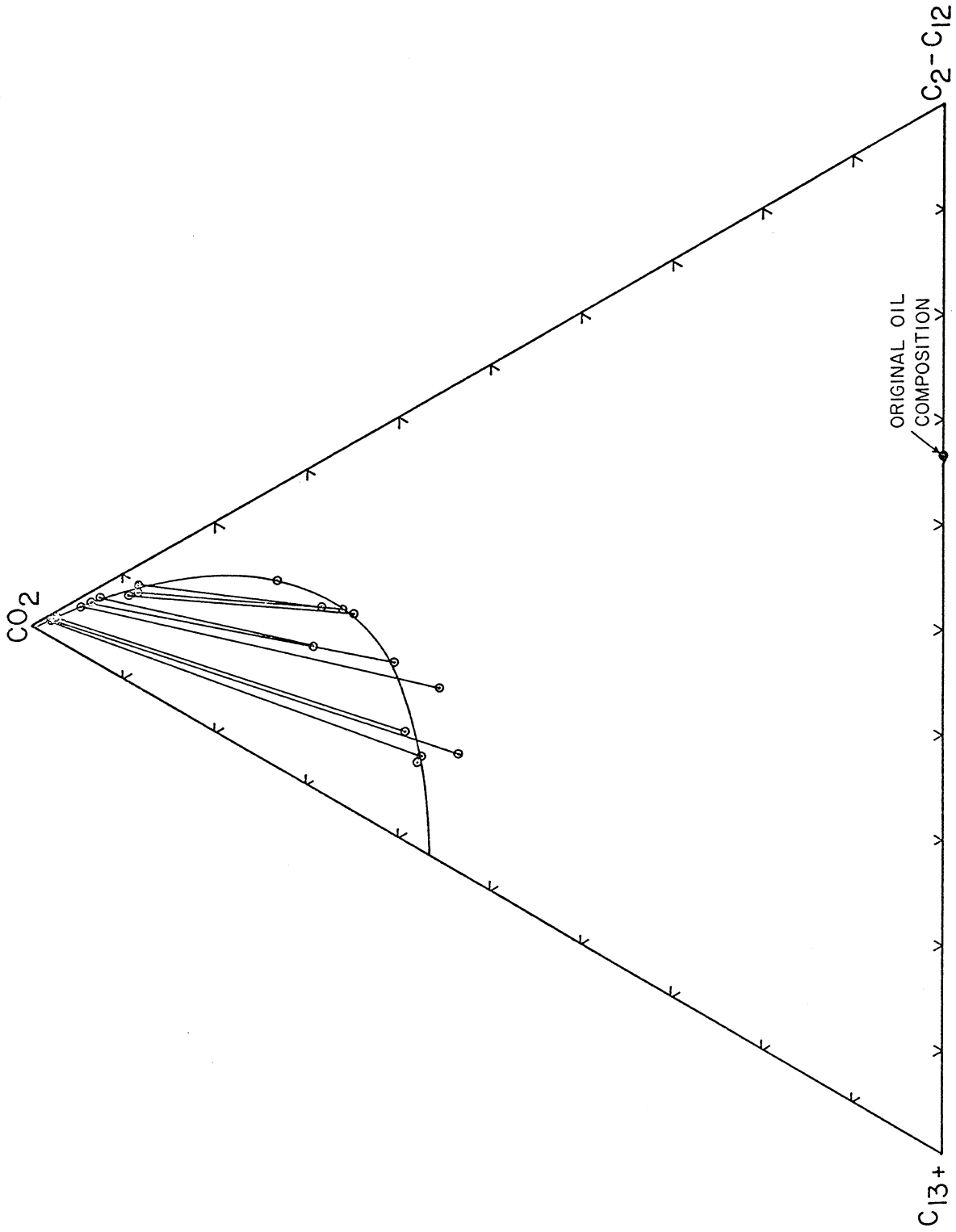


Figure 3.21 Pseudo-ternary phase diagram (in mole fractions) for CO<sub>2</sub> and Maljamar separator oil at 8274 kPa (1200 psi) and 32.2°C (90°F).

Figure 3.20 compares the composition of the original oil with compositions of liquid hydrocarbon samples collected from the produced upper and lower phase samples. Again, the trend is clear. Hydrocarbons in the C<sub>5</sub>-C<sub>20</sub> range are extracted preferentially into the CO<sub>2</sub>-rich liquid phase. The hydrocarbons produced in the upper phase became lighter with continued injection while those produced in the lower phase became heavier.

Figure 3.21 shows a pseudo-ternary plot of phase compositions and tie lines for the CO<sub>2</sub>-Maljamar separator oil system. The mole fractions shown in Figure 3.21 were calculated from the weight fraction data obtained by chromatography by assigning the molecular weight of the appropriate normal alkane to each carbon number cut. The molecular weight of the C<sub>37+</sub> fraction was assumed to be that of C<sub>40</sub>. Since gas samples were not analyzed for the lower phase, the analysis of the gas from the corresponding upper phase sample was used as an estimate of the gas composition from the lower phase. Produced gas compositions varied from about 95 to 99 mol % CO<sub>2</sub> during the run, and since the amount of gas produced with lower phase samples was relatively small, the lower phase compositions were not strongly affected by this assumption. Typical composition results are given in Table 3.7 for the original oil and upper and lower phase samples taken at 1.57 cell volumes CO<sub>2</sub> injected. Detailed compositions were then lumped as C<sub>2</sub>-C<sub>12</sub> and C<sub>13+</sub> pseudo-components for the plot shown in Figure 3.21.

The results for lower phase compositions presented in Figure 3.21 show substantial scatter. The principal cause of that scatter was the fact that the viscosity of the lower phase increased dramatically as the run progressed. This caused the production of lower phase across the metering valve to decrease when the apparatus was running unattended. The resulting gas volumes were too small to determine accurately. Design of a modification of the apparatus which will alleviate that problem has been completed. Even with the scatter in the lower phase composition data, the results shown in Figure 3.21 establish that equilibrium phase compositions can be obtained much more rapidly in a continuous experiment than in static equilibrium experiments. The continuous experiment has several additional advantages over single contact phase equilibrium studies. It reaches portions of the phase diagram which are difficult to investigate in single contact experiments. Samples need not be maintained at high pressure, and the results are not sensitive to the production rates of the two phases. In addition, density data could be obtained simultaneously if a high pressure densitometer such as the Mettler/Paar DMA 512 were installed in the sample lines ahead of the back pressure regulator or metering valve. It may also be possible to measure phase viscosities. Thus, the continuous multiple contact experiment offers a technique for measuring phase composition, and at least some fluid properties, which is much more efficient, and, therefore, less expensive than more standard static equilibrium experiments.

## Discussion

A variety of results have been presented which show clearly that CO<sub>2</sub> extracts hydrocarbons of a broad range in molecular weights if the pressure is high enough. Results of the mixing cell displacements and the continuous multiple contact experiments indicate that amounts of hydrocarbons extracted increase as the pressure increases and that substantially more extraction occurs when the CO<sub>2</sub>-rich phase is a liquid rather than a vapor. Furthermore, for the crude oil studied here, the "minimum miscibility pressure," as determined in slim tube displacements, was high enough that the CO<sub>2</sub>-hydrocarbon mixtures formed two liquid phases rather than liquid-vapor mixtures. That behavior is consistent with the idea that CO<sub>2</sub> extracts hydrocarbons more efficiently when the density of the CO<sub>2</sub>-rich phase is close to that of the oil. Holm and Josendal (1980) have argued persuasively that minimum miscibility pressures correlate well with the pressure required to make the CO<sub>2</sub> density "close enough" to that of the oil. The results presented here provide both quantitative and qualitative evidence to support that view. Accordingly, the simple correlation given by equation (3.3) can be used as a preliminary estimate of the minimum miscibility pressure for low temperature (below 50°C) CO<sub>2</sub> floods.

It can be argued that the presence of three phases might be beneficial if mutual interference to flow provided some mobility control (Metcalf and Henry 1980). For instance, some evidence of higher resistance of flow was observed in the slim tube displacement at 6890 kPa (1000 psi) which passed through the L<sub>1</sub>-L<sub>2</sub>-V region (see Figures 3.1, 3.2 and 3.9). Nevertheless, resistance to flow is not the only requirement. Phase behavior must be sufficiently favorable as well. The slim tube displacement at 5520 kPa (800 psi) also showed larger pressure drops than the two high pressure displacements because a large residual oil saturation was left behind, but hydrocarbon extraction was not efficient and the displacement yielded low recovery. While not conclusive, the results of the slim tube displacements considered here suggest that the possible benefits of mobility control from three phases are outweighed by the loss of effectiveness of extraction. It seems reasonable therefore to choose operating pressures so that the presence of a highly mobile vapor phase is avoided. Equation 3.3 gives a simple way to make that choice. Considerable evidence has been presented here that development of multiple contact miscibility in low temperature CO<sub>2</sub> floods occurs through extraction of hydrocarbon by a CO<sub>2</sub>-rich liquid phase. This view is not universally held, however. Metcalfe and Yarborough argued that a condensation mechanism generates miscible displacements when two liquid phases occur. They suggested that condensation of CO<sub>2</sub> into the oil in place created a phase which could then be miscibly displaced by injected CO<sub>2</sub>. Their argument was based on phase equilibrium and core displacement experiments with a synthetic oil containing components C<sub>1</sub>-C<sub>14</sub>. The oil was too light and their experimental temperature too high, however, to produce the liquid-liquid separations which will be the rule for CO<sub>2</sub>-crude oil mixtures in the low temperature reservoirs of New Mexico, West Texas and West Virginia (see Appendix A).

Experiments in our laboratory proved that liquid-liquid separations do occur for synthetic oils if the oil contains enough heavy components (see Appendix B for details of those experiments). Experiments with a synthetic oil which better modeled crude oil behavior would be appropriate if conclusions are to be drawn from such experiments concerning CO<sub>2</sub>-crude oil displacement mechanisms. In any case, the direct experimental evidence presented here for CO<sub>2</sub>-crude oil mixtures argues strongly that extraction of hydrocarbons by CO<sub>2</sub> generates an efficient displacement in low temperature CO<sub>2</sub> floods by a mechanism similar to that described by Hutchinson and Braun (1961) and Rathmell et al. (1971) for vapor-liquid systems.

### 3.4 Summary and Conclusions for Task 2

Results of displacement experiments have been presented which include not only oil recovery data but also extensive data on the compositions of produced fluids. In addition, results of extensive phase behavior and fluid property measurements, necessary for detailed interpretation of displacement tests, have been given. Specific conclusions drawn from the results presented above are:

- (1) CO<sub>2</sub> is only partially miscible with crude oil at typical reservoir conditions. CO<sub>2</sub>-crude oil mixtures will separate into two liquid phases at high pressure (and high CO<sub>2</sub> concentration) if the temperature is below about 50°C (120°F).
- (2) Liquid-liquid-vapor phase behavior occurs in CO<sub>2</sub>-crude oil systems at temperatures below about 120°F at pressures near the vapor pressure (extrapolated if necessary) of CO<sub>2</sub> at the system temperature.
- (3) Available data for CO<sub>2</sub>-crude oil systems indicate that liquid-liquid phase behavior will occur if the pressure exceeds the vapor pressure of CO<sub>2</sub> by about 1750 kPa (250 psi).
- (4) Synthetic oils composed of alkanes can be found which exhibit liquid-liquid and liquid-liquid-vapor phase behavior qualitatively similar to that observed for CO<sub>2</sub>-crude oil systems if sufficient quantities of components heavier than C<sub>14</sub> are present.
- (5) If CO<sub>2</sub>-rich liquid and vapor phases coexist, the liquid phase extracts hydrocarbons from crude oil more efficiently than the vapor.

- (6) Comparison of measurements of compositions of produced fluids in slim tube displacements with those of static and dynamic phase behavior experiments, indicates that efficient displacement occurs when extraction of hydrocarbons by CO<sub>2</sub> is also efficient.
- (7) Comparison of slim tube displacement results with those of core flood and mixing cell displacements indicates that the scale over which mixing occurs strongly influences displacement efficiency.
- (8) Slim tube displacements are more efficient than core floods because a transition zone long enough to stabilize the otherwise unstable displacement develops in the inlet region of the slim tube.
- (9) Viscous fingering not only reduces sweep efficiency, but also reduces displacement efficiency in the swept zone because it increases the volume scale on which mixing occurs and therefore reduces the effectiveness of the extraction of hydrocarbons by the CO<sub>2</sub>-rich displacing phase.
- (10) The continuous multiple contact experiment is an effective technique for rapid measurement of CO<sub>2</sub>-crude oil phase equilibrium data.

#### 4. TASK 3. MATHEMATICAL MODELING OF CO<sub>2</sub> DISPLACEMENTS

Numerical simulation of tertiary oil recovery processes is an essential feature of current research on such techniques and of methods for evaluation of field scale floods. Completely scaled experiments, in which rock and fluid properties are chosen to reflect the balance of physical forces which will occur in a reservoir displacement, are a practical impossibility when the effects of complex exchanges of components between flowing phases must be included. Scale-up of laboratory experiments to field predictions must rely, therefore, on detailed calculations of the effects of competing physical phenomena: compositional effects on phase densities and viscosities, rock-fluid interactions such as wetting behavior, phase relative permeabilities and dispersion, and the resultant convection of components at different rates. Such calculations can only be performed by computer simulation of the process.

A one-dimensional process simulator designed for carbon dioxide (CO<sub>2</sub>) flooding applications is described in detail in a separate report (Orr 1980c). The simulator follows convection of four components, three of which enter into phase equilibrium calculations for up to three phases containing hydrocarbons and CO<sub>2</sub>. The fourth component is water which appears only in a separate phase. Material balance equations for the four components are solved by a fully explicit finite difference method which allows the use of numerical dispersion to simulate the effect of physical dispersion, which is not modeled explicitly.

The calculations performed in the simulator are based on the following assumptions:

- (1) Darcy's law describes the flow of each of up to four phases.
- (2) The flow system has uniform cross-section and properties and fluids are uniform and well mixed in the direction transverse to flow.
- (3) Capillary pressure effects are negligible.
- (4) Local chemical equilibrium exists between phases.
- (5) There is no volume change on mixing.
- (6) Changes in pressure over the length of the displacement have negligible effect on the phase behavior of the hydrocarbon-CO<sub>2</sub> mixtures.
- (7) CO<sub>2</sub>-crude oil phase behavior can be represented in terms of three components: CO<sub>2</sub>, light hydrocarbons, and heavy hydrocarbons.

These assumptions are similar to those made by Pope and Nelson (1978) in their development of a one-dimensional compositional simulator for surfactant flooding applications.

Assumption (1) carries with it the assumption that relative permeabilities can be calculated for the water phase and the three CO<sub>2</sub>-hydrocarbon phases (two liquids and a vapor) which sometimes occur for CO<sub>2</sub>-crude oil mixtures. Stone's model (1973) was used to calculate relative permeabilities for three phase systems and a simple extension, in which the two phases closest in composition shared in proportion to their saturations the relative permeability of one phase (see Orr 1980c for details), was used for four phase systems.

Assumption (2) is a statement that the flow is one-dimensional. Thus, the simulator does not model viscous fingering or gravity segregation. While capillary pressures for oil-water systems are well known, those for multiphase CO<sub>2</sub>-hydrocarbon systems are not, and hence, are not modeled here (Assumption (3)). Assumption (4) is reasonable for secondary displacements but may be less so if trapped oil droplets are shielded by water films (Raimondi et al. 1961, Stalkup 1970, Shelton and Schneider 1975). Assumption (5) is reasonable if the pressure is high enough that the density of CO<sub>2</sub> is not too different from that of the oil. The work of Holm and Josendal (1980) and the results presented here (see §3.3) suggest that for pressures near and above the minimum miscibility pressure, assumption (5) is acceptable. Assumptions (6) and (7) simplify representation of phase behavior. The limitations of a ternary representation of CO<sub>2</sub>-crude oil phase behavior have been discussed by Gardner et al. (1979). Results given below indicate that the representation is remarkably successful given its simplicity.

#### 4.1 Validation of the Simulator

Extensive experiments to test the validity of the one-dimensional simulator were performed by Pongpitak (1980). He compared displacement results in a bead pack with simulations for a ternary system of oil (isooctane, IC<sub>8</sub>), brine (2 wt % CaCl<sub>2</sub>), and alcohol (isopropanol, IPA). The ternary phase diagram for this system is shown in Figure 2.9. Figures 4.1 and 4.2 show typical comparisons of experimental results with simulation results. Figure 4.1 compares simulation with experimental results for a displacement of a 50 vol % IPA-50 vol % brine mixture by IC<sub>8</sub>. That displacement was not miscible (see Figure 2.9), but extraction of IPA by the IC<sub>8</sub> produced better recovery for IPA than brine. Agreement between experimental and calculated results was excellent. Figure 4.2 gives similar results for a run in which IC<sub>8</sub> displaced an 85-15 vol % mixture of IPA and brine. In that run, sufficient IPA was present that extraction of IPA by IC<sub>8</sub> came close to generating a miscible displacement and the recovery of both brine and IPA was substantially better than that shown in Figure 4.1. Again, agreement between calculation and experiment was very good.

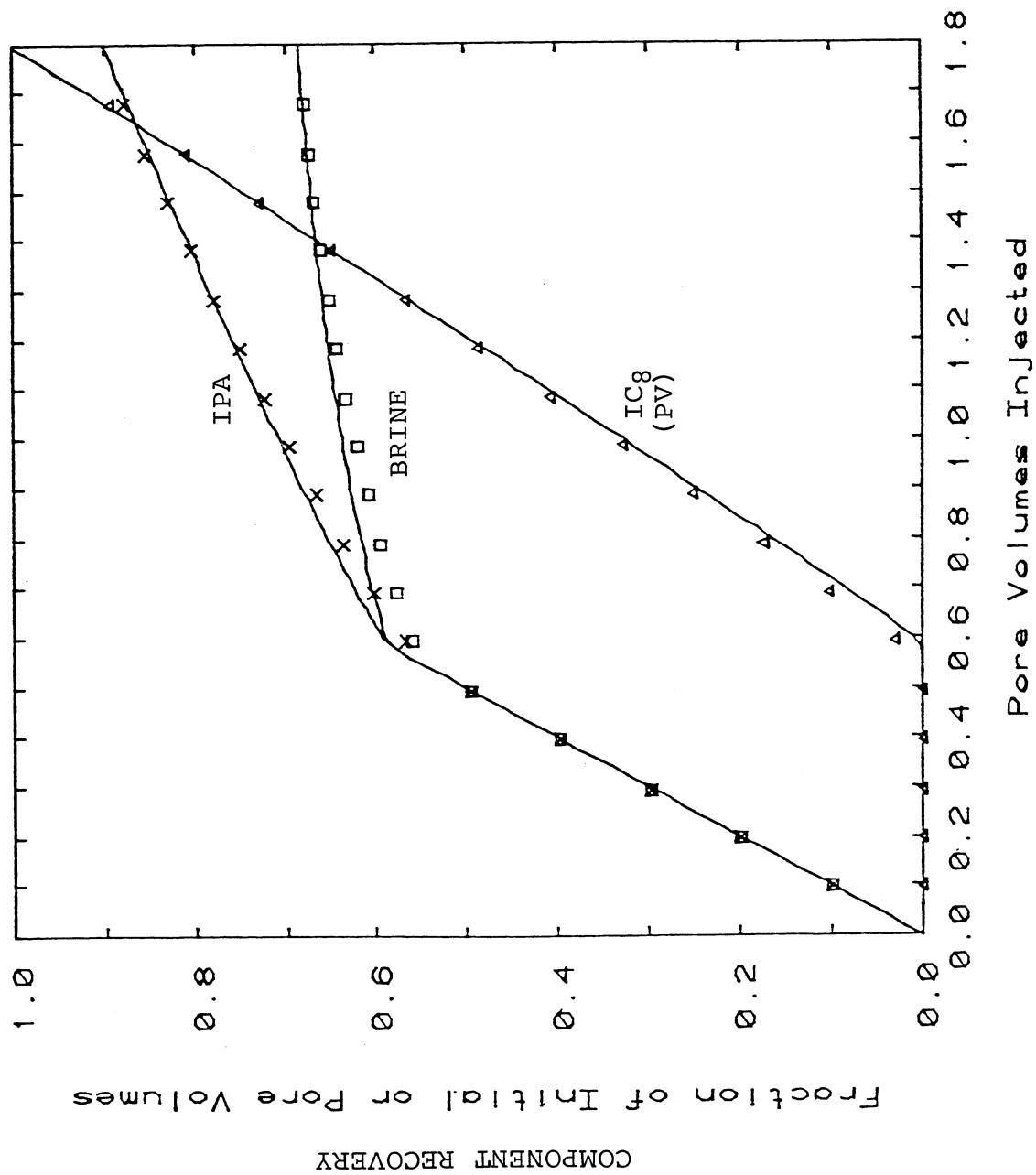


Figure 4.1 Comparison of calculated (solid line) and experimental (data points) component recovery for isooctane (IC8) displacing 50 vol % isopropanol (IPA) - 50 vol % brine (2 wt. %  $\text{CaCl}_2$ ).

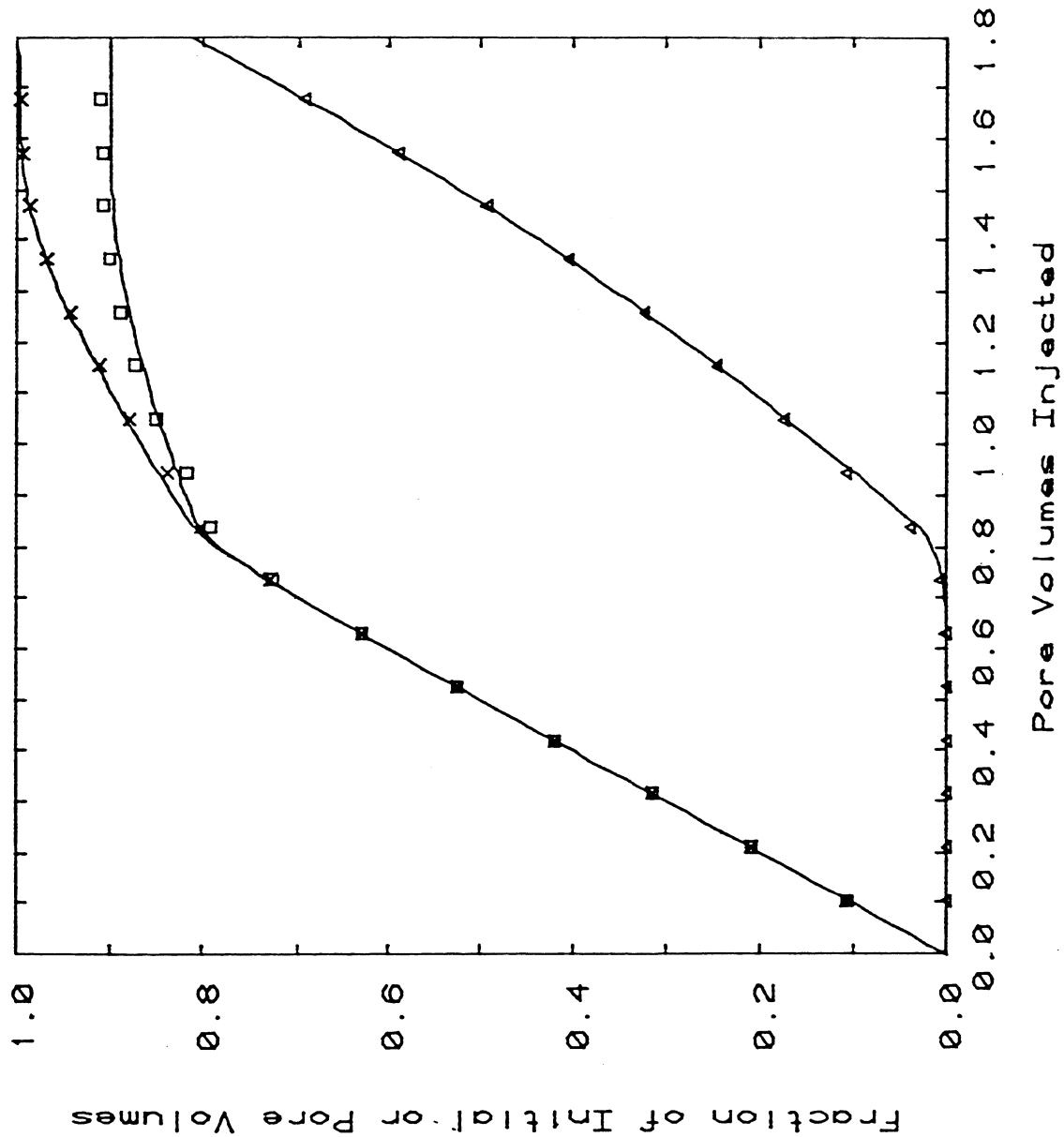


Figure 4.2 Comparison of calculated (solid line) and experimental (data points) component recovery for isooctane (IC<sub>8</sub>) displacing 85 vol % IPA - 15 vol % brine.

Pongpitak's (1980) results show clearly that the simulator developed in this project can accurately represent flow of several phases in one-dimension for multicomponent mixtures, provided that the phase behavior of the mixtures and the viscosities of the phases are known. Calculated composition paths and component recoveries agreed beautifully once provision was made to handle the unusual viscosity behavior of alcohol-brine mixtures.

#### 4.2 Simulation of Slim Tube Displacements

Simulations were performed of slim tube displacements discussed in §3.2. Properties of the components are given in Table 4.1. Phase diagrams used for CO<sub>2</sub>-crude oil mixtures at 5516, 6895, and 8274 kPa (800, 1000, and 1200 psi) are given in Figures 4.3, 4.4 and 4.5 respectively. The phase diagram shown in Figure 4.5 (8274 kPa, 1200 psi) was matched to the experimental data for the continuous multiple contact experiment. Data points shown in Figure 4.5 are from Figure 3.21. Gas-oil relative permeability data given by Naar et al. for unconsolidated sands were used without adjustment. Simulations of the slim tube displacements were performed with 100 grid blocks and a time step size of 0.00125 PV.

Figure 4.6 shows computed oil recovery curves for the three displacements, and Figure 4.7 compares experimental and computed oil recovery at 1.0 PV injected. To reduce the distortion of the time scale by volume change on mixing, actual pore volumes injected were estimated for the experimental points with the assumption that all volume change had occurred by the time that CO<sub>2</sub> broke through. Thus, the oil recovery at breakthrough was used as the pore volume injected at that point. After breakthrough, the injection rate was used to calculate additional pore volumes injected. Agreement between calculation and experiment is reasonable at the two higher pressures but poor at 5516 kPa (800 psi). The principal reason for the discrepancy is the fact that the simulator does not account for volume change on mixing. In the simulator, the mole fraction of CO<sub>2</sub> in the oil-rich phase is fixed by the assumption of local equilibrium and the phase diagram entered as input data. In addition, the density of CO<sub>2</sub> is the same regardless of the phase in which it appears. The experimental results given in Tables 3.2 and 3.3 indicate clearly, however, that CO<sub>2</sub> dissolved in crude oil has a much higher apparent density than low pressure CO<sub>2</sub> vapor. Thus, in the calculation, the volume occupied in the oil phase by dissolved CO<sub>2</sub> is much greater than in the actual displacement. In this immiscible displacement, the average remaining oil saturation at CO<sub>2</sub> breakthrough is determined primarily by the phase viscosities and relative permeabilities, which are insensitive to the density used for CO<sub>2</sub>. The calculated amount of oil phase remaining at CO<sub>2</sub> breakthrough is about the same, therefore, regardless of the density of CO<sub>2</sub>. However, the fraction of the oil phase which is actually oil is quite sensitive to the density of CO<sub>2</sub>. When the density of CO<sub>2</sub> in the oil phase is too low, the volume fraction occupied by dissolved CO<sub>2</sub> is too high. The amount of oil left in the oil phase is therefore too low and hence, the amount of

Table 4.1 Component Properties for Slim Tube Simulations

Component	Molecular Weight	Viscosity (cp)			Density (g/cm <sup>3</sup> )		
		5515 kPa	6895 kPa	8274 kPa	5515 kPa	6895 kPa	8274 kPa
CO <sub>2</sub>	44	0.0176	0.0207	0.052	.142	.230	.670
C <sub>5</sub> -C <sub>12</sub>	119.1	0.89	0.89	0.89	.689	.696	.702
C <sub>13+</sub>	322.5	18.96	18.96	18.96	.978	.978	.978

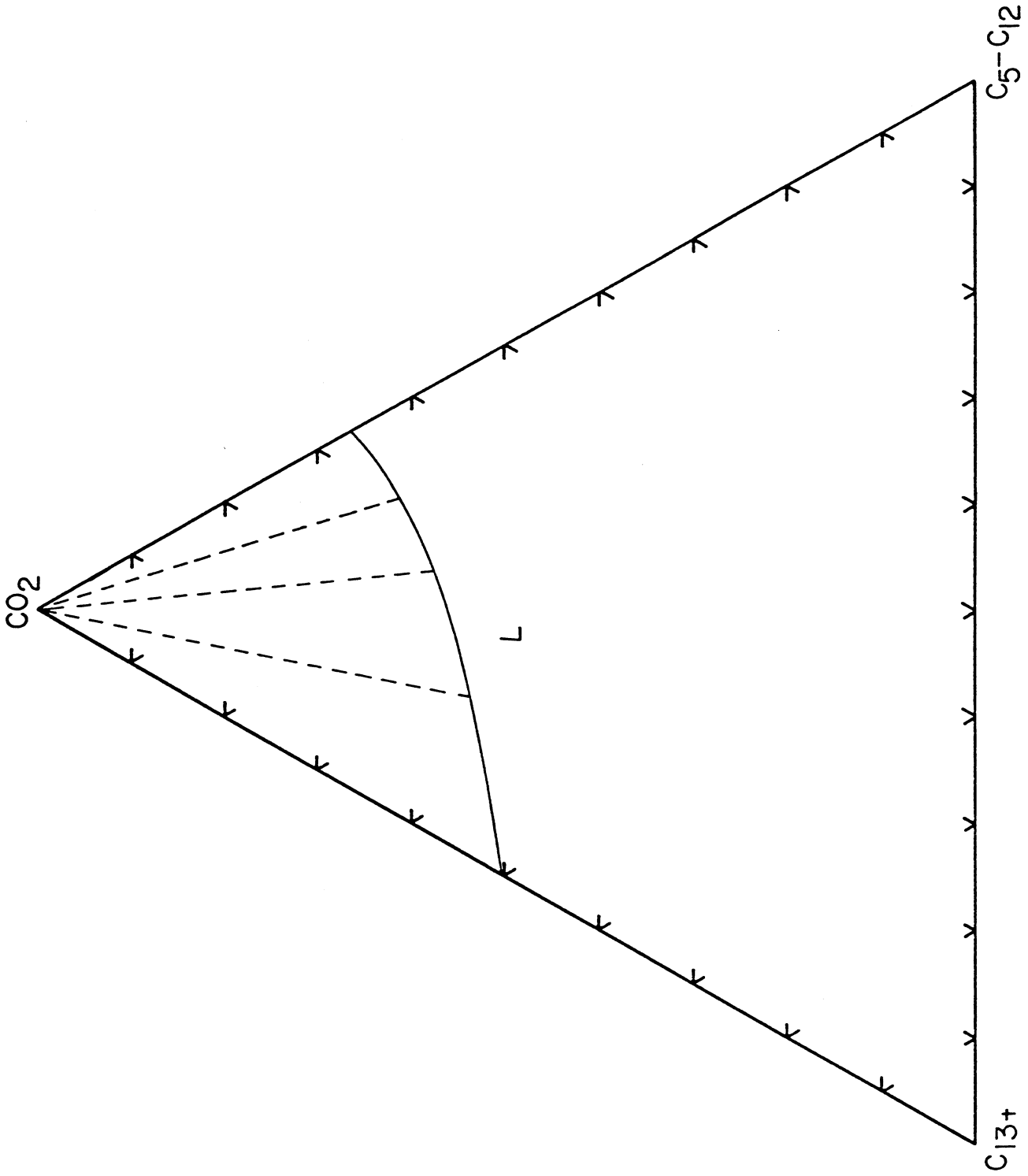


Figure 4.3 Pseudo-ternary phase diagram used in one-dimensional simulation of slim tube displacement at 5516 kPa (800 psi).

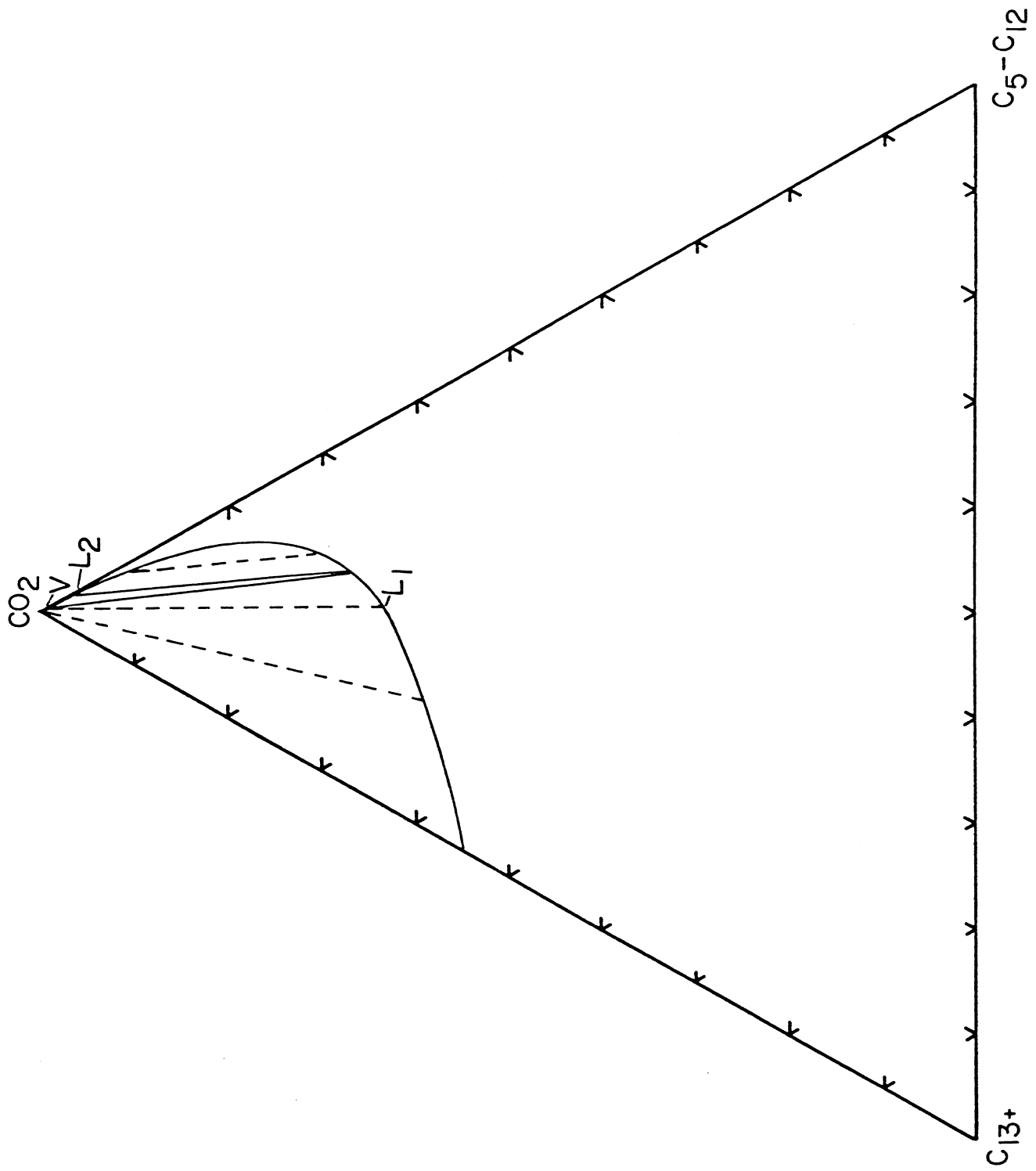


Figure 4.4 Pseudo-ternary phase diagram used in one-dimensional simulation of slim tube displacement at 6895 kPa (1000 psi).

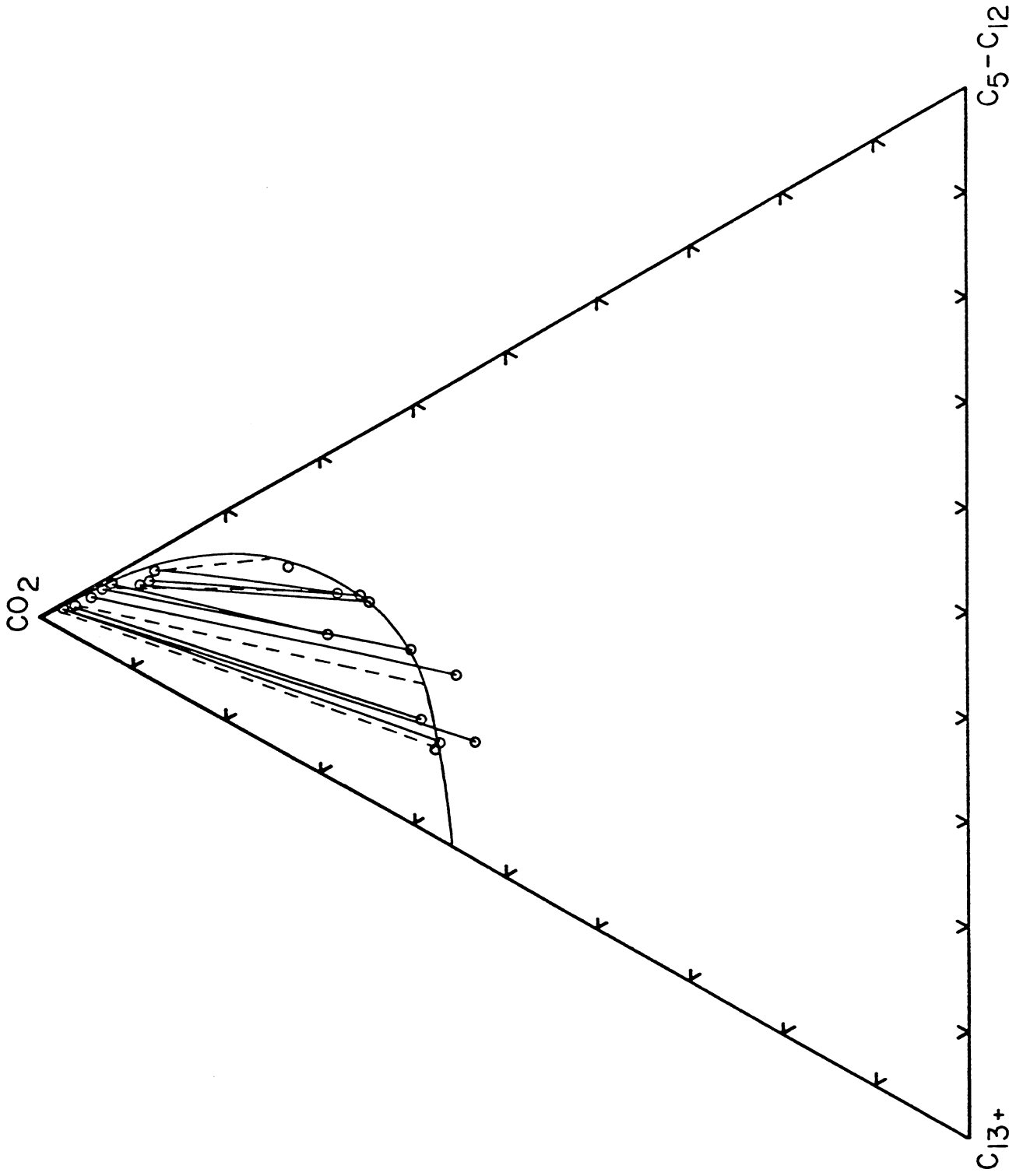


Figure 4.5 Pseudo-ternary phase diagram used in one-dimensional simulation of slim tube displacement at 8274 kPa (1200 psi).

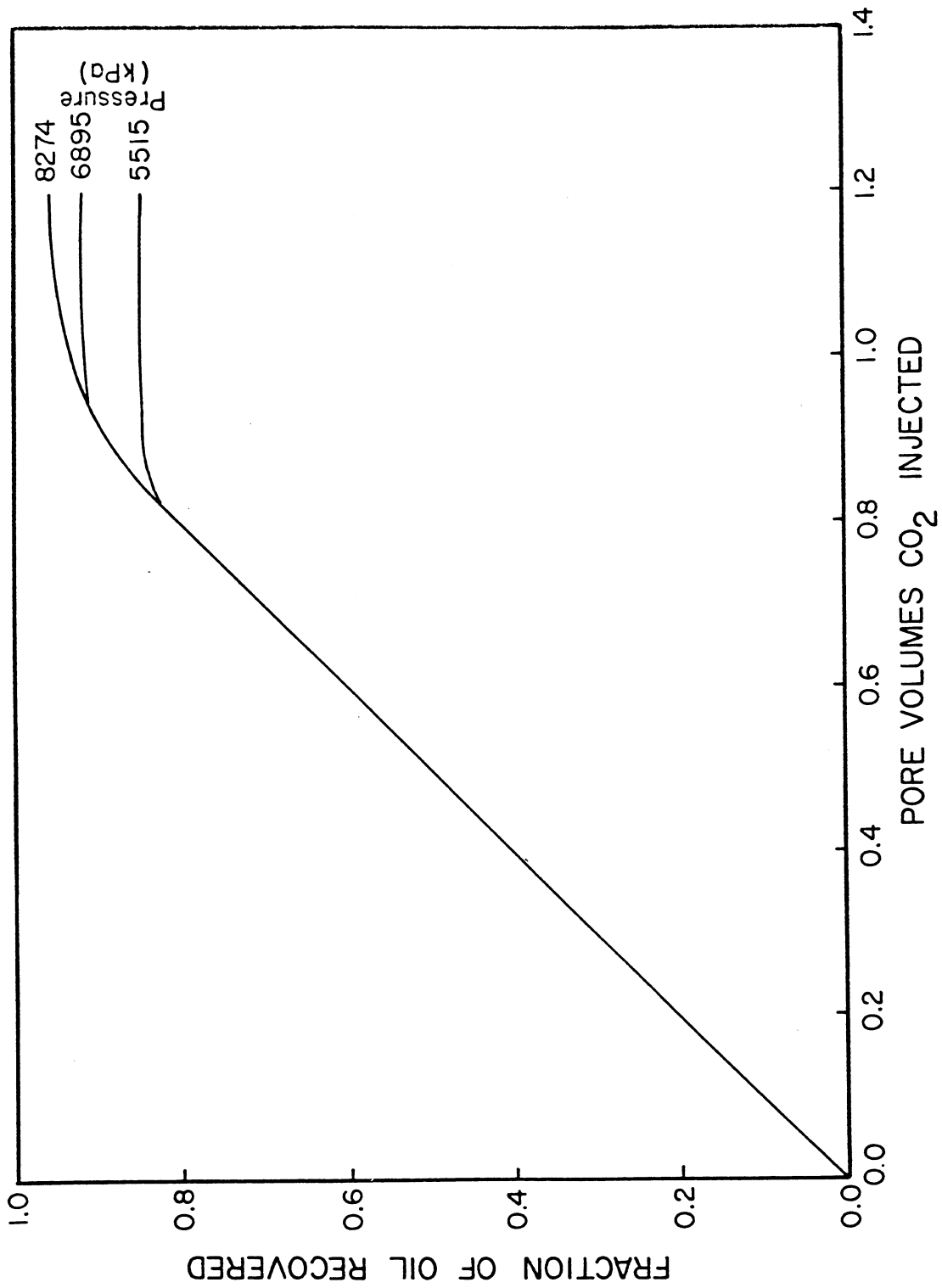


Figure 4.6 Calculated oil recovery in slim tube displacements.

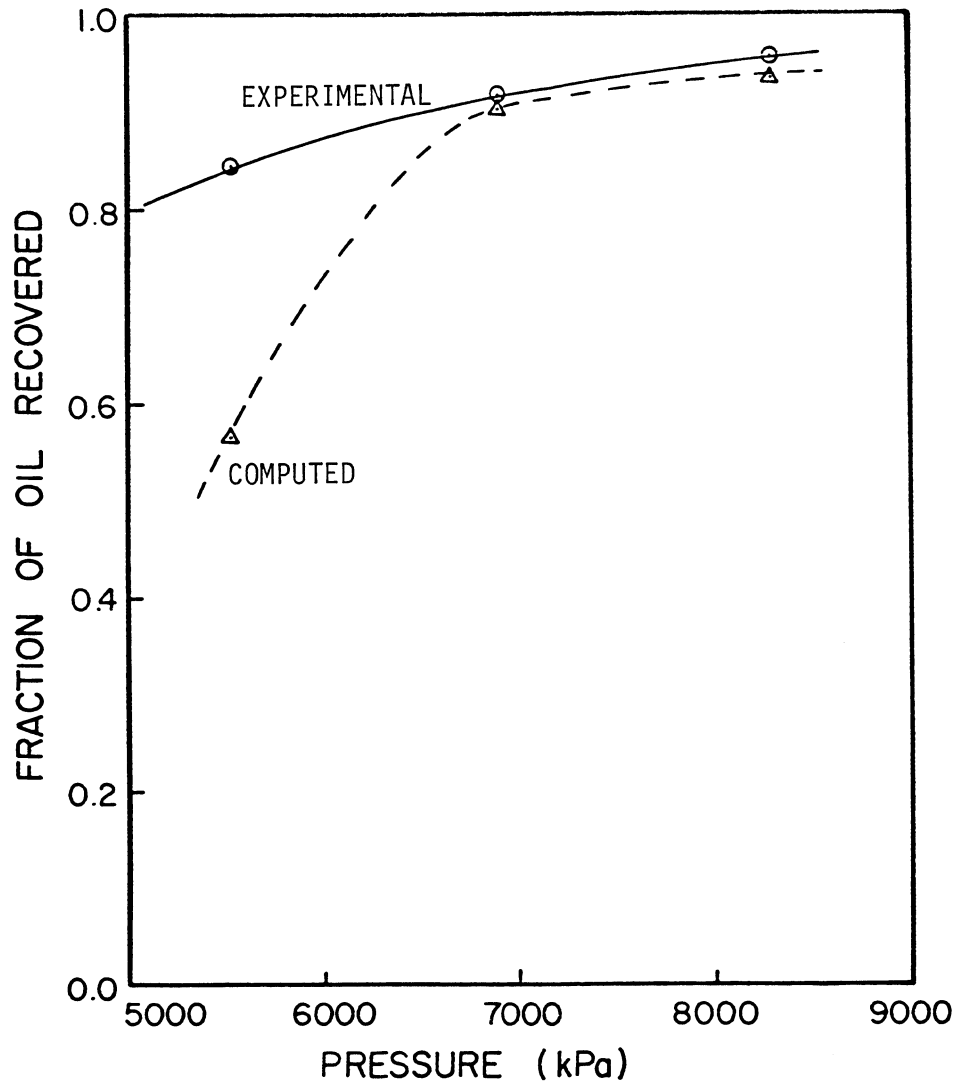


Figure 4.7 Comparison of computed and experimental oil recovery at one pore volume injection in slim tube displacements.

oil recovered at breakthrough is too high. Figure 4.8 compares calculated oil recovery curves for the 5516 kPa (800 psi) displacement using the density of pure CO<sub>2</sub> at the run conditions, 0.142 g/cm<sup>3</sup>, and the estimated apparent density of dissolved CO<sub>2</sub> from Table 3.2, 0.795 g/cm<sup>3</sup>. The higher density reduced the oil recovery substantially, which confirms the argument given above.

Figure 4.9 compares calculated and experimental oil recovery curves for the three displacements, again with the assumption that oil recovery at breakthrough was equivalent to the effective pore volumes injected. Agreement is good for the higher pressures, but still less satisfactory for the low pressure displacement. It is apparent that accurate modeling of immiscible CO<sub>2</sub> displacements will require that the assumption of no volume change on mixing be eliminated. Results of the higher pressure calculations are much less sensitive to volume change effects because extraction of intermediate hydrocarbons leads to a composition path which results in a small residual oil phase saturation. Figures 4.10, 4.11, and 4.12 show computed saturation and composition distributions at 0.5 PV injected for the three simulations. The displacement shown in Figure 4.10 (5516 kPa, 800 psi) is clearly immiscible. The simulator essentially performs a Buckley-Leverett calculation except that some CO<sub>2</sub> dissolves in the oil. There is no preferential extraction of C<sub>5</sub>-C<sub>12</sub> components. CO<sub>2</sub> merely replaces some of the oil. Figure 4.13 shows the overall composition path for the outlet grid block. As the displacement progressed, the composition in the outlet region changed from that of the original oil to mixtures containing oil and CO<sub>2</sub>, but since almost no oil was extracted into the CO<sub>2</sub> phase, the CO<sub>2</sub>-oil mixtures lie on the straight line connecting the oil composition with the CO<sub>2</sub> vertex.

At 6895 kPa (1000 psi), the displacement is much more complex (Figure 4.11). The small oscillations in the lower liquid (L<sub>1</sub>) phase saturation are the result of an instability which occurs in the explicit finite difference method if the time step is too large (Orr 1980c). A small reduction in the time step eliminates the oscillations but has negligible effect on the computed oil recovery, in this case. As the concentration of CO<sub>2</sub> rises through the transition zone, a second, CO<sub>2</sub>-rich liquid appears. In that region, the concentration of C<sub>5</sub>-C<sub>12</sub> hydrocarbons declines less rapidly than that of C<sub>13+</sub> because the C<sub>5</sub>-C<sub>12</sub> hydrocarbons are preferentially extracted by CO<sub>2</sub>. Closer to the inlet, the CO<sub>2</sub> concentration is higher, and consequently vapor phase CO<sub>2</sub> coexists with a residual oil phase containing dissolved CO<sub>2</sub>. Figure 4.14 shows the path followed by the overall composition of the fluids present in the outlet grid block. Again, as the displacement progresses, the composition changes from original oil to mixtures containing CO<sub>2</sub> and extracted C<sub>5</sub>-C<sub>12</sub>. In contrast with the composition path shown in Figure 4.13, that in Figure 4.15 lies on the C<sub>5</sub>-C<sub>12</sub> side of the straight line connecting the original oil composition with the CO<sub>2</sub> vertex. The displacement does not avoid the multiphase region entirely, but when the multiphase region is entered, the amount of residual oil left behind is smaller than in the lower pressure displacement.

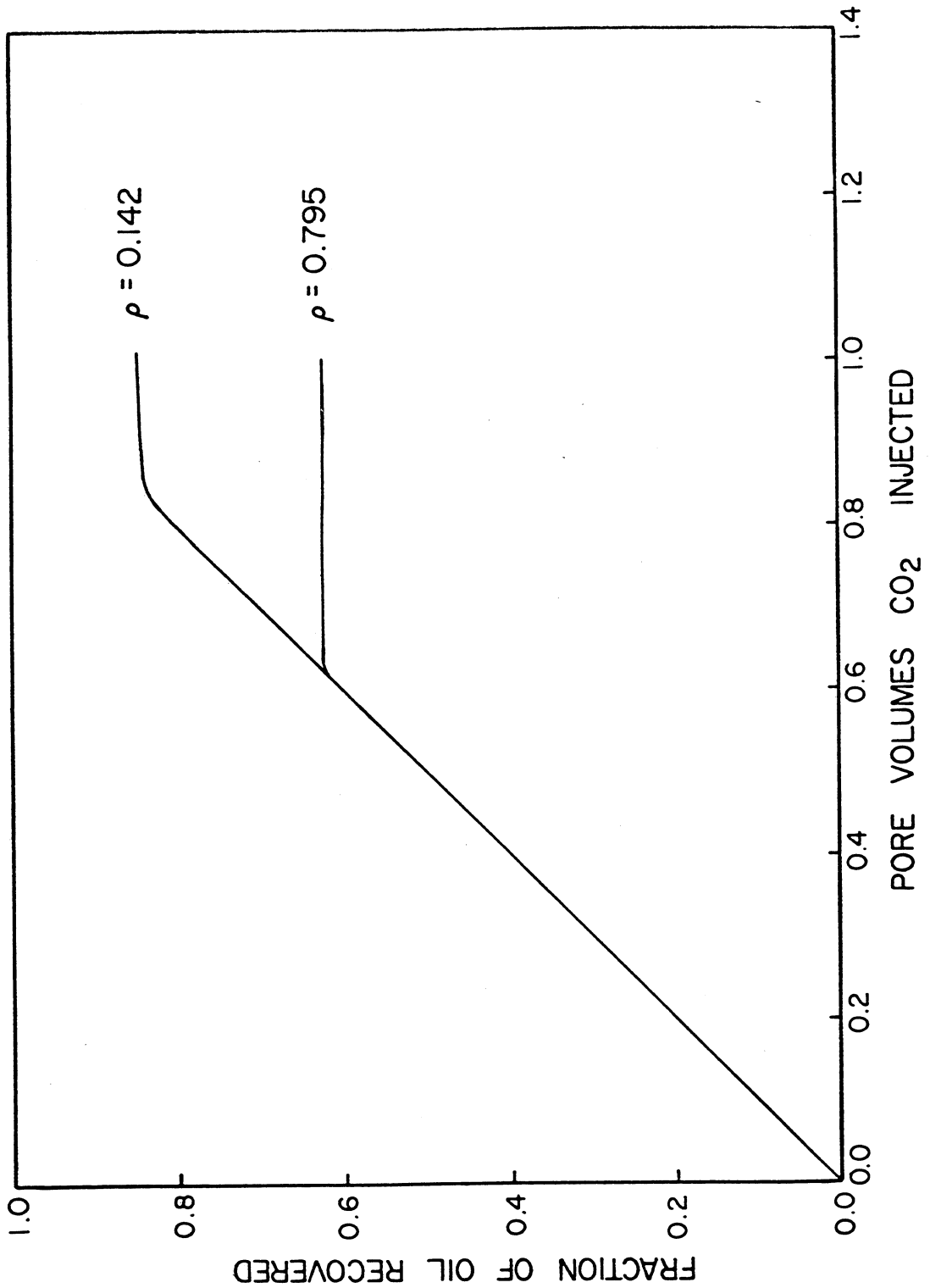


Figure 4.8 Effect of CO2 density on computed recovery for a slim tube displacement at 5516 kPa (800 psi).

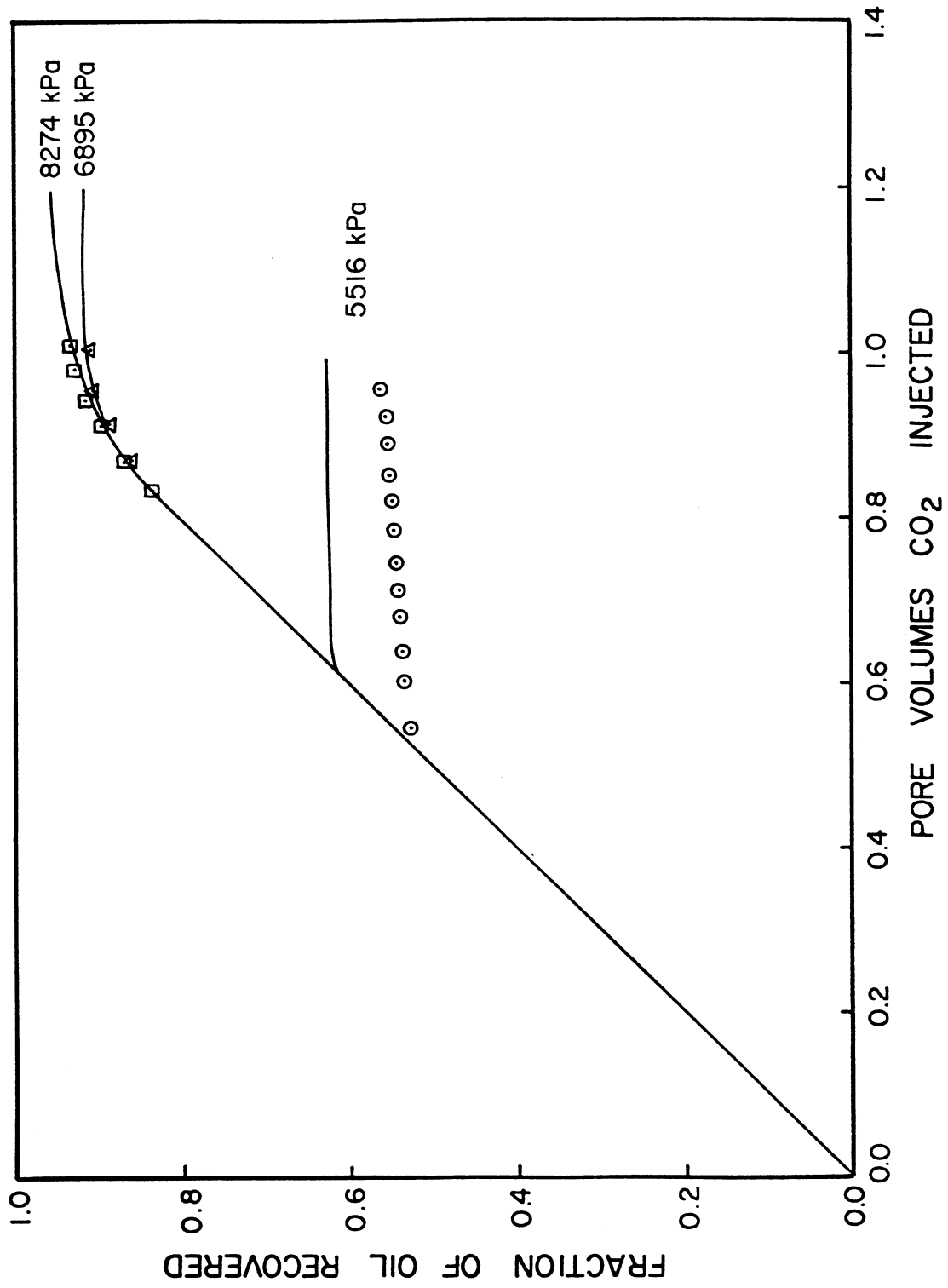


Figure 4.9 Comparison of calculated to experimental oil recovery in slim tube displacements.

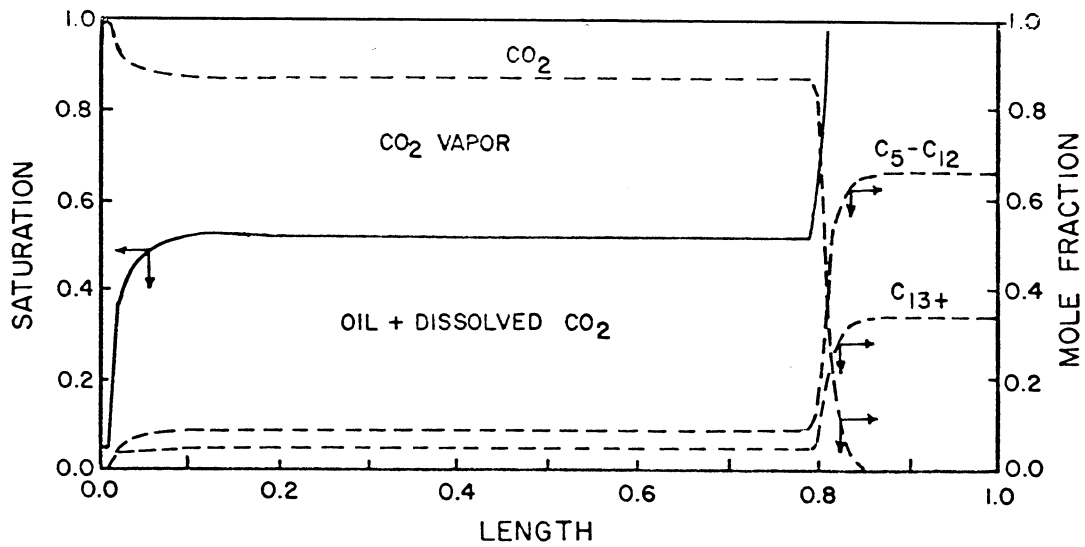


Figure 4.10 Computed saturation and composition distributions for slim tube displacement at 5516 kPa (800 psi).

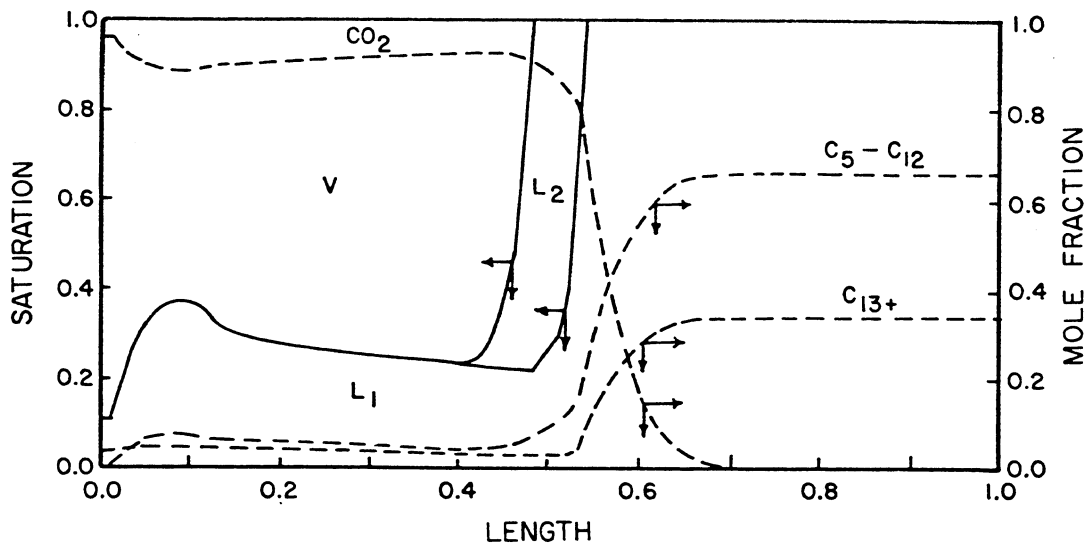


Figure 4.11 Computed saturation and composition distributions for slim tube displacement at 6895 kPa (1000 psi).

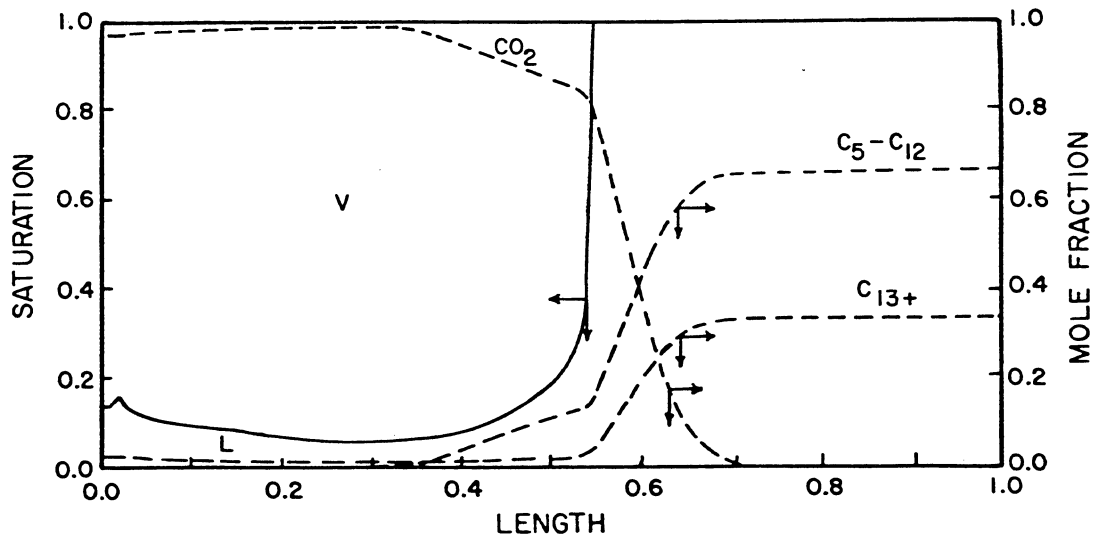


Figure 4.12 Computed saturation and composition distributions for slim tube displacement at 8274 kPa (1200 psi).

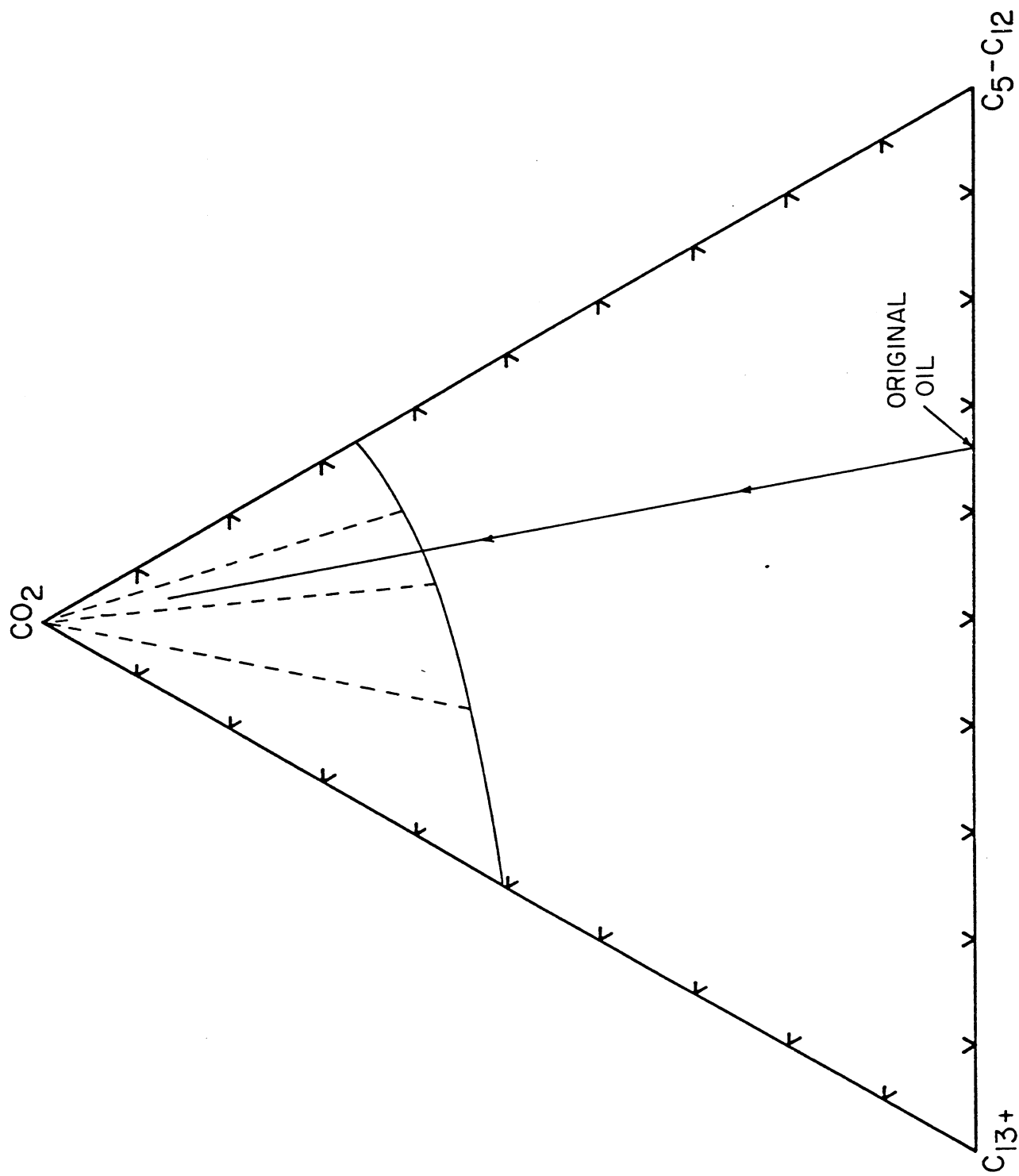


Figure 4.13 Overall composition path of fluids present at the outlet grid block at 5516 kPa (800 psi).

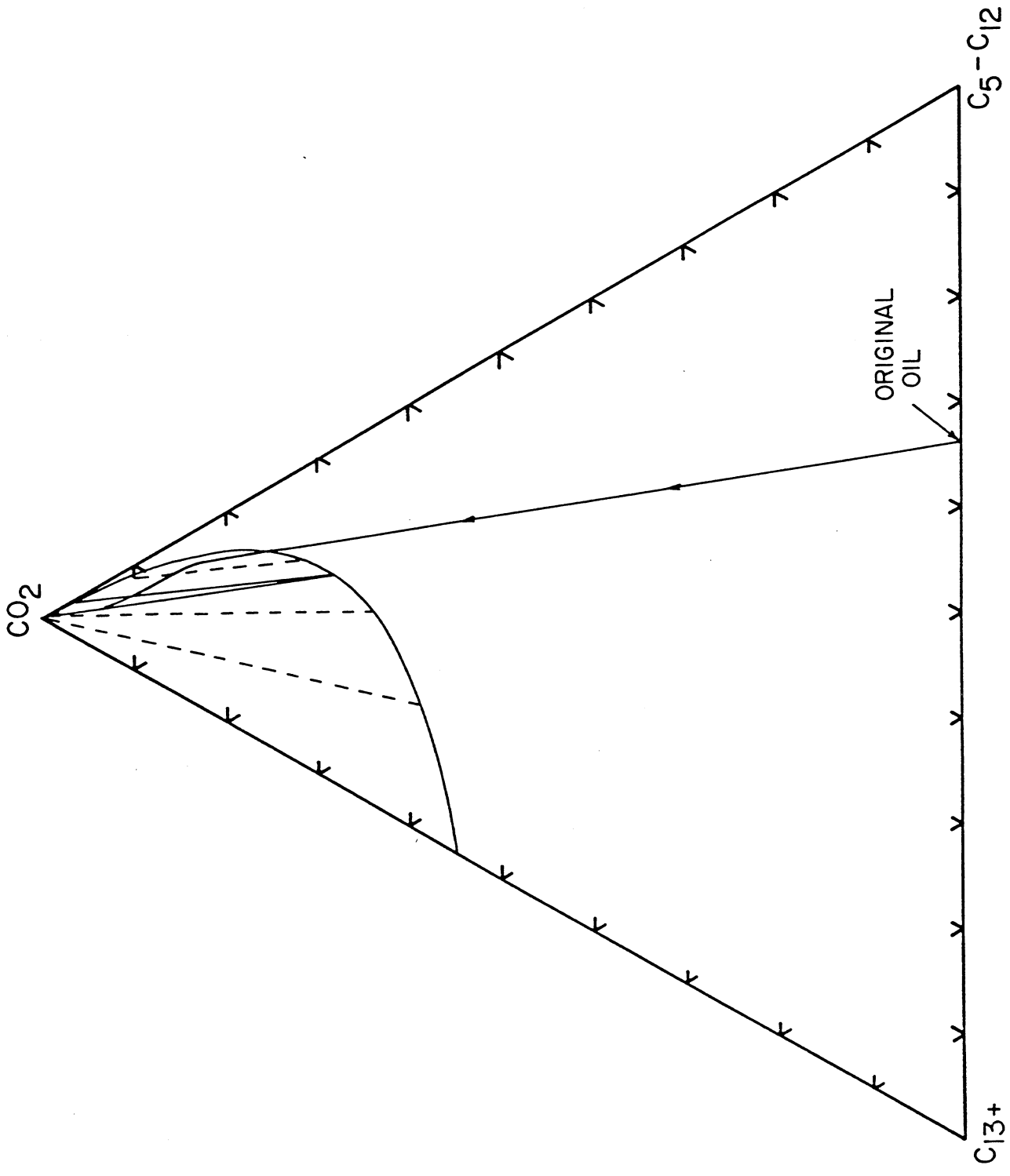


Figure 4.14 Overall composition path of fluids present at the outlet grid block at 6895 kPa (1000 psi).

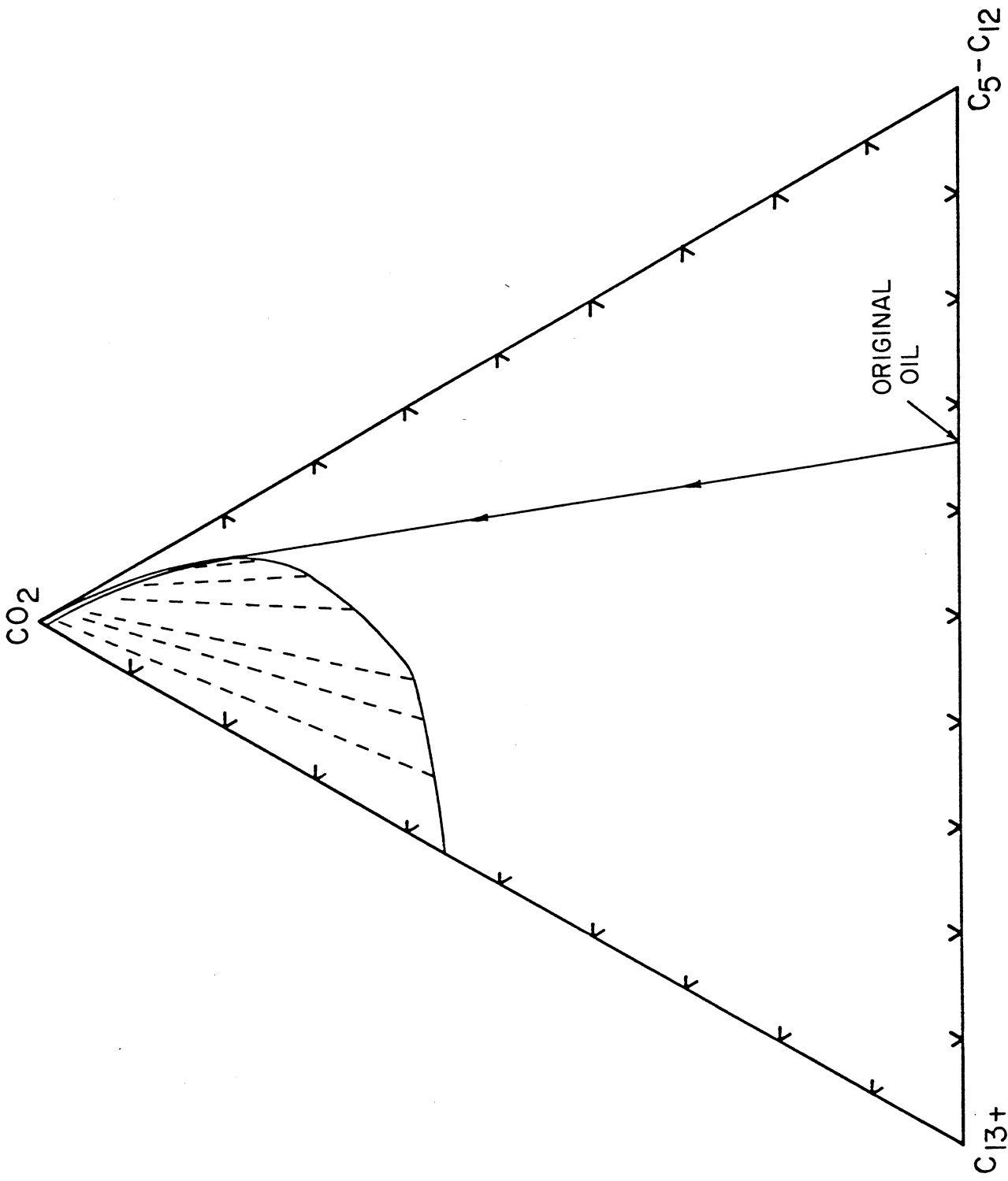


Figure 4.15 Overall composition path of fluids present at the outlet grid block at 8274 kPa (1200 psi).

At 8274 kPa (1200 psi), the displacement is still more favorable (Figures 4.12 and 4.15). The zone containing additional extracted C<sub>5</sub>-C<sub>12</sub> is larger, and the residual oil saturation is smaller. Correspondingly, the overall composition path lies closer to the binodal curve (Figure 4.15). In fact, because the original oil composition lies at the boundary of the region of the ternary diagram which contains tie line extensions, the displacement would have avoided the two phase region entirely had there been no numerical dispersion (Hutchinson and Braun 1961; Helfferich 1979). Numerical (or physical) dispersion increases the volume over which mixing occurs. This causes the composition path to fall deeper into the two phase region which in turn increases the residual oil saturation and reduces recovery (Gardner et al. 1979; Orr et al. 1980a). Viscous fingering couples to phase behavior in a similar way.

#### 4.3 Summary and Conclusions for Task 3.

Recovery of oil from a slim tube displacement increases when the displacement pressure increases, as has long been known. Even in a very simple porous medium, however, displacement of oil by CO<sub>2</sub> is the result of a complex interplay of phase behavior, fluid properties and multiphase flow. The simulation results presented here serve to delineate the roles of phase behavior, densities and viscosities in determining displacement efficiency. Study of the displacement, phase equilibrium and simulation results produces the following observations:

- (1) The viscosity of CO<sub>2</sub>, or of a CO<sub>2</sub>-rich phase, is sufficiently low that the increase in that viscosity with increasing pressure produces a negligible increase in oil recovery if all other factors are held constant. The efficiency of such adverse mobility displacements remains low. Thus, changes in the viscosity of CO<sub>2</sub> do not account for improved recovery with increasing pressure.
- (2) An increase in the density of injected CO<sub>2</sub>, with other factors constant, reduces oil recovery because the volume occupied by CO<sub>2</sub> dissolved in the oil phase is lower.
- (3) An increase in the solubility of CO<sub>2</sub> in oil increases recovery because the fraction of the remaining oil phase which is actually oil is reduced. However, the solubility of CO<sub>2</sub> in crude oil usually does not exceed 60-80 mol % at reasonable pressures (see Figure 3.9), and typical CO<sub>2</sub> volume fraction at such pressures would be less than 0.50. Thus, solubility increases alone do not explain recoveries of 95% either.

- (4) Improvement in the efficiency with which CO<sub>2</sub> extracts light and intermediate hydrocarbons from the oil, with all other factors constant, does produce an increase in recovery. Simulations presented here and by Gardner et al. (1979) and Orr et al. (1980a) clearly establish that improved extraction can account for improved recovery with increasing pressure in CO<sub>2</sub>-crude oil systems in which liquid-liquid phase behavior occurs.

The simulator developed and used here is simple in its mathematical approach and in the representation of the complex phase behavior of CO<sub>2</sub>-crude oil systems. Nevertheless, it produces results which agree well with experimental displacements, and it is a valuable tool for understanding the interplay of competing physical effects. The results presented here offer encouragement that representations of CO<sub>2</sub>-crude oil phase behavior in terms of a small number of pseudo-components may be feasible. Such representations are essential if field scale simulations which account for phase behavior are to be successful.

## 5. TASK 4. APPLICATION OF LABORATORY RESULTS TO FIELD PROBLEMS\*

The experimental techniques discussed in §2 were designed to provide data with which mechanisms by which CO<sub>2</sub> displaces oil could be better understood, and the discussions given in §3 and §4 centered on interpreting displacement experiments in terms of the physical behavior of CO<sub>2</sub>-crude oil mixtures. The rationale for that approach lies in the need for improvements in the accuracy of performance predictions for field scale CO<sub>2</sub> floods, improvements which inevitably will be based on better understanding of process mechanisms. In addition, there is a need for a more or less standard set of laboratory experiments with which to evaluate a particular field for CO<sub>2</sub> flooding.

Despite the fact that CO<sub>2</sub> flooding has been investigated since the early 1950's, consensus as to the laboratory experiments required for the evaluation of a CO<sub>2</sub> flooding prospect has not developed. Laboratory experiments most often performed, however, fall into three general areas: (1) slim tube displacements, (2) core displacements, and (3) high pressure volumetric (PVT) and vapor-liquid equilibrium (VLE) experiments. The three types of experiments yield different information about a potential CO<sub>2</sub> flood. This section reviews briefly the uses and limitations of the information obtained in the various laboratory experiments.

Design of any large scale CO<sub>2</sub> flood inevitably involves the use of numerical reservoir simulators (Henderson 1974; Bilhartz et al. 1978; Graue and Zana 1978; Delaney and Fish 1980; and Drennon et al. 1980). Those which are applicable to CO<sub>2</sub> flooding also fall into three general groups: (1) miscible simulators (Todd and Longstaff 1972), (2) compositional simulators (McDonald 1971; Nolen 1973; Kazemi et al. 1978; Fussell and Fussell 1977; Coats 1979; and Sigmund et al. 1979), and (3) hybrid miscible-compositional simulators (Todd 1979).

The type of data required to support a simulation effort depends, in part at least, on the choice of the simulator. Miscible simulators, which are based on the work of Todd and Longstaff (1972), treat CO<sub>2</sub> as completely miscible with the oil, and require little more than the permeability, relative permeability, capillary pressure, viscosity and density data common to black oil simulators. Routine reservoir fluid volumetric and fluid property measurements in addition to standard core characterizations (permeability, relative permeability and capillary pressure) are adequate to support such simulations.

Compositional simulators follow the transport of individual components where black oil simulators follow only the gas, oil and water phases. The distribution of components between phases is calculated using either convergence pressure correlations for equilibrium K-values (McDonald 1971; Nolen 1973; and Kazemi 1978) or an equation of state (Fussell and Fussell

\* Much of the material presented in this section is also available in a paper by Orr, Silva, Lien and Pelletier (1980b).

1977; Coats 1979; and Sigmund et al. 1979), and phase viscosities and densities are then calculated from the phase compositions. Thus, considerable input data are needed, in addition to the usual reservoir description data, to define the composition of the reservoir fluids and to specify the parameters used in the computations for phase compositions and fluid properties. Because the crude oil is generally represented as a set of pseudo-components, input data describing such components, such as critical pressures, temperatures and volumes must be estimated. If the resulting predictions of phase behavior and fluid properties are to be used with confidence, the accuracy of the predictions must be tested against experimental data. Usually, adjustment of the input data is required to achieve an acceptable match. For CO<sub>2</sub>-crude oil mixtures, measurements of the properties of equilibrium mixtures such as saturation pressures for various CO<sub>2</sub> concentrations, swelling of the oil by CO<sub>2</sub>, volume fractions of vapor and liquid, mixture viscosities, and occasionally, component K-values can be used to tune representations of phase behavior and fluid properties.

A hybrid miscible-compositional simulator, such as that described by Todd (1979), does not attempt to calculate component partitioning in as much detail as the compositional simulators described above. It treats CO<sub>2</sub> as miscible with the oil at pressures above an experimentally determined "minimum miscibility pressure (MMP)," models viscous fingering of CO<sub>2</sub> through a mixing parameter model (Todd and Longstaff 1972), but provides some capability to model component distribution between phases when the local pressure falls below the MMP. Particularly useful for simulations of this sort are data giving the solubility of CO<sub>2</sub> in the oil and K-values for other light components such as methane or nitrogen at various pressures, measurements of the MMP and the residual oil saturation to CO<sub>2</sub> at pressures above the MMP.

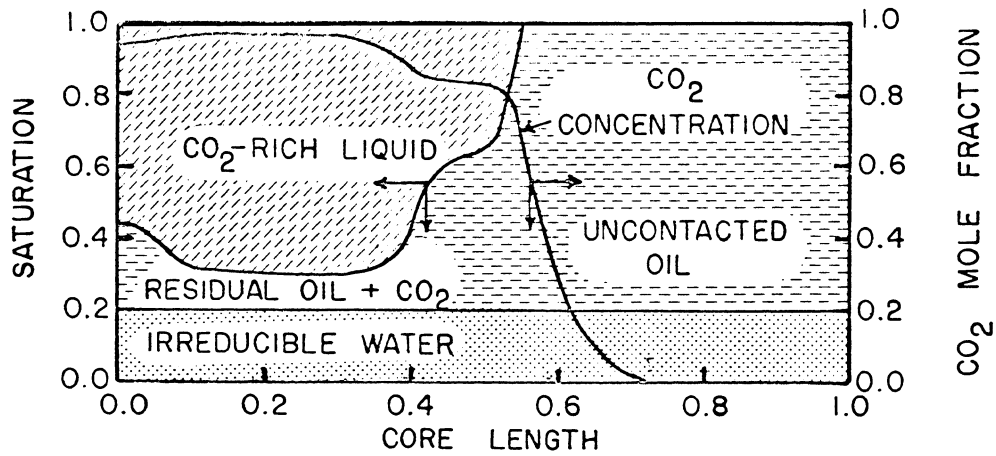
None of the simulators currently available models all of the factors which are known to influence the efficiency of the process, and, therefore, all have limitations which should be considered when simulation results are evaluated. Miscible simulators ignore phase behavior, an important part of the CO<sub>2</sub> flooding process, but attempt to model the effects of viscous fingering. Compositional simulators model phase behavior but do not account for viscous fingering and are affected by numerical dispersion which alters the calculated composition path, and, hence, the calculated process efficiency. Nevertheless, there is really no tractable alternative to the use of numerical simulation for CO<sub>2</sub> flood design. It is simply not possible to perform experiments in which all of the relevant variables have been properly scaled (Heller 1963; and, Gharib and Doscher 1979). Predictions of process efficiency, recovery rates and economics as well as evaluations of alternative operating procedures require the use of numerical simulation.

It seems prudent, therefore, to choose a set of laboratory experiments not only to provide data directly needed for flood design, such as minimum operating pressures, but also to yield information which will at least reduce the amount of data which must be estimated to conduct numerical

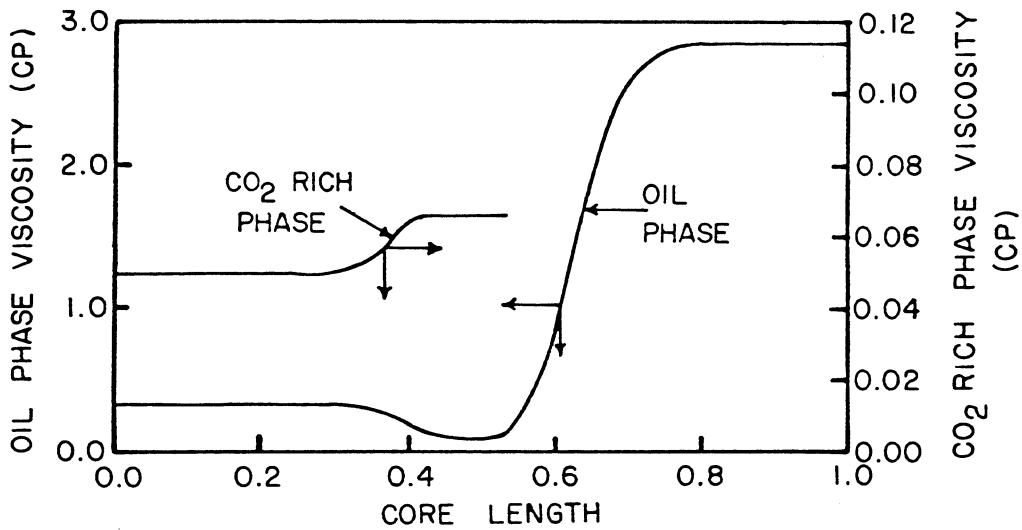
simulations. Because reservoirs and CO<sub>2</sub> injection processes vary widely, it is not possible to list a set of laboratory experiments appropriate to all situations. Numerical simulation prior to performing experimental work can help to identify the sensitivity of oil recovery projections to particular variables. For instance, phase density data may be crucial for designing gravity stabilized downward displacements but less important for reservoirs consisting of thin layers. Below, the experimental techniques most commonly used are reviewed, and the limitations of each are discussed.

## 5.1 Process Description

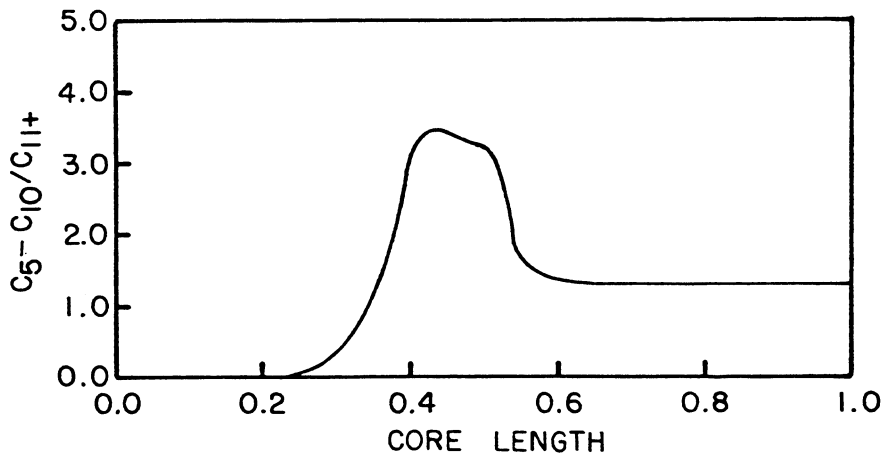
Figure 5.1 shows a schematic of an ideal one-dimensional CO<sub>2</sub> displacement as it might occur in a single porous medium, such as a slim tube, at a pressure close to the MMP. In this schematic CO<sub>2</sub> is injected from the left and fluids are produced from the right end. Injected CO<sub>2</sub> displaces water, mixes with the oil, dissolves in it, and extracts hydrocarbons from it. When the CO<sub>2</sub> concentration in the inlet region exceeds the solubility of CO<sub>2</sub> in the oil, a CO<sub>2</sub>-rich phase appears (it may be a liquid if the temperature is below 50°C; otherwise, it is a vapor). Because the CO<sub>2</sub>-rich phase has a viscosity close to that of CO<sub>2</sub>, that is, much lower than that of the oil, the CO<sub>2</sub>-rich phase flows more rapidly than the oil-rich phase, contacting fresh oil. Again, CO<sub>2</sub> displaces water and oil swollen by dissolved CO<sub>2</sub> and dissolves into the fresh oil ahead of the front until the solubility of CO<sub>2</sub> has been reached. Eventually, the CO<sub>2</sub>-rich phase contains enough extracted hydrocarbons to efficiently bank up residual oil. Figure 5.1a shows a simulated saturation distribution after injection of 0.4 PV of CO<sub>2</sub>. The one-dimensional simulator used was similar to that described by Gardner et al. (1979), which represents the oil as two components. At the outlet, only water is flowing because the oil saturation is still at its residual value. An oil bank has formed just ahead of the transition zone between the oil and CO<sub>2</sub>. Closer to the inlet, the CO<sub>2</sub> concentration rises and the CO<sub>2</sub>-rich phase appears. Behind the CO<sub>2</sub> front, most of the water has been displaced down to near its residual saturation, and there is a small residual oil phase saturation which contains substantial quantities of dissolved CO<sub>2</sub>. In the inlet region, the remaining water and oil saturations are higher because the pure CO<sub>2</sub> injected initially displaces oil and water less efficiently than it does after repeated contacts with the oil. Figure 5.1b shows the distribution of viscosities (calculated using a quarter power blending rule) (Todd and Longstaff 1972). The viscosity of the oil phase drops sharply when CO<sub>2</sub> is dissolved in it, and the CO<sub>2</sub>-rich phase viscosity is increased by the presence of extracted hydrocarbons. The preferential transport of the lighter hydrocarbon components is clearly shown in Figure 5.1c. Oil in the outlet region has not yet been affected by CO<sub>2</sub>, so the ratio of intermediate hydrocarbons (C<sub>5</sub>-C<sub>10</sub>) to heavier hydrocarbons (C<sub>11+</sub>) is the same as the original value for the oil. In the transition zone, the hydrocarbon mixtures are much richer in intermediate hydrocarbons



a) SATURATION DISTRIBUTION



b) VISCOSITY DISTRIBUTION



c) DISTRIBUTION OF RATIO OF INTERMEDIATE TO HEAVY HYDROCARBON CONCENTRATIONS

Figure 5.1 Ideal one-dimensional displacement of oil by CO<sub>2</sub>.

than the original oil, and in the inlet region, all the intermediate hydrocarbons have been extracted, so that the oil phase left behind is essentially all  $C_{11+}$  with  $CO_2$  dissolved in it.

The saturation and composition distributions shown in Figure 5.1 were calculated with the assumption that the flow is one-dimensional, that the fluids are locally well mixed, and that any phases present are in chemical equilibrium (Orr 1980c). These assumptions are not unreasonable for slim tube displacements, but they may lead to optimistic predictions of the amount of oil recovered for displacements in cores and on a reservoir scale. Because the flow is assumed to be one-dimensional, the effects of viscous fingering, reservoir heterogeneity, and gravity segregation are not modeled. Because the fluids are assumed to be well mixed, the effects of dead end pores and of shielding of trapped oil droplets from contact with  $CO_2$  are excluded. Furthermore, the effects of phase behavior, viscous fingering and trapping are not independent. If the  $CO_2$  injected initially fingers through the mobile water phase, the water saturation will remain high, oil will remain trapped, and hence may be contacted less efficiently by  $CO_2$ , and extraction of hydrocarbons by  $CO_2$  may proceed more slowly. Viscous fingering of injected  $CO_2$  through oil which has been mobilized causes mixing of  $CO_2$  that is poor in extracted hydrocarbons with fluids near the  $CO_2$  front. That mixing partly negates the beneficial effect of extraction. Finally, the effects of reduced  $CO_2$ -oil interfacial tensions, which could improve displacement efficiency by reducing the residual oil saturation to  $CO_2$  (Rosman and Zana 1977), have not been modeled. Thus, at reservoir conditions, the displacement process is a collection of complex and competing interactions of the phase behavior of  $CO_2$ -crude oil mixtures, with all its effects on the properties of the fluids, with multiphase flow behavior in the reservoir rock. It is important, therefore, to understand which of these competing effects is operating in a particular set of laboratory experiments.

## 5.2 Slim Tube Displacements

Displacements of recombined reservoir fluid samples from a slim tube packed with sand or glass beads come closest to a standard experiment to evaluate operating pressures for a potential  $CO_2$  flood. Even so, experimental techniques have differed substantially, as Yellig and Metcalfe (1980) observed, and as Table 5.1 reemphasizes. Displacement lengths range from 1.5 to nearly 26m (5-84 ft.), flow geometries vary from a vertical tube to flat coils to spirals, and flow velocities vary over nearly two orders of magnitude. The differences in experimental procedures probably stem from the fact that early work on truly miscible displacements showed that oil recovery is insensitive to flow rate. Investigators have also disagreed on the definition of "minimum miscibility pressure." Holm and Josendal (1974, 1980) define "miscible-type" displacements as those which recover more than 80 percent of oil in place at  $CO_2$  breakthrough, and more than 94 percent when the GOR reaches 40,000 SCF/BBL. Metcalfe and Yellig (1980) defined as "miscible" displacements, those in which recovery at 1.2 PV was "very near" the maximum recovery obtained in a series of displacements, and in which transition zone fluids appeared (in a

Table 5.1 Characteristics of Slim Tube Displacement Experiments

Author(s)	Length (m)	ID (cm)	Geometry	Packing (mesh)	Perm. (darcies)	Porosity (%)	Rate cm/hr*
Rutherford (1962)	1.5	1.98	Vertical Tube	50-70 mesh Ottawa Sand	24	35	37
Yarborough & Smith (1970)	6.7	.46	Flat Coil	No. 16 AGS Ottawa Sand (140-200 mesh)	2.74	?	66
Holm & Josendal (1974)	14.6 25.6	.59	?	No. 60 Crystal Sand	?	?	3.81
Holm & Josendal (1980)	15.8	.59	Coil	No. 60 Crystal Sand	20	39	101-254
Huang & Tracht (1974)	6.1	1.65	?	?	1.78	43	4.7
Yelling & Metcalfe (1980)	12.2	.64 OD	Flat Coil	160-200 mesh sand	2.5	?	5.2-10.2
Peterson (1978)	17.1	.64	?	60-65 mesh sand	19	?	?
Wang & Locke (1980)	18.0	.62	Spiral Coil	80-100 mesh glass beads	13	35	381
This work	12.2	.64	Spiral Coil	170-200 mesh glass beads	5.8	37	42
Gardner, Orr & Patel (1979)	6.1	.46	Flat Coil	230-270 mesh glass beads	1.4	37	32 64
Sigmund (1979)	17.9	.78	?	140 mesh glass beads	5	42	?

\*1 cm/hr = 0.787 ft/day

capillary sight glass) "to be the result of a multiple-contact miscible process." They took as an indication of a multiple-contact miscible process color gradations from dark oil to a yellow fluid. Floods which produced clear vapor and dark oil simultaneously were judged "immiscible."

Neither definition is completely satisfactory for comparisons of results from different laboratories, though both are reasonable for comparison of a series of runs performed in the same slim tube at the same displacement rate. Metcalfe and Yellig's definition requires a subjective judgment about transition zone appearance. Holm and Josendal's definition would not necessarily produce the same MMP in different laboratories because oil recovery from a slim tube depends not only on CO<sub>2</sub>-oil phase behavior, but also on displacement rate and the level of dispersion (Gardner et al. 1979) which in turn depends on displacement rate and the particle diameter of the packing material (Perkins and Johnson 1963). Furthermore, displacements of oil by CO<sub>2</sub> are generally unstable, even in slim tubes, so differences in tube diameters and lengths could be expected to have some effect on the magnitude of viscous fingering, and hence on recovery. Thus, a definition of the MMP which would produce repeatable results in different laboratories should include, in addition to breakthrough and final recovery amounts, a specification of the tube length and diameter, packing material and particle size and displacement rates.

While a definition of MMP which would produce repeatable measurements from one laboratory to another would be useful for testing and improving MMP correlations, it should be emphasized that for evaluation of operating pressures for a particular field application, it matters only that the series of displacements be performed in the same slim tube at the same displacement rate. Displacements in slim tubes come closest to the ideal displacements described by the simulations shown in Figure 5.1. Because the porous medium is nearly uniform, and because the diameter of the tube is small, the assumption that fluids are well mixed is reasonable. Because viscous finger growth is inhibited by the walls of the tube, the flow is nearly one-dimensional. Hence, the slim tube displacement experiment comes close to isolating the effects of phase behavior at different pressures in a setting which generates multiple contacts of CO<sub>2</sub> with the oil. Results of a slim tube displacement, therefore, provide the simplest test available of the accuracy of a numerical simulator. The simulations presented in §4 are an example of that type of test. Sigmund et al. (1979), in the only other such test published thus far, found reasonable agreement between the predictions of their compositional simulator and actual slim tube displacements.

Thus, the slim tube experiment is a useful one which provides a simple test of the effect of pressure on displacement efficiency. It provides direct evidence concerning minimum pressures for efficient operation of the phase behavior portion of the process, and it can be used effectively to investigate effects of contamination of the CO<sub>2</sub> with methane or nitrogen. It should be emphasized, however, that the experiment does not yield information about the oil recovery to be expected from a core flood, let alone from a field scale displacement. Neither can it be used to design slug sizes for field applications--it is simply not scaled to produce such information. Nevertheless, the slim tube displacement is a simple experiment

which gives immediate information about potential operating pressures, and it should be performed early in the evaluation of a field prospect for CO<sub>2</sub> flooding.

### 5.3 Core Floods

Of the three types of experiments, CO<sub>2</sub> core floods are the most difficult to interpret because even in linear cores, displacement efficiency can be affected by viscous fingering, gravity segregation, channeling or bypassing of oil due to core heterogeneities, and trapping or shielding of oil from contact with CO<sub>2</sub> by high mobile water saturations (Stalkup 1970; Shelton and Schneider 1975) as well as by the complexities of CO<sub>2</sub>-crude oil phase behavior. As is indicated in Table 5.2, a partial listing of CO<sub>2</sub> core flood investigations, most laboratory core flood work has been performed with sandstone cores. Emphasis has been on understanding displacement mechanisms rather than on measurements designed for use in scale-up calculations for particular reservoirs. However, core floods do seem appropriate to answer at least three questions directly. (1) Can CO<sub>2</sub> mobilize tertiary oil under conditions which are closer to field displacement conditions than those occurring in slim tube displacements? (2) What is the residual oil saturation in the swept zone of a CO<sub>2</sub> displacement? (3) Does CO<sub>2</sub> injection alter core permeability?

Core flood results which answer the first question build confidence that CO<sub>2</sub> can displace oil under conditions which are more realistic than in slim tubes. Even so, the recovery efficiency obtained in core displacements is significantly higher than can be expected in a field displacement, because vertical conformance and areal sweep will be less favorable in the field.

Watkins (1978) showed that residual oil saturations to a CO<sub>2</sub> flood can be measured for reservoir cores provided care is taken to avoid the effects of viscous fingering by generating a transition zone of graded viscosity and density upstream of the core. He found that at pressures well above the MMP, residual oil saturations to CO<sub>2</sub> were below 5% when viscous fingering was controlled, and that such measurements can be made on short pieces of reservoir core. Thus, estimates of maximum oil recovery for the portion of the reservoir swept by CO<sub>2</sub> can be obtained. Core floods can also provide some evidence as to whether interactions of CO<sub>2</sub> with reservoir brine, clays and cementing materials will cause unexpected problems. The main question is whether CO<sub>2</sub> will alter the permeability near the injection well in a way that would reduce the rate at which CO<sub>2</sub> could be injected. Injectivity problems have been reported in one CO<sub>2</sub> (Pontius and Tham 1978) flood, but there is no consensus as to the cause of the problem. There is some evidence that permeability may actually increase with continued CO<sub>2</sub> injection (Holm 1959; Holm and Josendal 1974).

Core floods were used by Huang and Tracht (1974) to investigate the effect of CO<sub>2</sub> slug size on oil recovery. Because slug size requirements are influenced by the amount and distribution of the residual oil saturation, there appears to be no alternative to core displacements if the question is to be investigated experimentally. Nevertheless, it is not obvious that slug sizes determined in relatively short cores are those

Table 5.2 Characteristics of CO<sub>2</sub> Displacements in Cores

Author(s)	Length (m)	Diameter (cm)	Rock Type	Permeability (md)	Porosity (%)	Velocity cm/hr*	Core Orientation	Secondary Tertiary (s, t)
Kathmell, Stalkup & Hassinger (1971)	1.8, 6.1, 13.0	5.1	Boise Outcrop Sandstone	1000	27	12.7-25.40	Vertical	s
Shelton & Schneider (1975)	0.3, 1.2, 2.4	5.1	Berea Sandstone	135-890	16-22	.3-40.6	Horizontal	s, t
Shelton & Yarborough (1977)	4.9	5.1	Berea Sandstone	688	20	3.8	Horizontal	s
Holm (1959)	0.15, 0.3, 2.3	8.9	Berea Sandstone McCook Dolomite	150-250	14-21	6.3-31.2	Horizontal	s
Sigmund, et al. (1979)	0.4	3.2	Butted Reservoir Cores	100-140	16-20	?	Horizontal	s, t
Huang & Tracht (1974)	1.8	5.1	Berea Sandstone	440-470	24	2.5	Horizontal	t
Rosman & Zana (1977)	0.8	2.5	Butted Reservoir Cores	11	15	3.6	Horizontal	
Graue & Zana (1978)	0.9	2.5	Rangely Reservoir Cores	59	18	1.3	Horizontal	t
Metcalf & Yarborough (1979)	2.4	5.1	Berea Sandstone	450		2.7	Horizontal	s
Watkins (1978)	0.3	3.5-5.1	Berea Sandstone	290-670	17-22	0.4-19.1	Vertical	s, t
	0.15	5.1-6.4	San Andres Carbonate Reservoir Cores	6.2-16.8	11-15	0.3- 5.1	Vertical	s, t

\*1 cm/hr = 0.787 ft/day

appropriate for field scale displacements.

Core floods may also be an important tool for testing numerical simulation methods. Oil recovery, pressure drop, and produced fluid compositions can all be compared against simulator predictions. For instance, Leach and Yellig (1979) successfully simulated displacements of a synthetic oil by CO<sub>2</sub> with an equation of state compositional simulator. In some cases, history matches of laboratory displacements may be used to determine unknown input data. One possible technique would be to use independent phase behavior and fluid property data (see discussion of PVT experiments below) to tune phase behavior calculations, to simulate core floods to check the accuracy of the simulator for the combination of phase behavior and flow at representative reservoir conditions, and then to use the validated simulator for field scale predictions, with appropriate attention to the effects of grid size (Gardner et al. 1979; Camy and Emmanuel 1977). It should be noted, however, that no example of such a method has yet been published for a CO<sub>2</sub> flood, though a very similar technique was used by Todd et al. (1978) to evaluate chemical flood designs for the Bell Creek micellar-polymer pilot.

#### 5.4 PVT Experiments

Equilibrium phase behavior and fluid property measurements provide direct evidence concerning the physical behavior of mixtures of CO<sub>2</sub> and crude oil. The measurement most commonly made determines saturation pressures for binary mixtures of the recombined reservoir fluid with CO<sub>2</sub> (Graue and Zana 1978; Sigmund et al. 1979; Gardner et al. 1979; Huang and Tracht 1974; Peterson 1978; Rathmell et al. 1971; Shelton and Yarborough 1977; Simon et al. 1977; and Orr et al. 1980a). In a typical experiment, CO<sub>2</sub> and oil are metered into a high pressure visual cell to produce a mixture of known overall composition. The volume, and hence the pressure, of the mixture is then changed, usually by injecting or removing mercury from the cell. Thus, the experiment is identical to a standard constant composition expansion performed for a reservoir fluid sample. At each pressure, the volumes of any phases present are measured. If only one phase is present, then the phase density (often represented as swelling of oil by CO<sub>2</sub>) is easily obtained from the known masses of CO<sub>2</sub> and oil charged and the measured volume of the cell. Bubble point pressures for the CO<sub>2</sub>-oil mixtures can be accurately measured by plotting cell pressure against cell volume. A sharp change is observed in the pressure-volume curve when gas appears or disappears. Liquid-liquid saturation pressures and dew point pressures must be detected visually because the overall compressibility of the system does not change dramatically when the second phase appears.

Typical results of a single contact phase behavior study are shown in Figure 3.9. Phase diagrams such as that shown in Figure 3.9 and the phase volume data used to construct that diagram can be predicted using the phase behavior routines built into compositional reservoir simulators. Therefore, saturation pressure measurements can be used to test phase behavior

predictions of the simulators. Graue and Zana (1978) reported good agreement between observed and calculated saturation pressures and liquid densities after adjustment of parameters used in the equilibrium K-value and liquid density calculations in their compositional simulator. Sigmund et al. (1979) adjusted binary interaction parameters used in the Peng-Robinson equation of state to match saturation pressures for a CO<sub>2</sub>-crude oil system prior to simulating slim tube displacements. Thus, saturation pressure data are useful as an independent measure of the accuracy of predictions from simulator phase packages.

More detailed experimental data on phase compositions can also be obtained, though the difficulties associated with sampling and analysis of high pressure mixtures make such measurements time consuming and expensive, and hence less common. Phase composition data have been reported for CO<sub>2</sub>-crude oil systems by Rathmell et al. (1971), Shelton and Yarborough (1977), Simon et al. (1977), Graue and Zana (1978), and Gardner et al. (1979). Phase composition data can be extremely valuable for improving understanding of the effects of component partitioning on the displacement process. Furthermore, comparison of observed and calculated phase compositions is a much more rigorous test of a phase behavior routine than matching saturation pressures alone. In addition, if phase density and viscosity data are also obtained, detailed tests of the accuracy of fluid property calculations can be made. Simultaneous measurements of composition, viscosity and density of a phase are, unfortunately, rare.

It is important to recognize that the binary mixtures of oil and CO<sub>2</sub> which are studied in a single contact phase equilibrium study are not necessarily those which will occur during a displacement process in a reservoir. When CO<sub>2</sub> is injected, it eventually forms a CO<sub>2</sub>-rich phase containing extracted hydrocarbons, and an oil-rich phase which also contains substantial quantities of dissolved CO<sub>2</sub>. The two phases will have different densities and viscosities as well as different relative permeabilities, and hence will move at different rates. The mixtures which occur away from an injection well will result from mixing of those phases with reservoir fluids and may, therefore, be quite different from the binary mixtures.

It is the differences between the multiple contact and single contact mixtures which account for the improvement in local displacement efficiency which comes about due to extraction of hydrocarbons by the CO<sub>2</sub>. Unfortunately, it is not a simple procedure to relate the displacement process to results of single contact phase behavior studies. Again, some sort of numerical simulation is required to account for compositional effects on phase volumes, densities and viscosities (Gardner et al. 1979, and Orr et al. 1980a). Multiple contact experiments such as those reported by Gardner et al. (1979) which mix CO<sub>2</sub>-rich phase from a binary mixture with fresh reservoir fluid or which mix the oil-rich phase with fresh CO<sub>2</sub> can be used to investigate qualitatively how phase behavior will change along a composition path which more closely simulates the displacement process. Measurements of this sort are sufficiently time consuming so that it is unlikely that they will be performed as frequently as slim tube displacements, however. Nevertheless, they are needed if progress is to be made in representing the phase

behavior of CO<sub>2</sub>-oil mixtures in terms of a small number of pseudo-components. Such a representation is required if compositional simulations are to be performed for reservoir scale processes (Todd 1979).

### 5.5 Continuous Multiple Contact Experiment

Much of the phase behavior information collected in batch single and multiple contact PVT experiments can be obtained efficiently with the continuous multiple contact (CMC) experiment described in §2.2. That experiment produces phase behavior data at one pressure for mixtures which change composition continuously through the experiment. A standard PVT experiment, on the other hand, examines the behavior of a mixture of fixed composition at different pressures. While the CMC experiment can be used efficiently to measure the solubility of CO<sub>2</sub> in the oil and to detect multiple phases, it is most useful for direct measurements of equilibrium phase compositions. While such measurements can be made in a PVT apparatus, they are not as convenient as the CMC experiment, partly because batch experiments are inherently more time consuming than continuous one, and partly because it is difficult to obtain representative samples from the PVT apparatus. Sample collection in the CMC experiment is automatic and continuous. Phase composition data can be used to test directly the accuracy of an equation of state or phase behavior correlations, and the CMC experiment produces information which can be used directly in simulations of the type described in §4 and by Gardner et al. (1979). The CMC experiment also has the advantage that results are not sensitive to production rates of the two phases. Finally, the installation of high pressure density measuring equipment (such as the Mettler/Paar DMA 512 densitometer used in our PVT apparatus) in the sample lines would allow simultaneous phase density measurements. In addition, techniques for on-line phase viscosity measurements are being investigated. Thus, with additional development of the CMC experiment it may be possible to make rapid and efficient simultaneous measurements of phase compositions and fluid properties in an experiment which is not much more difficult to perform than a slim tube displacement.

### 5.6 Task 4: Conclusions

- (1) The suite of laboratory experiments used to evaluate a particular field for CO<sub>2</sub> flooding should be chosen, based on the characteristics of the field and on the type of numerical simulation to be used for field scale recovery predictions.
- (2) Because they eliminate effects of viscous fingering, gravity segregation and rock heterogeneity, slim tube displacement experiments offer the simplest method for evaluating the effectiveness of the phase behavior portion of the displacement process.

- (3) Core floods do not necessarily always eliminate such effects and hence must be interpreted with care.
- (4) Equilibrium phase behavior experiments provide data useful for tuning phase behavior calculations in reservoir simulators but are time consuming and expensive.
- (5) Continuous multiple contact experiments can be used to measure phase compositions for CO<sub>2</sub>-crude oil mixtures much more rapidly than in static equilibrium cell studies.

## 6. SUMMARY

This report presents research results in four areas:

- (1) Experimental equipment and techniques.
- (2) Displacement tests and extensive supporting data on phase behavior of CO<sub>2</sub>-crude oil mixtures.
- (3) One-dimensional simulation of CO<sub>2</sub>-crude oil displacements.
- (4) Review of experimental techniques for evaluation of field prospects for CO<sub>2</sub> flooding.

In the first area, design of an apparatus to perform batch single and multiple contact PVT experiments has been presented. That apparatus is unusual because it includes provision for measurements of phase volumes, densities and viscosities. A technique for obtaining high pressure samples of CO<sub>2</sub>-crude oil mixtures from the PVT apparatus has also been developed. While that technique was successful for mixtures of CO<sub>2</sub> with well-characterized hydrocarbons, substantial scatter was observed for high pressure CO<sub>2</sub>-crude oil samples. A much more reliable technique was developed for measurement of compositions of phases which form in CO<sub>2</sub>-crude oil mixtures at reservoir conditions. The continuous multiple contact experiment offers a simple displacement technique for rapid, continuous measurement of phase compositions. It relies upon the use of a precise back pressure regulator developed as part of the project and upon the adaptation of chromatographic techniques for characterization of crude oil samples. In addition, the experiment provides direct evidence of the extraction of hydrocarbons by CO<sub>2</sub> at the experimental conditions.

In the second area, results of displacement tests in slim tubes and cores have been presented. The interpretation of the displacement tests has been based on detailed measurements of the physical behavior of the CO<sub>2</sub>-crude oil mixtures which occur during the displacement and on the results of model calculations performed with the one-dimensional simulator developed as part of the project. The complex phase behavior of CO<sub>2</sub>-crude oil mixtures has been studied in some detail, and the reservoir conditions under which liquid-liquid, liquid-liquid-vapor and liquid-vapor behavior should be expected have been delineated. The combination of displacement results, phase behavior measurements and model calculations provides strong evidence that for the low temperature CO<sub>2</sub> floods studied here, the very high displacement efficiency observed in slim tube displacements is the result of efficient extraction of a broad range of hydrocarbons by a CO<sub>2</sub>-rich liquid phase. Furthermore, the comparison of slim tube and core flood results suggests that even in laboratory core floods, viscous fingering can significantly reduce oil recovery, and that the adverse effect of viscous fingering is aggravated by interactions of phase behavior with viscous fingering. Future investigations will deal with those interactions where high water saturations are present.

Results presented in areas (3) and (4) focused on the interpretation and uses of laboratory experimental data. Factors which influence various types of laboratory experiments have been reviewed and the uses and limitations of slim tube, core flood and PVT data have been summarized.

The research presented here has concentrated on the mechanisms acting to influence displacement efficiency in secondary CO<sub>2</sub> floods. The experimental techniques developed and the results obtained provide a base of understanding upon which additional investigations of the interactions of phase behavior, viscous fingering, gravity segregation, rock heterogeneity and trapping or shielding of oil from contact with CO<sub>2</sub> by high water saturations can proceed. It is the understanding of those interactions and the development of techniques to model them that will lead to more accurate methods for performance prediction for field scale CO<sub>2</sub> floods.

## ACKNOWLEDGEMENT

The research effort reported on here was the result of much hard work by H.K. Wainwright, who designed much of the experimental equipment, including the improved back pressure regulator and the continuous multiple contact apparatus; C.L. Lien, who developed sampling and chromatographic techniques; and, M.K. Silva and M.T. Pelletier, who built, operated, and steadily improved the PVT and displacement equipment. Without their contributions progress would have been slow indeed. We also thank R.K. Spaulding for her help in performing static equilibrium phase behavior experiments. We are especially indebted to J.P. Heller for many useful suggestions. We thank K.A. Grattan for all her able assistance in assembling this and other manuscripts. We are grateful to Conoco, Inc. for providing crude oil samples and for a grant used to purchase the gas chromatograph used extensively in this project. Finally, we thank the U.S. Department of Energy and the New Mexico Energy and Minerals Department for the support that made this work possible. In particular, we thank Royal Watts and Leo Noll for their active interest and encouragement. We are also indebted to C.C. Nathan of the New Mexico Energy Institute for his assistance throughout this project.

## REFERENCES

- American Society for Testing and Materials 1976, "Proposed Test Method for Boiling Range Distribution of Crude Petroleum by Gas Chromatography," ASTM Standards, Part 25, Philadelphia, PA, 716-722.
- Bilhartz, H. L., Charlson, G. S., Stalkup, F. I. and Miller, C. C. 1978, "A Method for Projecting Full-Scale Performance of CO<sub>2</sub> Flooding in the Willard Unit," SPE 7051, presented at SPE 5th Symposium on Improved Oil Recovery, Tulsa, April 16-19.
- Camy, J. P. and Emmanuel, A. S. 1977, "Effect of Grid Size in the Compositional Simulation of CO<sub>2</sub> Injection," SPE 6894, presented at SPE 52nd Annual Meeting of SPE of AIME, Denver, October 9-12.
- Coats, K. H. 1979, "An Equation-of-State Compositional Model," SPE 8284, presented at SPE 54th Annual Fall Meeting, Las Vegas, September 23-26.
- Delaney, R. P. and Fish, R. M. 1980, "Judy Creek CO<sub>2</sub> Flood Performance Predictions," presented at 31st Annual Meeting of the Petroleum Society of CIM, Calgary, May 25-28.
- Drennon, M. D., Kelm, C. H. and Whittington, H. M. 1980, "A Method for Appraising the Feasibility of Field-Scale CO<sub>2</sub> Miscible Flooding," SPE 9323, presented at SPE 55th Annual Fall Meeting, Dallas, September 21-24.
- Dumore, J. M. 1964, "Stability Considerations in Downward Miscible Displacements," Soc. Pet. Eng. J. (December) 356-362.
- Fussell, L. T. 1977, "A Technique for Calculating Phase Equilibria of Three Coexisting Hydrocarbon Phases," SPE 6722, presented at 52nd Annual Fall Technical Conference of SPE of AIME, Denver, October 9-12.
- Fussell, L. T. and Fussell, D. D. 1977, "An Iterative Sequence for Compositional Models Incorporating the Redlich-Kwong Equation of State," SPE 6891, presented at SPE 52nd Annual Fall Meeting, Denver, October 9-12.
- Gardner, J. W., Orr, F. M. and Patel, P. D. 1979, "The Effect of Phase Behavior on CO<sub>2</sub> Flood Displacement Efficiency," SPE 8367, presented at SPE 54th Annual Fall Meeting, Las Vegas, September 23-26.
- Gharib, S. and Doscher, T. M. 1979, "Solvent Displacement of Residual Oil," presented at 5th Annual DOE Symposium on Enhanced Oil and Gas Recovery & Improved Drilling Technology, Tulsa, August 22-24.

- Graue, D. J. and Zana, E. 1978, "Study of a Possible CO<sub>2</sub> Flood in the Rangely Field, Colorado," SPE 5th Symposium on Improved Methods for Oil Recovery, Tulsa, April 16-19.
- Helfferich, F. G. 1979, "General Theory of Multicomponent, Multi-Phase Displacement in Porous Media," SPE 8372, presented at SPE 54th Annual Fall Meeting, Las Vegas, September 23-26.
- Heller, J. P. 1963, "The Interpretation of Model Experiments for the Displacement of Fluids Through Porous Media," AICHE J 9 (July) 452-459.
- Henderson, L. E. 1974, "The Use of Numerical Simulation to Design a Carbon Dioxide Miscible Displacement Project," J. Pet. Tech. 26 (December) 1327-1334.
- Henry, R. L. and Metcalfe, R. S. 1980, "Multiple Phase Generation During CO<sub>2</sub> Flooding," SPE 8812, presented at the First Joint SPE/DOE Symposium on Enhanced Oil Recovery, Tulsa, April 20-23.
- Hill, S. 1949, "Channeling in Packed Columns," Chem. Eng. Sci. 1 No. 6, 247.
- Holm, L. W. 1959, "Carbon Dioxide Solvent Flooding for Increased Oil Recovery," Trans. AIME 216, 225-231.
- Holm, L. W. and Josendal, V. A. 1974, "Mechanisms of Oil Displacement by Carbon Dioxide," J. Pet. Tech. 16 (December) 1427-1438.
- Holm, L. W. and Josendal, V. A. 1980, "Effect of Oil Composition on Miscible-Type Displacement by Carbon Dioxide," SPE 8814, presented at 1st SPE/DOE Symposium on Enhanced Oil Recovery, Tulsa, April 20-23.
- Huang, E. T. S. and Tracht, J. H. 1974, "The Displacement of Residual Oil by Carbon Dioxide," SPE 4735, presented at the SPE 3rd Symposium on Improved Oil Recovery, Tulsa, April.
- Hutchinson, C. A., Jr. and Braun, P. H. 1961, "Phase Relations of Miscible Displacement in Oil Recovery," AICHE J 7 (March) 64-72.
- Kazemi, H., Vestal, C. R. and Shank, G. D. 1978, "An Efficient Multicomponent Numerical Simulator," Soc. Pet. Eng. J. 18 (October) 355-368.
- Leach, M. P. and Yellig, W. F. 1979, "Compositional Model Studies: CO<sub>2</sub>-Oil Displacement Mechanisms," SPE 8368, presented at SPE 54th Annual Fall Meeting, Las Vegas, September 23-26.
- Lee, A. L. 1965, "Viscosity of Light Hydrocarbons," Monograph on API Research Project 65, American Petroleum Institute, New York.

- McDonald, R. C. 1971, "Numerical Simulation with Interphase Mass Transfer," Report No. U7-71-a, Texas Petroleum Research Committee, Austin.
- Meldrum, A. H. and Nielsen, R. F. 1955, "A Study of Three-Phase Equilibria for Carbon Dioxide-Hydrocarbon Mixtures," *Prod. Monthly* (August) 22-35.
- Metcalfe, R. S. and Yarborough, L. 1979, "The Effect of Phase Equilibria on the CO<sub>2</sub> Displacement Mechanism," *Soc. Pet. Eng. J.* 19 (August) 242-252.
- Michels, A., Botzen, A. and Schuurman, W. 1957, "The Viscosity of Carbon Dioxide between 0°C and 75°C at Pressures up to 2000 Atmospheres," *Physica* 23, 95-102.
- Naar, J., Wygal, R. J. and Henderson, J. H. 1962, "Imbibition Relative Permeability in Unconsolidated Porous Media," *Soc. Pet. Eng. J.* 2, 13-17.
- Newitt, D. M., Pai, M. U., Kuloor, N. R. and Huggill, J. A., 1956, "Carbon Dioxide" in *Thermodynamic Functions of Gases*, Vol. 1., F. Din, Ed., Butterworths, London, 102-134.
- Nolen, J. S. 1973, "Numerical Simulation of Compositional Phenomena in Petroleum Reservoirs," SPE 4274, presented at SPE 3rd Symposium on Numerical Simulation, Houston, January 11-12.
- Orr, F. M., Yu, A. D. and Lien, C. L. 1980a, "Phase Behavior of CO<sub>2</sub> and Crude Oil in Low Temperature Reservoirs," SPE 8813, presented at the First Joint SPE/DOE Symposium on Enhanced Oil Recovery, Tulsa, April 20-23.
- Orr, F. M., Silva, M. K., Lien, C. L. and Pelletier, M. T. 1980b, "Laboratory Experiments to Evaluate Field Prospects for CO<sub>2</sub> Flooding," SPE 9534, presented at Eastern Regional Meeting, November 5-7.
- Orr, F. M. 1980c, "Simulation of One-Dimensional Convection of Four Phase, Four Component Mixtures," Topical Report DOE/ET/12082-8, U. S. Department of Energy, Bartlesville, Oklahoma.
- Orr, F. M., Lien, C. L. and Pelletier, M. T. 1981, "Liquid-Liquid Phase Behavior in CO<sub>2</sub>-Hydrocarbon Systems," Symposium on Chemistry of Enhanced Oil Recovery, American Chemical Society, Atlanta, March 29-April 3.
- Perkins, T. K. and Johnson, O. C. 1963, "A Review of Diffusion and Dispersion in Porous Media," *Soc. Pet. Eng. J.* (March) 70-75.

- Perrine, R. L. 1961a, "Stability Theory and Its Use to Optimize Solvent Recovery of Oil," Soc. Pet. Eng. J. (March) 9-16.
- Perrine, R. L. 1961b, "The Development of Stability Theory for Miscible Liquid-Liquid Displacement," Soc. Pet. Eng. J. (March) 17-25.
- Perry, G. E., Guillory, A. J., Baron, J. D. and Moranville, M. B. 1978, "Weeks Island 'S' Sand Reservoir B Gravity Stable Miscible CO<sub>2</sub> Displacement, Iberia Parish, Louisiana," presented at the 4th Annual DOE Symposium on Enhanced Oil and Gas Recovery, Tulsa, August 29-31.
- Peterson, A. V. 1978, "Optimal Recovery Experiments with N<sub>2</sub> and CO<sub>2</sub>," Pet. Eng. (November) 40-50.
- Pongpitak, S. D. 1980, "Interaction of Phase Behavior with Multi-phase Flow in Porous Media," M.Sc. Thesis, New Mexico Institute of Mining and Technology.
- Pontius, S. B. and Tham, M. J. 1978, "North Cross (Devonian) Unit CO<sub>2</sub> Flood -- Review of Flood Performance and Numerical Simulation," J. Pet. Tech. 30 (December) 1706-1714.
- Pope, G. A. and Nelson, R. C. 1978, "A Chemical Flooding Compositional Simulator," Soc. Pet. Eng. J. 18, 339-354.
- Raimondi, P., Torcaso, M. A. and Henderson, J. H. 1961, "The Effect of Interstitial Water on the Mixing of Hydrocarbons during a Miscible Displacement Process," Mineral Industries Experimental Station Circular No. 61, The Pennsylvania State U., University Park (October 23-25).
- Raimondi, P. and Torcaso, M. A. 1964, "Distribution of the Oil Phase Obtained Upon Imbibition of Water," Soc. Pet. Eng. J. (March) 49-55.
- Rathmell, J. J., Stalkup, F. I. and Hassinger, R. C. 1971, "A Laboratory Investigation of Miscible Displacement by Carbon Dioxide," SPE 3483, presented at SPE 46th Annual Fall Meeting, New Orleans, October 3-6.
- Rosman, A. and Zana, E. 1977, "Experimental Studies of Low IFT Displacement by CO<sub>2</sub> Injection," SPE 6723, presented at SPE 52nd Annual Fall Meeting, Denver, October 9-12.
- Rutherford, W. M. 1962, "Miscibility Relationships in the Displacement of Oil by Light Hydrocarbons," Soc. Pet. Eng. J. (December) 340-346.

- Shelton, J. L. and Schneider, F. N. 1975, "The Effects of Water Injection on Miscible Flooding Methods Using Hydrocarbons and Carbon Dioxide," Soc. Pet. Eng. J. 15 (June) 217-226.
- Shelton, J. L. and Yarborough, L. 1977, "Multiple Phase Behavior in Porous Media During CO<sub>2</sub> or Rich-Gas Flooding," J. Pet. Tech. 19 (September) 1171-1178.
- Sigmund, P. M., Aziz, K., Lee, J. J., Nghiem, L. X. and Mehra, R. 1979, "Laboratory CO<sub>2</sub> Floods and Their Computer Simulation," World Petroleum Congress, Bucharest, Romania, September.
- Simon, R., Rosman, A. and Zana, E. 1978, "Phase Behavior Properties of CO<sub>2</sub> Reservoir Oil Systems," Soc. Pet. Eng. J. 18 (February) 20-26.
- Spaulding, R. K., Yu, A. D. and Orr, F. M. 1980, "Calibration Experiments for the Measurement of Density at Elevated Temperatures and Pressures," Report No. 80-2, New Mexico Petroleum Recovery Research Center, New Mexico Institute of Mining and Technology.
- Stalkup, F. I. 1970, "Displacement of Oil by Solvent at High Water Saturation," Soc. Pet. Eng. J. 10 (December) 337-348.
- Stalkup, F. I. 1978, "Carbon Dioxide Miscible Flooding: Past, Present and Outlook for the Future," J. Pet. Tech. 30 (August) 1102-1112.
- Stone, H. L. 1973, "Estimation of Three-Phase Relative Permeability and Residual Oil Data," J. Can. Pet. Tech. 12, 53-61.
- Todd, M. R. 1979, "Modeling Requirements for Numerical Simulation of CO<sub>2</sub> Recovery Processes," SPE 7998, presented at the California Regional Meeting of SPE, Ventura, California, April 18-20.
- Todd, M. R., Dietrich, J. K., Goldberg, A. J. and Larson, R. G. 1978, "Numerical Simulation of Competing Chemical Flood Designs," SPE 7077, presented at SPE 5th Symposium on Improved Methods for Oil Recovery, Tulsa, April 16-19.
- Todd, M. R. and Longstaff, W. J. 1972, "The Development, Testing and Application of a Numerical Simulator for Predicting Miscible Flood Performance," J. Pet. Tech. 24 (July) 874-882.
- Wang, G. C. and Locke, D. C. 1980, "A Laboratory Study of the Effects of CO<sub>2</sub> Injection Sequence on Tertiary Oil Recovery," Soc. Pet. Eng. J. 20 (August) 278-280.

Watkins, R. W. 1978, "A Technique for the Laboratory Measurement of Carbon Dioxide Unit Displacement Efficiency in Reservoir Rock," SPE 7474, presented at SPE 53rd Annual Fall Meeting, Houston, October 1-3.

Whitehead, W. R., Kimbler, O. K., Hoshman, R. M. and Hervey, J. R. 1980, "Investigation of Enhanced Oil Recovery Through Use of Carbon Dioxide," U.S. Dept. of Energy Progress Report for the period July 7, 1978-December 31, 1979. Louisiana State University, Baton Rouge, February.

Yarborough, L. and Smith, L. R. 1970, "Solvent and Driving Gas Compositions for Miscible Slug Displacement," Soc. Pet. Eng. J. (September) 298-310.

Yellig, W. F. and Metcalfe, R. S. 1980, "Determination and Prediction of CO<sub>2</sub> Minimum Miscibility Pressures," J. Pet. Tech. 32 (January) 160-168.

Yu, A. D. 1980, "Volumetric Calibrations of Windowed Cells for PVT Measurements," Report No. 80-22, New Mexico Petroleum Recovery Research Center, New Mexico Institute of Mining and Technology.

Appendix A

Phase Behavior of CO<sub>2</sub> and Crude Oil in Low  
Temperature Reservoirs

## PHASE BEHAVIOR OF CO<sub>2</sub> AND CRUDE OIL IN LOW TEMPERATURE RESERVOIRS

by F.M. Orr Jr., A.D. Yu, and C.L. Lien,  
New Mexico Petroleum Recovery Research Center

© Copyright 1980, Society of Petroleum Engineers

This paper was presented at the First Joint SPE/DOE Symposium on Enhanced Oil Recovery at Tulsa, Oklahoma, April 20-23, 1980. The material is subject to correction by the author. Permission to copy is restricted to an abstract of not more than 300 words. Write: 6200 N. Central Expwy., Dallas, Texas 75206.

### ABSTRACT

Phase behavior of carbon dioxide-crude oil mixtures which exhibit liquid-liquid and liquid-liquid-vapor equilibria is examined. Results of single contact phase behavior experiments for CO<sub>2</sub> separator oil mixtures are reported. Experimental results are interpreted using pseudo-ternary phase diagrams based on a review of phase behavior data for binary and ternary mixtures of CO<sub>2</sub> with alkanes. Implications for the displacement process of liquid-liquid-vapor phase behavior are examined using a one-dimensional finite difference simulator. Results of the analysis suggest that liquid-liquid and liquid-liquid-vapor equilibria will occur for CO<sub>2</sub>-crude oil mixtures at temperatures below about 50°C (122°F), and that development of miscibility occurs by extraction of hydrocarbons from the oil into a CO<sub>2</sub> rich liquid phase in such systems.

### INTRODUCTION

The efficiency of a displacement of oil by carbon dioxide (CO<sub>2</sub>) depends on a variety of factors; these include phase behavior of CO<sub>2</sub>-crude oil mixtures generated during the displacement, densities and viscosities of the phases present, relative permeabilities to individual phases and a host of additional complications such as dispersion, viscous fingering, reservoir heterogeneities and layering, and so on. It is generally acknowledged that phase behavior and attendant compositional effects on fluid properties strongly influence local displacement efficiency<sup>1,2,3,4,5</sup> though it is also clear that on a reservoir scale, poor vertical and areal sweep efficiency, caused by the low viscosity of the displacing CO<sub>2</sub>, may negate the favorable effects of phase behavior.<sup>3</sup>

Interpretation of the effects of phase behavior on displacement efficiency is made difficult by the complexity of the behavior of CO<sub>2</sub>-crude oil mixtures. The standard interpretation of CO<sub>2</sub> flooding phase behavior, given first by Rathmell *et al.*<sup>1</sup> is that CO<sub>2</sub> flooding behaves much like a vaporizing gas drive, as described originally by Hutchinson

and Braun.<sup>6</sup> During a flood, vapor phase CO<sub>2</sub> mixes with oil in place and extracts light and intermediate hydrocarbons. After multiple contacts, the CO<sub>2</sub>-rich phase vaporizes enough hydrocarbons to develop a composition which can displace oil efficiently, if not miscibly. The picture presented by Rathmell *et al.*<sup>1</sup> appears to be consistent with phase behavior observed for CO<sub>2</sub>-crude oil mixtures as long as the reservoir temperature is high enough. Table 1 summarizes data reported for CO<sub>2</sub>-crude oil mixtures. Of the ten systems studied, all those at temperatures above 50°C show only liquid-vapor equilibria while those below 50°C exhibit liquid-liquid vapor separations (Stalkup<sup>3</sup> also reports two phase diagrams which are qualitatively like the other low temperature diagrams but does not give temperatures). Thus, at temperatures not too far above the critical temperature of CO<sub>2</sub> (31°C), mixtures of CO<sub>2</sub> and crude oil exhibit multiple liquid phases and at some pressures liquid-liquid-vapor equilibria are observed.<sup>5,7,8</sup> It has not been established whether Rathmell *et al.*'s<sup>1</sup> interpretation of the process mechanism can be extended to cover the more complex phase behavior of low temperature CO<sub>2</sub>-crude oil mixtures. In a recent paper, Metcalfe and Yarborough<sup>4</sup> argued that low temperature CO<sub>2</sub> floods behave more like condensing gas drives<sup>6,2</sup> while Kamath *et al.*<sup>13</sup> concluded that CO<sub>2</sub> solubility effects dominate in low temperature displacements. In contrast, Huang and Tracht<sup>7</sup> argued that swelling and stripping of hydrocarbons from the oil by a CO<sub>2</sub>-rich liquid phase are the dominant mechanisms for tertiary recovery in low temperature displacements in the liquid-liquid region. This paper examines the phase behavior of low temperature CO<sub>2</sub>-crude oil mixtures with the goal of understanding the influence of liquid-liquid and liquid-liquid-vapor phase behavior on the displacement mechanism. Results of phase behavior experiments with an eastern New Mexico crude oil are presented and compared with the behavior of binary and ternary mixtures of CO<sub>2</sub> with normal alkanes. The results of the phase behavior experiments are interpreted in terms of a simple ternary representation similar to that used by Gardner *et al.*<sup>5</sup> and the influence of the phase behavior on displacement efficiency is predicted using a simple numerical model.

References and illustrations at end of paper.

Phase Behavior of CO<sub>2</sub> with Maljamar Crude Oil

Single contact phase equilibrium experiments were performed with separator oil from the Maljamar Field, Lea County, New Mexico. Properties of the oil are given in Table 2. The oil composition was determined using a Hewlett-Packard 5840A gas chromatograph with an OV-101 column which separates hydrocarbons in boiling point order. As the Figure 1 illustrates, the oil is rich in components in the C<sub>5</sub> to C<sub>20</sub> range, with about 65 weight percent (85 mol percent) of the crude oil lighter than C<sub>20</sub>.

In a typical experiment, metered amounts of CO<sub>2</sub> and oil were charged into a 190 cm<sup>3</sup> high pressure cell which has windows on both sides which permit observation of the upper 50% of the cell volume. The cell could be inverted to view an interface or phase in the blind portion of the cell. The cell was installed in an air bath within which the temperature was controlled to 32.2°C ± .4°C. Cell contents could be viewed in either transmitted or reflected light. Volume of the cell contents was varied by injecting or removing mercury from the cell; cell pressure was measured by a Setra 204 transducer (0-65 MPa) with a digital display.

Results of the phase behavior experiments are summarized in Figure 2. At overall CO<sub>2</sub> concentrations below about 80 mole percent, the CO<sub>2</sub>-crude oil mixtures exhibited bubble points. That is, as the pressure in the cell was reduced from high levels, a vapor phase appeared at the top of the cell. With further pressure reductions, the volume of the vapor phase grew with attendant shrinkage of the liquid phase.

For CO<sub>2</sub> concentrations of 79.3 mole percent and above, two liquid phases were observed. At the highest pressure investigated (27.58 MPa) two phases, both black to reflected and transmitted light, could be detected in ultraviolet (uv) light. The fact that both phases were very dark suggests that heavy hydrocarbons were present in both phases. When pressure was reduced from 27.58 MPa to 24.13 MPa, the upper phase increased in volume slightly and took on a dark burgundy color to transmitted light. At the higher pressures, the phases were very slow to separate, indicating a small density difference between phases. With additional pressure reductions, the upper liquid phase grew in volume and its color gradually changed to a light yellow or straw color. In the neighborhood of 6.89 MPa, vapor appeared at the top of the cell, and over a small pressure range, but with a large volume change, the upper liquid phase changed from a liquid to a vapor. This sequence of phase appearances was observed even when the overall CO<sub>2</sub> mole fraction was as high as .9949. Evidently, addition of even a small amount of crude oil to pure CO<sub>2</sub> raises the critical temperature of the mixture from that of CO<sub>2</sub> (31°C) to above the operating temperature (32.2°C).

In all of the experiments in which the CO<sub>2</sub> concentration was above about 70 mol percent, a small amount of heavy resinous material was observed on the cell window, and the exact level of the mercury-oil interface was obscured by the formation of beads of mercury surrounded by oil. The beads of mercury failed to coalesce even after waiting periods of up to two days.

Properties of the upper and lower phases for a mixture of 79.3 mol % CO<sub>2</sub> and separator oil were measured and are reported in Table 3. Densities were measured using a Mettler/Paar DMA 512 high pressure densitometer. The density listed for the lower phase at 14.92 mPa seems too low. We believe the discrepancy is probably due to temporary difficulties with the temperature controller for the high pressure densitometer, and that the value given for 15.13 mPa is more accurate. Viscosities were measured by transferring the phase in question to a second cell at a known rate through a capillary tube while measuring the pressure drop. These data clearly indicate that at conditions typical for Permian basin fields, the two liquid phases which form for at least one mixture of oil and CO<sub>2</sub> show densities which are very nearly the same and viscosities which differ by much less than those of the original oil and pure CO<sub>2</sub>. The CO<sub>2</sub>-rich liquid phase was nearly three times more viscous than pure CO<sub>2</sub> at 32.2°C, presumably because substantial quantities of hydrocarbons were dissolved in it. In addition, the viscosity of the hydrocarbons remaining in the oil-rich liquid phase was more than three times lower than that of the original oil. Thus, compositional effects on fluid properties may have an important effect on displacement behavior.

Carbon number distributions were obtained for the hydrocarbons contained in both the upper and lower phases. Figure 3 compares the distribution of the original oil with the CO<sub>2</sub>-rich and oil-rich phase distributions. The high pressure sampling scheme used did not permit estimation of the heavy portion of the oil which was not eluted from the gas chromatograph column. Thus, Figure 3 compares the distributions up through C<sub>24</sub> only. The three carbon number distributions differ only slightly in the range C<sub>5</sub>-C<sub>24</sub>. What is remarkable is the effectiveness of the extraction of hydrocarbons into the CO<sub>2</sub>-rich phase which contained substantial quantities of components as heavy as C<sub>24</sub>. These and similar data reported by Gardner *et al.*<sup>5</sup> suggest that even in liquid-liquid systems, CO<sub>2</sub> can efficiently extract hydrocarbons from the oil.

One additional experiment was performed to assess the effect of solution gas on the phase behavior of mixtures of CO<sub>2</sub> and Maljamar crude. Gas of the composition given in Table 4 was added to separator oil to give a recombined reservoir fluid (RRF) with a bubble point of 10.52 mPa (~500 SCF/BBL). A mixture of 74.4 mol % CO<sub>2</sub> and RRF was then examined in the high pressure cell for pressures between 7.58 and 31.03 mPa. A comparison of the volumetric behavior of this mixture with that observed for the mixture containing 79.7% CO<sub>2</sub> and separator oil is shown in Figure 4. At low pressures both mixtures formed a dark liquid and a clear vapor, and as pressure was increased, a second liquid phase appeared. With additional increases in pressure, the vapor phase disappeared, leaving two liquids. Substantial differences occurred at higher pressures, however. The separator oil mixture showed small reductions in the volume of the upper phase with increasing pressure, while in the RRF mixture the upper phase grew at the expense of the lower phase. While the actual disappearance of the lower phase was not observed, an extrapolation of the volume of the L<sub>31</sub> phase vs. pressure gives a saturation pressure of above 30.06 mPa. Thus, it appeared that

for the separator oil mixture, the single-phase region would be approached with the disappearance of the upper phase—a bubble point except that these are liquid-liquid equilibria rather than vapor-liquid equilibria—while in the RRF mixture it would occur with the disappearance of the lower phase—a dew point in vapor-liquid parlance. These data suggest that the full phase diagram for CO<sub>2</sub>-RRF mixtures would be similar to those reported<sup>2</sup> by Gardner *et al.*<sup>5</sup> and Stalkup,<sup>3</sup> with retrograde behavior in the liquid-liquid region of the pressures and compositions. Apparently, addition of the solution gas to the separator oil causes a substantial change in the location of the liquid-liquid critical point. Thus, at high CO<sub>2</sub> concentrations and high pressure, the RRF mixture is more easily extracted into the CO<sub>2</sub> rich phase.

The phase behavior reported here is qualitatively similar to that reported for five other CO<sub>2</sub>-crude oil systems. Rathmell *et al.*<sup>1</sup> described liquid-liquid separations in a CO<sub>2</sub>-crude oil mixture, and phase diagrams qualitatively similar to Figure 2 have been reported by Huang and Tracht,<sup>7</sup> Shelton and Yarborough,<sup>8</sup> Stalkup<sup>3</sup> and Gardner *et al.*<sup>5</sup> While the phase diagrams all show the existence of liquid-liquid and liquid-liquid vapor regions, there is sufficient variation in the details of the phase diagrams to provide a challenge for interpreters of the implications of such phase behavior for the displacement process.

#### Phase Behavior of CO<sub>2</sub> and Normal Alkanes

##### Binary Mixtures

The complex phase behavior shown in Figure 2 can be understood qualitatively by examining the behavior of mixtures of CO<sub>2</sub> and normal alkanes. Mixtures of CO<sub>2</sub> with hydrocarbons methane through hexane show only liquid-vapor immiscibility. Binary mixtures of CO<sub>2</sub> with normal alkanes between heptane (C<sub>7</sub>) and tridecane (C<sub>13</sub>) exhibit phase behavior similar to that shown schematically for CO<sub>2</sub> and decane in Figures 5 and 6. Such mixtures can exist as two liquid phases for pressures and temperatures lying to the left of the L-L critical locus and above the L-L-V locus in Figure 5. Liquid-vapor mixtures occur within the envelope bounded by the vapor pressure curves of CO<sub>2</sub> and C<sub>10</sub> (dashed curves), and the L-V critical locus.

Figure 6 shows a set of qualitative constant temperature pressure-composition (P-X) diagrams for CO<sub>2</sub> and decane (C<sub>10</sub>) at six temperatures. Detailed data for CO<sub>2</sub>-C<sub>10</sub> mixtures are given by Meldrum and Nielsen,<sup>14</sup> Stewart and Nielsen,<sup>15</sup> Reamer and Sage,<sup>16</sup> Schneider *et al.*,<sup>17</sup> Zarah *et al.*<sup>18</sup> and Kulkarni *et al.*<sup>19</sup> The phase diagram for T<sub>1</sub> in Figure 6 corresponds to a temperature which lies somewhere below that given by the liquid-liquid critical locus (L-L) in Figure 5. At T<sub>1</sub>, binary mixtures of CO<sub>2</sub> and C<sub>10</sub> separate into liquid and vapor phases at low pressures. There is one pressure (at a given temperature T<sub>1</sub>) at which three phases, a decane rich liquid (L<sub>1</sub>), a CO<sub>2</sub> rich liquid (L<sub>2</sub>) and a CO<sub>2</sub> rich vapor (V) occur (Figure 6, T<sub>1</sub>). The L-L-V locus in Figure 5 is the set of temperatures and pressures at which three phases can coexist. For pressures between the three phase pressure and the vapor pressure of CO<sub>2</sub>, either L<sub>1</sub>-L<sub>2</sub>, L<sub>2</sub>-V or single phase mixtures may be observed, depending on the mixture composition. At higher

pressures only L<sub>1</sub>-L<sub>2</sub> separations occur.

With increasing temperature (Figure 6, T<sub>2</sub>, T<sub>3</sub>, T<sub>4</sub>), the L<sub>1</sub>-L<sub>2</sub> region separates from the L<sub>1</sub>-V region.<sup>A</sup> A critical point, which corresponds to the L-L critical locus in Figure 5, appears at the base of the L<sub>1</sub>-L<sub>2</sub> region, and that critical pressure rises sharply with increasing temperature. For CO<sub>2</sub> and hydrocarbons C<sub>13</sub> and lighter, the liquid-liquid region separates from the liquid vapor region at temperatures below the critical temperature of CO<sub>2</sub>. When the critical temperature of CO<sub>2</sub> is reached, the remaining L-V envelope separates from the CO<sub>2</sub> side of the diagram, and a liquid-vapor critical point appears (Figure 6, T<sub>5</sub>). At still higher temperatures, L-V separations occur at pressures well above the critical pressure of CO<sub>2</sub> (Figure 6, T<sub>6</sub>), though the two phase region shrinks again as the critical temperature of C<sub>10</sub> (345°C) is approached (not shown).

Normal alkanes C<sub>14</sub> and heavier also show liquid-liquid immiscibility,<sup>14,15,17,20,21,22</sup> but in contrast to the separation of L<sub>1</sub>-L<sub>2</sub> and L<sub>2</sub>-V regions for light hydrocarbons, the L-L critical locus and the L-V critical locus merge into a continuous critical curve (Figure 7). Figure 8 shows the qualitative behavior of CO<sub>2</sub>-hexadecane mixtures for various temperatures (see Schneider *et al.*<sup>17</sup> for detailed data for this system). At temperatures below the critical temperature of CO<sub>2</sub>, the qualitative behavior is the same as that described for C<sub>10</sub> (Figure 8, T<sub>1</sub>). In this case, however, the region of L<sub>1</sub>-L<sub>2</sub> separations persists at temperatures above the critical temperature of CO<sub>2</sub>. A critical point appears in the L<sub>2</sub>-V region (Figure 8, T<sub>2</sub>). With further temperature increases, the L<sub>2</sub>-V region shrinks, eventually disappearing, leaving a large region in which the distinction between L<sub>1</sub>-L<sub>2</sub> and L-V separations is ambiguous (Figure 8, T<sub>3</sub> and T<sub>4</sub>). That is, above the L<sub>2</sub>-V critical temperature, a mixture can pass from what appears to be an L-V state at low pressure to a L<sub>1</sub>-L<sub>2</sub> state at high pressure without showing an L<sub>1</sub>-L<sub>2</sub>-V transition. Higher temperatures cause the L<sub>1</sub>-L<sub>2</sub> region to separate from the L-V region and a return to more familiar L-V immiscibility (Figure 8, T<sub>4</sub>, T<sub>5</sub> and T<sub>6</sub>). As the molecular weight of the alkane increases, the maximum temperature at which liquid-liquid immiscibility can occur also increases, as data reported by Liphard and Schneider for CO<sub>2</sub>-squalane (C<sub>30</sub>) mixtures clearly show.<sup>22</sup> Their results suggest that maximum temperatures at which L<sub>1</sub>-L<sub>2</sub> immiscibility can occur will vary with the composition of the crude oil. Oils with a C<sub>14+</sub> fraction of high molecular weight can be expected to show L<sub>1</sub>-L<sub>2</sub> behavior at higher temperatures than for oils with a lower molecular weight C<sub>14+</sub> fraction. CO<sub>2</sub>-C<sub>16</sub> mixtures show L<sub>1</sub>-L<sub>2</sub> immiscibility up to at least 135°C and CO<sub>2</sub>-squalane mixtures up to about 60°C,<sup>22</sup> hence it appears that the limit of about 50°C for such behavior in CO<sub>2</sub>-crude oil mixtures is in rough agreement with CO<sub>2</sub>-alkane behavior, since the molecular weight of C<sub>14+</sub> fractions normally will lie between that of C<sub>16</sub> (226) and squalane (422). Huang and Tracht observed liquid-liquid equilibrium for one CO<sub>2</sub>-crude oil mixture at 43.9°C but found only L-V immiscibility at 49.4°C.<sup>7</sup> Apparently, Metcalfe and Yarborough<sup>4</sup> failed to see liquid-liquid immiscibility in their synthetic oil system at 120°F (48.9°C) because their oil was very light, containing 30% C<sub>10</sub> and only 5% C<sub>14</sub>, and because their oper-

ating temperature was near the maximum temperature for such immiscibility even for much heavier oils.

Thus, the liquid-liquid immiscibility reported here and elsewhere<sup>1,3,5,7,8</sup> for CO<sub>2</sub>-crude oil mixtures appears to be consistent with the occurrence of such behavior in binary CO<sub>2</sub>-alkane mixtures. Liquid-liquid phase behavior will be a factor, therefore, in many of the CO<sub>2</sub> floods being considered for Permian basin fields.

### Ternary Mixtures

#### Type I. Phase behavior with a subcritical light hydrocarbon component

Ternary mixtures containing CO<sub>2</sub> have been studied by Snedeker,<sup>20</sup> Huie *et al.*,<sup>23</sup> Zarah *et al.*,<sup>18</sup> Yang *et al.*,<sup>24</sup> Gupta,<sup>25</sup> Francis,<sup>26,27</sup> and Meldrum and Nielsen<sup>14</sup> and useful discussions of phase behavior in ternary systems with one supercritical component have been given by Snedeker<sup>20</sup> and Elgin and Weinstock.<sup>28</sup> At low pressures ternary CO<sub>2</sub>-hydrocarbon mixtures will show liquid-vapor separations while high pressure mixtures may form two liquid phases, just as binary mixtures do, if one hydrocarbon component is heavy enough and the temperature is low enough. At intermediate pressures, two liquids and a vapor may coexist. There appear to be at least two ways in which the L<sub>1</sub>-L<sub>2</sub>-V region can appear with increasing pressure, depending on the ranges of pressures at which the three binary pairs exist as L-V or L<sub>1</sub>-L<sub>2</sub> mixtures. One way is illustrated by the data of Meldrum and Nielsen<sup>14</sup> which are plotted in Figure 9 along with estimated phase envelopes constructed with their data as well as data from the CO<sub>2</sub>-propane binary from Poettman and Katz.<sup>29</sup> At 4.21 MPa, the two-phase envelope is a band across the diagram (the dew point curves at high CO<sub>2</sub> concentrations are not shown). At 4.85 MPa, the band has shrunk, with the solubility of CO<sub>2</sub> in liquid propane increasing more than that in C<sub>16</sub>. With a further increase in pressure to 5.52 MPa, the three phase L<sub>1</sub>-L<sub>2</sub>-V triangle has appeared. It is as if with increasing pressure, the liquid propane phase becomes so rich in CO<sub>2</sub> that it is no longer miscible with a phase containing C<sub>16</sub>. Meanwhile, the CO<sub>2</sub>-C<sub>16</sub> binary is still showing L<sub>1</sub>-V equilibria. Thus, in the three phase region, the vapor phase, which is richest in CO<sub>2</sub>, is in equilibrium with a CO<sub>2</sub>-rich liquid phase and a hydrocarbon rich liquid (which even so contains more than 75 mol % CO<sub>2</sub>). As the pressure is increased above 5.52 Pa, the L<sub>2</sub> (CO<sub>2</sub>-rich liquid) phase becomes closer in composition to the vapor phase, and eventually the L<sub>2</sub> and V phases coincide at very high CO<sub>2</sub> concentrations) leaving only liquid-liquid equilibria. The resulting migration of the three phase triangle with increasing pressure toward lower propane concentration is shown in Figure 10. In this case, therefore, the three phase region occurs when the CO<sub>2</sub>-rich liquid generated by the CO<sub>2</sub>-light hydrocarbon component binary becomes immiscible with liquid mixtures containing the heavy component. At the same pressure, mixtures containing amounts of the light component show liquid-vapor equilibria similar to those observed for binary mixtures of CO<sub>2</sub> and the heavy hydrocarbon component, and at intermediate compositions, three phases exist. It should be noted that the data of Meldrum and Nielsen<sup>14</sup> are at 21.1°C which is below the critical temperature of CO<sub>2</sub>. Snedeker<sup>20</sup> argues, however, that similar diagrams

can occur at temperatures above the critical temperature of CO<sub>2</sub>, though a light hydrocarbon heavier than C<sub>3</sub> may be required.

#### Type II. Phase behavior with a supercritical light hydrocarbon component

If the intermediate hydrocarbon component (C<sub>3</sub>) is replaced with a lighter component (C<sub>1</sub>), or the temperature of the system is increased,<sup>1</sup> the resulting sequence of phase diagrams may behave differently with increasing pressure. Figure 11 shows a hypothetical sequence of phase diagrams when both CO<sub>2</sub> and the light hydrocarbon component are supercritical. At low pressures, the two-phase region is again a band across the diagram, though this time the CO<sub>2</sub>-C<sub>1</sub> binary is miscible, and the C<sub>1</sub>-C<sub>16</sub> binary is not. Increasing pressure shrinks the two-phase region, detaching it from the C<sub>1</sub>-C<sub>16</sub> side of the diagram when the C<sub>1</sub>-C<sub>16</sub> critical pressure is passed, and with further increases, the three-phase region appears with a split in a tie line near the CO<sub>2</sub>-C<sub>16</sub> side of the diagram. This split occurs when pressures are reached that are sufficient to cause L<sub>1</sub>-L<sub>2</sub> behavior in the CO<sub>2</sub>-C<sub>16</sub> binary while L-V separations still occur for the C<sub>1</sub>-C<sub>16</sub>-CO<sub>2</sub> mixtures rich in C<sub>1</sub>. In this case, the L<sub>2</sub> phase is richer in CO<sub>2</sub> than the V phase. It is likely that the disappearance of the three-phase region occurs with the L<sub>2</sub> phase becoming richer in C<sub>1</sub> and, hence, moving toward the V composition with increasing pressure. That is, with increasing pressure, more C<sub>1</sub> is compressed into the liquid phases which would cause the three-phase triangle to translate to higher C<sub>1</sub> concentrations. Thus, in both cases, the three-phase region apparently disappears when the L<sub>2</sub> and V phases coincide.

The two types of ternary diagrams proposed here offer a possible explanation for the effects of solution gas on phase behavior. If an oil composed of, say 50% C<sub>3</sub> and 50% C<sub>16</sub> is mixed with varying amounts of CO<sub>2</sub> at 21.1°C, then a P-X diagram similar to that shown in Figure 12a results. The pressure range over which L<sub>1</sub>-L<sub>2</sub>-V equilibria occur increases with increasing CO<sub>2</sub> concentration and the L<sub>1</sub>-L<sub>2</sub> critical point (C) is at a very high pressure. The phase diagram for CO<sub>2</sub> and Maljamar separator oil (Figure 2) is qualitatively like that shown in Figure 12a.

In contrast, a mixture of CO<sub>2</sub> and an oil (say 50% C<sub>1</sub> and 50% C<sub>16</sub>) from Figure 11 would produce a P-X diagram of the type shown in Figure 12b. The L<sub>1</sub>-L<sub>2</sub>-V pressure range now decreases with increasing CO<sub>2</sub> concentration, and the critical point (a L-V critical in this case) is at a much lower pressure than in Figure 12a. Thus, it is possible to obtain dew points at lower CO<sub>2</sub> concentration and lower pressures in this system than in one without solution gas. Phase diagrams similar to Figure 12b have been reported by Gardner *et al.*,<sup>5</sup> Stalcup,<sup>3</sup> and Huang and Tracht,<sup>7</sup> and it is likely that a full P-X diagram for CO<sub>2</sub>-RRF mixtures would resemble Figure 12b.

It is apparent from the proposed ternary diagrams that changes in oil composition, temperature, location of plait points, etc. alter the details of the resulting P-X diagrams. Nevertheless, the L<sub>1</sub>-L<sub>2</sub>-V equilibria observed for CO<sub>2</sub>-crude oil mixtures are not inconsistent with the phase behavior of CO<sub>2</sub>-alkane mixtures. Such behavior occurs because some components in the oil form two liquid phases when mixed with CO<sub>2</sub>, while at the same pressure others form a

liquid and a vapor. It is possible, therefore, for some intermediate mixture compositions to have all three phases present.

#### Ternary Diagrams for CO<sub>2</sub>-Crude Oil Mixtures

The limitations of pseudo-ternary representations of CO<sub>2</sub>-crude oil phase behavior have been discussed by Gardner.<sup>5</sup> Nevertheless, such diagrams are extremely useful for describing compositional effects in displacement processes. Figure 13 shows a hypothetical ternary phase diagram for CO<sub>2</sub>-Maljamar separator oil mixtures at three pressures. The oil is represented as two pseudo-components, a light component containing hydrocarbons C<sub>5</sub>-C<sub>10</sub> and a heavy component C<sub>11+</sub>. Binary mixtures of the separator oil and CO<sub>2</sub> lie on the straight line connecting the CO<sub>2</sub> vertex with the oil composition (56.5 mol % C<sub>5</sub>-C<sub>10</sub>, 43.5 mol % C<sub>11+</sub>). It should be noted that the only experimental data available to construct the phase diagrams shown are the CO<sub>2</sub> concentrations at which phase boundaries are crossed and whether the phase transition is a bubble point or a dew point. The phase envelopes are speculations, therefore, but speculations based on the behavior of CO<sub>2</sub> and hydrocarbons in well-characterized binary and ternary systems.

At 5.52 MPa and 32.2°C, CO<sub>2</sub> should show vapor-liquid immiscibility with both the light component (average molecular weight 111) and the heavy component (average molecular weight 286). Stewart and Nielsen's data<sup>15</sup> for octane (molecular weight 114) and hexadecane (molecular weight 226) were used to estimate solubilities of CO<sub>2</sub> in each of the pseudo-components. At 6.21 MPa, both components still show binary liquid-vapor immiscibility, but the solubility of CO<sub>2</sub> in C<sub>5</sub>-C<sub>10</sub> has increased more than that in C<sub>11+</sub>. At 6.90 MPa, the solubility of CO<sub>2</sub> in the light component has increased substantially as the critical pressure in that binary is approached. Apparently, the condensed phase in CO<sub>2</sub>-light component binary has become so rich in CO<sub>2</sub> that it is immiscible with the oil rich liquid phase, and the resulting diagram is similar to those reported by Meldrum and Nielsen<sup>14</sup> for CO<sub>2</sub>-C<sub>3</sub>-C<sub>16</sub> and CO<sub>2</sub>-C<sub>10</sub>-C<sub>16</sub> systems at 21.1°C. With additional pressure increases, the CO<sub>2</sub> concentrations on the L<sub>2</sub>-V envelope (see Figure 2) move to higher levels.<sup>1</sup> This suggests that the three-phase region for this system moves with increasing pressure as do the triangles shown in Figure 10, finally disappearing around 7.58 MPa (see Figure 2). The critical pressure of the CO<sub>2</sub>-C<sub>5</sub>-C<sub>10</sub> binary will be near that of CO<sub>2</sub>, so in the neighborhood of 7.58 MPa the L<sub>2</sub>-V region will detach from the right side of the diagram at a high CO<sub>2</sub> concentration leaving a small two-phase L<sub>2</sub>-V region bounding one side of the three-phase triangle.

The phase diagrams shown in Figure 13 are consistent with the single contact phase behavior experiments reported in Figure 2 and fit the type I sequence of diagrams described above. The addition of solution gas to the separator oil necessarily lightens the pseudo-component used to represent the light portion of the oil and probably alters the phase diagrams to the type II sequence.

It would be unrealistic to expect the phase diagrams shown here to describe the actual phase behavior with complete accuracy because of the representation of the oil as only two components

and because only single contact data were available to locate the phase envelopes. Multiple contact data such as obtained by Shelton and Yarborough<sup>7</sup> for rich gas-oil mixtures and by Gardner<sup>5</sup> for CO<sub>2</sub>-oil mixtures would improve the accuracy of the phase envelopes. Such experiments are underway and will provide a test of the validity of the phase diagrams proposed here. Even so, the sequences of phase diagrams provide a useful framework for understanding the results of single contact experiments and can be used to assess the impact of the complex low temperature phase behavior on the displacement process.

#### Effect of Phase Behavior on Displacement Efficiency

To assess the impact of the phase behavior postulated in Figure 13 on the displacement process, numerical simulations were conducted for displacements of Maljamar separator oil by CO<sub>2</sub> at three pressures. The simulator used is similar to those described by Pope and Nelson<sup>30</sup> and Gardner *et al.*<sup>5</sup> It follows pure convection of CO<sub>2</sub> and two hydrocarbon components in as many as three hydrocarbon phases plus water and uses numerical dispersion to model physical dispersion.<sup>31</sup> Stone's model<sup>32</sup> is used to calculate relative permeabilities for gas, oil and water with the additional proviso that if three hydrocarbon phases are present, the two phases closest in composition share the relative permeability of the appropriate phase in proportion to their saturations. Relative permeability functions and fluid property data used are summarized in Table 5. Phase behavior is entered into the simulator by a simple polynomial representation of the phase boundary curves from a ternary diagram. Phase densities are calculated assuming no volume change on mixing and phase viscosities are calculated from phase compositions using a quarter power blending rule.<sup>33</sup>

In order to isolate the effects of changing phase behavior with increasing pressure, simulations of CO<sub>2</sub> displacing Maljamar separator oil were made with fluid properties held constant. The phase envelopes shown in Figure 13 were used in the simulations of displacements at 5.52 and 6.90 MPa. A third displacement at 8.27 MPa used the same phase envelope as that for 6.90 MPa with the exceptions that the three-phase triangle was no longer present and the tie line slopes at the higher pressure reflect somewhat better extraction of the light hydrocarbon component into the CO<sub>2</sub>-rich liquid phase (compare the phase diagrams in Figures 15 and 16).

Paths of the overall mixture composition in the middle grid block shown for the three displacements are in Figures 14, 15 and 16, and recovery curves for each component are given in Figure 17. At 5.52 MPa (Figure 14), the displacement is clearly immiscible. When CO<sub>2</sub> is injected, it mixes with the oil, eventually splitting into two phases when the CO<sub>2</sub> concentration is high enough. The upper phase that results is very nearly pure CO<sub>2</sub>, and the oil phase which is left behind contains hydrocarbons in the original concentration ratios though the remaining oil is now saturated with dissolved CO<sub>2</sub>. There is no enrichment of the upper phase with C<sub>5</sub>-C<sub>10</sub> so the fraction of C<sub>5</sub>-C<sub>10</sub> recovered is identical to that of C<sub>11+</sub> (Figure 17). Thus, with all fluid properties held constant, an increase in the solubility of CO<sub>2</sub> in the oil leads to a calculated increase in oil recovery, because the oil phase left behind contains

more CO<sub>2</sub> and hence less oil.

At 6.90 MPa (Figure 15), the displacement composition path enters the L<sub>1</sub>-L<sub>2</sub> region along the extension of a tie line, as it must,<sup>6,34</sup> and the composition path stays well inside the two and three-phase regions throughout the displacement. The extraction of hydrocarbons into the L<sub>2</sub> and V phases is not efficient enough to generate a miscible displacement, but as the component recovery curves in Figure 17 show, the overall recovery of hydrocarbons is better than at 5.52 MPa because the two-phase region is smaller and because improved extraction of C<sub>5</sub>-C<sub>10</sub> by CO<sub>2</sub> causes continuing recovery of that component after CO<sub>2</sub> breakthrough, while C<sub>11+</sub> recovery levels off rapidly once CO<sub>2</sub> production starts. Comparison of the composition path (Figure 16) and recovery curves for the 8.27 MPa displacement with those of 6.90 MPa shows clearly the effect of increased extraction of hydrocarbons into the upper phase. The two-phase regions used in the two displacements are the same size, reflecting the fact that phase envelopes are less sensitive to pressure in liquid-liquid systems, but tie line slopes at 8.27 MPa give higher C<sub>5</sub>-C<sub>10</sub> concentrations in the CO<sub>2</sub> rich liquid. Increased extraction of C<sub>5</sub>-C<sub>10</sub> leads to better recovery of both C<sub>5</sub>-C<sub>10</sub> and C<sub>11+</sub>, as Figure 17 demonstrates.

Further improvement of the extraction of light hydrocarbon components would lead to still higher component recoveries. Hutchinson and Braun<sup>6</sup> argued and Helfferich proved<sup>34</sup> that (in the absence of dispersion) a displacement composition path will develop which avoids the two-phase region if there is no tie line extension which passes through the initial oil composition. The presence of dispersion, however, pulls the composition path back into the two-phase region, as simulations of displacements with varying levels of dispersion clearly show.<sup>5</sup> This causes some oil to be left behind as the transition zone passes. The amount of oil so trapped depends on the competition between the enrichment of the upper phase by extraction and the smoothing of longitudinal concentration gradients by dispersion.

Figure 18 is a plot of combined recovery of C<sub>5</sub>-C<sub>10</sub> and C<sub>11+</sub> vs. pressure. According to the criteria proposed by Yellig and Metcalfe,<sup>35</sup> the minimum miscibility pressure for this system would be in the neighborhood of 8.27 MPa, which agrees reasonably well with their experimental determination of 7.58-7.93 MPa at 35°C for a dead West Texas oil not too different in composition from that considered here. The 8.27 MPa displacement fits their criteria because the oil recovery is near the maximum recovery for simulations conducted with the level of numerical dispersion used, and because the two phases produced as the transition zone reached the outlet both were enriched by C<sub>5</sub>-C<sub>10</sub> and, of course, contained large amounts of CO<sub>2</sub>. Yellig and Metcalfe<sup>35</sup> argued, based on simulation results,<sup>36</sup> that two-phase production does not necessarily indicate an immiscible displacement. That is certainly true if "immiscible" is defined as the sort of displacement shown for 5.52 MPa in Figure 14. It is also true, however, that the 8.27 MPa simulated displacement does not quite develop miscibility in the sense that, in the absence of dispersion, the composition path of the displacement avoids the two-phase region completely, though not much additional improvement in the extraction of C<sub>5</sub>-C<sub>10</sub> would be required to meet the more stringent definition. Because the recovery of hydrocarbons improves continuously with the effectiveness of the

extraction of hydrocarbons with the CO<sub>2</sub>-rich phase, a displacement which penetrates the two-phase region near the plait point, as does the 8.27 MPa run, may be nearly as efficient as one which penetrates the two-phase region only because dispersion alters the composition path. In addition, for mixtures sufficiently close to the plait point, interfacial tensions will be low, and in such a case the distinction between miscible and immiscible may have little to do with recovery efficiency. Thus, the operating definition of "minimum miscibility pressure" proposed by Yellig and Metcalfe<sup>35</sup> is broader than that originally discussed by Hutchinson and Braun<sup>6</sup> and Rathmell et al.<sup>1</sup> In any case, the criteria given by Yellig and Metcalfe are probably sufficient to insure that phase behavior will be favorable enough to produce an efficient displacement, which is, of course, what matters, whether or not it is strictly miscible.

#### CONCLUSIONS

1. The occurrence of liquid-liquid and liquid-liquid-vapor phase behavior in CO<sub>2</sub>-crude oil mixtures is consistent with similar behavior reported for binary and ternary mixtures of CO<sub>2</sub> with alkanes at temperatures not too far above the critical temperature of CO<sub>2</sub>. CO<sub>2</sub> shows liquid-liquid immiscibility with hydrocarbons heavier than C<sub>13</sub> at temperatures above 31°C (88°F).
2. Since essentially all crude oils contain substantial quantities of components C<sub>14</sub> and heavier, liquid-liquid phase behavior can be expected if the reservoir temperature is low enough. While the maximum temperature at which such behavior will occur probably depends on oil composition, a reasonable estimate of a temperature limit for liquid-liquid immiscibility is about 50°C (122°F).
3. Preliminary fluid property measurements for the two liquid phases indicate that extracted hydrocarbons can substantially increase the viscosity of the CO<sub>2</sub>-rich liquid over that of CO<sub>2</sub> while dissolved CO<sub>2</sub> reduces the viscosity of the hydrocarbons remaining in the oil-rich liquid.
4. Pseudo-ternary representations of CO<sub>2</sub>-crude oil phase behavior are useful tools for interpreting single contact phase behavior experiments. When used in simple displacement simulations, such diagrams provide insight into the effects of the complex phase behavior observed for CO<sub>2</sub> crude oil mixtures.
5. Displacements of oil by CO<sub>2</sub> can develop miscibility by extraction of hydrocarbon components into a CO<sub>2</sub>-rich phase when liquid-liquid phase behavior occurs. This conclusion is based on simulation results which show increased oil recovery when extraction improves, and on experimental evidence that extraction of hydrocarbons by a CO<sub>2</sub>-rich liquid phase improves with increasing pressure.

#### ACKNOWLEDGMENT

The work reported in this report was supported by the U. S. Department of Energy and the New Mexico Energy and Minerals Department. Oil and gas samples used in this study were provided by Conoco, Inc. We especially appreciate the encouragement and assistance of Lowell Deckert, Peter Lingane and other Conoco engineers. Experimental data presented here were obtained with much assistance from R. Spaulding and M. T. Pelletier using equipment designed and

constructed by H. K. Wainwright and M. T. Pelletier. We also thank N. R. Morrow, J. P. Heller and especially J. J. Taber for encouragement and careful reviews of the manuscript.

#### REFERENCES

- Rathmell, J. J., Stalkup, F. I. and Hassinger, R. C., "A Laboratory Investigation of Miscible Displacement by Carbon Dioxide," SPE 3483, presented at SPE 46th Annual Fall Meeting, New Orleans, Oct. 3-6, 1971.
- Holm, L. W. and Josendal, V. A., "Mechanisms of Oil Displacement by Carbon Dioxide," J. Pet. Tech. **16** (December, 1974) 1427-1438.
- Stalkup, F. I., "Carbon Dioxide Miscible Flooding: Past, Present and Outlook for the Future," J. Pet. Tech. **30** (August, 1978) 1102-1112.
- Metcalfe, R. S. and Yarborough, L., "The Effect of Phase Equilibria on the CO<sub>2</sub> Displacement Mechanism," Soc. Pet. Eng. J. **19** (August, 1979) 242-252.
- Gardner, J. W., Orr, F. M. and Patel, P. D., "The Effect of Phase Behavior on CO<sub>2</sub> Flood Displacement Efficiency," SPE 8367, presented at SPE 54th Annual Fall Meeting, Las Vegas, September 23-26, 1979.
- Hutchinson, C. A., Jr. and Braun, P. H., "Phase Relations of Miscible Displacement in Oil Recovery," AIChE J **7** (March 1961) 64-72.
- Huang, E. T. S. and Tracht, J. H., "The Displacement of Residual Oil by Carbon Dioxide," SPE 4735, presented at the SPE 3rd Symposium on Improved Oil Recovery, Tulsa, April, 1974.
- Shelton, J. L. and Yarborough, L., "Multiple Phase Behavior in Porous Media During CO<sub>2</sub> or Rich-Gas Flooding," J. Pet. Tech. **19** (September 1977) 1171-1178.
- Simon, R., Rosman, A. and Zana, E., "Phase Behavior Properties of CO<sub>2</sub> Reservoir Oil Systems," Soc. Pet. Eng. J. **18** (February, 1978) 20-26.
- Graue, D. J. and Zana, E., "Study of a Possible CO<sub>2</sub> Flood in the Rangely Field, Colorado, SPE 7060, presented at the SPE 5th Symposium on Improved Oil Recovery, Tulsa, April 16-18, 1978.
- Peterson, A. V., "Optimal Recovery Experiments with N<sub>2</sub> and CO<sub>2</sub>," Pet. Eng. (November, 1978) 40-50.
- Perry, G. E., Guillory, A. J., Baron, J. D. and Moranville, M. B., "Weeks Island 'S' Sand Reservoir B Gravity Stable Miscible CO<sub>2</sub> Displacement, Iberia Parish, Louisiana," presented at the 4th Annual DOE Symposium on Enhanced Oil and Gas Recovery, Tulsa, August 29-31, 1978.
- Kamath, K. I., Comberati, J. R. and Zamerilli, A. M., "The Role of Reservoir Temperature in CO<sub>2</sub> Flooding," presented at the 5th Annual DOE Symposium on Enhanced Oil and Gas Recovery, Tulsa, August 22-24, 1979.
- Meldrum, A. H. and Nielsen, R. F., "A Study of Three-Phase Equilibria for Carbon Dioxide-Hydrocarbon Mixtures," Prod. Monthly (August, 1955) 22-35.
- Stewart W.C. and Nielson, R. F., "Phase Equilibria for Mixtures of Carbon Dioxide and Several Normal Saturated Hydrocarbons," Prod. Monthly (January, 1954) 27-32.
- Reamer, H. H. and Sage, B. H., "Phase Equilibria in Hydrocarbon Systems. Volumetric and Phase Behavior of the n-Decane-CO<sub>2</sub> System," J. Chem. Eng. Data **8** (1963) 508-513.
- Schneider, G., Alwani, Z., Heim, W., Horvath, E. and Franck, E. U., "Phasengleichgewichte und kritische Erscheinungen in binären Michsystemen bis 1500 bar: CO<sub>2</sub> mit n-Octan, n-Undecan, n-Tridecan und n-Hexadecan," Chem. Ing. Tech. **39** (1967) 649-656.
- Zarah, B. Y., Luks, K. D. and Kohn, J. P., "Phase Equilibria Behavior of Carbon Dioxide in Binary and Ternary Systems with Several Hydrocarbon Components," AIChE Symposium Series **70**, No. 140 (1974) 91-101.
- Kulkarni, A. A., Zarah, B. Y., Luks, K. D. and Kohn, J. P., "Phase Equilibria Behavior of Carbon Dioxide-n-Decane at Low Temperatures," J. Chem. Eng. Data **19** (1974) 92-94.
- Snedeker, R. A., "Phase Equilibria in Systems with Supercritical Carbon Dioxide," Ph.D. Thesis, Princeton University (1955).
- Schneider, G., "Phase Equilibria in Binary Fluid Systems of Hydrocarbons with Carbon Dioxide, Water and Methane," AIChE Symposium Series **64** (1968) 9-15.
- Liphard, K. G. and Schneider, G. M., "Phase Equilibria and Critical Phenomena in Fluid Mixtures of Carbon Dioxide + 2, 6, 10, 15, 19, 23-hexamethyltetracosane up to 423°K and 100 MPa," J. Chem. Thermodynamics **7** (1975) 805-814.
- Huie, N. C., Luks, K. D. and Kohn, J. P., "Phase Equilibria Behavior of Systems Carbon Dioxide-n-Eicosane and Carbon Dioxide-n-Decane-n-Eicosane," J. Chem. Eng. Data **18** (1973) 311-313.
- Yang, H. W., Luks, K. D. and Kohn, J. P., "Phase Equilibria Behavior of the System Carbon Dioxide-n-Butylbenzene-2 Methyl-naphthalene," J. Chem. Eng. Data **21** (1976) 330-335.
- Gupta, V. S., "Measurement and Prediction of Phase Equilibria in Liquid Carbon Dioxide-Hydrocarbon Ternary Systems," Ph.D. Thesis, Pennsylvania State University (1969).

PHASE BEHAVIOR OF CO<sub>2</sub> AND CRUDE OIL IN LOW TEMPERATURE RESERVOIRS

26. Francis, A. W., "Ternary Systems of Liquid Carbon Dioxide," <u>J. Phys. Chem.</u> <u>58</u> (1954) 1099-1114.	32. Stone, H. L., "Estimation of Three-Phase Relative Permeability and Residual Oil Data," <u>J. Can. Pet. Tech.</u> <u>12</u> , No. 4 (1973) 53-61.
27. Francis, A. W., "Solvent Extraction with Liquid Carbon Dioxide," <u>Ind. Eng. Chem.</u> <u>47</u> (1955) 230-233.	33. Todd, M. R. and Longstaff, W. J., "The Development, Testing and Application of a Numerical Simulator for Predicting Miscible Flood Performance," <u>J. Pet. Tech.</u> <u>14</u> (July, 1972) 874-881.
28. Elgin, J. C. and Weinstock, J. J., "Phase Equilibria at Elevated Pressures in Ternary Systems of Ethylene and Water with Organic Liquids, Salting out with a Supercritical Gas," <u>J. Chem. Eng. Data</u> <u>4</u> (1959) 2-12.	34. Helfferich, F. G., "General Theory of Multi-component, Multiphase Displacement in Porous Media," SPE 8372, presented at SPE 54th Annual Fall Meeting, Las Vegas, September 23-26, 1979.
29. Poettman, F. H. and Katz, D. L., "Phase Behavior of Binary Carbon Dioxide-Paraffin Systems," <u>Ind. Eng. Chem.</u> <u>37</u> (1945) 847-853.	35. Yellig, W. F. and Metcalfe, R. S., "Determination and Prediction of CO <sub>2</sub> Minimum Miscibility Pressures," <u>J. Pet. Tech.</u> <u>32</u> (January, 1980) 160-168.
30. Pope, G. A. and Nelson, R. C., "A Chemical Flooding Compositional Simulator," <u>Soc. Pet. Eng. J.</u> <u>18</u> (October, 1978) 339-354.	36. Leach, M. P. and Yellig, W. F., "Compositional Model Studies: CO <sub>2</sub> -Oil Displacement Mechanisms," SPE 8368, presented at SPE 54th Annual Fall Meeting, Las Vegas, September 23-26, 1979.
31. Lantz, R. B., "Quantitative Evaluation of Numerical Diffusion (Truncation Error)," <u>Soc. Pet. Eng. J.</u> <u>11</u> (September, 1971) 315.	

TABLE 1

Summary of CO<sub>2</sub>-Crude Oil Systems for which  
Phase Behavior Has Been Reported

<u>Authors</u>	<u>Crude Oil</u>	<u>Temperature (°C)</u>	<u>Phase Behavior</u>
Huang & Tracht <sup>7</sup>	West Texas Oil	32.2	L <sub>1</sub> -L <sub>2</sub> -V
Shelton & Yarborough <sup>8</sup>	Oil B	34.4	L <sub>1</sub> -L <sub>2</sub> -V
Gardner <u>et al</u> <sup>5</sup>	Wasson	40.6	L <sub>1</sub> -L <sub>2</sub> -V
Rathmell <u>et al</u> <sup>1</sup>	Oil A	42.8	L <sub>1</sub> -L <sub>2</sub> -V
Simon <u>et al</u> <sup>9</sup>	Oil A	54.4	L-V
Graue & Zana <sup>10</sup>	Rangely	71.1	L-V
Peterson <sup>11</sup>	Painter	73.3	L-V
Rathmell <u>et al</u> <sup>1</sup>	Oil C	85.6	L-V
Perry <u>et al</u> <sup>12</sup>	Weeks Island	107.2	L-V
Simon <u>et al</u> <sup>9</sup>	Oil B	123.9	L-V

TABLE 2

## Properties of Maljamar Separator Oil

Density (15.6°C)	0.8294 g/cm <sup>3</sup>
Density (34.4°C)	0.7959 g/cm <sup>3</sup>
Viscosity (34.4°C)	0.0028 Pa.S
Molecular Weight	183.7
Molecular Weight of C7+*	199.3
Density of C7+ (15.6°C) *	0.8441 g/cm <sup>3</sup>

\* Calculated from measured values of molecular weight and density and oil composition.

TABLE 3

## Properties of Upper and Lower Liquid Phases at 32.2°C

Overall Composition (Mol % CO <sub>2</sub> )	Oil	Phase	Pressure (MPa)	Density (g/cm <sup>3</sup> )	Viscosity (mPa s)
79.3	Separator	Upper	14.92	.8520	0.185
79.3	Separator	Lower	14.92	.8495	0.760
79.3	Separator	Lower	15.13	.8802	0.774
74.4	RRF*	Upper	17.23	.7700	0.165
74.4	RRF	Lower	17.23	.7840	-
0	RRF	-	12.41	.7393	0.840
0	RRF	-	14.82	.7419	0.845
0	RRF	-	17.23	.7444	0.870
0	RRF	-	20.68	.7474	0.900

\* Recombined reservoir fluid

TABLE 4

## Composition and Properties of Maljamar

	Recombined Reservoir Fluid		
	Gas (Mol %)	Oil (Mol %)	RRF <sup>1</sup> (Mol %)
C <sub>1</sub>	56.55	-	25.71
C <sub>2</sub>	19.61	-	8.91
C <sub>3</sub>	16.06	-	7.30
C <sub>4</sub>	6.37	-	2.90
C <sub>5</sub>	1.41	3.90	2.77
C <sub>6</sub>	-	9.37	5.11
C <sub>7</sub>	-	10.27	5.60
C <sub>8</sub>	-	13.54	7.39
C <sub>9</sub>	-	11.91	6.50
C <sub>10</sub>	-	7.50	4.09
C <sub>11+</sub>	-	43.51	23.72
	<u>100.00</u>	<u>100.00</u>	<u>100.00</u>
Mol. Wt.	26.77	183.7	112.4
Density	-	.8405 <sup>2</sup>	0.7393 <sup>3</sup>
Bubble Point Pressure (MPa)		-	10.51

<sup>1</sup> Calculated for the approximate recombination GOR of 89 standard M<sup>3</sup>/M<sup>3</sup> (500 SCF/BBL)

<sup>2</sup> At 13.79 MPa and 32.2°C

<sup>3</sup> At 12.41 MPa and 32.2°C

TABLE 5

Fluid Properties and Relative Permeabilities  
for Simulated Displacements of Maljamar Separator  
Oil by CO<sub>2</sub>

Component	Density (g/cm <sup>3</sup> )	Viscosity (mPa.S)	Molecular Weight
CO <sub>2</sub>	0.35	0.05	44.0
C <sub>5</sub> -C <sub>10</sub>	0.70	1.00	111.5
C <sub>11+</sub>	0.92	7.00	286.1

$$\text{Oil relative permeability} = k_{ro} = [(S_o - 0.3)/0.7]^2$$

$$\text{Gas relative permeability} = k_{rg} = [(0.7 - S_o)/0.7]^2$$

S<sub>o</sub> = oil saturation

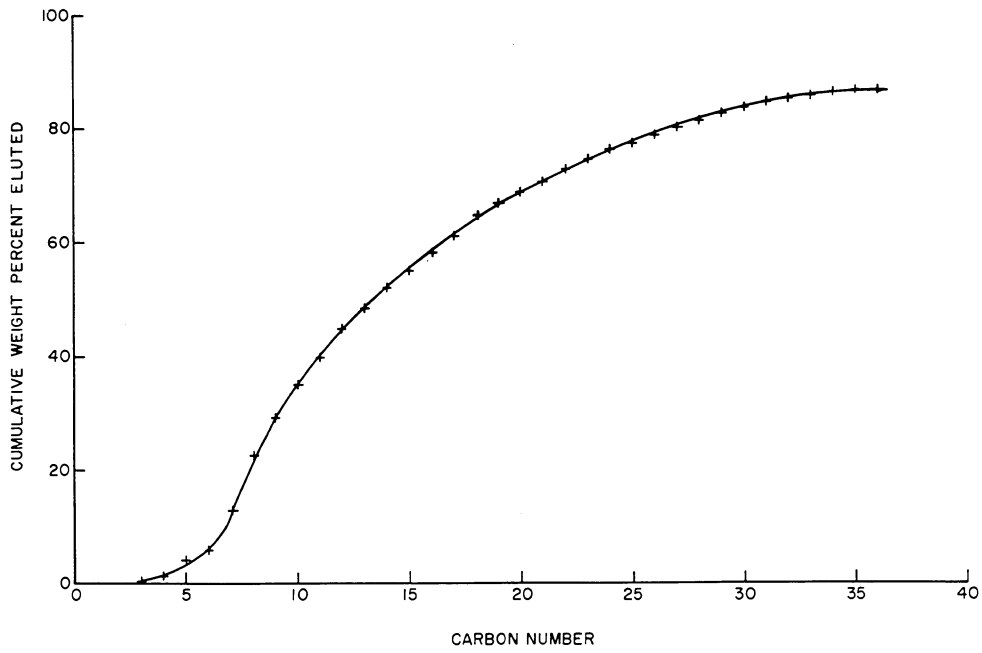


Fig. 1 - Composition of Maljamar separator oil.

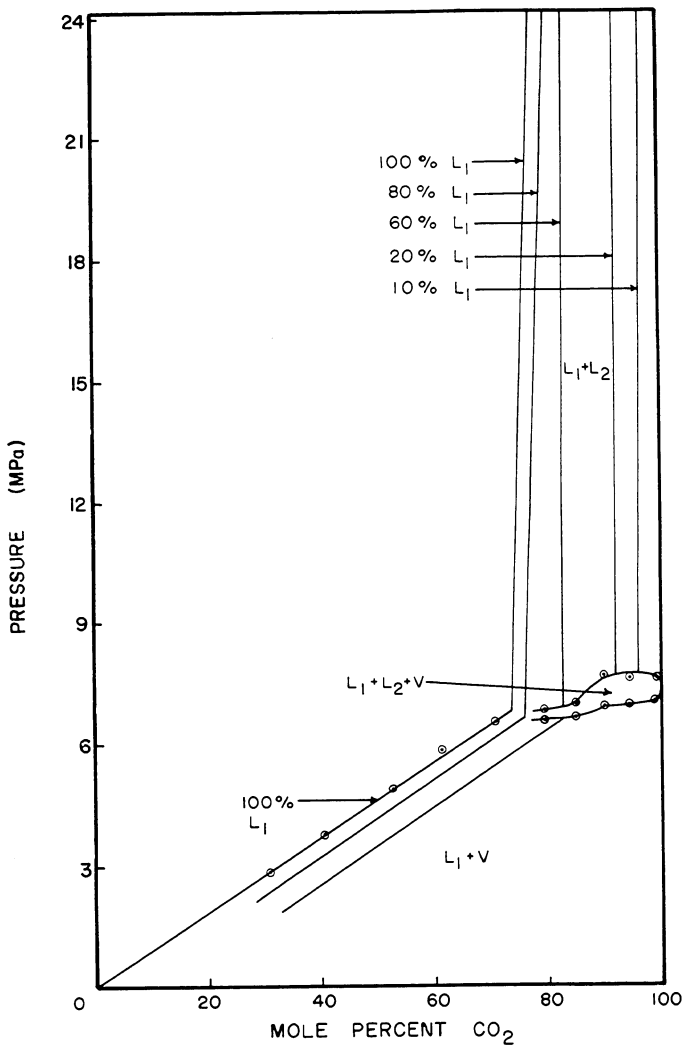


Fig. 2 - Phase behavior of binary mixtures of CO<sub>2</sub> and Maljamar separator oil.

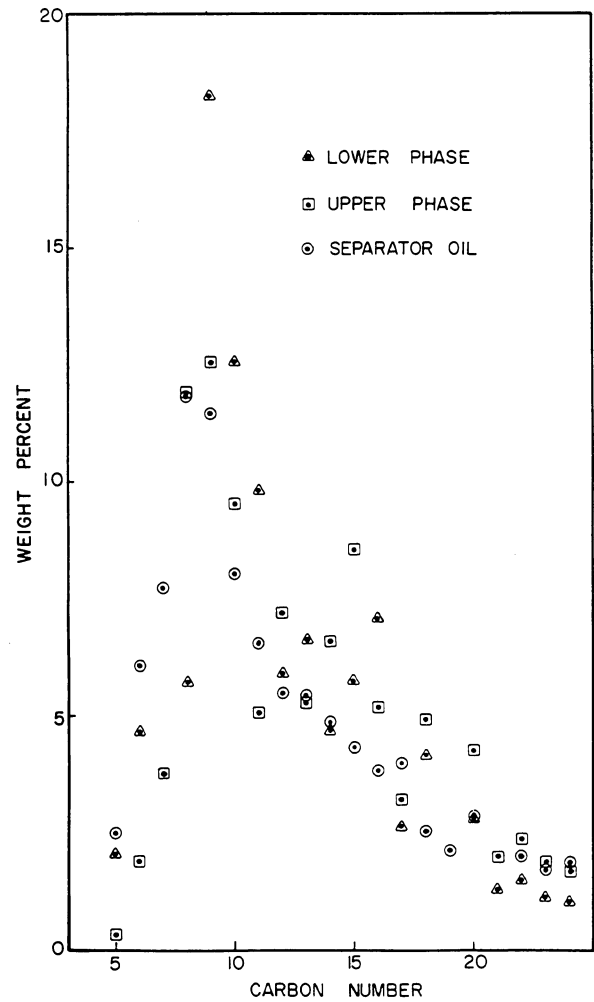


Fig. 3 - Carbon number distribution for hydrocarbons in the CO<sub>2</sub>-rich liquid, oil-rich liquid and separator oil. Samples were taken at 14.92 MPa and 32.2°C.

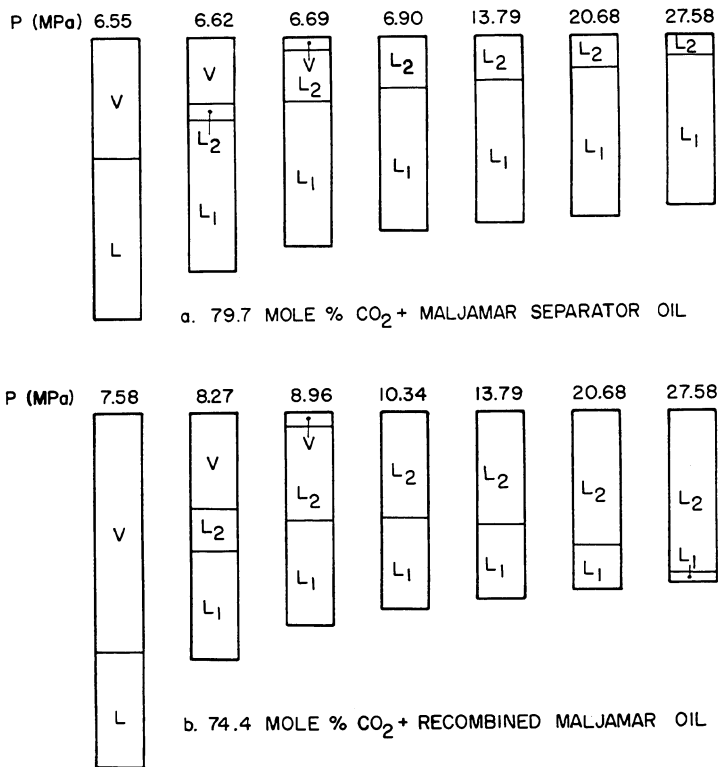


Fig. 4 - Volumetric behavior at various pressures of CO<sub>2</sub> mixed with (a) separator oil and (b) recombined oil.

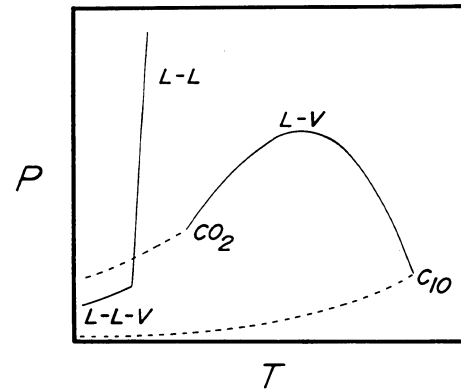


Fig. 5 - Critical loci for CO<sub>2</sub>-decane mixtures.

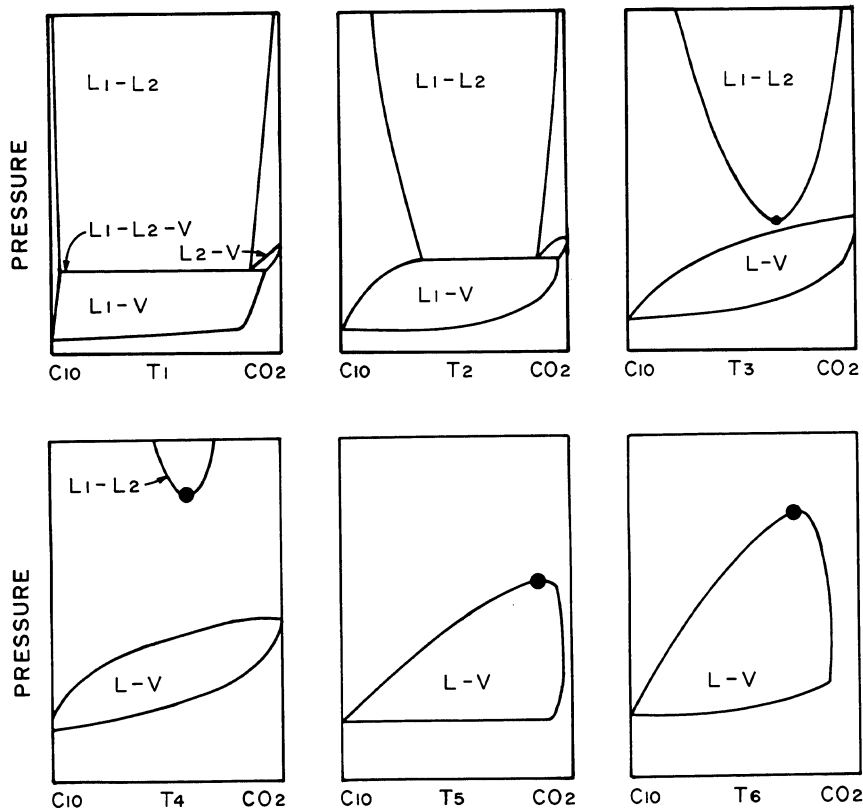


Fig. 6 - Evolution of pressure-composition diagrams with increasing temperature for binary mixtures of CO<sub>2</sub> and decane.

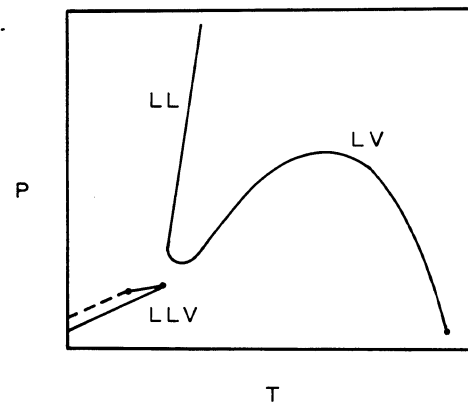


Fig. 7 - Critical loci for CO<sub>2</sub>-hexadecane mixtures.

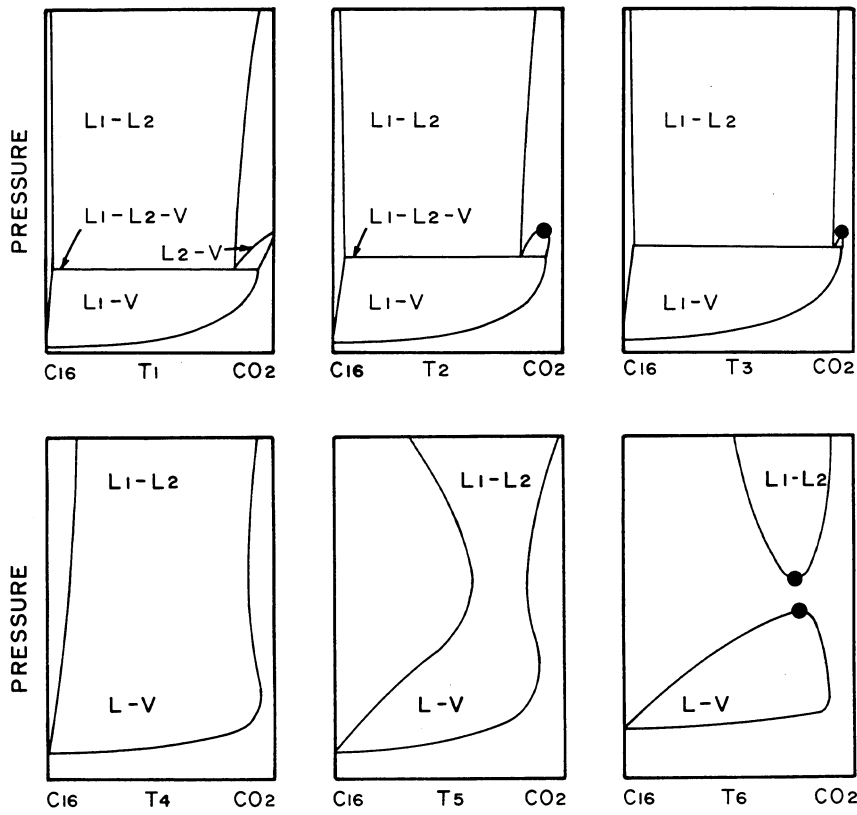


Fig. 8 - Evolution of pressure-composition diagrams with increasing temperature for binary mixtures of CO<sub>2</sub> and hexadecane.

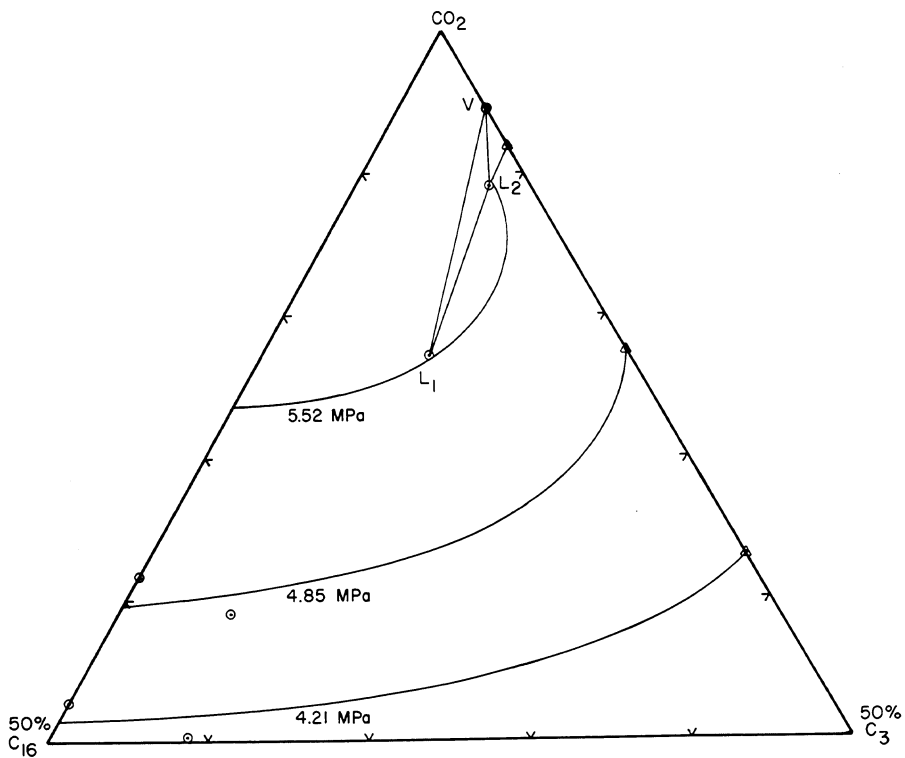


Fig. 9 - Phase behavior of CO<sub>2</sub>-propane-hexadecane mixtures at 21°C (after Meldrum and Nielsen<sup>14</sup>).

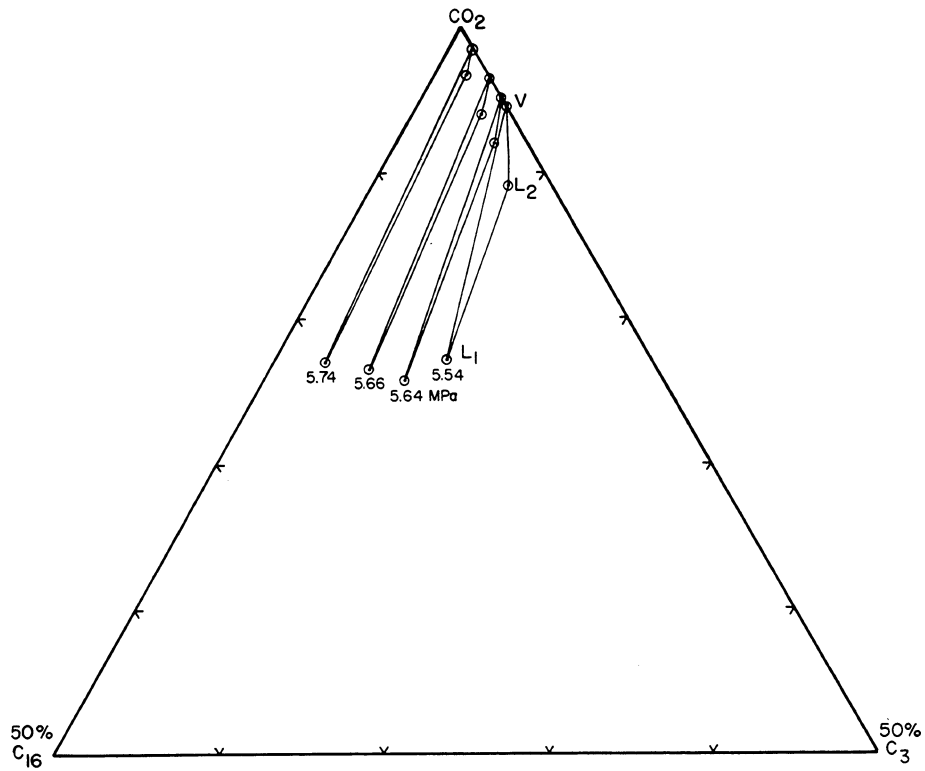


Fig. 10 - Effect of pressure on the  $L_1$  -  $L_2$  -  $V$  region for  $\text{CO}_2$ -propane-hexadecane mixtures at  $21^\circ\text{C}$  (after Meldrum and Nielsen<sup>14</sup>).

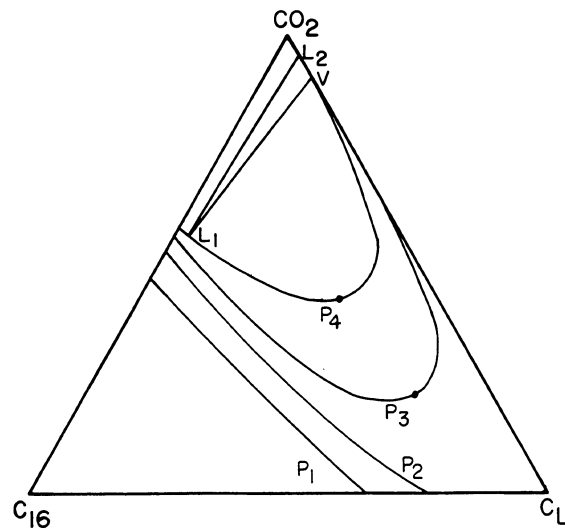


Fig. 11 - Postulated phase diagram for  $\text{CO}_2$ , hexadecane and a supercritical light hydrocarbon.

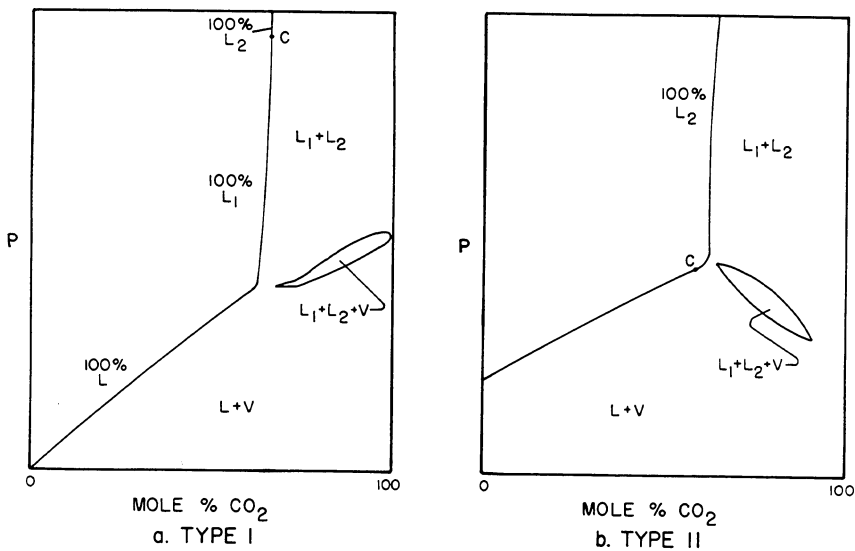


Fig. 12 - Pressure-composition plots for (a) type I (without solution gas) and (b) type II (with solution gas) ternary diagrams.

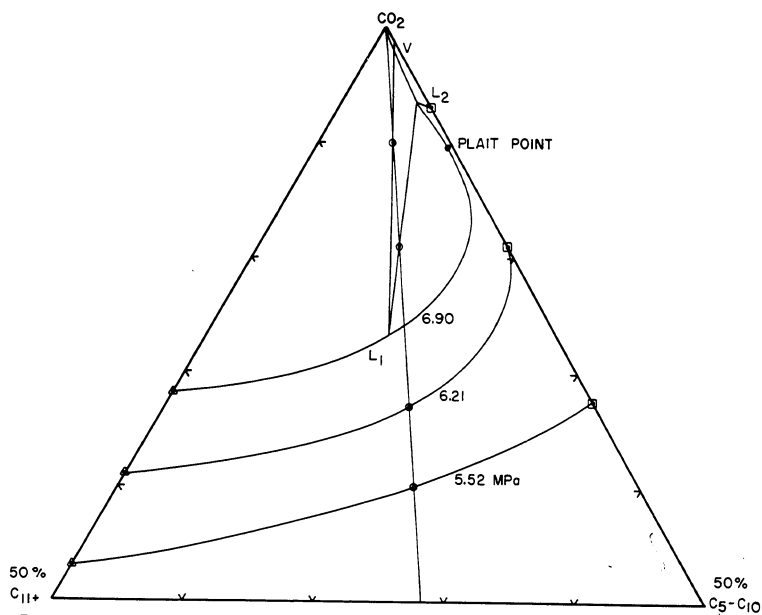


Fig. 13 - Postulated phase diagrams for CO<sub>2</sub> and Maljamar separator oil at various pressures (Only the upper half of the phase diagram is shown.)

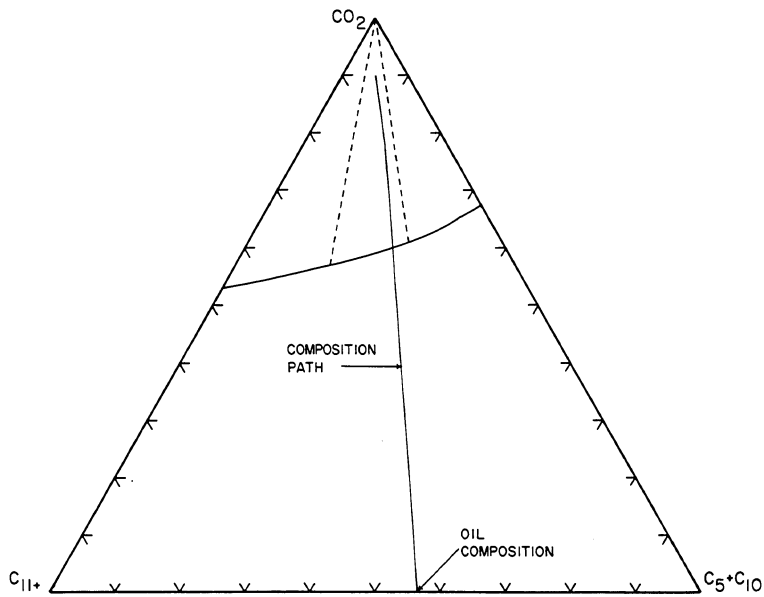


Fig. 14 - Simulated composition path for displacement of Maljamar separator oil by CO<sub>2</sub> at 5.52 MPa and 32.2°C.

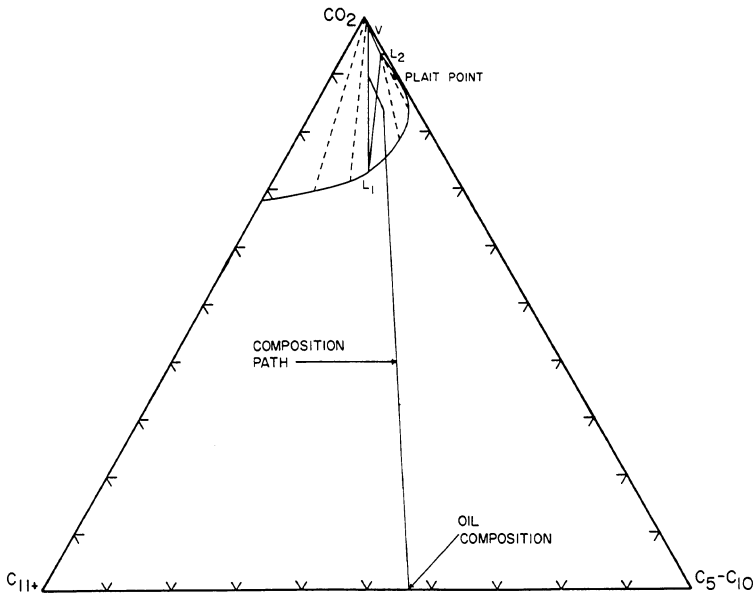


Fig. 15 - Simulated composition path for displacement of Maljamar separator oil by CO<sub>2</sub> at 6.90 MPa and 32.2°C.

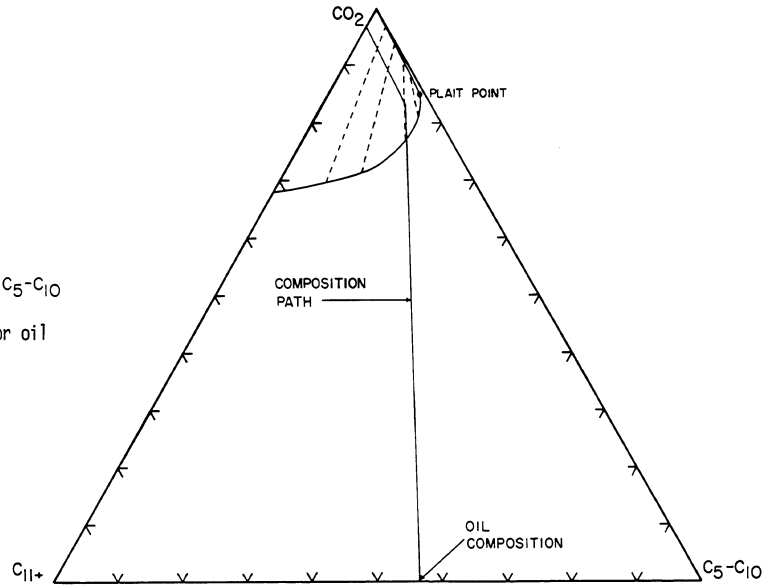


Fig. 16 - Simulated composition path for displacement of Maljamar separator oil by CO<sub>2</sub> at 8.27 MPa and 32.2°C.

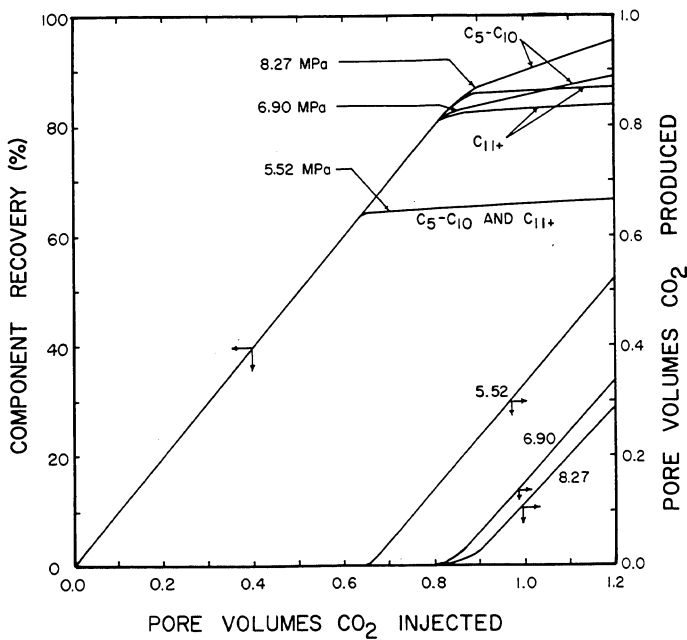


Fig. 17 - Simulated recovery of individual components during displacements of Maljamar separator oil by CO<sub>2</sub> at various pressures and 32.2°C.

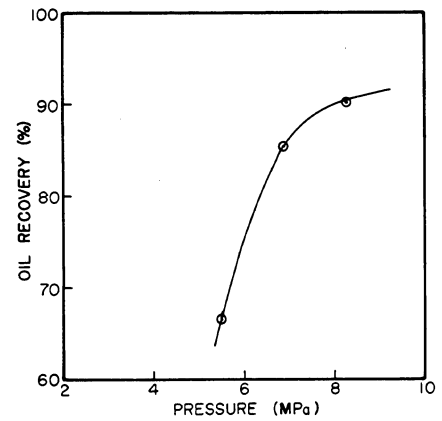


Fig. 18 - Simulated recovery of Maljamar separator oil.

Appendix B

Liquid-Liquid Phase Behavior in CO<sub>2</sub> -  
Hydrocarbon Systems

LIQUID - LIQUID PHASE BEHAVIOR IN CO<sub>2</sub> - HYDROCARBON SYSTEMS

By

F. M. Orr, Jr., C. L. Lien and M. T. Pelletier  
New Mexico Petroleum Recovery Research Center  
New Mexico Institute of Mining and Technology  
Socorro, New Mexico 87801  
505-835-5432

INTRODUCTION

Phase behavior of CO<sub>2</sub> - crude oil mixtures is only one of many factors which influence process efficiency in CO<sub>2</sub> floods, but it is an essential feature of a successful flood. At temperatures above about 50°C, CO<sub>2</sub> - crude oil mixtures form an oil-rich liquid and a CO<sub>2</sub>-rich vapor phase (1) with a small volume of a very heavy asphaltic phase also possible (2). At temperatures below 50°C but still above the critical temperature of CO<sub>2</sub> (31°C), liquid-vapor (L-V), liquid-liquid (L<sub>1</sub>-L<sub>2</sub>) or liquid-liquid-vapor (L<sub>1</sub>-L<sub>2</sub>-V) phase separations may occur (small amounts of asphaltene precipitation have also been observed in such systems (3)). Since many of the oil fields which are being considered for CO<sub>2</sub> flooding are at temperatures below 50°C, it is important to understand when L<sub>1</sub>-L<sub>2</sub> and L<sub>1</sub>-L<sub>2</sub>-V phase behavior will occur and how that phase behavior will affect displacement efficiency at reservoir conditions. This paper reports results of phase behavior experiments with two CO<sub>2</sub>-hydrocarbon systems: CO<sub>2</sub> plus methane (C<sub>1</sub>) and hexadecane (C<sub>16</sub>), and CO<sub>2</sub> mixed with a synthetic oil containing pentane (C<sub>5</sub>), decane (C<sub>10</sub>), hexadecane (C<sub>16</sub>) and squalane (C<sub>30</sub>). Results of those experiments are compared with the phase behavior of CO<sub>2</sub> - crude oil systems and with qualitative predictions of the Peng-Robinson equation of state.

## EXPERIMENTAL PROCEDURES

Mixtures of known overall composition were made by metering volumes of  $\text{CO}_2$ ,  $\text{C}_1$  and oil into one of two high pressure windowed cells mounted in an air bath for temperature control (4). Temperature and pressure of the gases charged were measured and the masses transferred to the cell calculated from literature density values. The volume of the mixture was then changed by injecting or removing mercury from the cell. The pressure at which a phase appeared or disappeared was determined by visual observations and by measurements of the overall compressibility of the mixture. Phase volumes were determined by measuring meniscus heights with a cathetometer calibrated against cell volume.

Phase compositions were measured by gas chromatography. Samples were analyzed on a 10 ft. x 1/8 in. OV-101 column installed in an HP5840A gas chromatograph. The chromatograph oven temperature was set at  $-65^\circ\text{C}$  initially to separate  $\text{C}_1$  from  $\text{CO}_2$ , then programmed upward at  $15^\circ\text{C}/\text{min.}$  to elute the hydrocarbon components. High pressure samples were obtained by the procedure outlined schematically in Figure 1. Before sampling, the sample groove (volume  $3\mu\text{l}$ ) in the sampling valve was cleaned and filled with carbon disulfide ( $\text{CS}_2$ ). The valve was then rotated to the vent position and a very small amount of sample vented to remove the  $\text{CS}_2$  from the system. Then, with the valve in the load position a large volume of the phase to be sampled was displaced from one windowed cell to the other through the sample groove. Finally, the sample was allowed to relieve pressure into a  $50\mu\text{l}$  syringe which could stand pressures up to 1700 kPa. Any hydrocarbons which condensed in the valve during blowdown were displaced into the sample syringe with  $\text{CS}_2$ . The nose valve on the syringe was

then closed and the sample injected immediately into the gas chromatograph. Contamination of the sample with  $\text{CS}_2$  did not alter the analysis because it was not detected by the flame ionization detector in use when the  $\text{CS}_2$  eluted. A thermal conductivity detector was used to measure the amount of  $\text{CO}_2$  present. Response factors were obtained by sampling and analyzing single phase mixtures of known composition.

#### PHASE BEHAVIOR OF $\text{CO}_2$ - $\text{C}_1$ - $\text{C}_{16}$ MIXTURES

Volumetric behavior of three  $\text{CO}_2$ - $\text{C}_1$ - $\text{C}_{16}$  mixtures and one  $\text{CO}_2$ - $\text{C}_{16}$  mixture determined at  $32.2^\circ\text{C}$  is shown in Figure 2. The overall compositions of the four mixtures and phase compositions for two ternary mixtures which formed three phases ( $\text{L}_1$ - $\text{L}_2$ -V) are given in Figure 3. In a binary mixture of  $\text{CO}_2$  and an alkane heavier than  $\text{C}_{13}$ , three phases can coexist at a given temperature at one pressure only, according to the phase rule (see reference 1 for a discussion of the phase behavior of binary mixtures of  $\text{CO}_2$  with various alkanes). For instance, Mixture 1 (see Figure 3), which contained 97.0 mol %  $\text{CO}_2$  and 3.0 mol %  $\text{C}_{16}$ , split into  $\text{L}_1$ ,  $\text{L}_2$  and V phases at 7488 kPa. Above that pressure,  $\text{L}_1$ - $\text{L}_2$  phase behavior was observed. A substantial additional increase in pressure caused the  $\text{C}_{16}$ -rich  $\text{L}_1$  phase to be completely extracted into the  $\text{CO}_2$ -rich liquid ( $\text{L}_2$ ).

The volumetric behavior of Mixture 2, obtained by adding a small amount of  $\text{C}_1$  to Mixture 1, was very nearly the same as that of Mixture 1. Three phases were observed over a narrow pressure range which had shifted to slightly higher pressure levels with the addition of  $\text{C}_1$ . The dew point pressure also increased somewhat.

Mixture 3 contained more  $\text{C}_1$  and  $\text{C}_{16}$  than Mixture 2. With more  $\text{C}_1$  present, the pressure range in which three phases coexisted again shifted to higher pressure levels. Mixture 4, however, which was still richer in

$C_1$  and  $C_{16}$ , did not form three phases. Instead, at pressures below 10000 kPa it showed compressibilities typical of vapor-liquid systems, while at higher pressures its compressibility was similar to that of liquid-liquid mixtures. Thus, with increasing pressure, the upper phase changed from a vapor-like state to a liquid-like state without exhibiting a phase change, much as a supercritical fluid does.

In Mixtures 1 and 2, the  $C_{16}$ -rich ( $L_1$ ) phase disappeared at high pressure while in both Mixtures 3 and 4, the  $CO_2$ -rich ( $L_2$ ) phase disappeared. That is, the transition from  $L_1$ - $L_2$  mixtures to a single phase mixture was analogous to a vapor-liquid dew point for Mixtures 1 and 2 and to a bubble point for Mixtures 3 and 4. The distinction between bubble points and dew points was somewhat ambiguous in this study since three of the four mixtures exhibited phase inversions. For all mixtures except that richest in  $C_1$  (Mixture 4), the  $CO_2$ -rich liquid phase was more dense than the  $C_{16}$ -rich liquid at pressures above about 14000 kPa. In the discussion below, the terms "dew point" and "bubble point" (for liquid-liquid phase transitions) refer to the appearance or disappearance of oil-rich ( $L_1$ ) and  $CO_2$ -rich ( $L_2$ ) phases respectively.

The phase compositions shown in Figure 3 indicate that the  $L_2$  and V phases had nearly the same composition. Both were rich in  $CO_2$ , but the vapor phase contained slightly more  $C_1$ . Thus, the appearance of the second liquid phase with increasing pressure was the result of liquefaction of the vapor phase, and was accompanied by little change in the lower liquid phase. Figure 3 also shows the effect of increasing pressure on the location of the three phase region on the ternary diagram. Higher pressure caused the three phase triangle to move to higher  $C_1$  concentrations as more  $C_1$  was compressed into the two liquid phases.

The behavior of the two and three phase mixtures outlined in Figures 2 and 3 is consistent with the sequence of qualitative phase

diagrams shown in Figure 4. The sequence was constructed with the aid of the Peng-Robinson equation of state (5) (the program used was obtained from the Gas Processors Association). At low pressures, the two phase region is a band across the diagram (Figure 4a). The band is narrower near the  $\text{CO}_2\text{-C}_{16}$  side of the diagram because  $\text{CO}_2$  is more soluble than  $\text{C}_1$  in  $\text{C}_{16}$ . Binary mixtures of  $\text{CO}_2$  and  $\text{C}_{16}$  that are rich enough in  $\text{CO}_2$  split into a  $\text{C}_{16}$ -rich liquid ( $\text{L}_1$ ), a  $\text{CO}_2$ -rich liquid ( $\text{L}_2$ ) and a vapor (V) at 7488 kPa. At higher pressures, mixtures of  $\text{CO}_2$  and  $\text{C}_{16}$  containing more than about 75 mol %  $\text{CO}_2$  form two liquid phases (Figure 4b). Such a  $\text{CO}_2\text{-C}_{16}$  mixture with a small amount of  $\text{C}_1$  added forms three phases in equilibrium: a liquid phase ( $\text{L}_1$ ) rich in  $\text{C}_{16}$ , a liquid phase ( $\text{L}_2$ ) rich in  $\text{CO}_2$ , and a vapor phase (V) with a composition very close to that of the  $\text{L}_2$  phase but containing slightly more  $\text{C}_1$ . Addition of more  $\text{C}_1$  to that mixture causes it to revert to a two phase system, though now the phases present are a liquid and a vapor. With additional increases in pressure, the  $\text{L}_1\text{-L}_2\text{-V}$  region migrates to higher  $\text{C}_1$  concentrations as more  $\text{C}_1$  is compressed into the  $\text{L}_1$  and  $\text{L}_2$  phases. Eventually, the  $\text{L}_1\text{-L}_2\text{-V}$  region disappears at a critical tie line as the  $\text{L}_2$  and V phases become identical (a type - k singular point), and the remaining  $\text{L}_1\text{-L}_2$  region (at high  $\text{CO}_2$  concentrations) separates from the  $\text{L}_1\text{-V}$  region at high  $\text{C}_1$  concentrations (Figure 4d). At still higher pressures both the remaining two phase regions are smaller (Figure 4e).

The phase behavior data given in Figures 2 and 3 and sequence of phase diagrams shown in Figure 4 give the first experimental confirmation of what Orr et al. (1) referred to as type II phase behavior for three phase  $\text{CO}_2$  - hydrocarbon systems. Phase equilibrium calculations for the  $\text{CO}_2\text{-C}_1\text{-C}_{16}$  system, performed with the Peng-Robinson equation of state, were reported by Mehra et al. (6). Their results clearly indicate that the Peng-Robinson equation of state, if used with a carefully

designed iterative scheme, can effectively model the complexity of  $\text{CO}_2$  - hydrocarbon phase behavior. The need for an effective iterative scheme of the type they describe became apparent when we attempted to calculate  $L_1$ - $L_2$  and  $L_1$ - $L_2$ - $V$  equilibria for the  $\text{CO}_2$ - $\text{C}_1$ - $\text{C}_{16}$  system. The rudimentary iterative procedure used in our equation of state program converged very slowly for  $L_1$ - $L_2$  systems and failed to converge for the  $L_1$ - $L_2$ - $V$  systems. In spite of the computational difficulties, however, it became clear that an equation of state can be a very useful tool for interpreting, interpolating and extrapolating high pressure phase behavior data which are difficult and expensive to obtain. Improvements of the sort described by Mehra et al. (6) and by Turek et al. (7) for a Redlich-Kwong equation of state will make such calculations still more valuable as the accuracy of a priori predictions improves.

#### PHASE BEHAVIOR OF $\text{CO}_2$ - SYNTHETIC OIL MIXTURES

Volumetric measurements were made for four binary mixtures of  $\text{CO}_2$  with a synthetic oil composed of 14.0 mol %  $\text{C}_5$ , 53.7%  $\text{C}_{10}$ , 19.0%  $\text{C}_{16}$  and 13.3%  $\text{C}_{30}$ . Phase volumes and saturation pressures were measured at  $37.8^\circ\text{C}$  for mixtures of  $\text{CO}_2$  and the oil containing 29.5, 54.2, 76.7 and 91.1 mol %  $\text{CO}_2$ . Then approximately 4 mol %  $\text{C}_1$  was added to the 91.1% mixture and the phase volumes and saturation pressures measured again. Figure 5 reports results of the volumetric measurements, and Figure 6 shows the effect of  $\text{CO}_2$  concentration on saturation pressures. Bubble points were observed for the mixtures containing 76.7%  $\text{CO}_2$  or less. As  $\text{CO}_2$  was added to the oil, the bubble point pressure increased. The mixture richest in  $\text{CO}_2$  showed a range of pressures in which  $L_1$ ,  $L_2$  and  $V$  phases coexisted, as did the same mixture when  $\text{C}_1$  was added. The liquid-liquid saturation pressures for those mixtures were dew points (see Figure 5).

Also shown in Figure 6 are saturation pressures calculated with the Peng-Robinson equation of state for binary mixtures of the synthetic oil with  $\text{CO}_2$  and for mixtures of  $\text{CO}_2$  with the synthetic oil plus  $\text{C}_1$ . Binary interaction parameters for  $\text{CO}_2$  and the heavy hydrocarbons  $\text{C}_{16}$  and  $\text{C}_{30}$  were obtained by matching binary saturation pressure data of Stewart and Nielsen (8) and Liphard and Schneider (9). Values used for  $\text{CO}_2$ - $\text{C}_{16}$  and  $\text{CO}_2$ - $\text{C}_{30}$  were 0.10 and 0.12 respectively. No attempt was made to further adjust interaction parameters to match measurements made in this study. The calculated saturation pressures shown in Figure 6 are predictions based on independent determinations of the required parameters. Agreement between calculated and measured bubble point pressures for the  $\text{CO}_2$  - synthetic oil mixtures is good at low  $\text{CO}_2$  concentrations but is less satisfactory at high  $\text{CO}_2$  levels. Again, computational difficulties were encountered for pressures and compositions in the liquid-liquid region. Measurements were not made at low  $\text{CO}_2$  concentrations for the system containing  $\text{C}_1$ . The saturation pressure curve shown in Figure 6 for that system was estimated from the calculated bubble point pressures.

Figure 6 indicates that the presence of  $\text{C}_1$  in this system increased both saturation pressures and the pressure levels at which  $\text{L}_1$ - $\text{L}_2$ -V phase separations occurred. Figure 7 shows compositions of three phase systems with and without  $\text{C}_1$ . Mole fractions of components  $\text{CO}_2$  and  $\text{C}_1$ ,  $\text{C}_5$  and  $\text{C}_{10}$  and those of  $\text{C}_{16}$  and  $\text{C}_{30}$  have been lumped for representation on the ternary diagram. The principal effect of the added  $\text{C}_1$  was to reduce the solubility of  $\text{CO}_2$  in the  $\text{L}_1$  phase. The preferential extraction of  $\text{C}_5$  and  $\text{C}_{10}$  into the  $\text{L}_2$  phase was not strongly affected. Clearly, the  $\text{L}_2$  phase extracted hydrocarbons from the oil more efficiently than did the V phase.

The phase behavior of the synthetic oil system without  $\text{C}_1$  is an

example of what Orr et al. (1) called type I phase behavior and is qualitatively similar to that reported by Meldrum and Nielsen (10) for a ternary system containing  $\text{CO}_2$ , propane ( $\text{C}_3$ ) and  $\text{C}_{16}$ . In that system,  $L_1$ - $L_2$ -V phase behavior appeared, with increasing pressure, when the solubility of  $\text{CO}_2$  in the  $\text{C}_3$ -rich liquid phase increased to the point that the  $\text{C}_3$ -rich liquid, which is more accurately described as a  $\text{CO}_2$ -rich liquid containing dissolved  $\text{C}_3$ , became immiscible with the lower liquid ( $L_1$ ) phase which contained more  $\text{C}_{16}$ . The sequence of phase diagrams for such a system (1) is shown in Figure 8. At low pressures, the two phase (L-V) region is a band across the ternary diagram (Figure 8a). As the pressure is increased, the solubility of  $\text{CO}_2$  in the light hydrocarbons increases more rapidly than that in the heavier component (Figure 8b). Eventually, the liquid phase on the  $\text{CO}_2$ - $\text{C}_5$ + $\text{C}_{10}$  side of the diagram becomes so rich in  $\text{CO}_2$  that it is immiscible with the liquid phase which contains most of the  $\text{C}_{16}$  and  $\text{C}_{30}$ . Additional increases in pressure cause the  $L_1$ - $L_2$ -V region to migrate toward the  $\text{CO}_2$ - $\text{C}_{16}$ + $\text{C}_{30}$  side of the diagram. When the three phase pressure for the  $\text{CO}_2$ - $\text{C}_{16}$ + $\text{C}_{30}$  binary is reached, the  $L_1$ - $L_2$ -V region disappears.

#### PRESSURE RANGES FOR $L_1$ - $L_2$ -V BEHAVIOR

In the  $\text{CO}_2$ - $\text{C}_1$ - $\text{C}_{16}$  system, the experimental temperature exceeded the critical temperature of both  $\text{CO}_2$  and  $\text{C}_1$ . In such systems, the lower limit of pressures at which  $L_1$ - $L_2$ -V phase behavior will occur is the three phase pressure for  $\text{CO}_2$  and the heavy component (see Figure 4). In  $\text{CO}_2$  - hydrocarbon systems in which  $\text{CO}_2$  is the only supercritical component, the three phase pressure will be the upper bound for  $L_1$ - $L_2$ -V separations. Measurements of the three phase pressure for  $\text{CO}_2$  - hydrocarbon binary mixtures by Meldrum and Nielsen (10), Leder and Irani (11) and in our laboratory indicate that the locus of  $L_1$ - $L_2$ -V pressures

at various temperatures lies slightly below but very close to the vapor pressure curve for CO<sub>2</sub>. Therefore, while the L<sub>1</sub>-L<sub>2</sub>-V pressure range for a specific CO<sub>2</sub> - hydrocarbon mixture will depend on the mixture composition, L<sub>1</sub>-L<sub>2</sub>-V phase behavior will occur at pressures in the neighborhood of the vapor pressure of CO<sub>2</sub> at a given temperature. Figure 9 compares the vapor pressure of CO<sub>2</sub>, calculated from the equation given by Newitt et al. (12), with L<sub>1</sub>-L<sub>2</sub>-V pressure ranges for CO<sub>2</sub> - crude oil systems (1, 3, 10, 13-15). Despite wide variations in the compositions of the crude oils, pressure ranges reported for L<sub>1</sub>-L<sub>2</sub>-V behavior lie within a band given by the vapor pressure plus 1750 kPa and minus 1000 kPa. Thus, a reasonable estimate of the pressure required to avoid L<sub>1</sub>-L<sub>2</sub>-V phase behavior for temperatures from 10 to 50°C is given by Equation 1.

$$P = 101.325 \exp \left\{ \frac{-2015.19}{T} + 10.9122 \right\} + 1750 \quad 1)$$

where P is the pressure in kPa, and T the temperature in °K.

Operation of a low temperature (below 50°C) CO<sub>2</sub> flood above the pressure given by Equation 1 would avoid adverse affects of a highly mobile gas phase and would ensure that the density of any CO<sub>2</sub>-rich phase would be near that required for efficient extraction of hydrocarbons from the oil (16).

#### CO<sub>2</sub> - CRUDE OIL PHASE BEHAVIOR

Comparison of the results shown in Figures 3, 6 and 7 with phase behavior results for low temperature CO<sub>2</sub> - crude oil systems reported by Shelton and Yarborough (3), Huang and Tracht (14), Gardner et al. (13) and Orr et al. (17) indicates that the qualitative features of CO<sub>2</sub> - crude oil phase diagrams can be reproduced with CO<sub>2</sub>-alkane systems. The synthetic oil considered here came closer to matching

CO<sub>2</sub> - crude oil behavior than that used by Metcalfe and Yarborough (18) because it contained hydrocarbons heavy enough to produce liquid-liquid phase behavior. It should be noted, however, that the solubility of CO<sub>2</sub> in the synthetic oil is higher at high CO<sub>2</sub> concentrations than it is in CO<sub>2</sub> - crude oil systems. In particular, the L<sub>1</sub>-L<sub>2</sub> region extends to lower CO<sub>2</sub> concentrations and to much higher pressures in CO<sub>2</sub> - crude oil systems (1, 13, 17). The higher solubility of CO<sub>2</sub> in the synthetic oil probably stems from the fact that the heaviest component present was C<sub>30</sub>. Crude oils, however, contain some components much heavier than C<sub>30</sub>. Since saturation pressures at high CO<sub>2</sub> concentrations are sensitive to the amounts and properties of the heaviest hydrocarbon components, it is not surprising that the L<sub>1</sub>-L<sub>2</sub> region is larger in CO<sub>2</sub> - crude oil systems.

The results presented here suggest that synthetic oil mixtures can be found which reproduce the behavior of crude oils when mixed with CO<sub>2</sub>. Combinations of phase behavior and displacement experiments with synthetic oils, such as those reported by Metcalfe and Yarborough (18), can be extremely useful for developing understanding of the types of behavior which may occur in CO<sub>2</sub> - crude oil systems. Nevertheless, caution should be used in the interpretation of such experiments if conclusions about CO<sub>2</sub> - crude oil displacement mechanisms are sought. For instance, the higher solubility of CO<sub>2</sub> in the synthetic oil discussed here would lead to higher recovery in a displacement than would be achieved with a crude oil because any residual L<sub>1</sub> phase would contain a larger volume fraction of CO<sub>2</sub>. Thus, in the synthetic oil system recovery would improve with increasing pressure because the solubility of CO<sub>2</sub> improves, while in a crude oil system the improvement in displacement efficiency comes primarily from the improvement in the efficiency of extraction of hydrocarbons by the

CO<sub>2</sub>-rich phase.

#### CONCLUSIONS

Results of phase behavior measurements for CO<sub>2</sub> and two well characterized hydrocarbon systems indicate that:

- (1) High pressure samples can be obtained reliably by flushing samples trapped at system temperature and pressure from a liquid sampling valve into a pressure tight syringe.
- (2) At temperatures below about 50°C, L<sub>1</sub>-L<sub>2</sub>-V phase behavior occurs for CO<sub>2</sub> - hydrocarbon mixtures at pressures near the vapor pressure of CO<sub>2</sub>.
- (3) The second liquid phase is predominantly CO<sub>2</sub> with some hydrocarbons dissolved in it. The L<sub>2</sub> phase extracts hydrocarbons from the oil more efficiently than the vapor phase.
- (4) At temperatures below 50°C, the range of pressures within which L<sub>1</sub>-L<sub>2</sub>-V occurs is bounded above by the vapor pressure of CO<sub>2</sub> if methane is not present. If it is, the pressure required to eliminate the vapor phase is somewhat higher than the vapor pressure of CO<sub>2</sub> (extrapolated if necessary). A reasonable estimate of the pressure required to produce L<sub>1</sub>-L<sub>2</sub> behavior in CO<sub>2</sub> - crude oil systems is the vapor pressure plus 1750 kPa.
- (5) Conclusions about CO<sub>2</sub> - crude oil displacement mechanisms should be drawn with caution from CO<sub>2</sub> - synthetic oil displacement studies.

#### ACKNOWLEDGEMENT

The work reported in this paper was performed with support from the U. S. Department of Energy, the New Mexico Energy and Minerals Department, and the New Mexico Petroleum Recovery Research Center. We thank R. K. Spaulding for her help with the phase behavior experiments. Finally, we thank especially J. J. Taber for his unflagging enthusiasm and support.

#### LITERATURE CITED

- (1) Orr, F. M., Jr., Yu, A. D. and Lien, C. L., SPE 8813, presented at the First Joint SPE/DOE Symposium on Enhanced Oil Recovery, Tulsa, April 20-23 (1980).

- (2) Simon, R., Rosman, A. and Zana E., Soc. Pet. Eng. J. 18, 20 (1978).
- (3) Shelton, J. L. and Yarborough, L., J. Pet. Tech. 19, 1171 (1977).
- (4) Orr, F. M., Jr. and Taber, J. J., Annual Report on Petroleum Research, U. S. Department of Energy, January (1981).
- (5) Peng, D. Y. and Robinson, D. B., Ind. Eng. Chem. Fund., 15, 304 (1976).
- (6) Mehra, R. K., Heidemann, R. A. and Aziz, K., SPE 9232, presented at SPE 55th Annual Fall Meeting, Dallas, September 21-24 (1980).
- (7) Turek, E. A., Metcalfe, R. S., Yarborough, L. and Robinson, R. L., SPE 9231, presented at SPE 55th Annual Fall Meeting, Dallas, September 21-24 (1980).
- (8) Stewart, W. C. and Nielsen, R. F., Prod. Monthly, 27 January (1954).
- (9) Liphard, K. G. and Schneider, G. M., J. Chem. Thermodynamics 7, 805 (1975).
- (10) Meldrum, A. H. and Nielsen, R. F., Prod. Monthly, 22 August (1955).
- (11) Leder, F. and Irani, C. A., J. Chem. Eng. Data, 20, 323 (1975).
- (12) Newitt, D. M., Pai, M. U. and Kuloor, N. R., Thermodynamic Functions of Gases, Vol. 1, F. Din, Ed., Butterworths, London 102 (1956).
- (13) Gardner, J. W., Orr, F. M., Jr. and Patel, P. D., SPE 8367, presented at SPE 54th Annual Fall Meeting, Las Vegas, September 23-26 (1979).
- (14) Huang, E. T. S. and Tracht, J. H., SPE 4735, presented at the SPE 3rd Symposium on Improved Oil Recovery, Tulsa, April (1974).
- (15) Henry, R. L. and Metcalfe, R. S., SPE 8812, presented at the First Joint SPE/DOE Symposium on Enhanced Oil Recovery, Tulsa, April 20-23 (1980).
- (16) Holm, L. W. and Josendal, V. A., SPE 8814, presented at the First Joint SPE/DOE Symposium on Enhanced Oil Recovery, Tulsa, April 20-23 (1980).
- (17) Orr, F. M., Jr., Silva, M. K., Lien, C. L. and Pelletier, M. T., SPE 9534, presented at Eastern Regional Meeting of SPE, Morgantown, Nov. 5-7 (1980).
- (18) Metcalfe, R. S. and Yarborough, L., Soc. Pet. Eng. J. 19, August (1979).

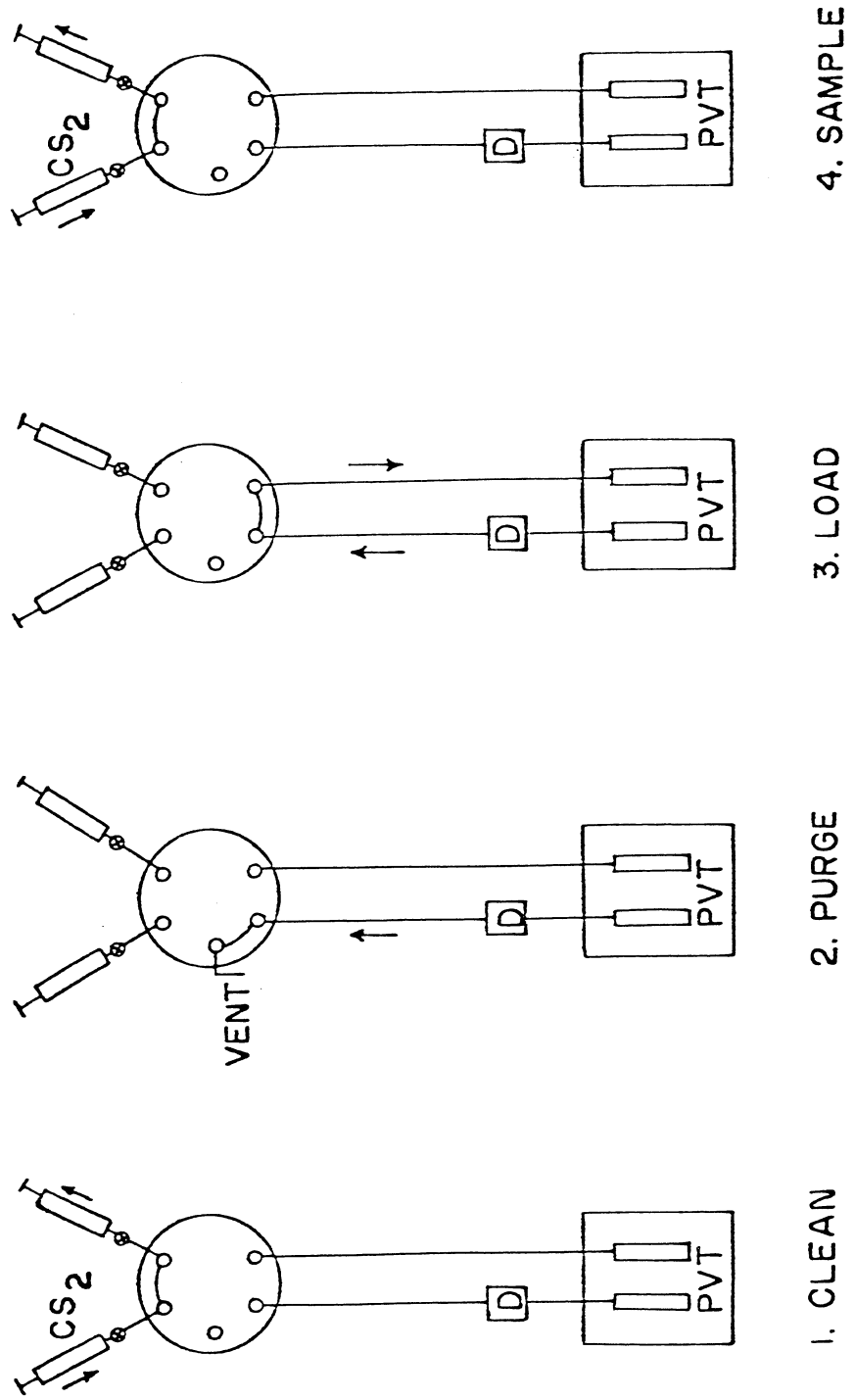


Figure 1. High pressure sampling system

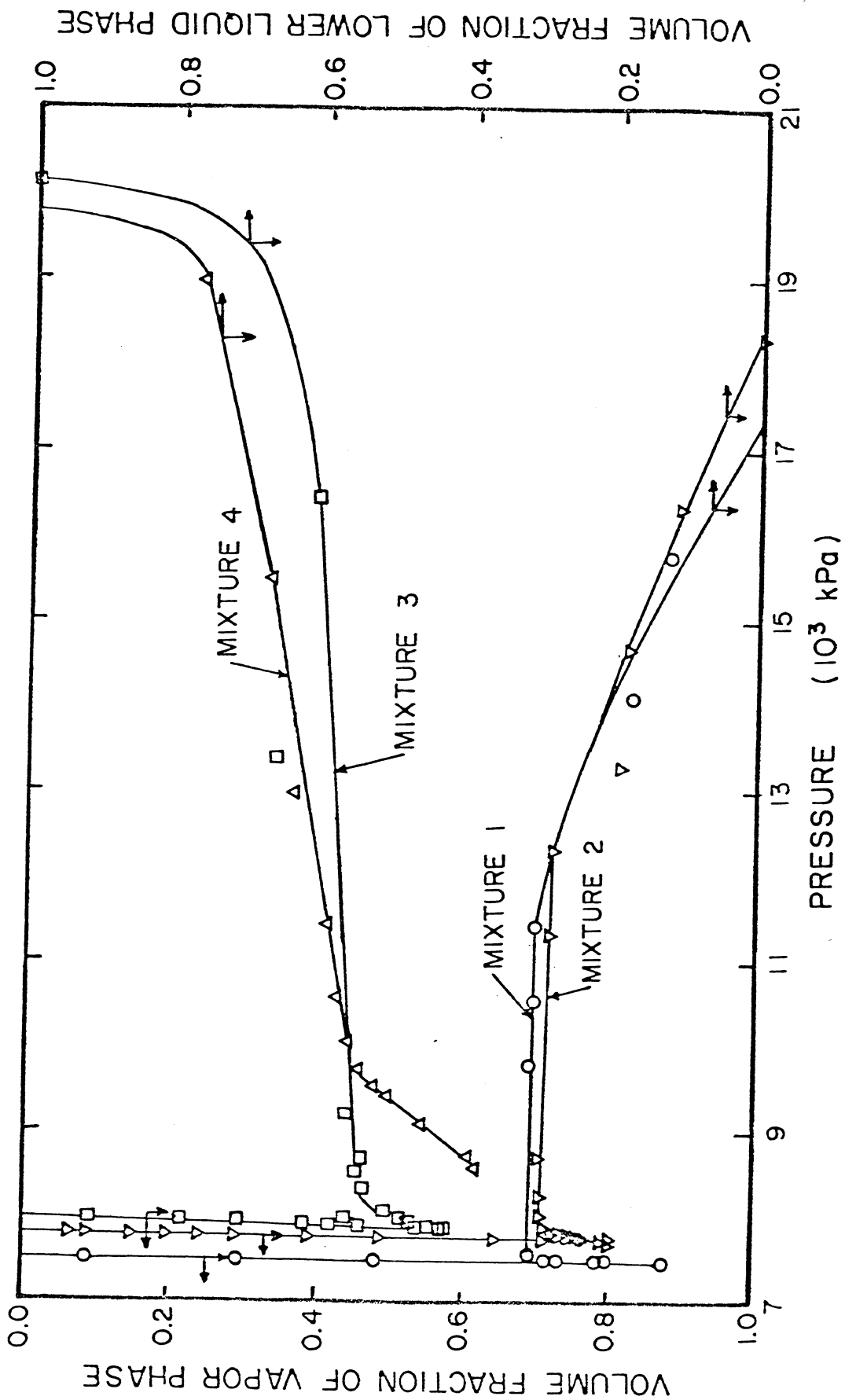


Figure 2. Volumetric behavior of CO<sub>2</sub>-C<sub>1</sub>-C<sub>16</sub> mixtures at 32.2°C

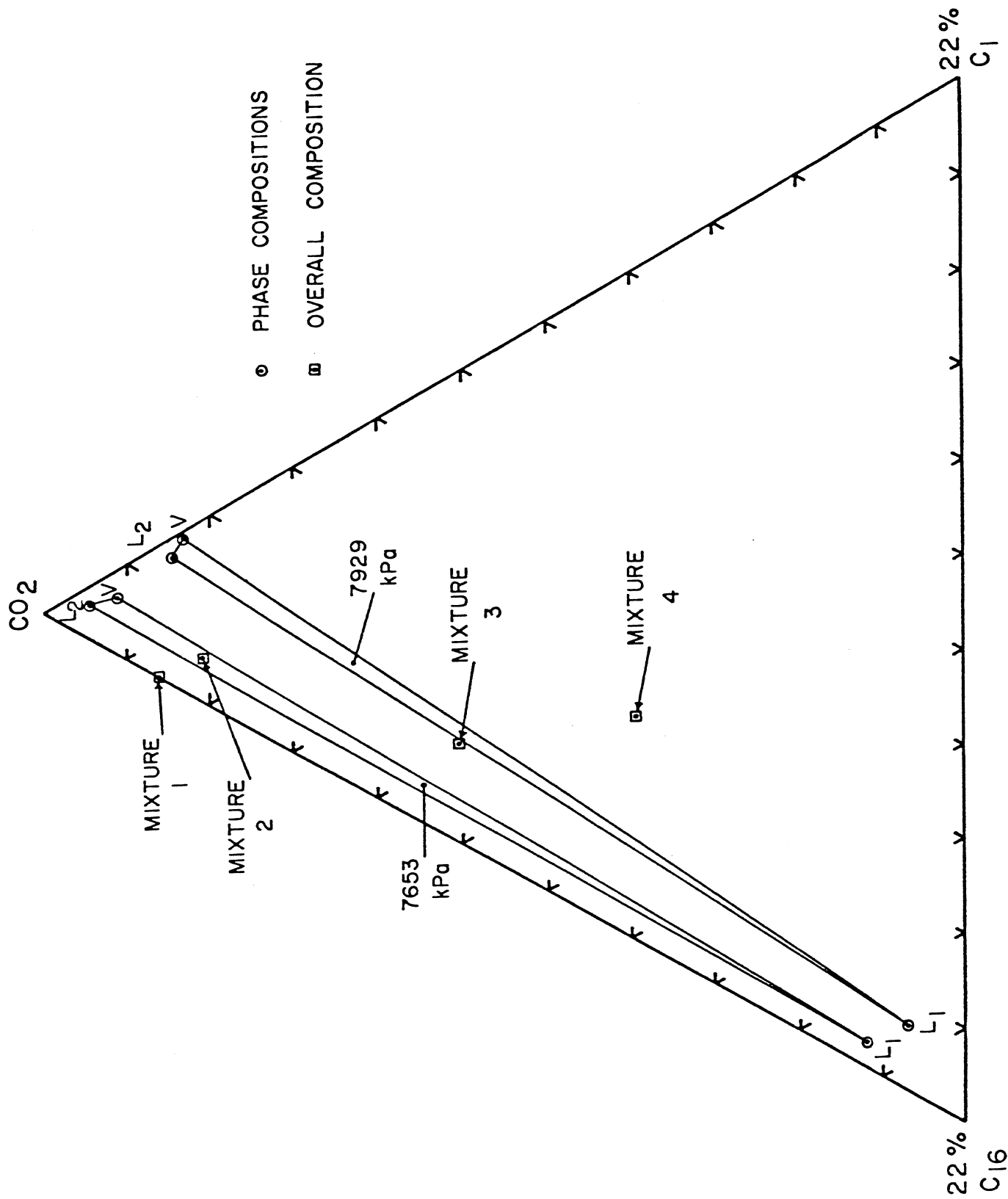


Figure 3. Compositions of  $L_1$ - $L_2$ - $V$  mixtures of  $\text{CO}_2$ ,  $\text{C}_1$  and  $\text{C}_{16}$  at  $32.2^\circ\text{C}$

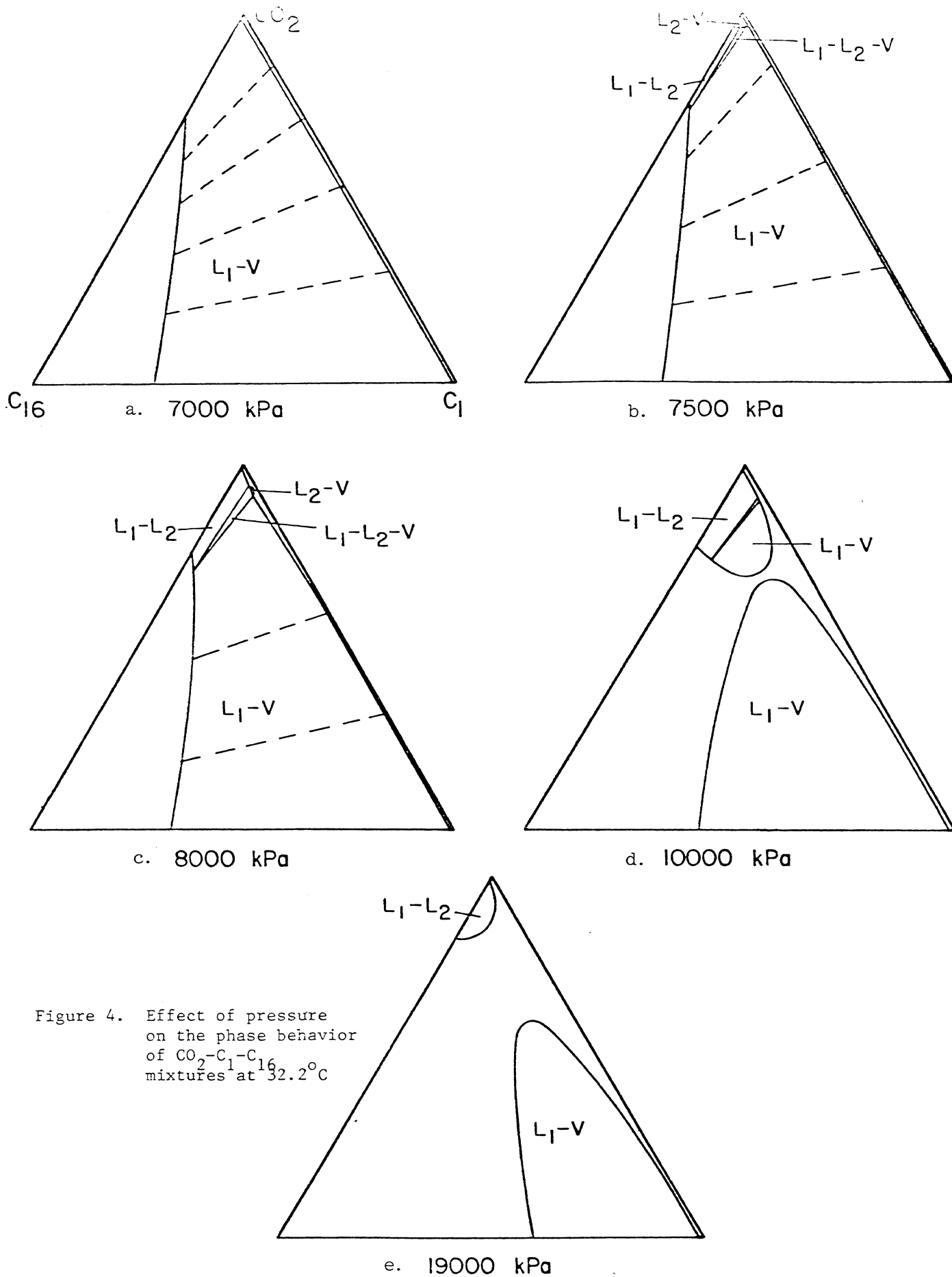


Figure 4. Effect of pressure on the phase behavior of  $CO_2$ - $C_1$ - $C_{16}$  mixtures at  $32.2^\circ C$

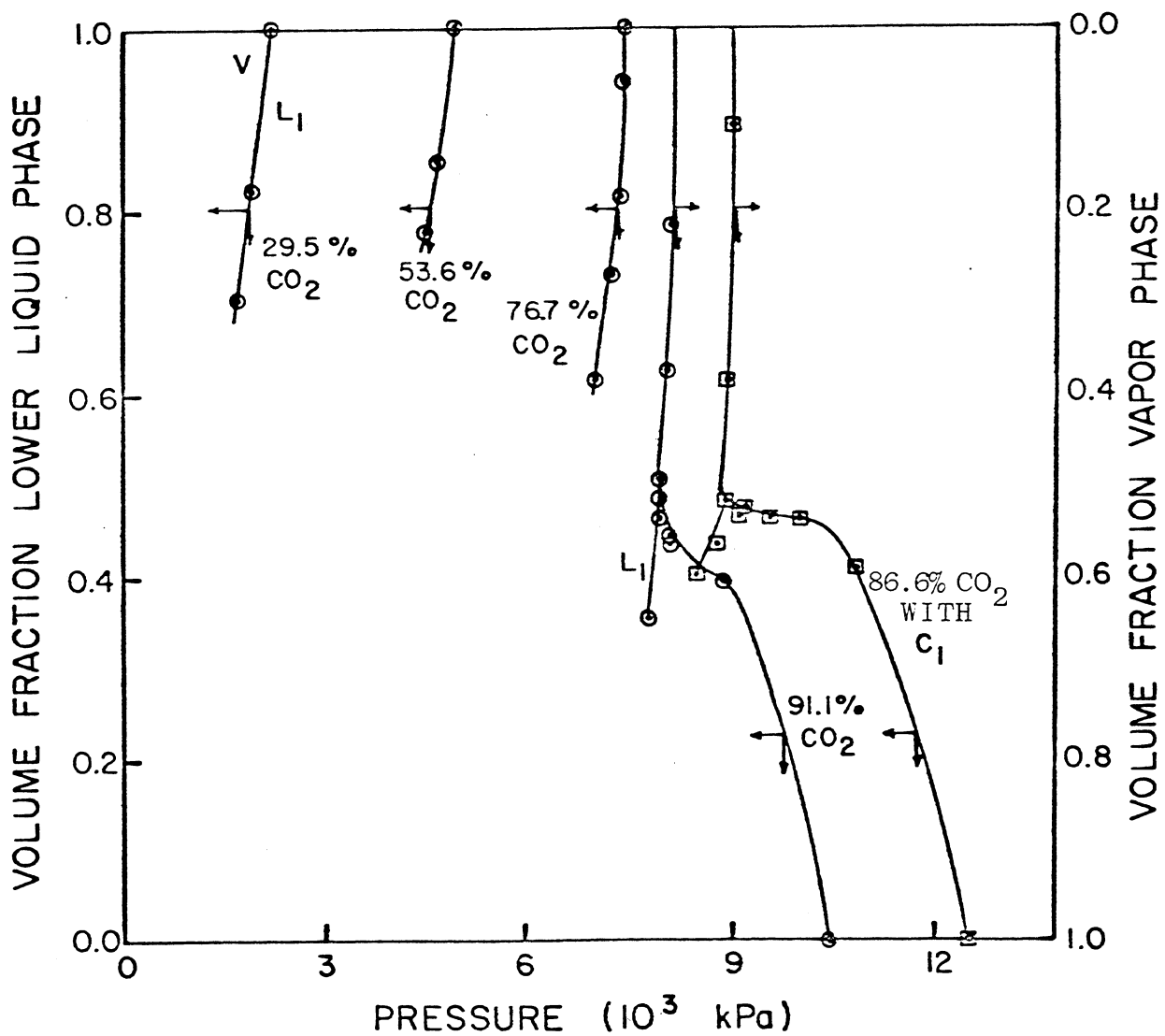


Figure 5. Volumetric behavior of CO<sub>2</sub> - synthetic oil mixtures at 37.8°C

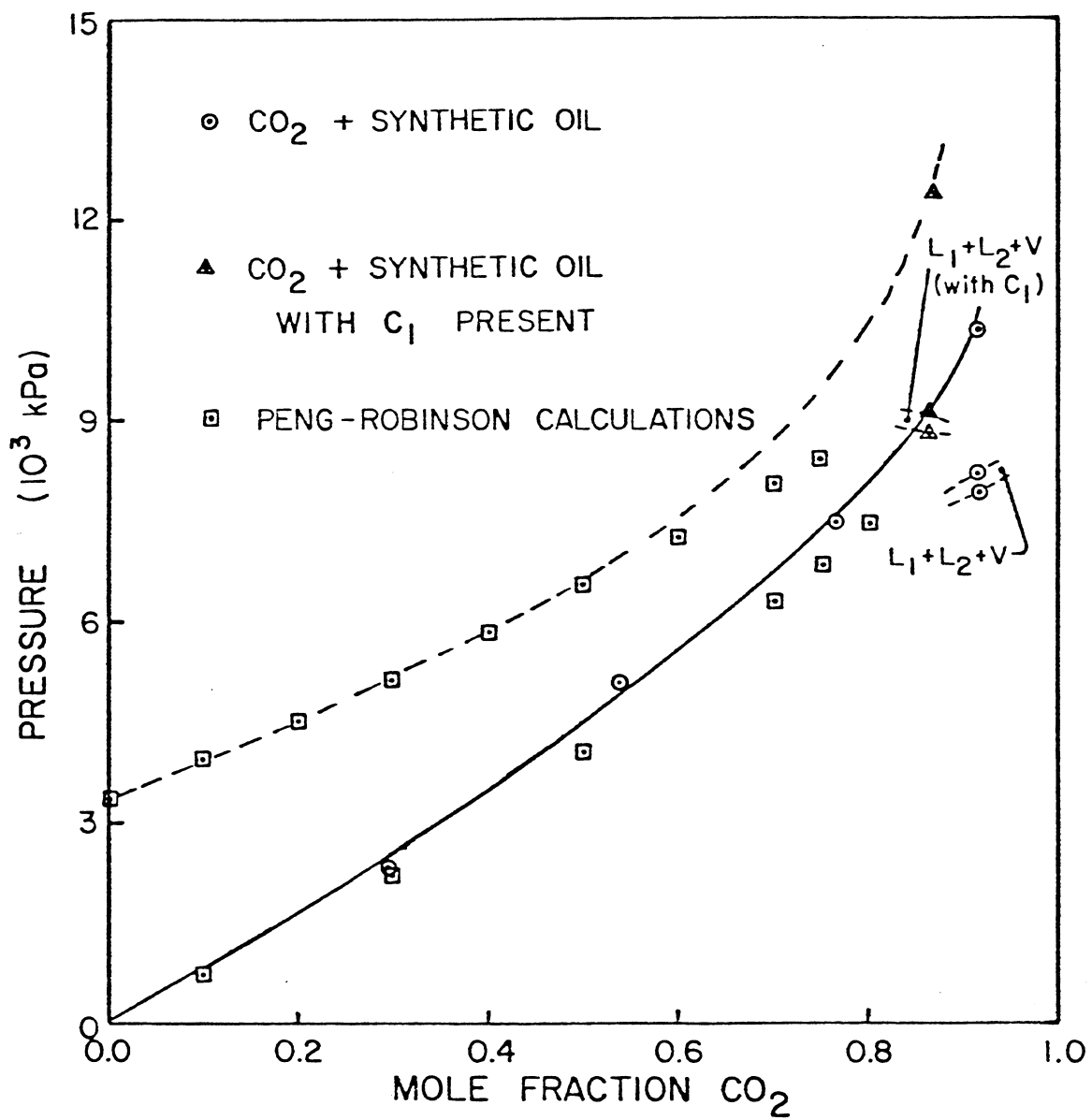


Figure 6. Phase behavior of  $CO_2$  and synthetic oil at  $37.8^\circ C$

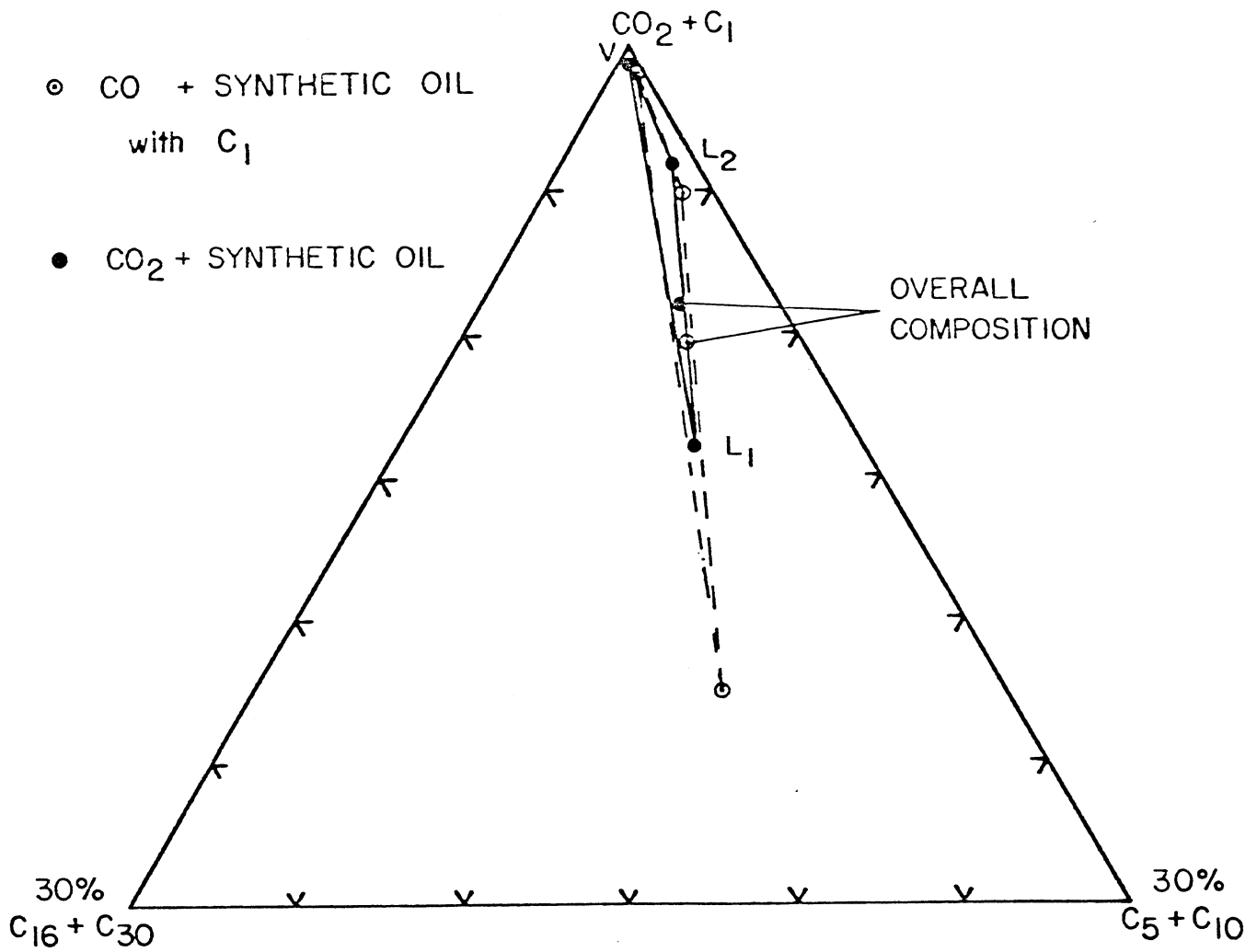


Figure 7. Comparison of compositions of  $L_1$ ,  $L_2$  and  $V$  phases for a  $\text{CO}_2$  - synthetic oil mixture at 7998 kPa and a  $\text{CO}_2$  -  $\text{C}_1$  - synthetic oil mixture at 8894 kPa and  $37.8^\circ\text{C}$

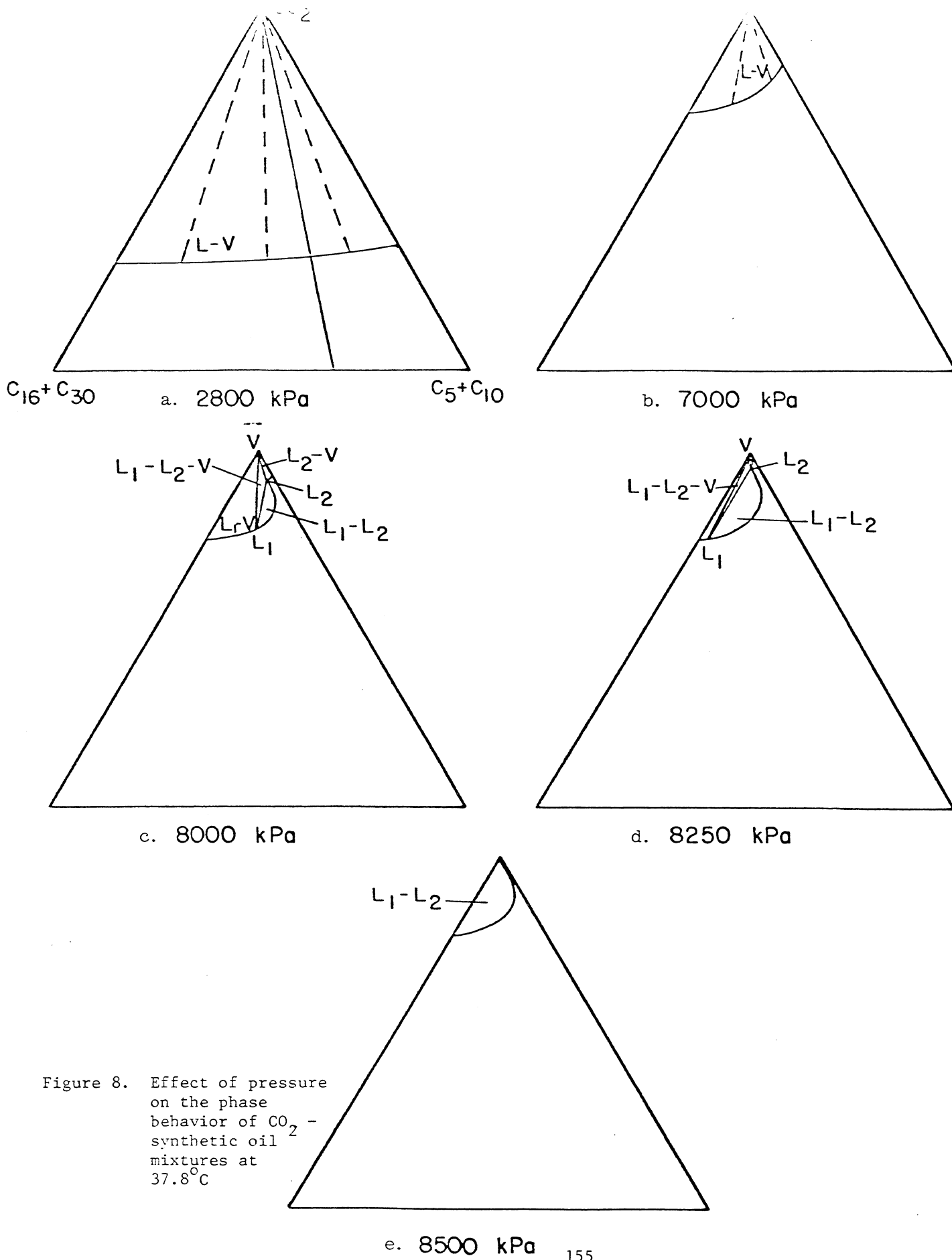


Figure 8. Effect of pressure on the phase behavior of  $\text{CO}_2$  - synthetic oil mixtures at  $37.8^\circ\text{C}$

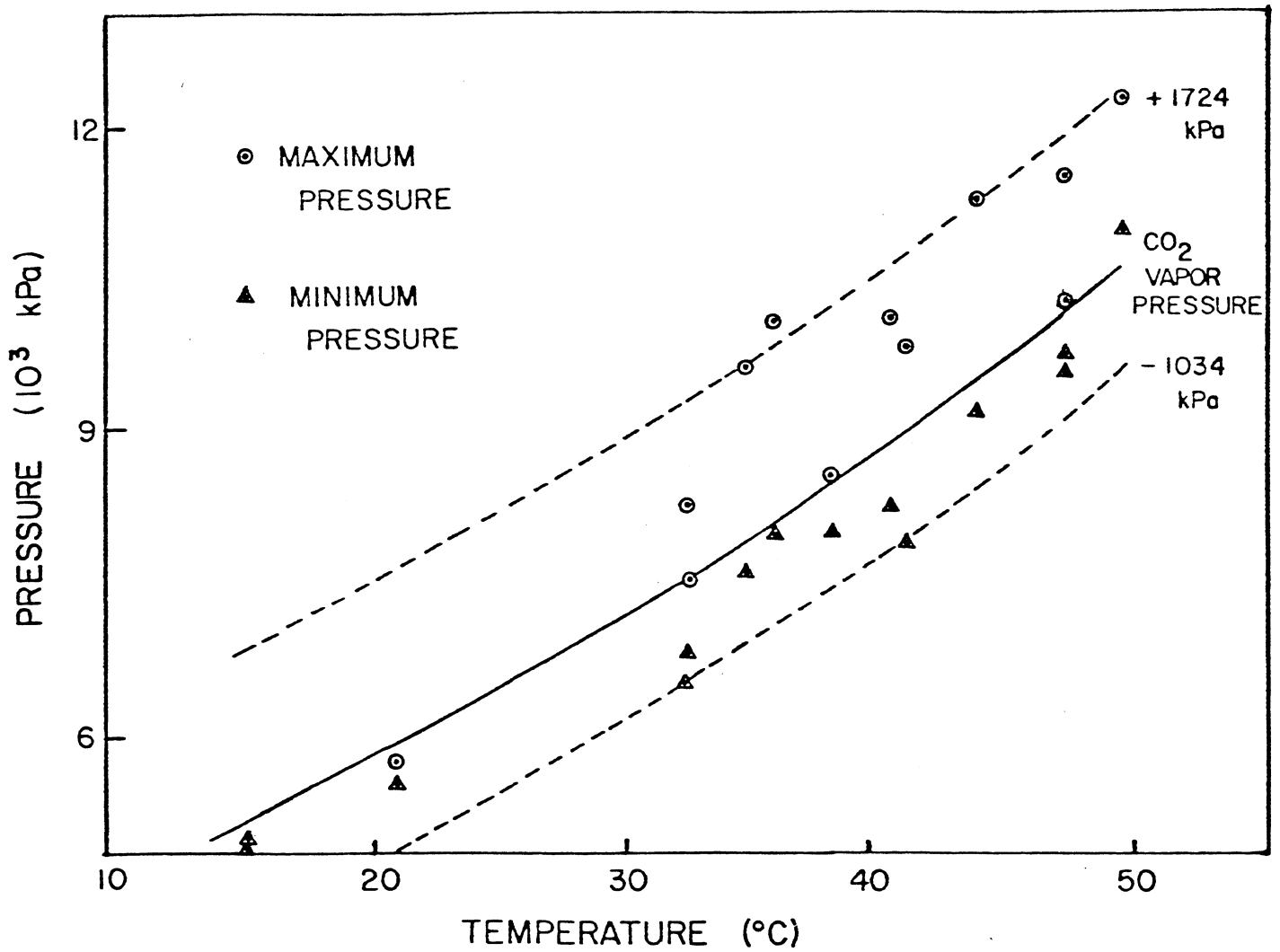


Figure 9. Pressure ranges for  $L_1$ - $L_2$ -V phase behavior in CO<sub>2</sub> - crude oil systems





